Regulation of dematin by the p38 MAPK and the adaptor protein 14-3-3

Holly Baum

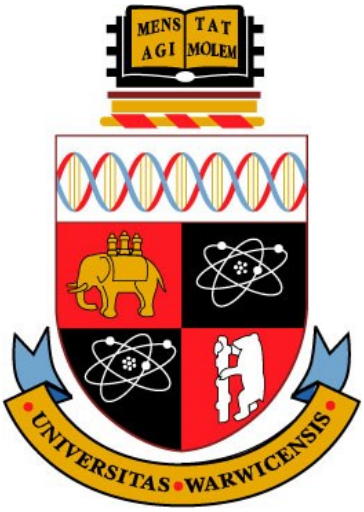

A thesis submitted for the degree of Doctor of Philosophy

The University of Warwick

Warwick Medical School

June 2014

‘Research is what I'm doing when I don't know what I'm doing.’

Werner Von Braun

I. Table of contents

II. Table of figures

III. Table of tables

IV. Acknowledgements

I would like to thank my supervisor, Dr Jürgen Müller, for both giving me the opportunity to complete this PhD, and for the support and guidance he has given me throughout the process. His advice on all aspects of my experimental and written work has been greatly appreciated, and I value the broad range of new techniques that I have learnt. Thank you also to Dr Tine Tingholm for conducting the mass spectrometry analysis of my protein.

Thank you to all of the support staff at Gibbet Hill; those in media prep, stores, the workshop, and the technicians. You do so much behind the scenes to keep things running smoothly, and I'm extremely grateful for all the help you have given me.

A big thank you to everyone in C030, in Neuroscience, and those in C126. There are far too many of you to name individually, but in your own unique ways you've all made the past four years far more enjoyable than they otherwise could have been. We got through this together, with the help of a lot of tea, a substantial amount of moaning, and some good cakes!

Finally an extra special thank you to Mike and Sandrine, you've both always been there for me, and my time at Warwick wouldn't have been the same without you.

V. Declaration

This thesis is submitted to the University of Warwick in support of my application for the degree of Doctor of Philosophy. It has been composed by myself, under the supervision of Dr Jürgen Müller, and has not been submitted in any previous application for another degree.

I hereby declare that I have conducted all of the work presented here, with the exception of the following experiments:

1. The in vitro kinase and micro-array experiments, described in section 3.3.1 and presented in figure Figure 3.3, were conducted by Dr Jürgen Müller.

2. The mass spectrometry analysis of dematin, detailed in section 3.3.3 and presented in figure Figure 3.5B, was conducted by Dr Tine Tingholm of Lund University, Sweden.

Holly Baum

June 2014

VI. Summary

Dematin is an actin-binding and -bundling protein that was first identified in human erythrocytes where it is important for providing mechanical stability. Two splice variants exist in vivo of 48 KDa and 52 KDa, each of which comprises a disordered C-terminal core domain and a short, highly-ordered, N-terminal headpiece (HP). Expression of dematin has now been demonstrated in a wide range of tissues and functional roles are emerging for dematin as a tumour suppressor, and regulator of wound healing, via negative regulation of RhoA. Despite these advances, the in vivo regulation of dematin remains poorly understood. This thesis therefore aimed to characterise the regulation of dematin by two known cytoskeletal coordinators; the p38 mitogen-activated protein-kinase (MAPK), and the adaptor protein 14-3-3.

Dematin was confirmed as a substrate of p38, and multiple phosphorylation sites were identified in both the core and HP regions of the protein using mass spectrometry and in vitro kinase assays. Moreover pulse-chase degradation analysis identified dematin as a short-lived protein, with a calculated half-life of 5.49 +/- 0.44 hours. Further experiments confirmed that this propensity for degradation is at least in part due to the presence of a PEST motif, with the half-life of the dematin_ΔPEST construct significantly increased compared to wild-type dematin at 7.64 +/- 0.72 hours. Despite identifying p38 phosphorylation sites within and flanking the PEST motif, hyper-activation or inhibition of p38 had no significant effect on protein stability. Finally, it was shown that although p38 phosphorylated the dematin HP at Ser^{383}, this was not sufficient to disrupt the association of the HP and core regions which is known to inhibit actin bundling.

Additionally dematin was identified as a novel substrate of the 14-3-3 family of adaptor proteins. The 14-3-3β isoform was shown to bind to 52 KDa dematin at two phosphorylated motifs; $RKTRS_{269}LP$ and $RGNS_{333}LP$. It was not possible to identify the kinases that regulate these motifs, but Akt, PKA, or AMPK were ruled out as potential candidates. Immunofluorescence staining and confocal imaging confirmed that 14-3-3 regulates dematin by altering its subcellular distribution, which is likely to be via masking of an actin-binding motif. Wild-type dematin was distributed throughout the cytoplasm in C2C12 skeletal muscle cells, whereas the dematin_S269/333A binding mutant localised strongly to the F-actin cytoskeleton. This localisation result was confirmed in quantitative sedimentation experiments, which showed a statistically significant decrease in both the actin-binding (42.8%) and -bundling (30.1%) ability of dematin upon 14-3-3 association.

In this thesis I have characterised both the p38 MAPK and the adaptor protein 14-3-3 as novel regulators of dematin, adding considerably to the understanding of dematin regulation in vivo. This provides a basis for further investigation into the ability of dematin to coordinate the actin cytoskeleton, which has implications for a wide array of dematin functions due to its ubiquitous tissue expression profile.

VII. List of Abbreviations

α - alpha

β - beta

γ - gamma

δ - delta

ε - epsilon

ζ - zeta

η - eta

θ - theta

ΔPEST - deletion of PEST motif

µm - micro meter

µM - micro molar

A - absorbance

Aa - amino acids

Amp - ampicillin

ABP - actin-binding protein

AF - actin filament

APS - ammonium persulphate

BCA - bicinchoninic acid

BSA - bovine serum albumin

Co-IP - co-immunoprecipitation

DMSO - dimethyl sulphoxide

DNA - deoxyribonucleic acid

dNTP - deoxynucleotide triphosphate

DTT - dithiothreitol

ECL - enhanced chemiluminescence

F-actin - filamentous actin

G-actin - globular actin

G - gravitational force

GAP - GTPase activating protein

GDI - GDP dissociation inhibitor

GEF - guanine nucleotide exchange factor

GFP - Green fluorescent protein

HBSS - Hank's Balanced Salt Solution

HP - headpiece

HPKO - headpiece knock-out

Kb - Kilobase

IP - immunoprecipitation

LB - Luria-Bertami

MAPK - mitogen-activated protein kinase

min - Minutes

ml - Millilitre

MS - mass spectrometry

MPM2 - Mitotic Protein Monoclonal #2

OD - Optical density

p - phosphorylated

PCR - polymerase chain reaction

PFA - paraformaldehyde

PKA - Protein kinase A

PKC - Protein Kinase C

PKD - Protein Kinase D

rpm - Revolutions per minute

RT - room temperature

SD - standard deviation

SDS - sodium dodecyl sulphate

TBE - Tris / Borate / EDTA

TBST - Tris-buffered…… / Tween-20

TEMED - tetramethylethylenediamine

w/v - weight/volume

Ser^{381} [Ser^{403}] - number in brackets refers to position in the 52 KDa dematin isoform

NOTE - In the literature the system used to number the residues within a particular dematin construct traditionally begins at 0 from the first amino acid of that specific construct. This can lead to confusion when studies focus on just the N-terminal headpiece of dematin, or use the shorter 48 KDa isoform of dematin, as a particular residue can then by referred to by three different numbers. For example, Ser^{403} in the 52 KDa isoform = Ser^{381} in the 48 KDa isoform = Ser^{74} in the headpiece. For simplicity, all constructs created for use in this thesis are numbered relative to the 52 KDa isoform of dematin - which ranges from 0-405 aa. Therefore the headpiece domain, which is referred to in the literature as 0-76 aa, is here annotated as 315-405. In line with this numbering approach, where a reference is made to a specific residue from the literature that does not correlate with this system, the relative position in the 52 KDa isoform of dematin is given in [ ].

1. Introduction

1.1 Dematin

Dematin, also known as EPB49 and protein 4.9, was first identified in 1985 as a component of the erythrocyte cytoskeleton (Siegel & Branton). The name derives from the Greek word Dema, which translates as 'to bundle', and refers to the ability of dematin to both bind and bundle actin filaments (AFs). Expression of dematin has subsequently been demonstrated in a wide variety of tissues, including the brain, heart, lungs, kidneys, and skeletal muscle (Kim *et al.*, 1998; Rana *et al.*, 1993). In erythrocytes dematin forms a linkage between the cell membrane and the actin cytoskeleton, providing mechanical stability to the cell (Khan *et al.*, 2008). The non-erythroid functions of dematin have yet to be fully characterised, but it has been implicated in wound healing (Mohseni & Chishti, 2008a; Mohseni & Chishti, 2009), and tumour suppression (Kim *et al.*, 1998).

1.1.1 Primary structural features of dematin

Dematin is composed of a large N-terminal core domain, and a shorter C-terminal headpiece domain (HP) (Figure 1.1). The dematin HP is homologous to that of villin, a protein found in the epithelial brush borders which is also known to bind to actin (Vardar *et al.*, 2002). In vivo two isoforms of dematin exist, of 48 and 52 KDa, which are the result of alternative splicing. The dematin gene consists of 15 exons and 14 introns (Kim *et al.*, 1998), with the 22-amino acid insert in the 52 KDa isoform encoded by exon 13 (Azim *et al.*, 1995). The primary structure of the 48 KDa isoform of dematin was first determined in 1993 (Rana *et al.*), followed by that of the 52 KDa variant in 1995 (Azim *et al.*). This confirmed that the sequences of the two isoforms are identical, except for the insert in the HP domain of the 52 KDa variant (Figure 1.2).

The 48 and 52 KDa human isoforms of dematin have sequences of 383 aa and 405 aa in length respectively (Azim *et al.*, 1995). Several regions of interest within the primary structure of dematin have been identified, based upon the presence of characterised sequence motifs. The functional implications of the majority of these

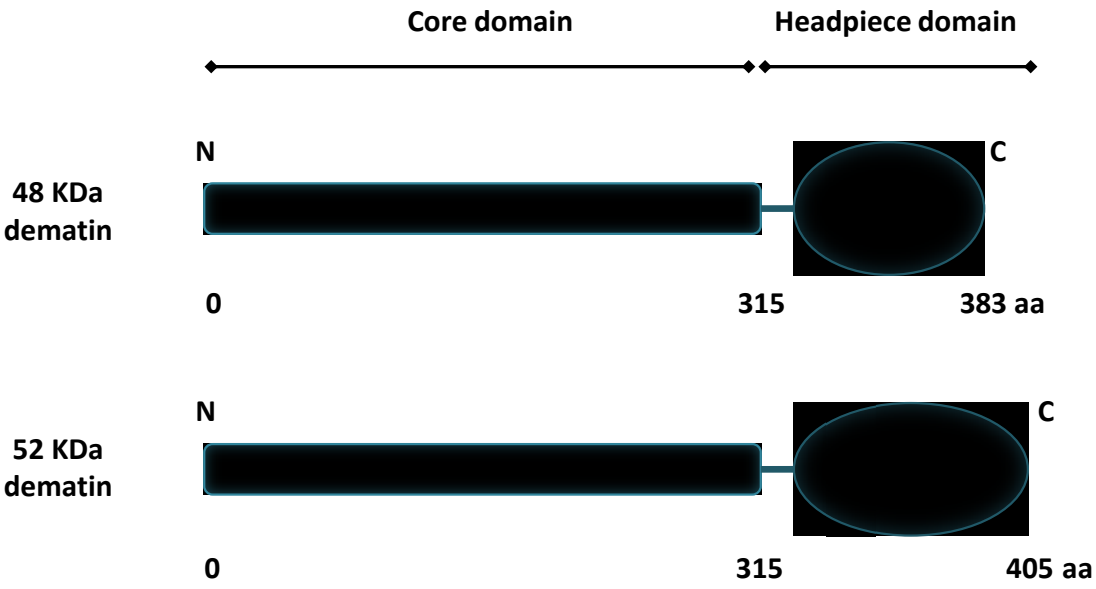

Figure 1.1: The domain structures of the two dematin isoforms

Dematin exists in vivo as two isoforms of 48 and 52 KDa. Both isoforms are composed of a large N-terminal core domain, with a shorter C-terminal headpiece. The sequence of the core domain of the two isoforms is identical, while the headpiece domains differ by a 22-amino acid insert (light blue shaded region) in the 52 KDa variant.

motifs have yet to be investigated, and so it is unclear as to the roles they may play in the regulation of dematin.

1.1.1.1 MAPK phosphorylation motifs

The mitogen-activated protein-kinase (MAPK) family are a large group of Ser/Thr specific kinases that regulate a vast array of cellular outcomes (Ashwell, 2006). These are classified as proline-directed kinases due to their preference for a Pro residue at the +1 position in the consensus recognition sequence, phosphorylating substrates at either Ser-Pro (SP) or Thr-Pro (TP) motifs. There are thirteen such motifs within the primary sequence of dematin (Figure 1.2; purple boxes).

1.1.1.2 MAPK docking motif (D-motif)

In addition to the presence of MAPK phosphorylation motifs, dematin contains the potential MAPK docking sequence ^{49}KDKAILDI^{56} (Figure 1.2; green box). D-motifs are found in MAPK substrates at sites distal to the phosphorylation motifs and act to enhance substrate recognition; however they are not essential for phosphorylation of a substrate (Bardwell *et al.*, 2009).

1.1.1.3 PEST degradation motif

PEST motifs are short sequences rich in the amino acids Pro, Glu, Ser, and Thr (Rogers *et al.*, 1986). Dematin contains the sequence ^{89}KSTSPPPSPEVWADSR^{104} (Figure 1.2; blue box), which meets the criteria for such a motif. The presence of a PEST motif in a protein sequence has been linked to a propensity for degradation, a process which is often regulated through phosphorylation of internal serine and threonine residues (Rechsteiner & Rogers, 1996).

1.1.1.4 14-3-3 binding motifs

The 14-3-3 family of adaptor proteins bind to a wide array of substrates at defined phospho-serine / phospho-threonine containing motifs. The dematin sequence contains seven of these motifs (Figure 1.2; yellow boxes). The association of 14-3-3 can have a wide variety of effects on a target, including altering the subcellular localisation and interaction properties (Bridges & Moorhead, 2005).

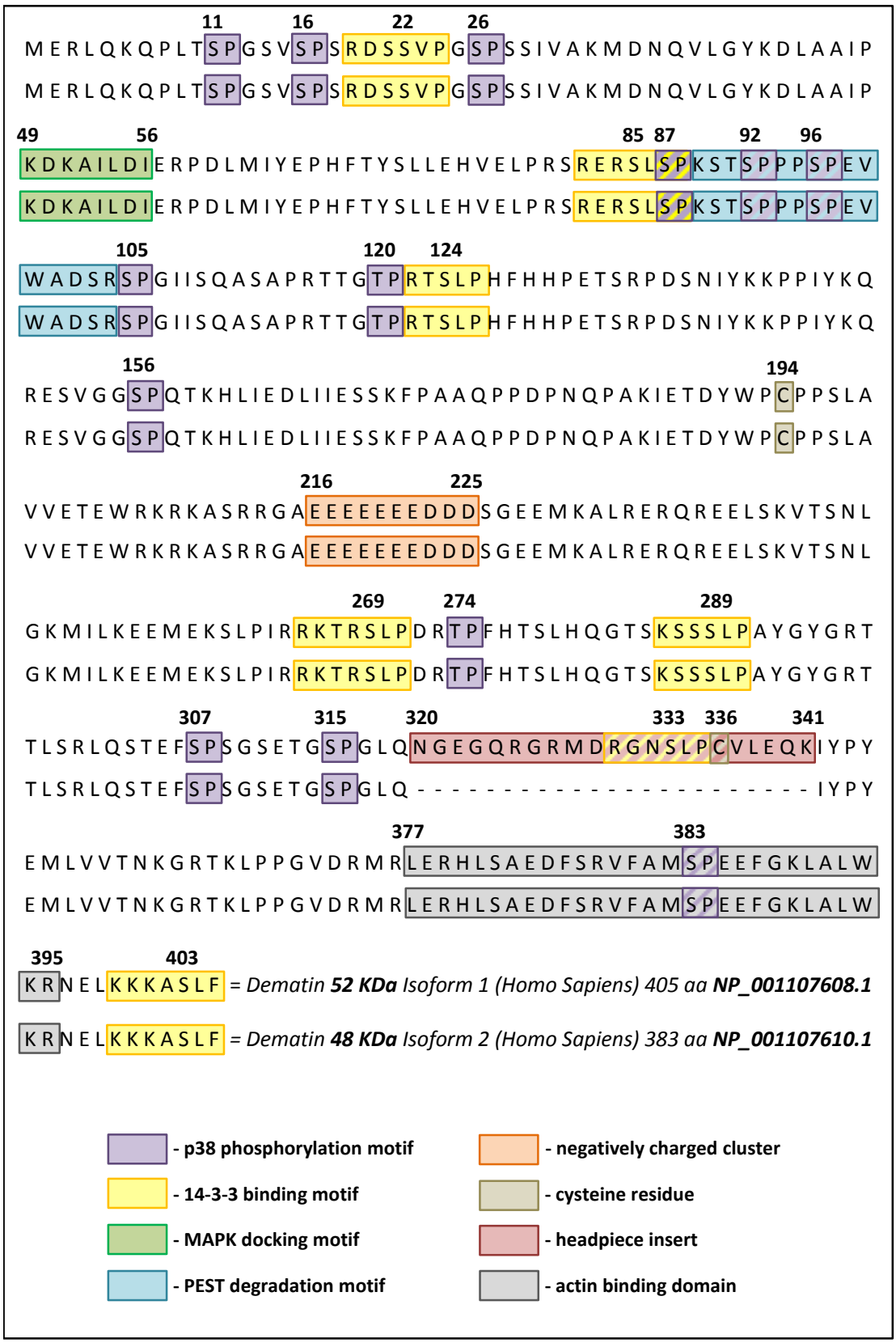

Figure 1.2: Notable features of the human dematin sequence

Identified sequence motifs in the 48 KDa and 52 KDa isoforms of human dematin.

1.1.1.5 Actin binding domains

Regulation of the actin cytoskeleton is coordinated by a large group of proteins capable of binding to actin and dynamically modulating its function. Dematin contains two actin binding sequences, one in the HP domain (Figure 1.2; grey box) and a second undefined site in the core domain (Azim *et al.*, 1995).

1.1.1.6 Cysteine residues

Both the 48 and 52 KDa isoforms of dematin contain a cysteine residue at Cys^{194}, and the 52 KDa variant has an additional site in the HP-insert at Cys^{336} (Figure 1.2; brown boxes). These residues have been implicated in the potential trimerisation of dematin through the formation of disulphide bonds between monomers (Azim *et al.*, 1995).

1.1.1.7 Cluster of negatively charged residues

Dematin contains a cluster of ten negatively charged residues ^{216}EEEEEEEDDD^{225} (Figure 1.2; orange box). This sequence is found in protein which associate with the cell nucleus (Rana *et al.*, 1993).

1.1.2 Secondary structure of dematin

The large N-terminal core region of dematin displays a natively unfolded structure, consistent with the high proline percentage of 10.7 % (double the average value of 5.2 % (Doolittle, 1989)), and any alpha-helical motifs present can be attributed to the folding of the HP region (Chen *et al.*, 2009). The core region also contains a large proportion of charged residues (128 / 405 in the 52 KDa isoform), a property shared by many intrinsically disordered proteins. Although disordered, the dematin core domain does not undergo fully unrestrained motions, and is instead thought to exist in a number of states that lack significant secondary structure but still possess some form of order. This theory is supported by the extremely high (> 94%) sequence conservation between dematin homologues in mammalian species (Chen *et al.*, 2013). The core domain of dematin also shares around 36% sequence homology with another actin binding protein called limatin (Kim *et al.*, 1997).

In contrast to the core domain, the C-terminal HP of dematin is highly ordered. The HP of the 48 KDa isoform shows a fully folded conformation (Figure 1.3A), whereas the extra 22-amino acid insertion in the longer isoform is mostly unfolded (Frank *et al.*, 2004). The dematin HP structure is similar to that of villin, with an N-terminal sub-domain of loops and turns, and 3 alpha helices in the C-terminal sub-domain (Frank *et al.*, 2004; Jiang & McKnight, 2006).

Folding of the dematin HP appears to be independent of the core domain. Overlaying the ^{1}H-^{15}N HSQC NMR spectrum for full-length dematin with that of just the HP showed that the two correlate (Chen *et al.*, 2009), confirming that the dematin HP is independently folded. The only exception to this was in the extreme N-terminal linker region where the two domains join, at which point a slight change in conformation was observed. This independent folding mechanism is also seen with the HP of villin (Smirnov *et al.*, 2007). The NMR spectrum for recombinant dematin shows narrow resonances and no chemical shift, indicating that the core and HP domains don't interact (Chen *et al.*, 2009).

Solving the 3D structure of the dematin HP using multidimensional NMR methods revealed that dematin has several novel characteristics compared to villin (Frank *et al.*, 2004). In dematin the HP has a buried cluster of charged residues: a salt bridge cluster of Glu^{39} [Glu^{368}], Arg^{66} [Arg^{395}], and Lys^{70} [Lys^{399}], and c-terminal carboxylate of Phe^{76} [Phe^{405}]. Villin has only a single buried salt bridge that holds N- and C-terminal domains together. Compared to villin, the variable loop (found in all HP domains; Figure 1.3A) of dematin can undergo a far greater range of movements than the rest of the protein. The conformational change in the V-loop is induced by phosphorylation of Ser^{74} [Ser^{403}] in the HP by PKA (Frank et al., 2004).

In order to further investigate the conformational change that occurs in dematin upon phosphorylation of the HP, Jiang and McKnight (2006) created a phospho-mimicking form of the HP with Ser^{74} [Ser^{403}] mutated to Glu^{74} (DHP_S74E). Initial NMR analysis confirmed that the conformation adopted by this construct closely resembled that of the phosphorylated wild-type HP. The NMR spectrum indicates

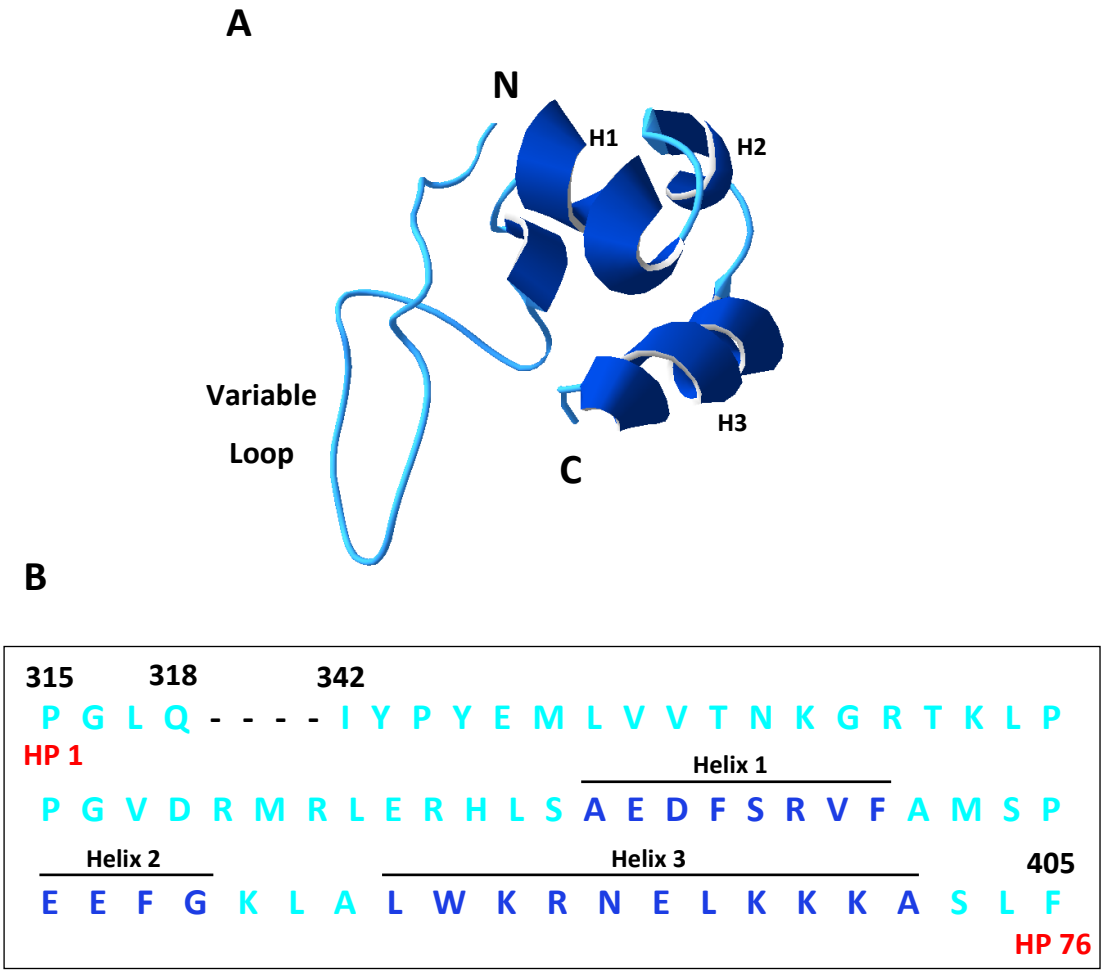

Figure 1.3: NMR structure of the headpiece domain of 48 KDa human dematin

(A) A ribbon representation of the minimised average solution NMR structure of the headpiece domain of the 48 KDa isoform of dematin. The predicted α-helices are shown in dark blue, with the linker regions in light blue. (B) The amino acid sequence of the 48 KDa dematin headpiece, colour coded to match the NMR structure. The sequence is numbered in black according to the longer 52 KDa isoform, with the dashed region indicating the 22-amino acid insert not present in this shorter variant. The numbers in red refer to the headpiece specific numbering that is often quoted in the literature. (The NMR structure was obtained from RCSB Protein Data Bank; structure of the human dematin headpiece domain, 1QZP. The image was created using Swiss-PDB viewer 4.1.0).

only very small changes in localised structure of the C-terminal region of DHP_S74E, with the majority of residues forming the hydrophobic core remaining buried. The most notable change is an increased distance between residues Arg^{66} [Arg^{395}], and Glu^{39} [Glu^{368}], which would prevent the formation of a salt bridge, and could potentially explain the reduction in actin-binding that has previously been reported upon phosphorylation of Ser^{74} [Ser^{403}] (Azim *et al.*, 1995). In contrast, the structure of the N-terminal region of DHP_S74E from residues 9-42 [346-379] altered dramatically. This lead to the hypothesis that the phosphate group attracts Lys^{24} [Lys^{353}] in the V-loop and this electrostatic interaction causes the N-terminal loop to move closer to the C-terminal helix, forming a structure that allows stabilising hydrophobic interactions to occur (Jiang & McKnight, 2006).

The V-loop region of DHP_S74E is much better resolved than the wild-type HP, indicating a greater number of constraints on the structure, and is located in closer proximity to the C-terminus. The altered conformation of the V-loop could potentially alter the relative orientations of the dematin core and HP domains making the two sites unfavourable for bundling. Alternatively if the two regions are connected by a flexible loop, then phosphorylation of the HP could lock the structure into a specific position relative to the core that is unfavourable. A selection of complimentary NMR approaches were employed to compare the backbone dynamics of DHP and DHP_S74E in more detail (Vugmeyster & McKnight, 2009). These results correlated with those seen previously, and suggested that the additional salt bridge formed between the core and HP domains is likely to be responsible for the reduction in mobility.

1.1.3 Oligomerisation of dematin

Rotary shadowed electron micrograph (EM) images of dematin revealed what appeared to be tri-lobed structures (Husain-Chishti *et al.*, 1989; Husain-Chishti *et al.*, 1988; Siegel & Branton, 1985). This correlated with the calculated molecular weight of the complex in solution of approximately 145 KDa. Analysis of these protein complexes revealed a 48:52 KDa isoform ratio of 2:1 (Husain-Chishti *et al.*, 1989). This led to the proposed model of dematin forming a functional trimer in vivo,

composed of two 48 KDa and one 52 KDa subunits (Figure 1.4). The formation of this structure was proposed to be mediated through interactions between cysteine residues, of which there are four in total in such a trimeric configuration; at Cys^{194} in each of the three core domains, and at Cys^{336} in the HP insert of the 52 KDa protomer (Azim *et al.*, 1995).

Not all data supports the trimerisation model of dematin, however. Recent experiments using analytical ultracentrifugation suggest that dematin actually exists in a monomeric state. Sedimentation velocity data indicated that dematin was present in a single oligomeric state, which was most consistent with the protein being monomeric. Further sedimentation equilibrium experiments, capable of detecting weak oligomeric interactions, were again unable to detect the presence of higher order structures (Chen *et al.*, 2013). It is currently unclear whether the trimerisation of dematin detected in the EM imaging is an artefact due to the experimental conditions used (Chen *et al.*, 2013), or whether dematin can form oligomeric structures in vivo. Interestingly it has recently been demonstrated that platelets predominantly express the 52 KDa isoform of dematin with very little of the 48 KDa isoform (Wieschhaus *et al.*, 2012), suggesting that the trimerisation mechanism may not be equally relevant in all cell types.

1.1.4 Dematin as an actin binding and bundling protein

The dematin HP shares sequence homology with the actin binding protein villin, which is found in epithelial brush-borders. Villin and dematin share common HP features but have unique core domains (Azim *et al.*, 1995). The actin binding and bundling properties of dematin have been well documented. Both isoforms contain two actin binding motifs, one at the extreme C-terminus of the protein, and the other in the core domain. The independent motions of the core and HP regions allows each of the actin binding sites within a dematin monomer to interact with separate AFs, forming parallel arrays of actin bundles (Chen *et al.*, 2013).

Despite the high structural homology with other villin-type HP proteins, the dematin HP is unique in its ability to be phosphorylated in vivo. Phosphorylation of

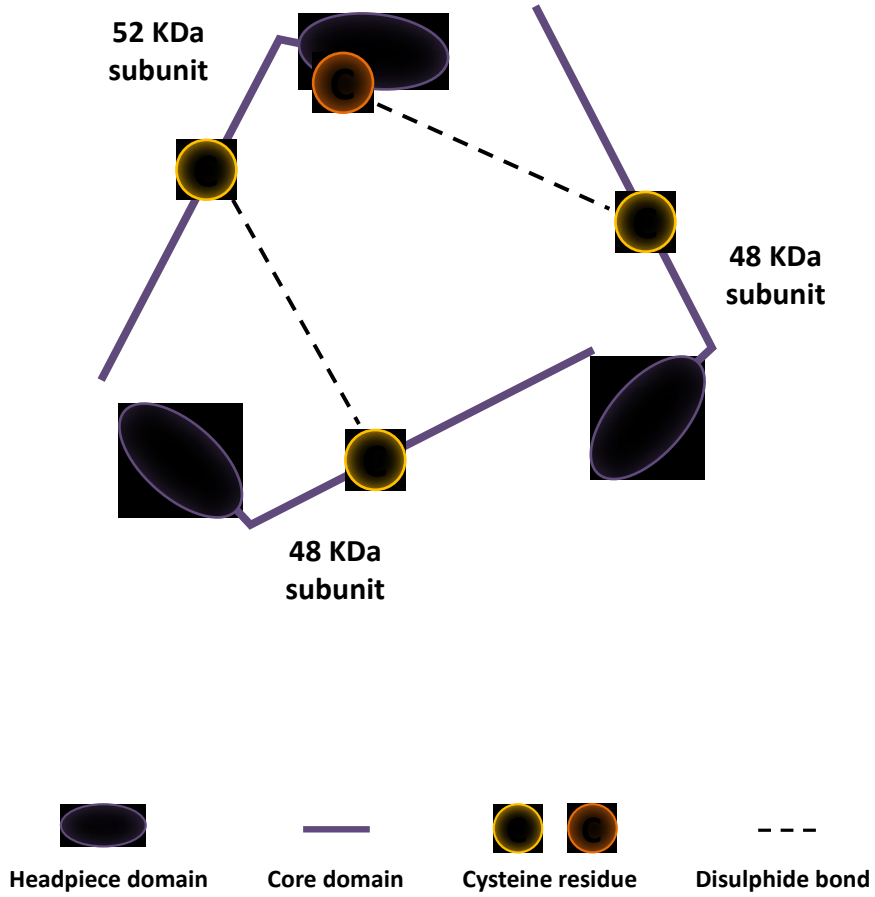

Figure 1.4: Proposed model of the trimerisation of dematin

Some evidence suggests that dematin may form a trimeric structure in vivo, consisting of two 48 KDa and one 52 KDa subunits. This model was proposed based upon rotary shadowed electron micrograph (EM) images that appear to show tri-lobed structures and the calculated molecular weight of the complex in solution of approximately 145 KDa. Oligomerisation is potentially mediated through interactions between cysteine residues. Each protomer contains a cysteine residue within the core domain, with an additional site in the headpiece of the 52 KDa variant.

dematin at Ser^{381} [Ser^{403}] by cAMP-dependent protein kinase induces a conformational change in the protein that controls its actin-bundling ability (Chen *et al.*, 2013; Frank *et al.*, 2004; Jiang & McKnight, 2006). In the phosphorylated state F-actin bundling is inhibited, with this function resuming rapidly upon dephosphorylation (Husain-Chishti *et al.*, 1988). Dematin is able to bind to actin in both the phosphorylated and un-phosphorylated states (Azim *et al.*, 1995; Chen *et al.*, 2013), however the binding affinity may be lower when phosphorylated (Vardar *et al.*, 2002). Recent NMR analysis of this process indicates that the inhibition of bundling is due to the normally independent core and HP regions coming into close proximity with one another (Chen *et al.*, 2013). Phosphorylation of the HP increases its affinity for the core domain, which sterically hinders one of the two actin binding sites. This leaves each monomer capable of binding to just a single AF, therefore losing its ability to bundle filaments together.

1.1.5 Characterised functions of dematin in erythrocytes

Dematin was first identified and characterised in human erythrocytes, where it is localised to spectrin-actin junctions (Husain-Chishti *et al.*, 1989; Husain-Chishti *et al.*, 1988; Siegel & Branton, 1985). This network of proteins is responsible for stabilising the cell and controlling morphological changes. The junctional complex assembly is coordinated around tetramers of spectrin and actin dimers, with which a number of other proteins, including tropomyosin, adducin, and protein 4.1 associate (Bennett, 1989; Mohandas & An, 2006).

A connection between the spectrin-actin network and the cell membrane occurs via two mechanisms: protein 4.1R and p55 associating with glycophorin C in the membrane, and ankyrin binding to band 3 (Bennett, 1989; Reid *et al.*, 1990). It was previously thought that the 4.1R connection was wholly responsible for maintaining erythrocyte structural integrity; however recent findings have indicated that this function may be shared across additional cytoskeletal proteins (Anong *et al.*, 2009; Chen *et al.*, 2007; Khan *et al.*, 2008). Confirmation of the presence of dematin in this region (Derick *et al.*, 1992), in addition to biochemical analysis of binding characteristics, led to the current model in which dematin acts as an additional

adaptor protein, binding to the transmembrane glucose-transporter 1 (GLUT1) and stabilising the cell (Figure 1.5) (Khan *et al.*, 2008). Knocking out the dematin HP domain (HPKO) in mice is non-lethal, but erythrocytes become fragile and more deformable, and as a result animals display compensatory anaemia (Chen *et al.*, 2007; Khanna *et al.*, 2002). As the primary sequences of human and mouse dematin share 95% homology (Azim *et al.*, 1999), phenotypic and functional data obtained from mouse knock out studies are of significant potential relevance when looking at the function of human dematin.

1.1.6 Characterised functions of dematin in non-erythroid cells

Dematin expression has now been demonstrated in a broad range of non-erythroid human tissues including the brain, heart, lungs, kidneys, testis, endothelial and epithelial cells, adipose tissue, and skeletal muscle (Kim *et al.*, 1998; Mohseni & Chishti, 2008b; Rana *et al.*, 1993). This suggests that dematin may have far more widespread functions than those that have been defined in erythrocytes. Several non-erythroid functions of dematin have been characterised, but there is still relatively limited understanding of these additional roles.

1.1.6.1 The involvement of dematin in wound healing

HPKO experiments have shown that loss of expression of the dematin HP domain, which leads to inhibition of actin binding, results in abnormal phenotypes in mouse embryonic fibroblasts. Cells displayed altered morphological, motile, and adhesive properties, resulting in a significantly decreased efficiency of wound healing. This was attributed to dematin acting as a negative regulator of the RhoA pathway, which was independent of Focal Adhesion Kinase (FAK) activation (Mohseni & Chishti, 2008a; Mohseni & Chishti, 2009). The current data is insufficient to precisely determine the mechanism by which dematin suppresses RhoA activation, however several plausible models have been proposed. Firstly, dematin may bind to guanine nucleotide exchange factor (GEF) thereby preventing it from associating with, and activating, RhoA. Alternatively dematin may act as a guanidine nucleotide dissociation inhibitor (GDI), or may bind to another GDI, tethering RhoA and again preventing activation (Mohseni & Chishti, 2008a).

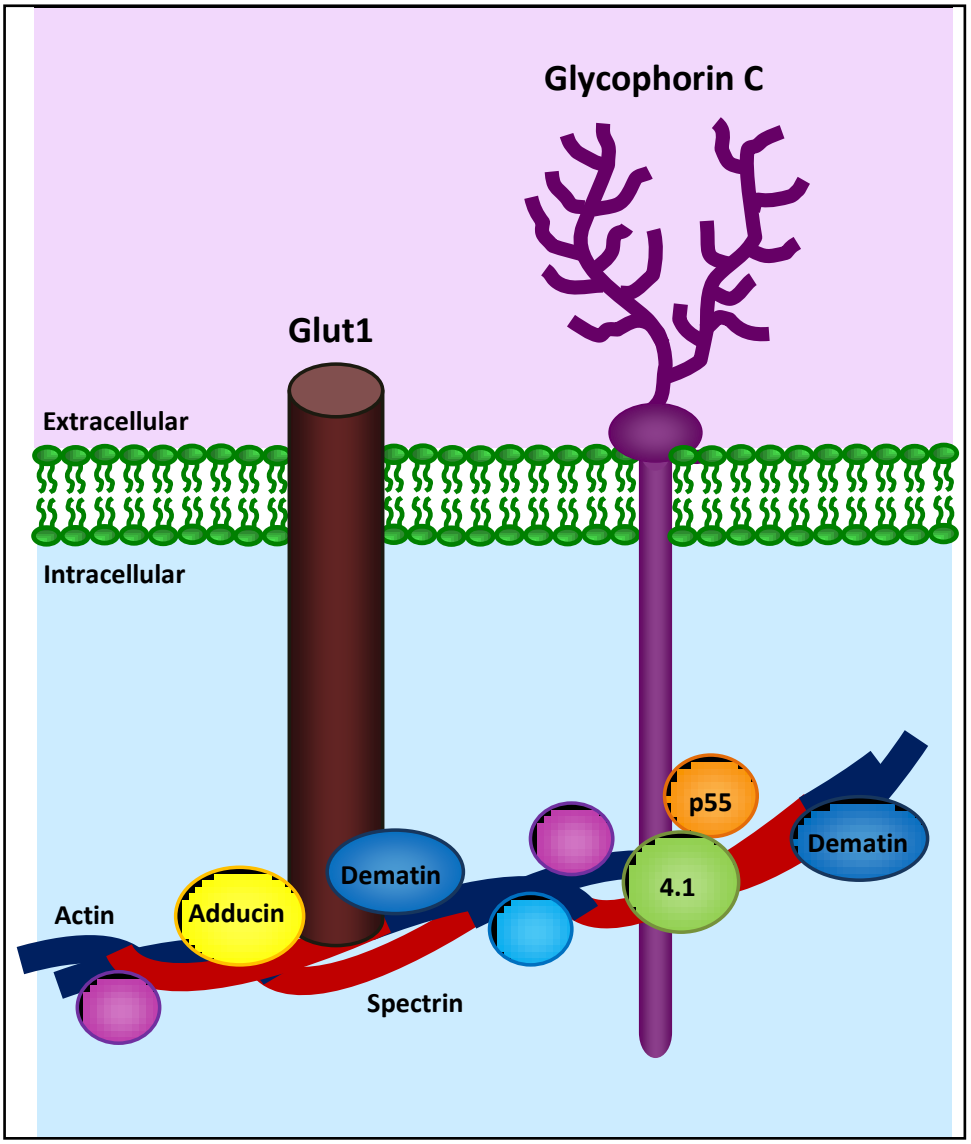

Figure 1.5: Dematin is located in the erythrocyte junctional complex

In erythrocytes dematin is located at the spectrin-actin network and has been shown to be important for mechanical stability. Previous research suggested that the link between the actin cytoskeleton and the cell membrane was coordinated by the interaction of glycophorin C in the membrane with p55 and protein 4.1. It has now been demonstrated that dematin is involved in an extra stabilising linkage, through direct binding to the basal glucose transporter GLUT1. Mice lacking the dematin headpiece therefore display erythrocyte spherocytosis and compensatory anaemia.

The delayed wound healing phenotype was further investigated through characterisation of the changes that occur in platelets of dematin HPKO mice (Wieschhaus *et al.*, 2012). Morphologically, HPKO platelets were comparable to wild-type and were of equal size and quantity; however they displayed reductions in adhesion and spreading, impaired aggregation resulting in poor clot retraction, and defects in granule secretion. Loss of dematin expression resulted in reduced expression of human inositol 1,4,5-triphosphate 3-kinase form B (IP3KB), an important regulator of calcium homeostasis, at the cell membrane while cytosolic concentrations increased. It remains to be determined whether this regulation of intracellular calcium by dematin is relevant in other cells types.

1.1.6.2 The role of dematin as a tumour suppressor

In humans dematin has been mapped to chromosome 8 at locus 8p21.1 (Azim *et al.*, 1995), a region frequently affected by oncogenic deletions (Huang *et al.*, 1996; Vocke *et al.*, 1996). Other actin-binding proteins including tropomyosin, gelsolin, and vinculin, have been identified as having roles in tumour suppression in epithelial cells (Hall, 2009). It was therefore proposed that dematin may have similar effects on cell proliferation through regulation of its actin-bundling ability (Kim *et al.*, 1998). Deletions in this region are seen particularly frequently in prostate cancer, and the loss of one dematin allele was observed in the majority of 8p21-linked prostate tumours (Kim *et al.*, 1998). Reduced dematin expression is therefore potentially linked to tumour progression and alterations in cell morphology, adding to increasing evidence that cytoskeletal proteins can function as tumour suppressors. The prostate adenocarcinoma cell line PC-3 has a single allele deletion of dematin. Overexpression of dematin in the PC-3 tumorigenic cell line changes cell morphology to a more typical polarised epithelial phenotype. Conversely overexpression of dominant negative dematin mutants compromises the normal morphology of 3T3 fibroblasts (Lutchman *et al.*, 1999).

1.1.6.3 Other non-erythroid functions of dematin

Dematin has been proposed as a candidate gene for Marie Unna Hereditary Hypotrichiosis (MUHH). Patients suffering from MUHH are born with hair of normal

to sparse density, but this gradually becomes wiry and eventually is lost permanently. Attempts to locate the gene responsible for MUHH pinpointed chromosomal region 8p21.2, which lies next to the dematin locus, as one region of interest. The involvement of dematin in this disorder was further supported by phenotypic observations in dematin HPKO mice, approximately a third of which display facial hair-loss as they age, with some losing all hair from their dorsal region. Skin samples from these mice showed decreased expression of the dematin core domain in the dermis, hypodermis, and skeletal muscle. This effect is not seen in heterozygous HPKO animals (Mohseni & Chishti, 2008b).

The majority of functions that have been investigated to date involve the HP of dematin, with relatively little still known about the function of the core domain. The lack of secondary structure led to one hypothesis that the region may act as a scaffold on which other junctional complex proteins can associate, however this has yet to be confirmed (Chen *et al.*, 2009).

Given the widespread tissue expression profiles, and limited understanding of the regulation of dematin, it is likely that there are numerous functions that have yet to be discovered. Dematin is expressed in skeletal muscle and adipose tissue, the two main metabolic tissues of the body, and yet there has been no specific research into its function in either of these systems. This thesis will focus on the function and regulation of dematin in skeletal muscle, with particular emphasis on the potential phospho-regulation of dematin by the p38 MAPK, and interaction with the adaptor protein 14-3-3. The effects of these regulatory mechanisms on the actin-binding and bundling properties, and stability, of dematin will be determined. The background to these areas is covered in sections 1.2-1.5.

1.2 The actin cytoskeleton

The actin cytoskeleton is a dynamic three-dimensional structure found in the cytoplasm of all eukaryotic cells. It plays essential roles in a diverse range of cellular processes, including the control of cell morphology and motility, and the

endocytosis and intracellular trafficking of proteins (Pollard & Cooper, 2009). In order to meet the continually changing demands of the cell, AFs form highly dynamic structures which are regulated by the actions of numerous actin-binding proteins (ABPs) (Blanchoin *et al.*, 2014).

1.2.1 Actin

Actin is a 42 KDa protein that comprises 10% of the total protein mass found in muscle, and approximately 1-5% in non-muscle cells. There are three main isotypes of actin in mammals: α-actin, β-actin, and γ-actin. These display greater than 90% sequence homology at the amino acid level, with the majority of variation in the N-terminal 30 residues (Herman, 1993). Three isoforms of α-actin exist, which are expressed in cardiac, skeletal and smooth muscle. The β-actin and γ-actin isoforms are expressed in both muscle and non-muscle cells (Perrin & Ervasti, 2010). Actin exists in two structural forms, monomeric or globular-actin (G-actin), and polymerised filamentous-actin (F-actin). Actin monomers are composed of a single polypeptide chain of 375 residues, which folds to form a two-lobed structure with a central cleft in which ATP and Mg^{2+} bind. A flexible hinge region connects the two lobes, allowing them to rotate relative to one another (Otterbein *et al.*, 2001).

1.2.2 Actin filaments

Monomers of G-actin are polymerised into F-actin chains, forming two right-handed long-pitch helices (Holmes *et al.*, 1990). Polymerisation begins with an initial activation phase where G-actin undergoes a conformational change to correctly align monomers for incorporation into a polymer; the two lobes of each actin monomer rotate approximately 20° relative to one another, creating a flatter molecule (Oda *et al.*, 2009). Following this is the nucleation phase. This involves the initial polymerisation of these conformationally altered G-actin monomers, a process that is energetically unfavourable until three monomers have associated. Once a sufficient number of these unstable dimers and trimers have accumulated, rapid polymerisation occurs (Wegner & Engel, 1975).

AFs are polar, with a fast growing barbed (+) end and a slow growing pointed (-) end (Pollard, 1986). Elongation of AFs involves the preferential addition of ATP-actin monomers to the + end of the filament, into the exposed ATP binding cleft of the neighbouring monomer (Figure 1.6). Actin has intrinsic ATPase activity and irreversible hydrolysis of the bound ATP leads to de-stabilisation of the AF, resulting in disassembly of ADP-actin monomers and phosphate from the - end. The available pool of ATP-actin is then restored through nucleotide exchange, ready for incorporation into a new polymer (Figure 1.6). Polymerisation rates are regulated by the availability of ATP-actin monomers; at high concentrations monomers are added to both ends of the filament, while at intermediate concentrations AFs extend only from the + end. At low concentrations elongation does not occur (Wegner & Engel, 1975). Cellular concentrations of actin monomers can reach 300 µM, and under these conditions 3000 subunits can be incorporated into the barbed end of the filament every second. At this speed filaments of 10 µm in length can be synthesised in less than two seconds, facilitating rapid remodelling of the cellular architecture (Pollard et al., 2000).

1.2.3 Regulation of actin polymerisation by actin-binding proteins

In order to meet the demands of the cell, the actin cytoskeleton must be highly dynamic and capable of continual and rapid remodelling in response to spatial and temporal requirements. AFs are regulated by signals from both within the cell and from the extracellular environment, leading to changes in the local organisation of the actin network (Blanchoin *et al.*, 2014). Control of actin dynamics is achieved through the coordinated actions of a set of structurally and functionally diverse ABPs. To date more than 150 proteins containing actin-binding domains have been identified, and these can be categorised based on the regulatory effect they have on actin (dos Remedios *et al.*, 2003).

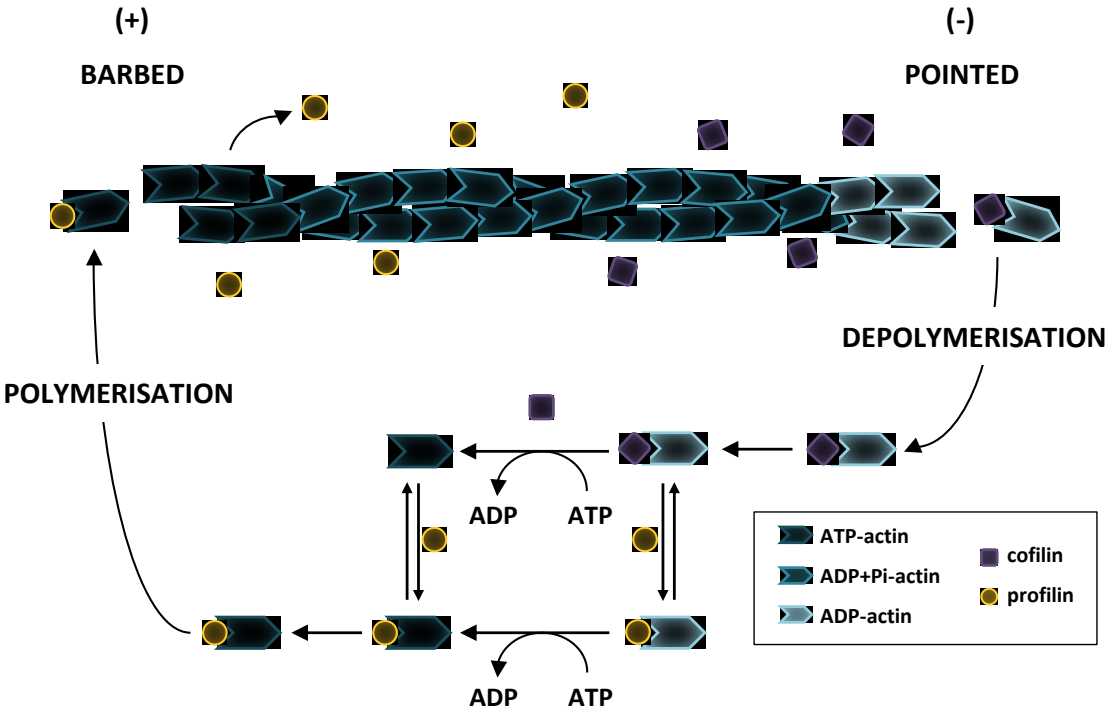

Figure 1.6: Polymerisation of monomeric G-actin to filamentous F-actin

Actin is found in vivo in two states, monomers of globular G-actin and polymers of these monomers known as filamentous or F-actin. Polymerised actin forms a polar structure, with a barbed (+) end where actin monomers are preferentially added and a pointed (-) end where depolymerisation occurs. Before incorporation into a polymer, G-actin monomers undergo a conformational change resulting in flatter molecules that align more readily. Actin polymerisation is facilitated by proteins such as profilin that sequester ATP-actin monomers and deliver them to the barbed end of the filament. Following incorporation into the polymer, the intrinsic ATPase activity of F-actin hydrolyses ATP to ADP resulting in ADP+Pi-actin. Upon cofilin-mediated depolymerisation at the pointed filament end, ADP-actin monomers undergo nucleotide hydrolysis, restoring the pool of ATP-actin available for the polymerisation of new filaments.

1.2.3.1 Nucleation promoting factors

As the initial polymerisation of monomers is energetically unfavourable, nucleating factors operate to overcome this lag-phase and enhance polymerisation rates. These include the Arp2/3 complex which is able to initiate the formation of a new AF protruding from an existing polymer, creating branched structures (Figure 1.7A) (Goley & Welch, 2006).

1.2.3.2 Monomer binding proteins

These proteins are involved in regulating the availability of actin monomers for incorporation into filaments. ABPs such as cofilin and twinfilin bind to ADP-F-actin at the pointed end of a filament and enhance the dissociation of ADP-actin monomers (Carlier *et al.*, 1997). Profilin then buffers these actin monomers and facilitates the nucleotide exchange of ADP for ATP. ATP-actin monomers are delivered exclusively to the barbed end of the AF ready for re-incorporation, enhancing the polarity of the growing structure (Pring *et al.*, 1992). Profilin also inhibits the formation of actin dimers and trimers, meaning that de novo synthesis of AFs can only occur in conjunction with nucleation-promoting factors (Pollard *et al.*, 2000).

1.2.3.3 Capping proteins

Capping proteins either stabilise AFs or promote filament disassembly. Gelsolin and tensin form a stabilising cap on the barbed end of AFs, preventing the addition of further actin monomers, whereas others such as emerin bind to the pointed end of the filament and inhibit depolymerisation (Figure 1.7A) (Pollard *et al.*, 2000).

1.2.3.4 Severing proteins

The formation of new polymers is enhanced by severing proteins which bind to existing filaments and cut them in two, allowing polymerisation to continue from the two barbed ends. These include cofilin, which binds to actin and perturbs the local structure, leading to severing of the filament at a neighbouring site where this force is felt most strongly (Figure 1.7A) (Pavlov *et al.*, 2007).

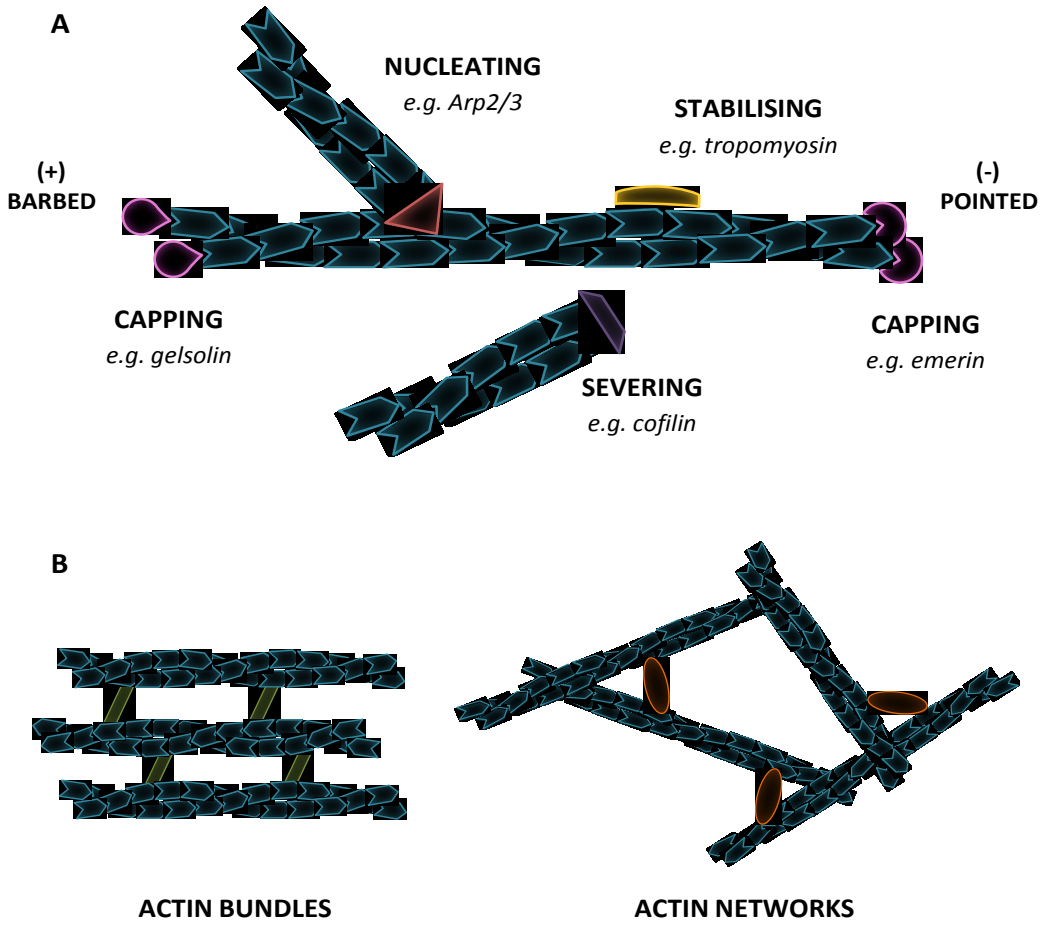

Figure 1.7: The regulation of actin by actin binding proteins

Regulation of the actin cytoskeleton relies on the coordinated actions of a large family of actin binding proteins. These diverse proteins each contain at least one actin binding motif, and perform functions that determine the nature of the actin structures that are formed. (A) Filamentous actin structures are stabilised by proteins such as the tropomyosin family that act to inhibit depolymerisation. Nucleation of new polymers from the sides of existing filaments is catalysed by the Arp2/3 complex, which overcomes the lag phase of de-novo polymerisation. Enhanced polymerisation rates may also be achieved through the severing of an existing polymer by proteins such as cofilin, to produce two barbed ends at which polymerisation can occur. Capping proteins such as gelsolin and emerin bind to the barbed and pointed ends of actin filaments, inhibiting polymerisation and depolymerisation respectively. (B) Actin polymers form two main types of higher order structure: actin bundles and actin networks. These structures are orchestrated by bundling and crosslinking proteins which are capable of simultaneously binding to two actin filaments, either monomers with two actin binding sites, or multimeric complexes of proteins. Actin bundles are either parallel or anti-parallel alignments of actin filaments held in a rigid orientation, whereas networks are a looser orthogonal arrangement of polymers.

1.2.3.5 Stabilising proteins

Proteins of the tropomyosin family bind along the length of AFs and have a stabilising role, preventing spontaneous depolymerisation. Some family members, including tropomyosin itself, also inhibit the actions of filament severing proteins as an additional method of increasing filament stability (Figure 1.7A) (Khaitlina *et al.*, 2013).

1.2.4 Higher-order actin structures

AFs in vivo organise themselves into two main types of structures: bundles and networks (Figure 1.7B). Formation of these higher-order structures is essential for cellular function, and is facilitated by two classes of ABPs - those that bundle F-actin, and those that crosslink F-actin. These ABPs either contain two distinct actin-binding domains, or form multimeric complexes where each monomer contains a single binding domain, allowing them to simultaneously bind to two different AFs. Such proteins play no role in the polymerisation of actin, but instead act upon pre-formed filaments (Blanchoin *et al.*, 2014).

1.2.4.1 Actin bundles

Actin bundles are composed of AFs aligned either parallel or anti-parallel (Figure 1.7B). Bundles can be either densely or loosely packed together, a property that is determined by the bundling protein involved. Proteins such as fimbrin, which contain two actin binding domains in closely proximity, aid the formation of dense, rigidly structured, bundles (Lieleg *et al.*, 2009). Conversely the loosely associated anti-parallel bundles in actin stress fibres are created by α-actinin, which forms a dimeric complex with an intermediate spacer region (Courson & Rock, 2010). Parallel actin bundles are found in filopodia and microvilli, while anti-parallel bundles are required for cytokinesis and cell adhesion (Blanchoin *et al.*, 2014).

1.2.4.2 Actin networks

The actin in networks is loosely packed and less organised than in bundles, with filaments lying perpendicular to one another (Figure 1.7B). Network formation is

coordinated by crosslinking proteins in which the two actin-binding domains are orientated at greater distances, such as in dimeric filamin or tetrameric spectrin, allowing for the formation of looser, less organised structures (Feng & Walsh, 2004). Planar networks are associated with the plasma membrane and form 2D web-like structures, whereas the cytosol gains gel-like qualities from 3D networks. In some instances, networks can form denser meshes, coordinated by smaller monomeric proteins such as fascin (Courson & Rock, 2010). Actin networks are important in controlling cell shape and maintaining mechanical integrity (Blanchoin *et al.*, 2014).

1.2.5 Functions of the actin cytoskeleton

The actin cytoskeleton has been shown to be involved in a wide array of important cellular functions. F-actin is essential in numerous processes including maintaining cell morphology, endocytosis and intracellular trafficking, cell motility, and cytokinesis (Pollard & Cooper, 2009).

1.2.5.1 Endocytosis and intracellular trafficking

F-actin assembles at the cell membrane at sites of endocytosis, forming structures known as actin patches. These patches are involved in the latter stages of endocytotic vesicle formation, and also provide the force required to deform the membrane and internalise the vesicle (Kaksonen *et al.*, 2006). Actin is essential for scission of the vesicle from the membrane, with filaments orientating themselves with all of the barbed ends around the neck of partially invaginated vesicles to constrict the membrane (Collins *et al.*, 2011). As the vesicle moves into the cytoplasm the AFs rapidly depolymerise (Kaksonen *et al.*, 2005).

1.2.5.2 Cell contractility and motility

Cell motility is dependent upon the actin cytoskeleton. This movement is coordinated by a dense branched network of short AFs under the membrane of the leading edge of the cell, which polymerise in the direction of migration (Pollard & Cooper, 2009). This locomotion is physiologically important during development, for example in the migration of neurons from the neural crest to the intestine

(Anderson *et al.*, 2006). Immune cells also employ this mechanism in the search for pathogens. Actin-mediated motility is also involved in pathological processes. Metastatic cancer cells employ actin bundles to generate protrusions with sufficient mechanical force to migrate through the extracellular matrix and invade surrounding tissues (Stevenson *et al.*, 2012).

1.2.5.3 Cytokinesis

The final stage of cytokinesis requires the physical separation of a dividing cell into two distinct daughter cells. This process involves a contractile ring of AFs, which needs to be perfectly positioned to bisect the anaphase spindle along a plane with sister chromosomes segregated on either side (Pollard, 2010). Mitotic exit signals then activate cell-cycle kinases which initiate the constriction of the actin ring by myosin II, which results in pinching of the membrane and the formation of a cleavage furrow (Glotzer, 2005). Membrane fusion then occurs to create two daughter cells, and the contractile ring structure rapidly disassembles (Montagnac *et al.*, 2008).

1.3 p38 MAPK

Reversible phosphorylation is an important mechanism for regulating protein function which is involved in a wide variety of cellular processes, and is essential for signal transduction (Ubersax & Ferrell, 2007). The human kinome consists of over 500 protein kinases. Phosphorylation of serine residues accounts for the 86% of phosphorylation reactions, with phosphorylation of threonine and tyrosine comprising the remaining 12% and 2% respectively. These kinases are classified into groups, families, and sub-families based upon their sequence conservation and biochemical function (Manning *et al.*, 2002).

1.3.1 The MAPK family

One well-characterised family of kinases are the MAPKs (Cargnello & Roux, 2011). These are a group of serine / threonine specific kinases that coordinate a range of intracellular functions in response to external stimuli. Four major subfamilies of

mammalian MAPKs have been characterised: the extracellular signal-regulated kinases (ERK) 1/2, ERK5, JUN N-terminal kinases (JNKs) and p38. Each subfamily is activated by specific extracellular stimuli that activate a kinase signalling-cascade, leading ultimately to transcription of target proteins in the nucleus, or regulation of cytosolic constituents (Ashwell, 2006).

Exposure to extracellular activating stimuli initiates a three-tiered downstream MAPK signalling cascade, where a series of phosphorylation reactions sequentially activate a MAPK kinase kinase (MAPKKK), MAPK kinase (MAPKK) and MAPK in turn (Cuadrado & Nebreda, 2010). Between them, the MAPKs regulate a vast array of biological processes, including apoptosis, differentiation, proliferation, and cytoskeletal rearrangement (Figure 1.8). Many of these processes are regulated by multiple MAPKs (Gehart *et al.*, 2010).

1.3.2 p38 MAPK

p38 is a 38 KDa protein involved in the cellular stress response. Four isoforms of p38, each encoded by separate genes, have been identified: p38α, p38β, p38γ, and p38δ. These can be further subdivided into p38α/β and p38δ/γ groupings based upon their sequences, and the observation that only p38α and p38β are susceptible to inhibition by SB203580 and SB202190 (Kuma *et al.*, 2005). Sequence homology at the amino acid level is approximately 74% between α and β, and 63% and 61% between α and γ / δ respectively (Jiang *et al.*, 1996). The p38α and p38β isoforms are fairly ubiquitously expressed, p38γ is found mainly in skeletal muscle and p38δ is expressed in the kidney, pancreas, small intestine and testes (Ono & Han, 2000).

1.3.3 Activation of p38 signalling

Along with the JNK family, p38 is classified as a stress-activated MAPK. Activation of p38 in vivo can occur in response to changes in pH, heatshock, high osmolarity, UV radiation and exposure to inflammatory cytokines or reactive oxygen species (ROS) (Freshney *et al.*, 1994) (Raingeaud *et al.*, 1995). These external stimuli activate receptor tyrosine kinase or G-protein coupled receptors, leading to activation of the

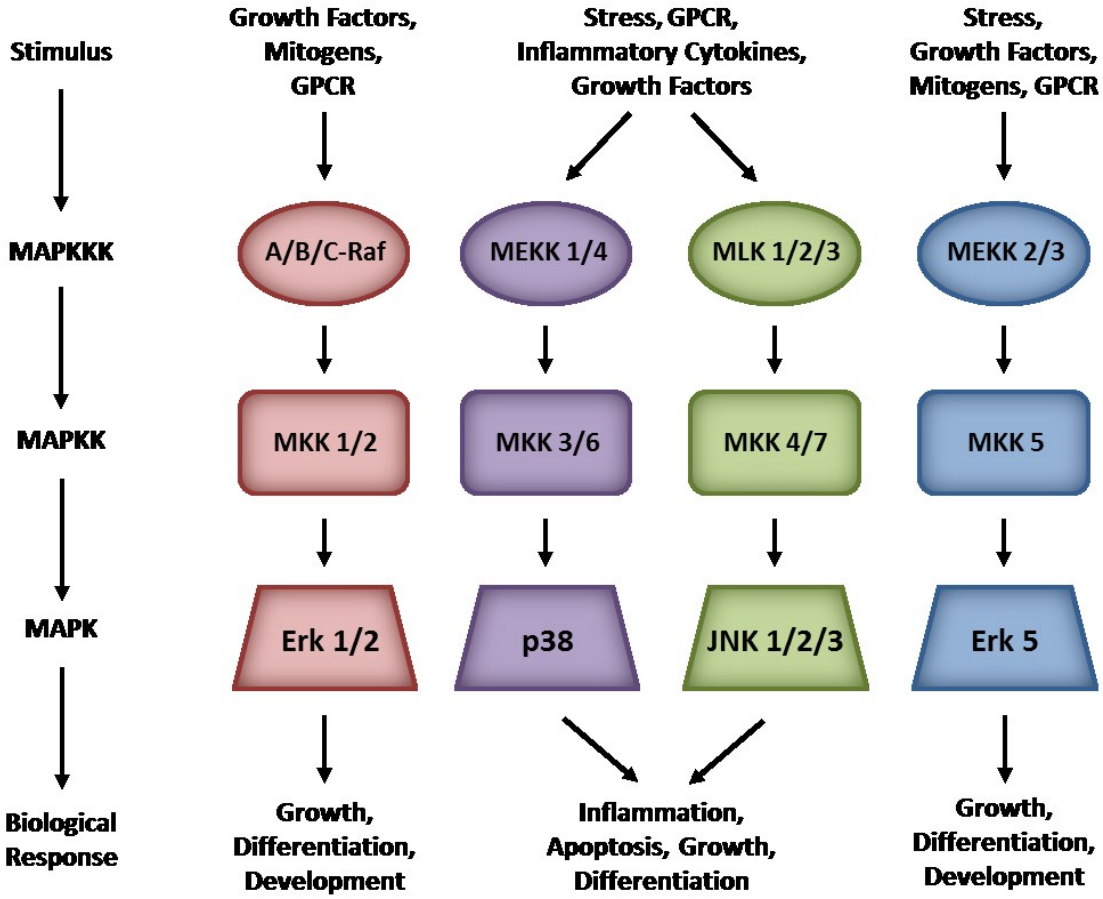

Figure 1.8: A simplified overview of the MAPK family signalling cascades

The MAPK family comprises four major sub-families: ERK 1 and 2, p38, JNKs, and ERK 5. These kinases respond to a variety of extracellular stimuli, which leads to activation of MAPKKKs, which in turn activate MAPKKs, which go on to activate the MAPKs themselves. Activation of MAPKs results in a variety of biological responses, some of which are specific to a particular subfamily whereas others involve multiple MAPK signalling pathways. (ERK; extracellular signal-regulated kinases, GPCR; G-protein coupled receptor, JNK; JUN N-terminal kinases, MAPK; mitogen-activated protein-kinase, MAPKK; mitogen-activated protein-kinase-kinase, MAPKKK; mitogen-activated protein-kinase-kinase-kinase, MEKK; MLK, mixed-lineage kinase, Raf; rapidly accelerated fibrosarcoma).

Rho family of GTP-binding proteins, including Rho, Rit, Rac1, and Cdc42 (Marinissen *et al.*, 2001; Sakabe *et al.*, 2002). These proteins activate an array of MAPKKKs including MEKK (MAPK/ERK kinase kinase) 1-3, ASK1 (apoptosis signal-regulating kinase 1), TAK1 (TGF (transforming growth factor) β-activated kinase 1), and TAO (thousand-and-one amino acid) 1 and 2 (Cheung *et al.*, 2003; Ichijo *et al.*, 1997). These MAPKKKs in turn phosphorylate the highly specific MAPKKs MKK3 and MKK6 through the phosphorylation of two conserved residues in their activation loops (Figure 1.9) (Dérijard *et al.*, 1995; Han *et al.*, 1996).

Activation of p38 results from the phosphorylation of a specific Thr^{180}-Gly-Tyr^{182} motif in the flexible activation loop of subdomain VIII, at both the threonine and tyrosine residues. The p38-specific activators MKK3 or MKK6 mediate this reaction, with the exception of p38β that can only be phosphorylated by MKK6 (Raingeaud *et al.*, 1996). MKK4 may also be capable of activating p38, however this is not specific and is better characterised as an activator of JNK (Dérijard *et al.*, 1995). This dual phosphorylation of Thr^{180} and Tyr^{182} induces a global conformational change in p38, altering the relative positions of the N- and C-terminal domains, and stabilising the activation loop in an open state which enables substrate binding (Bellon *et al.*, 1999; Canagarajah *et al.*, 1997).

Transient activation of p38 in vivo is essential for the fine control of signalling outcomes, and this regulation is primarily controlled through the balance of phosphorylation and dephosphorylation. MAPK phosphatases target the Thr^{180} and Tyr^{182} residues in the activation loop and revert kinases to their inactive state, thereby decreasing signalling through the pathway (Cuadrado & Nebreda, 2010). In mammalian cells the phosphatases PP2A, PP2C, and PTP have been shown to regulate p38 (Takekawa *et al.*, 2000; Takekawa *et al.*, 1998). This dynamic balance between the actions of MKK3 and MKK6 in activating p38, and the counter actions of these phosphatases enables tight control over the regulation of p38, and therefore the activation and function of p38 substrates.

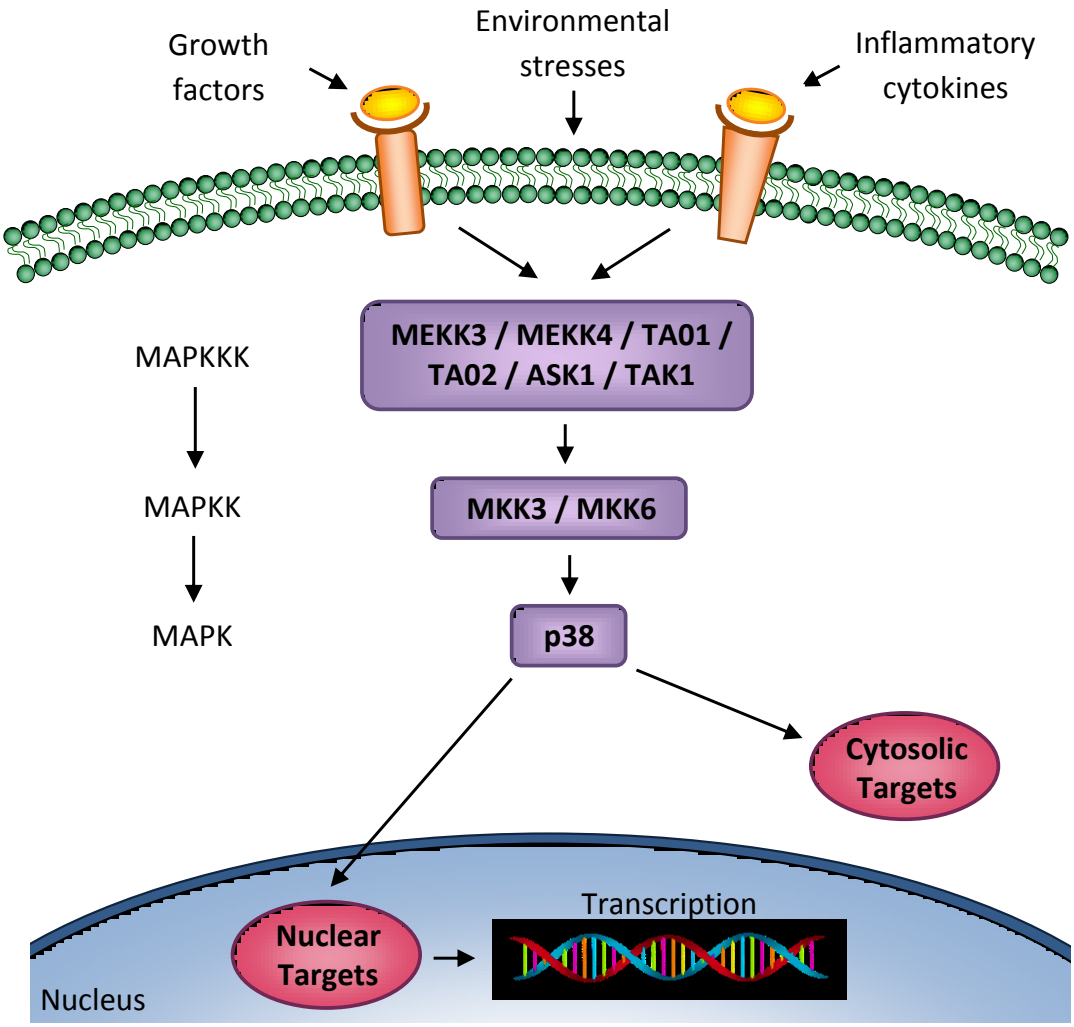

Figure 1.9: The p38 MAPK signalling cascade

Activation of p38 mitogen-activated protein-kinase (MAPK) in vivo can occur in response to growth factors, environmental stresses and inflammatory cytokines. These external stimuli activate receptor tyrosine kinase or G-protein coupled receptors on the cell surface, leading ultimately to activation an intracellular kinase signaling cascade. MAPKKKs phosphorylate the highly specific p38 MAPKKs MKK3 and MKK6 through the phosphorylation of two conserved residues in their activation loops. These then phosphorylate p38 at Thr^{180} and Tyr^{182} inducing and activating conformational change. Targets of p38 phosphorylation include both nuclear transcription factors and cytosolic proteins.

1.3.4 Substrates of the p38 MAPK

MAPKs including p38 phosphorylate substrates at serine or threonine residues that are followed by a small amino acid, preferably a proline. These are often referred to as Ser-Pro / Thr-Pro or SP / TP motifs. Current estimates suggest that MAPKs may each have around 200-300 substrates, although many of these have not been confirmed (Cuadrado & Nebreda, 2010). Known substrates of p38α include other protein kinases, nuclear proteins including transcription factors, and a wide array of cytosolic proteins including cytoskeletal components (Trempolec *et al.*, 2013).

As the presence of SP / TP motifs in proteins is very common, additional mechanisms of substrate recognition are essential for p38 signalling fidelity. Substrates for MAPKs often contain a docking or D-motif, a region consisting of positively charged and hydrophobic residues, often located 10-50 amino acids to the C-terminal side of the phosphorylation sites (Reményi *et al.*, 2005). These domains can be regulated by phosphorylation of either this sequence on the substrate, or the interacting region of p38 itself and act to enhance the efficiency and specificity of kinase substrate interactions. However the presence of a D-motif is not essential for the phosphorylation of a substrate by a MAPK.

1.3.5 Biological function of the p38 MAPK

Activation of p38 has been linked to a number of physiological and pathological conditions. Many of the studies involving gene-targeted mice have focused on the p38α isoform, and it has been demonstrated that the constitutive deletion of either p38α or of MKK3 and MKK6 is embryonically lethal (Adams *et al.*, 2000; Brancho *et al.*, 2003). Activation of the p38 pathway has been implicated in tissue homeostasis, cell migration, and inflammation (Cuenda & Rousseau, 2007).

1.3.5.1 Cell differentiation

Signalling through the p38 pathway is essential for myoblast differentiation into myotubes during embryogenesis, and constitutive overexpression of MKK6 in vitro leads to termination of proliferation and induction of differentiation (Wu *et al.*, 2000). These effects are mediated through control of transcription factors such as

myocyte enhancer factor-2 (MEF-2) (Han *et al.*, 1997), targeting of chromatin-remodelling enzymes to muscle specific loci (Simone *et al.*, 2004), and stabilisation of muscle-specific mRNA turnover (Briata *et al.*, 2005). The differentiation of many other cell types also involves alterations in p38 signalling, including in adipocytes (Aouadi *et al.*, 2006), osteoclasts (Huang *et al.*, 2006), intestinal epithelial cells (Houde *et al.*, 2001), and in neuronal plasticity (Butler *et al.*, 2004).

1.3.5.2 Cell migration

Chemotactic cell migration requires p38 signalling, a function which has been shown to be specific to the p38α isoform (Rousseau *et al.*, 2006). This process has been demonstrated in neutrophils, endothelial cells, epithelial cells, smooth muscle cells and neuronal cells (Cuenda & Rousseau, 2007). The majority of research into the role of p38 in cell migration focuses on the regulation of the actin cytoskeleton. Mice lacking MAPK-activated protein kinase 2 (MAPKAP-K2), which is a direct substrate of p38, display impaired migration of fibroblasts, macrophages, and vascular smooth muscle cells. This has been linked to the MAPKAP-K2 substrate heatshock protein 27 (HSP27), which can block actin polymerisation in its unphosphorylated state through binding to actin capping proteins (Lavoie *et al.*, 1995). LIM domain Kinase 1 (LIMK1), also a substrate of MAPKAP-K2, regulates actin remodelling through inhibition of the actin-depolymerising protein cofilin (Kobayashi *et al.*, 2006). p38 modulated regulation of cell migration and invasion also occurs through inhibition of matrix metalloprotease (MMP) proteins which degrade a range of extracellular matrix proteins (Simon *et al.*, 2001).

1.3.5.3 Inflammation

The p38 pathway has been implicated in a number of inflammatory disorders including Rheumatoid arthritis (Clark & Dean, 2012), Alzheimer's disease (Johnson & Bailey, 2003), and inflammatory bowel conditions (Hollenbach *et al.*, 2004). The production of inflammatory cytokines, such as Interleukin-1 (IL-1), IL-6, and tumour necrosis factor alpha (TNF-α), has been linked to p38 pathway activation. Again p38α is thought to be the main isoform mediating this function, with p38β knockout mice displaying no defects in cytokine production (Beardmore *et al.*, 2005).

1.4 The 14-3-3 protein family

The 14-3-3 proteins are a family of small acidic phospho-serine / phospho-threonine binding proteins that interact with substrates at specific motifs, resulting in a vast range of biological outcomes. Moore and Perez first purified these proteins from bovine brain tissue in 1967, with the name 14-3-3 deriving from this original purification procedure. The 14-3-3 protein eluted from a diethyl-aminoethyl (DEAE) cellulose chromatography column in the 14th fraction, and then migrated to position 3.3 during starch gel-electrophoresis (Moore, 1967).

1.4.1 Isoforms and expression patterns

The human brain homologue of 14-3-3 was purified in 1982 (Boston *et al.*), and 14-3-3 proteins have since been shown to be ubiquitously expressed throughout mammalian tissues. Expression of 14-3-3 has been demonstrated in all eukaryotic species examined to date, including Xenopus (Martens *et al.*, 1992), Drosophila (Swanson & Ganguly, 1992), and yeast (Ford *et al.*, 1994), and they are also found in plants (Hirsch *et al.*, 1992).

In humans, seven distinct genes encoding 14-3-3 isoforms β, γ, ε, ζ, η, θ and σ have been identified (Ichimura *et al.*, 1988; Toker *et al.*, 1992). These names derive from the fractions that each isoform eluted in during high performance liquid chromatography (HPLC) experiments (Ichimura *et al.*, 1988). The α and δ isoforms originally described are now known to be phosphorylated forms of the β and ζ isoforms respectively (Aitken *et al.*, 1995). The molecular weight of each isoform is in the region of 29-32 KDa, and they share a high degree of sequence homology (Figure 1.10). Isoform-specific knockouts in mice show no major changes in phenotype, indicating a high degree of functional compensation between isoforms (Aitken, 2006). The exception to this is the σ isoform, expressed primarily in epithelial cells, which is essential for control of DNA damage checkpoints (Chan *et al.*, 1999).

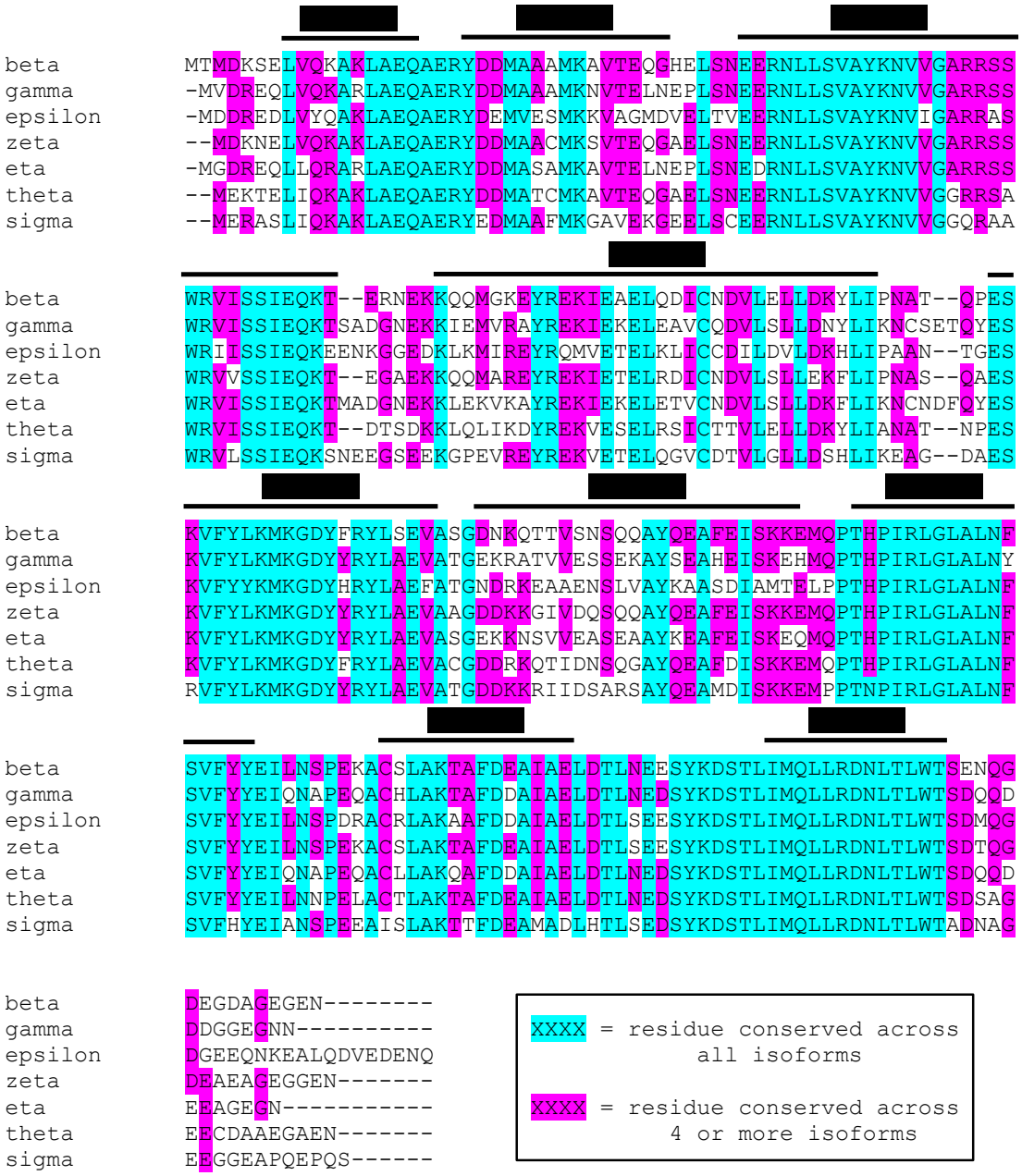

Figure 1.10: Sequence conservation across the seven human isoforms of 14-3-3

Seven isoforms of 14-3-3 are expressed in humans, each of which is composed of nine anti-parallel alpha helices connected by short loops. Human 14-3-3 isoforms show considerable sequence homology, with residues shared by all isoforms shown in blue and those shared by at least 4 isoforms in pink. A particularly high degree of sequence conservation is seen across helices 3, 5, 7 and 9, which are involved in ligand binding. The other helices form the outer surface of the 14-3-3 dimer, and the increased variability between isoforms may be responsible for isoform-specific ligand interactions. (Protein sequences were obtained from the NCBI database and aligned using Clustal X2 alignment software).

1.4.2 Structure of 14-3-3 proteins

The crystal structures of the θ and ζ isoforms of 14-3-3 were the first to be determined, and showed that monomers are composed of nine antiparallel α-helices each connected by short loops (Liu *et al.*, 1995; Xiao *et al.*, 1995). 14-3-3 monomers dimerise via their N-terminal domains (Jones *et al.*, 1995) to create a rigid, horseshoe-shaped, structure with two internal ligand-binding grooves (Liu *et al.*, 1995; Xiao *et al.*, 1995). Helices 1, 3, 5, 7 and 9, which are known to be the most highly conserved between the seven isoforms (Figure 1.10), form the internal surface of the dimer (Figure 1.11) and are involved in ligand binding. Helices 2, 4, 6 and 8, which display the greatest degree of variability, form the outer surfaces of the dimer (Figure 1.11) (Wang & Shakes, 1996; Wilker *et al.*, 2005). Most 14-3-3 isoforms are found as both homo- and hetero-dimers, the exception being the σ isoform that preferentially homo-dimerises. Unlike other isoforms the 14-3-3σ homo-dimer contains additional stabilising salt bridge interactions, and in the hetero-dimeric conformation it is thought the electrostatic interactions with other isoforms may destabilise the dimer in vivo (Wilker *et al.*, 2005).

1.4.3 Binding of 14-3-3 to target proteins

Binding of 14-3-3 involves residues Lys^{49}, Arg^{56}, Arg^{127}, and Tyr^{128}, which bind to the phosphate moiety of the target protein (Yaffe *et al.*, 1997). These are basic residues which are conserved across all isoforms, both within and across species (Rittinger *et al.*, 1999). 14-3-3 dimers are rigid structures, and it appears that binding causes conformational changes to the target protein leaving 14-3-3 relatively unchanged (Obsil *et al.*, 2001; Yaffe, 2002). 14-3-3 family members generally bind to specific motifs that have been designated as mode I RSx(pS/pT)xP and mode II Rxφx(pS/pT)xP, where pS/pT indicates a phosphorylated serine / threonine residue, φ is an aromatic or aliphatic residue, and x is any amino acid (Muslin *et al.*, 1996; Yaffe *et al.*, 1997). In some instances a 14-3-3 dimer can also interact with a substrate at the extreme C-terminal mode III –(pS/pT)$x_{1\text{-}2}$-COOH motif (Coblitz *et al.*, 2005).

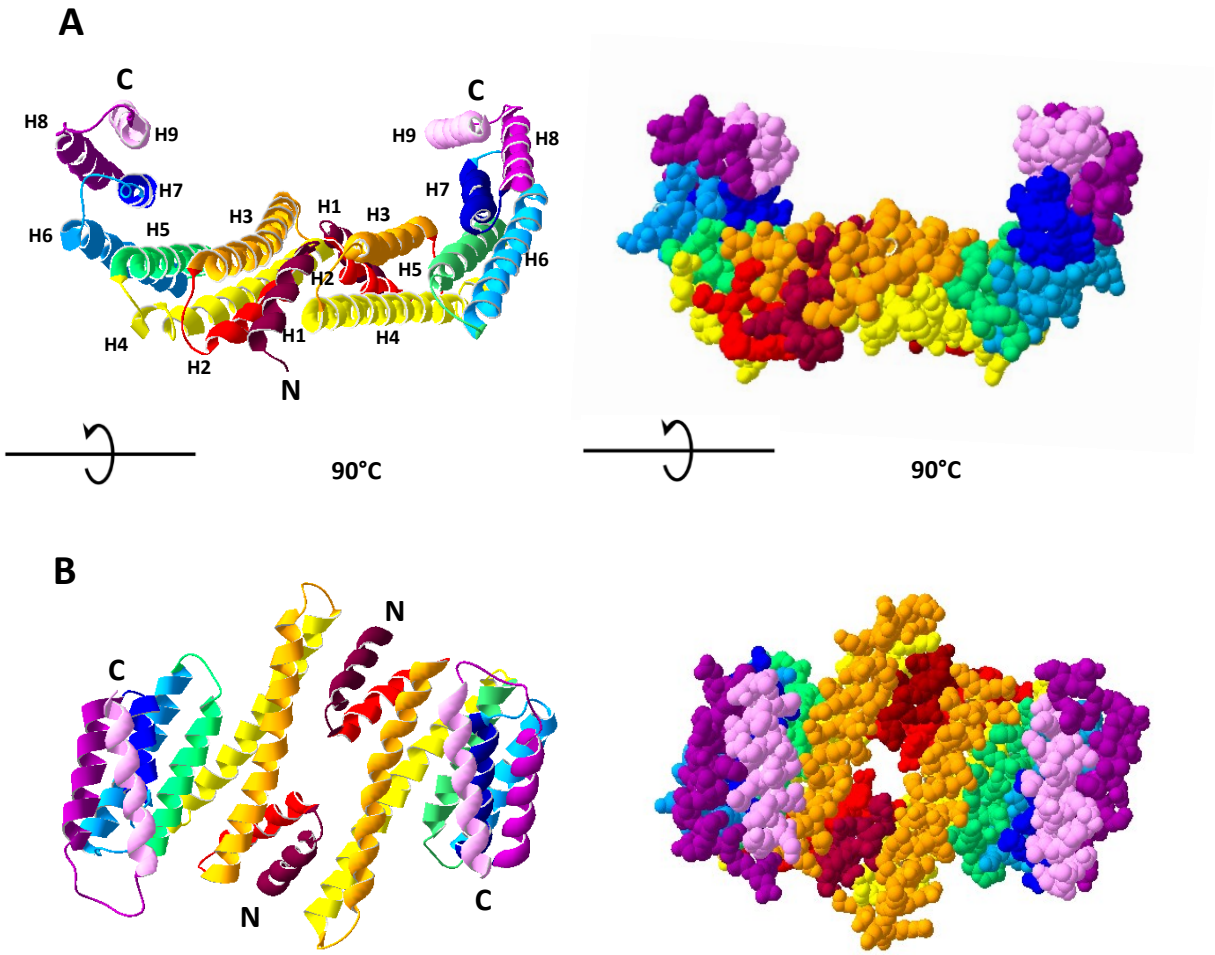

Figure 1.11: Crystal structure of the human 14-3-3β dimer.

The crystal structure of the human 14-3-3β dimer, with depictions of both the ribbon diagram (left) and space-filled models (right). Each 14-3-3 monomer is composed of nine α-helices, and the two monomers interact via their N-terminal regions to form a functional dimer. (A) The 14-3-3β dimer viewed from the side, showing the W shaped formation with two ligand-binding pockets. Note that odd-numbered helices, which are highly conserved between isoforms, form the internal ligand-binding grooves. Conversely all even-numbered helices are found on the external surfaces of the dimer, and are more variable between isoforms. (B) The 14-3-3β dimer depicted from above, showing the relative positions of the nine helices. (The crystal structure was obtained from RCSB Protein Data Bank; 14-3-3 Protein Beta (Human), 2BQ0, Biological Assembly 1. Images were created using Swiss-PDB viewer 4.1.0).

Many of the characterised 14-3-3 binding partners contain binding sequences that deviate to varying extents from the idealised mode I-III motifs (Johnson *et al.*, 2010). It has been proposed that deviations such as these may relate to the dimeric nature of 14-3-3 (Tzivion *et al.*, 2000). Each 14-3-3 monomer is capable of independent binding to a discrete motif in a target protein, either at two sites on the same target, or to two individual proteins. Affinity of a peptide with two binding motifs for a 14-3-3 dimer is over 30 times greater than for a ligand with a single binding site (Yaffe *et al.*, 1997). In proteins which lack a high affinity 14-3-3 binding site, a stable interaction may instead be achieved through coordinated binding at these two individual sites (Obsil *et al.*, 2003). It may also be of physiological relevance to have a sub-optimal binding site as 14-3-3 dissociates more readily from these proteins than those containing perfect consensus motifs (Bridges & Moorhead, 2005).

Although the majority of interactions with 14-3-3 appear to require a phosphorylated serine or threonine within the binding motif, there are rare examples of 14-3-3 interacting with non-phosphorylated targets. These include the ADP-ribosyltransferase toxin Exoenzyme S which interacts with 14-3-3 via a C-terminal DALDL motif (Masters *et al.*, 1999), and the RhoA-specific GEF p190RhoGEF which is bound by 14-3-3 at the motif IQAIQNL (Zhai *et al.*, 2001). A synthetic R18 peptide containing an LDL sequence was capable of binding to 14-3-3, and suggested that phosphorylation-independent binding of 14-3-3 is of the same affinity as binding at phosphorylated motifs (Wang *et al.*, 1999).

1.4.4 Regulation of 14-3-3 binding

Recognition of a target motif by 14-3-3 generally requires a phosphorylated residue within the consensus motif (Muslin *et al.*, 1996), a process which is regulated in vivo by the actions of protein kinases and phosphatases. Kinases known to phosphorylate 14-3-3 motifs include Akt (Mohammad *et al.*, 2013), PKA (Neukamm *et al.*, 2013), PKC (Hunter *et al.*, 2009), and AMPK (Shen *et al.*, 2013). Dephosphorylation of residues proximal to the binding motif may also be required for an interaction with 14-3-3. Phosphorylation at these sites provides an additional mechanism through which the interaction can be inhibited. The tumour suppressor

protein p53 is phosphorylated at residues Ser^{376} and Ser^{378}, with dephosphorylation of the Ser^{376} site exposing a consensus motif and leading to 14-3-3 association and DNA binding (Waterman *et al.*, 1998).

14-3-3 proteins themselves are also subject to regulation by phosphorylation (Mackintosh, 2004). Residues Ser^{58} and Ser^{63} are located at the interface of the two monomers, and phosphorylation of Ser^{58} in 14-3-3ζ disrupts the dimer both in vitro and in vivo (Woodcock *et al.*, 2003). This site is conserved across all isoforms except for 14-3-3θ and 14-3-3σ (Wilker *et al.*, 2005). A further two phosphorylatable residues at positions Ser^{184} and Ser / Thr^{232} are situated in close proximity to the ligand binding groove, and phosphorylation of either residue has been shown to decrease binding affinity (Aitken *et al.*, 2002; Obsilova *et al.*, 2004). The interaction between 14-3-3 and a target protein can also be regulated by the actions of small ligands. Binding of 14-3-3 to the plant plasma membrane H^+-ATPase is enhanced by fusicoccin, a molecule secreted by a plant pathogen, which acts by stabilising binding of H^+-ATPase to the binding groove of 14-3-3 (Würtele *et al.*, 2003).

There is some evidence to suggest that there may be isoform-specific functions of some 14-3-3 proteins, adding an additional layer of regulation to these interactions. A number of interactome studies have been conducted to identify novel 14-3-3 targets (Benzinger *et al.*, 2005). The binding proteins identified using 14-3-3σ as the bait showed only a 17% overlap with those which bound 14-3-3ζ, in studies using comparable methodologies and starting material (Bridges & Moorhead, 2005). Although some of this variation will be attributable to experimental conditions, or other regulatory mechanisms, it is likely that within this there are also examples of isoform-specific 14-3-3 binding. Sequence analysis shows that 14-3-3 isoforms are highly conserved within the ligand-binding groove. Helices 2, 4, 6 and 8, which form the outer surfaces of the dimer, are less well conserved and these amino acids may therefore be involved in mediating isoform-specific ligand interactions. Of the human isoforms, 14-3-3σ is evolutionarily distinct from the other family members and crystallisation of 14-3-3σ provided a structural explanation for its specificity in target interactions. A second ligand binding site, containing three residues which

are unique to 14-3-3σ, appears to regulate substrate discrimination (Wilker *et al.*, 2005). In isoforms other than 14-3-3σ, an additional layer of complexity is added through the potential for hetero-dimerisation, with the possibility of certain isoform combinations having specific binding characteristics not present in other pairings.

1.4.5 Modes of action of 14-3-3 proteins

Although 14-3-3 binding can mediate a vast array of biological outcomes, the mechanisms of action through which these changes occur can be broadly grouped into three categories. 14-3-3 binding may induce a conformational change in the ligand, mask a specific sequence in the ligand, or act as a scaffold protein to enhance the interactions between the ligand and other proteins (Figure 1.12) (Bridges & Moorhead, 2005).

1.4.5.1 Altering the structural conformation of a target protein

As 14-3-3 dimers are rigid structures, substrate binding has little effect on the conformation of 14-3-3 itself, and instead the dimer can act as a mould for the target protein. This conformational change can subsequently affect the intrinsic catalytic activity of the target protein. One example of this is the serotonin-*N*-acetyltransferase (AANAT), which is approximately 50% more active when 14-3-3 is bound than in the unbound state. Association of 14-3-3 alters the structure of the catalytic domain, promoting substrate binding, and thereby enhancing melatonin synthesis (Obsil *et al.*, 2001). Conversely 14-3-3 binding can induce an allosteric modification that catalytically inactivates a target protein. This is seen in plants in both the nitrate reductase (Athwal *et al.*, 1998) and ATP-synthase enzymes (Bunney *et al.*, 2001).

1.4.5.2 Masking a specific sequence on the target protein

The association of 14-3-3 with a target can prevent the ligand from localising in its usual site of action by masking a localisation signal, or a structural feature. Phosphorylation of Cdc25c facilitates binding of 14-3-3, which masks a nuclear localisation signal (NLS) leaving Cdc25c sequestered in the cytosol where it is unable

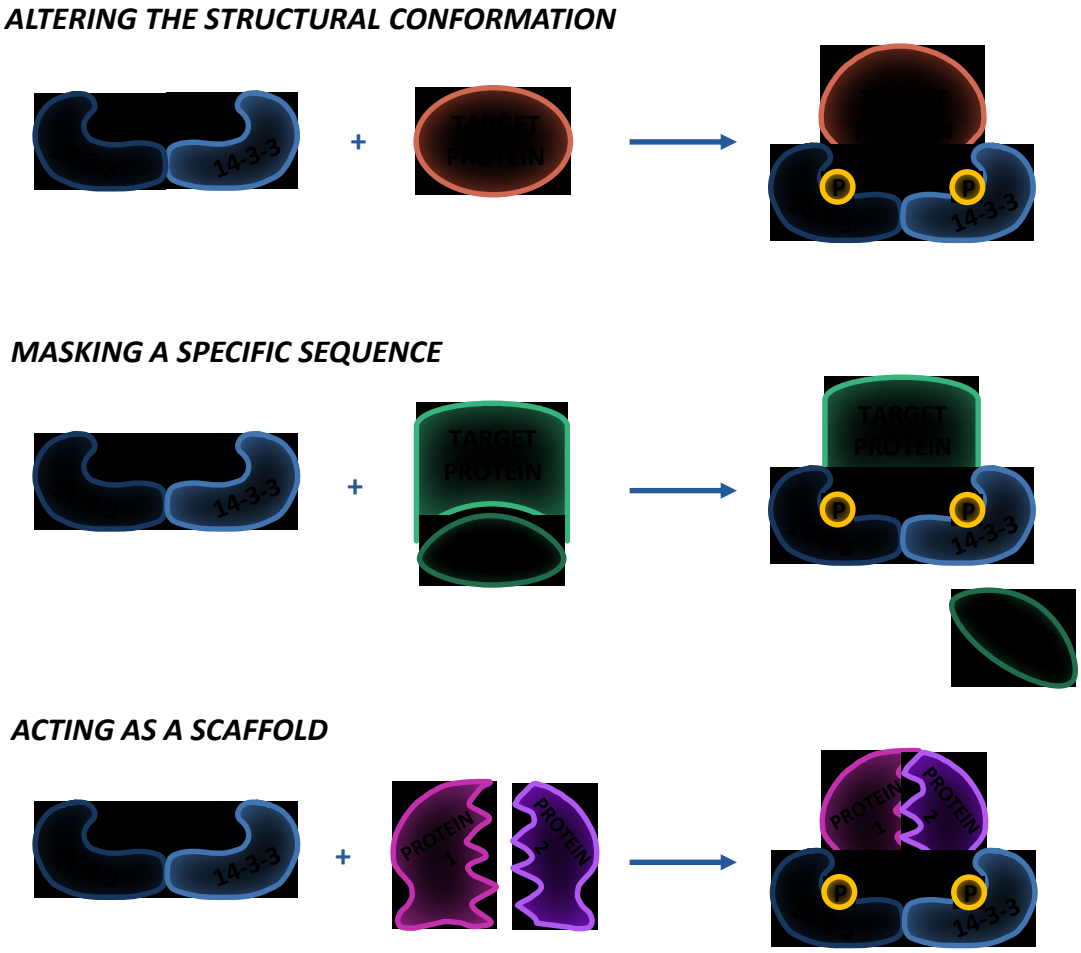

Figure 1.12: Mechanisms of action of 14-3-3 binding to a target protein

Binding of 14-3-3 can induce a wide variety of effects on a target protein, but these functional outcomes can be classified into three general modes of action. (A) Binding of 14-3-3 can induce a direct conformational change in a target protein, which may enhance or inhibit the intrinsic catalytic activity. (B) Association of 14-3-3 may mask a specific sequence within the target protein, which often results in a change in subcellular localisation of the target. Such sequences include localisation signals for the nucleus or membrane, binding motifs for other proteins, or sequences that interact with DNA. (C) The 14-3-3 dimer can act as a scaffold protein, binding to two separate proteins at each of the phosphate binding sites, and increasing the probability of an interaction.

to promote mitosis (Kumagai & Dunphy, 1999). There is some evidence to suggest that this may be due to direct interaction of 14-3-3 dimers with NLS sequences (Obsilova *et al.*, 2005). Alternatively, proteins such as telomerase reverse transcriptase (TERT) can be held in the nucleus upon 14-3-3 binding through masking of a nuclear export signal (NES) (Seimiya *et al.*, 2000). The Forkhead box O (FOXO) transcription factors are found in the unphosphorylated active state in the nucleus, and upon phosphorylation are exported to the cytosol. Phosphorylation by protein kinase B (PKB) at two sites leads to 14-3-3 association and masking of the DNA binding domain which lies between these residues, terminating gene transcription (Obsil *et al.*, 2003). Binding of 14-3-3 is essential for the cytoplasmic retention of of the kinase suppressor of Ras 1 (KSR1) protein in quiescent cells. Cdc25C-associated kinase 1 (C-TAK1) constitutively associates with the N-terminus of KSR1, and phosphorylates Ser^{392} to facilitate 14-3-3 binding. KSR1 is a cytoplasmic protein that translocates to the plasma membrane upon growth factor stimulation, resulting in MEK activation. In the absence of 14-3-3, KSR1 is constitutively localized to the membrane resulting in hyperactivated signaling through the Ras / MAPK pathway (Müller et al., 2001).

1.4.5.3 Acting as a scaffold protein to enhance protein-protein interactions

As dimeric 14-3-3 is capable of binding to two proteins, it can act as a scaffold to increase the likelihood of two proteins coming together. The first protein is bound to one binding pocket of the 14-3-3 dimer, and held in place bringing it in close proximity to the second protein that in turn binds to the other binding site (Bridges & Moorhead, 2005). For example one half of a dimer can bind a protein kinase, with its substrate bound by the other half – thereby upon activation of the kinase the substrate is in close proximity ready to be phosphorylated and continue the downstream signalling cascade. This scaffolding effect is known to enhance the phosphorylation of Tau by glycogen synthase kinase-3β (GSK-3β) (Agarwal-Mawal *et al.*, 2003), and of Raf-1 by protein kinase C (PKC) (Van Der Hoeven *et al.*, 2000).

1.4.6 Functions of 14-3-3 binding

The first function attributed to 14-3-3 proteins was the regulation of serotonin and noradrenaline biosynthesis in the brain, through activation of tryptophan 5-monooxygenase and tyrosine 3-monooxygenase (Ichimura *et al.*, 1987). Since this discovery the known functional roles of the 14-3-3 family have expanded dramatically, and they have been implicated in a vast array of both physiological and pathological processes. Novel functions are continually being discovered, in line with the identification of new 14-3-3 binding targets by mass spectrometry (Jin *et al.*, 2004), protein microarrays (Satoh *et al.*, 2006), and in vitro affinity chromatography (Pozuelo Rubio *et al.*, 2004). Current figures estimate that there are now over 300 known 14-3-3 binding proteins, but for many of these the physiological relevance of 14-3-3 binding has yet to be determined. Two characterised functions of 14-3-3 proteins are in regulating intracellular signalling pathways, and in coordinating the actin cytoskeleton.

1.4.6.1 14-3-3 and regulation of intracellular signalling

The 14-3-3 proteins have been implicated in the regulation of a wide variety of signalling pathways through interaction with both substrates and regulators of these pathways. Raf-1, an upstream activator of MAPK signalling, has been identified as a 14-3-3 binding protein and contains three interaction motifs at Ser^{259}, Ser^{621} and a third site between residues 136-187 (Tzivion *et al.*, 1998). Association with 14-3-3 holds Raf-1 in the inactive state in the absence of activation signals, however once these signals are present, 14-3-3 switches one of the binding sites resulting in Raf-1 activation and functions as a stabiliser of this active conformation (Fischer *et al.*, 2009). The growth factor receptor-bound protein 2 (Grb2) adaptor / GRB2-associated-binding protein 2 (Gab2) docking protein complex is also regulated by 14-3-3. Binding of 14-3-3 to Gab2 at phosphorylated Ser^{210} and Thr^{391} promotes the dissociation of the complex, thereby reducing Gab2 signalling. This phosphorylation is dependent upon the PI3K/PKD/Akt cascade (Brummer *et al.*, 2008).

1.4.6.2 14-3-3 and regulation of the actin cytoskeleton

The apparent co-localisation of actin and 14-3-3 using confocal microscopy was first demonstrated in astrocytes, and was initially taken as evidence for a direct interaction between these two proteins (Chen & Yu, 2002). Subsequent co-sedimentation experiments were not able to validate this hypothesis however, and it is now thought that this is more likely to be an indirect link mediated through the direct interaction of 14-3-3 with actin-binding proteins (Birkenfeld *et al.*, 2003).

A number of proteins involved in regulating the cytoskeleton have been shown to bind 14-3-3 (Angrand *et al.*, 2006; Jin *et al.*, 2004; Pozuelo Rubio *et al.*, 2004). These include slingshot 1-like (SSH1L) and cortactin, both of which contain 14-3-3 binding motifs that are phosphorylated by protein kinase D (PKD). SSH1L is a phosphatase which activates cofilin, an F-actin severing protein, through dephosphorylation of Ser^{3} (Andrianantoandro & Pollard, 2006). SSH1L itself is activated through interaction with F-actin, but when bound to 14-3-3 it loses this actin-binding ability (Nagata-Ohashi *et al.*, 2004). Localisation studies confirmed that upon activation of RhoA, PKD phosphorylates SSH1L within its F-actin binding domain at Ser^{978}, leading to 14-3-3 association, which sequesters SSH1L in the cytosol away from the actin-rich region (Eiseler *et al.*, 2009; Peterburs *et al.*, 2009). Cortactin is an F-actin binding protein found in a number of actin structures that interacts with the Arp2/3 complex to enhance actin polymerisation. Phosphorylation of the Ser^{298} motif by PKD results in 14-3-3 association and negative regulation of cortactin function (Eiseler *et al.*, 2010).

1.5 PEST-mediated protein degradation

The synthesis and degradation of proteins is tightly regulated to ensure that sufficient quantities of each protein are available to meet the spatial and temporal requirements of a cell. Proteins with rapidly changing requirements have short in vivo half-lives, and use degradation pathways as a method of regulating protein concentration. When combined with the temporary termination of protein synthesis, this provides a mechanism by which the total intracellular pool of a

protein can be rapidly depleted as required. This degradation process is largely mediated by the ubiquitin proteasome system, and to a lesser extent the lysosome pathway. These mechanisms are also essential for the degradation of proteins that have been incorrectly synthesised, damaged, or mis-folded, which must be rapidly removed from the cell to prevent potential problems with aberrant function (Bukau *et al.*, 2006).

1.5.1 Intracellular protein half-lives

The intracellular half-life of a protein is the time it takes for half of the protein that was originally synthesised within a cell to be depleted. Intracellular half-lives of proteins vary dramatically depending on their function. Ornithine decarboxylase, which catalyses the first committed reaction in polyamine synthesis and therefore needs to be tightly regulated, has an intracellular half-life of 16 minutes (Isomaa *et al.*, 1983). At the other end of the spectrum is collagen, which shows little variation in physiological requirements, and consequently has a calculated half-life of 117 years (Verzijl *et al.*, 2000). A large-scale analysis of the intracellular turnover rates of over 5000 mammalian proteins showed that half-lives fit a normal distribution, with a median half-life of 46 hours (Schwanhäusser *et al.*, 2013).

1.5.2 Regulators of intracellular protein half-lives

Several determinants of protein half-lives have been described. The N-end rule predicts the stability of a protein based upon its N-terminal amino acid, and first originated following observations that the N-terminal residue can have dramatic effects on protein stability (Bachmair *et al.*, 1986). Mutagenesis experiments using the protein beta-galactosidase showed that by changing only the extreme N-terminal residue the protein half-life could be dramatically altered. These experiments have now been conducted in yeast in vivo, mammalian reticulocytes in vitro, and in *E.coli* in vivo. The half-life of a given protein was also shown to be dependent upon the experimental model used (Bachmair *et al.*, 1986; Gonda *et al.*, 1989; Tobias *et al.*, 1991). In mammalian cells the half-life of beta-galactosidase

with an N-terminal glutamine was less than an hour, compared to over 100 hours when substituted for a valine residue (Bachmair *et al.*, 1986).

The half-live of a protein has also been linked to the presence of specific amino acid sequences within a substrate that serve as targets for ubiquitination and subsequent degradation. Many of these are classed as primary degrons, requiring phosphorylation of an internal residue(s) for activation. Some of these motifs, such as DpSGXXpS, show highly conserved sequences across substrates (Liu *et al.*, 2010; Zhao *et al.*, 2010). Others contain conserved and variable regions, including a 20-residue motif with a core sequence of ϕ-x-x-Ala-x-x-x-Ser-x-x-Ac, where ϕ is a large hydrophobic residue and Ac is an acidic residue (Hofmann & Falquet, 2001). Finally there are motifs that show no sequence conservation. These include PEST motifs, which are short regions rich in proline, glutamic acid, serine, and threonine residues in no particular sequence (Rogers *et al.*, 1986).

1.5.3 PEST degradation motifs

In an attempt to determine what makes some proteins degrade so much faster than others, Rogers *et al* (1986) scanned the sequence of ten proteins with intracellular half-lives of less than two hours. They found that all of these proteins contained one or more regions that were rich in the amino acids proline (P), glutamic acid (E), serine (S) and threonine (T) – which they designated PEST motifs. Analysis of proteins with longer half-lives indicated that they rarely contained such sequences. Estimates suggest that fewer than 10% of all proteins contain PEST motifs (Rechsteiner and Rogers, 1996). Deletion of a PEST motif can have dramatic effects on the stability of a protein, with the half-life of ornithine decarboxylase increasing ten-fold (Ghoda *et al.*, 1989). Conversely, transplanting a PEST motif into a protein that doesn't naturally contain one has been shown to have the opposite effect (Ghoda *et al.*, 1990; Loetscher *et al.*, 1991).

In their initial analysis, Rogers *et al* (1986) noted that although all of the rapidly degraded proteins that they examined contained a PEST motif, not all PEST containing proteins were unstable. For some proteins, such as the carboxy-

terminus of mouse ornithine decarboxylase, the presence of a PEST motif acts as a constitutive signal for degradation. However in the majority of proteins the PEST motif appears to act as a primary destruction signal, requiring activation by a second regulatory mechanism for protein degradation to occur. This conditional activation can occur through a number of mechanisms. Phytochrome has a half-life of approximately 100 hours before light activation induces a conformation change, thought to expose a PEST motif, which dramatically decreases the half-life to just one hour. Tetramerisation of the regulatory and catalytic subunits of cAMP-dependent protein kinase increases the protein half-life from one to ten hours compared to the monomers, which is likely to be caused by masking of external PEST motifs (Rechsteiner, 1990). However by far the most common regulatory mechanism identified is phosphorylation of the PEST motif at the integral serine and threonine residues (Rechsteiner & Rogers, 1996). Regardless of the mechanism, activation of a PEST domain acts as a signal for ubiquitination and subsequent degradation of the protein (Rechsteiner & Rogers, 1996).

1.5.4 Ubiquitination of degradation substrates

Ubiquitin is a 76 amino acid protein that is enzymatically attached to proteins destined for degradation. As it targets primary degrons within proteins, ubiquitin is classed as a secondary degron. The sequential addition of multiple ubiquitin tags to internal lysine residues of substrates allows the protein to be recognised by the proteolytic machinery and subsequently to be degraded (Varshavsky, 1991).

Three enzymes, E1, E2, and E3, control the addition of ubiquitin to proteins being targeted for destruction (Figure 1.13). E1 is the ubiquitin-activating enzyme, which binds to the C-terminus of ubiquitin at Gly^{76} in an ATP-dependent reaction. The ubiquitin moiety is then transferred to a cysteine residue on one of the E2 ubiquitin-conjugating enzymes. The E2 enzyme then associates with E3, the ubiquitin protein ligase, which facilitates the polymerisation of one or more ubiquitin molecules onto the substrate (Figure 1.13). In mammalian cells only a single E1 protein has been identified, however there are over 30 E2 enzymes and over 1000 different forms of

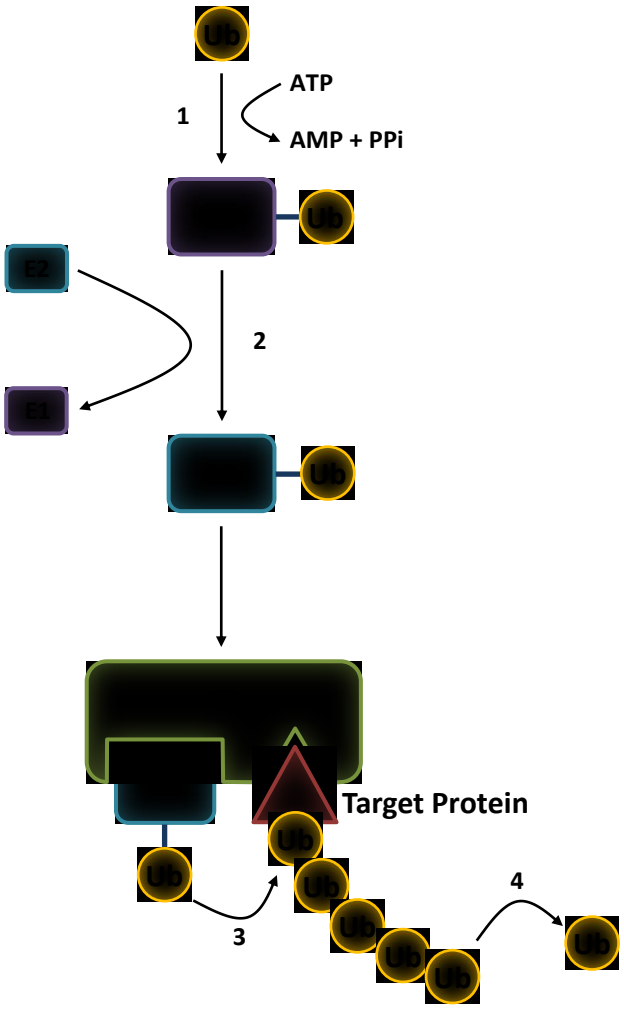

Figure 1.13: Ubiquitination of target proteins.

Ubiquitination of proteins in vivo is catalysed by the E1-E3 ubiquitin enzymes. Initially a single ubiquitin group is bound to the E1 ubiquitin-activating enzyme in an ATP-dependent reaction (1). The ubiquitin group is then transferred to one of the E2 ubiquitin-conjugating enzymes, and the unbound E1 recycled (2). E2 then associates with one of the hundreds of E3 ubiquitin-ligases, which transfers ubiquitin groups to the target protein (3). This process is reversible, and ubiquitin groups may also be removed through the actions of de-ubiquitinating enzymes (4). A protein with four or more attached ubiquitin groups is a target for degradation via the proteasome.

E3. The functions of the majority of these variants are not yet known, but the large number of proteins at the E2 and E3 stages enables the cell to have greater control over protein degradation. For a substrate to be recognised for proteolysis, it needs to be conjugated to a chain of four or more ubiquitin molecules. Whilst the E1-3 enzymes catalyse the polymerisation of these chains, there are also a large family of de-ubiquitinating enzymes that can reverse this process. This removal of ubiquitin groups provides an additional method of regulating the degradation process.

1.5.5 Degradation pathways

Two main structures mediate protein degradation in eukaryotic cells – lysosomes and proteasomes (Figure 1.14), and PEST-mediated proteolysis can involve either of these mechanisms (Rechsteiner & Rogers, 1996).

1.5.5.1 Proteasomal degradation

Proteasomes are responsible for the degradation of the majority of intracellular proteins, either those identified as being mis-folded or those targeted for degradation through activation of signalling pathways and subsequent phosphorylation (Rock *et al.*, 1994). The 26S proteasome is a 1.5 MDa complex consisting of over 60 proteins. These can be divided into 2 sub-domains; a central catalytic 20S core particle (CP) with 19S regulatory particle (RP) capping either one or both ends (Figure 1.14). The 20S CP forms a cylindrical structure composed of four layers of seven-subunit rings, with two interior β layers and two outer α layers. The 19S RP can be further divided into a base structure, and a lid complex.

A protein conjugated to a chain of ubiquitin molecules signals to the proteasome that it is a substrate for degradation. Ubiquitin is recognised by the 19S cap of the proteasome, which opens the outer α-ring to allow substrates into the central 20S domain (Baboshina & Haas, 1996). Proteins are unravelled by 19S and inserted into the central core, which contains proteases that digest the internalised proteins into short peptides. The ubiquitin molecules are not taken into the proteasome, but instead are released back into the cytosol and recycled (Kisselev *et al.*, 1999).

1.5.5.2 Lysosomal degradation

There is evidence that PEST mediated degradation may also occur through the lysosomal pathway (Zhuang *et al.*, 2012). Lysosomes are membrane-bound vesicles located in the cytoplasm that contain a wide range of proteases and other hydrolytic enzymes. They commonly degrade extracellular and transmembrane proteins that are brought into the cell in endocytotic vesicles (Figure 1.14). Cytosolic proteins may also be degraded in lysosomes if they are first engulfed in autophagic vesicles that fuse with lysosomes. This mechanism also regulates the digestion of intracellular organelles (Figure 1.14).

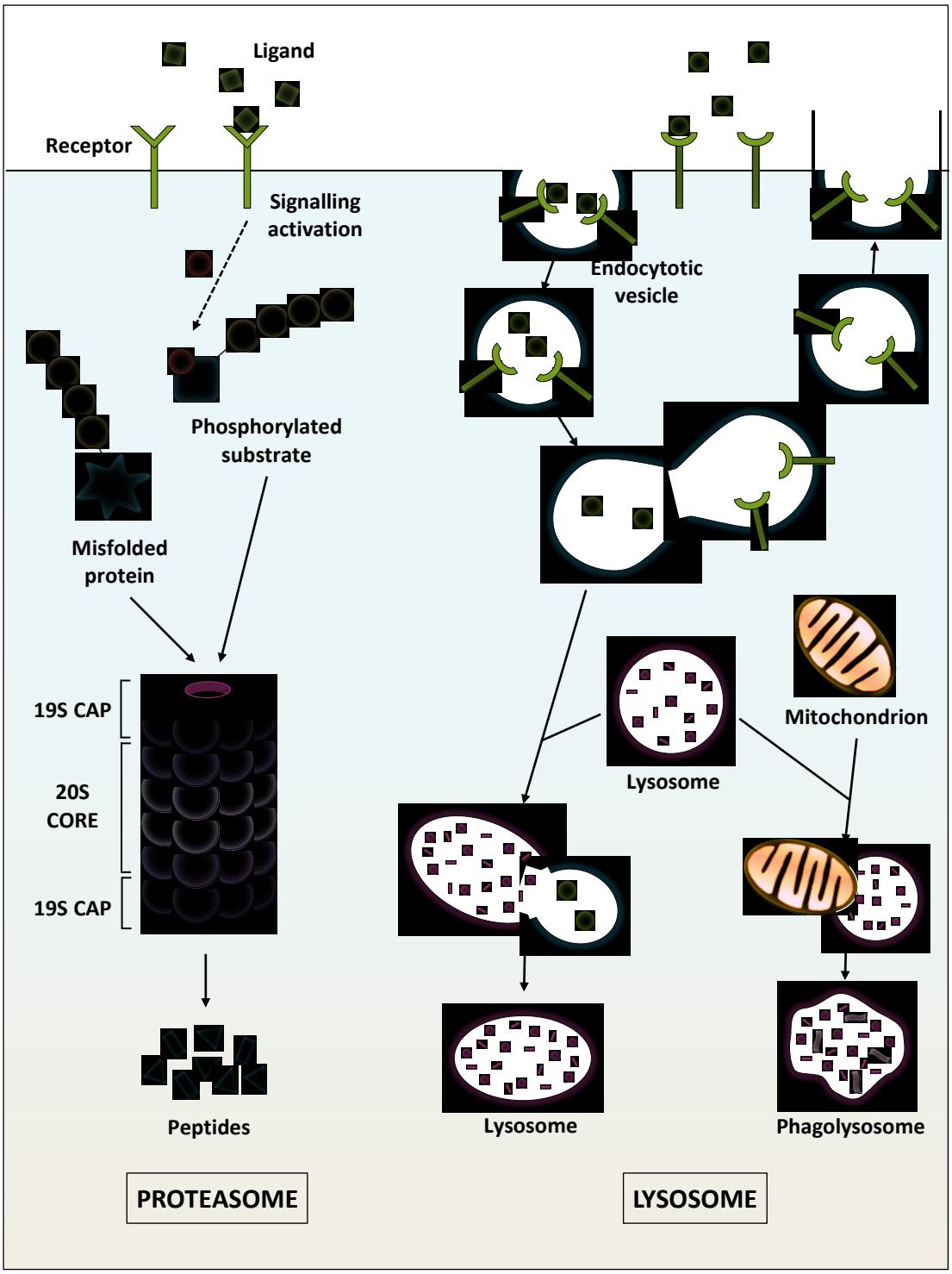

Figure 1.14: The proteasomal and lysosomal pathways of protein degradation

Intracellular protein degradation is mediated by two main pathways, the ubiquitin-proteasome pathway, and the lysosomal degradation pathway. Ubiquitin targets mis-folded or phosphorylated proteins to the proteasome where they are degraded into small peptides. Lysosomal degradation is commonly associated with the degradation of external and membrane proteins, in addition to intracellular organelles such as mitochondria.

1.6 Thesis aims

There is currently very little understanding of how dematin is regulated in vivo, and in particular what coordinates its ability to both bind and bundle actin. Given the ubiquitous expression of dematin, gaining a better understanding of this regulation has widespread implications not only for the known functions of dematin, but for those that have yet to be discovered. This thesis therefore aims to investigate the potential regulation of dematin by the p38 MAPK, and the adaptor protein 14-3-3, both of which have increasingly well documented roles in cytoskeletal regulation. Significant expression of dematin has been demonstrated in skeletal muscle and the C2C12 skeletal muscle cell line will therefore be used as a model system for investigating the regulation of dematin.

1.6.1 Aim 1 - To characterise the regulation of dematin by the p38 MAPK

Preliminary data from our lab has identified dematin as a novel substrate of the p38 MAPK (Müller 2010, unpublished). Furthermore, the primary sequence of dematin contains a number of phosphorylation motifs for the p38 MAPK (Figure 1.2). This thesis therefore aims to characterise the regulation of dematin by p38, with particular focus on PEST-mediated dematin instability and the core / HP interaction.

Objectives:

- To use a multi-technique approach to confirm that dematin is phosphorylated by p38, and begin to characterise the specific motifs in dematin that are phosphorylated both in vitro and in vivo.
- To assess whether the stability of dematin is regulated by its PEST degradation motif, and to determine whether p38 phosphorylation of internal residues within the motif regulates the degradation process.
- To identify the region of the dematin core domain that the HP binds to, and to determine whether p38 phosphorylation of the HP has a regulatory effect on this interaction.

1.6.2 Aim 2 - To characterise the regulation of dematin by 14-3-3

The 14-3-3 family are known to regulate the functions of a number of cytoskeletal proteins. Analysis of the primary sequence of dematin identified seven potential 14-3-3 binding motifs (Figure 1.2), suggesting that dematin may be a novel binding partner. This thesis therefore aims to characterise both the interaction and function of the dematin / 14-3-3 association.

Objectives:

- To determine whether dematin and 14-3-3 interact, to identify the 14-3-3 consensus motifs that are phosphorylated in vivo, and to confirm the specific motifs that are responsible for this interaction

- To identify which kinases phosphorylate the 14-3-3 binding motifs in dematin to facilitate a dematin / 14-3-3 interaction, and to determine whether p38 phosphorylation of neighbouring residues negatively regulates this interaction

- To characterise the function of the dematin / 14-3-3 interaction in C2C12 skeletal muscle cells, with particular focus on the known actin-binding and -bundling abilities of dematin

2. Materials and Methods

2.1 Suppliers of reagents and chemicals

Plastic lab-ware, including cell culture dishes and plates, were purchased from Beckton Dickinson (UK). Reagents were obtained from a variety of companies, as detailed at the relevant points throughout the methods. Chemicals were obtained from Fisher (UK) unless otherwise stated in the text.

2.2 Growth and maintenance of *E.coli*

2.2.1 Media

Liquid *E.coli* cultures were grown aerobically in Luria-Bertami medium (LB) (10 g/l NaCl; 10 g/l bactotryptone; and 5 g/l yeast extract) at 37°C with shaking at 220 rpm. *E.coli* cells were also grown on plates containing 16% (w/v) agar in LB, which were cultured at 37°C. Antibiotics were used in both solid and liquid cultures when required; 100 µg/ml ampicillin or 25 µg/ml kanamycin (Sigma, UK).

2.2.2 Preparation of competent *E.coli* cells

Starter cultures were prepared by inoculating 5 ml of LB with a single colony of TOP10 *E. coli* cells (Invitrogen, UK) and incubating overnight at 37°C with shaking at 220 rpm. This was used to inoculate 400 ml of LB, which was incubated at 37°C with shaking until it reached an OD_{590nm} = 0.35-0.4. The culture was divided into 8 x 50 ml aliquots and cooled on ice for 10 minutes. Cells were pelleted at 4000 x g at 4°C for 15 minutes, and each aliquot resuspended in 10 ml sterile-filtered ice-cold calcium buffer (60 mM $CaCl_2$, 15% (v/v) glycerol, 10 mM pipes; pH 7.0). Cells were then re-pelleted under the same conditions, resuspended in calcium buffer, and incubated on ice for 30 minutes. Following a final centrifugation, pellets were gently resuspended in 2 ml of ice-cold calcium buffer and aliquots stored at -80°C.

2.2.3 Transformation of competent *E.coli* cells

TOP10 competent *E.coli* cells (section 2.2.2) were transformed with 50 - 100 ng of plasmid DNA. Following 30 minutes incubation on ice, the DNA and cell mix was heat-shocked at 42°C for 45 seconds. After cooling on ice, samples were combined with 1 ml LB and incubated at 37°C for 1 hour with shaking at 220 rpm. Samples

were centrifuged at 5,000 x g for 2 minutes, supernatants removed and pellets resuspended in LB. Cells were plated onto LB agar plates containing the relevant antibiotic and incubated for 16-18 hours at 37°C.

2.3 DNA manipulation

2.3.1 DNA purification

Small-scale plasmid DNA isolation (1.5 ml of a 5ml LB culture) was conducted using a GeneJet Plasmid MiniPrep Kit (Thermo Scientific, UK). DNA extraction was performed according to the standard protocol, and eluted in 100 µl of buffer. Large scale DNA extraction (from 200 ml LB cultures) was conducted using the PureYield Midiprep System (Promega, UK) according to the standard vacuum-pump protocol with elution in 1 ml nuclease-free water. DNA concentration and purity were quantified using 1.5 µl samples on a Nanodrop ND1000 Spectrophotometer with NanoDrop 1000 3.6.0 software (Thermo Scientific, UK). The A260:280 nm and A260:230 nm ratios were used to asses DNA purity, with accepted values of ≈ 1.8 and 2.0-2.20 respectively. Samples were stored at -20°C.

2.3.2 DNA oligonucleotides

DNA oligonucleotides (Invitrogen, UK or Sigma, UK) were synthesised on a 25 nmol scales with desalting. Primer pairs were designed to have melting temperature within 5°C of one another, and minimal predicted dimer formation. Lyophilised primers were resuspended in sterile distilled water at a concentration of 100 µM and stored at -20°C.

2.3.3 Polymerase chain reaction (PCR)

PCR reactions were conducted in 25 µl volumes containing 50 ng template DNA, 0.1 µM each of sense and antisense primers, 0.2 mM dNTPs (from single nucleotide stocks), 1x *Pfu* buffer with 1.5 mM $MgSO_4$ and 0.5 units *Pfu* DNA polymerase (all Promega, UK). PCR was performed on an Eppendorf Mastercycler personal thermal cycler (Eppendorf, Germany) with a heated lid (105°C) using the following conditions:

Initial denaturation	95°C	3 minutes	
Denaturation	95°C	30 seconds	30 cycles
Annealing	Tm - 5°C	3 minutes	
Extension	72°C	2 min / Kb	
Final extension	72°C	15 minutes	
Hold	4°C		

PCR primers were designed to amplify the gene of interest, and add a unique restriction site onto the 3' and 5' ends of the PCR product to facilitate high efficiency cloning into the pENTR11 entry vector. The primer sequences, template DNA, and melting temperature (Tm) used for each reaction are detailed in (Table 2.1).

2.3.4 Agarose gel electrophoresis

Agarose gels were prepared by dissolving 1-2% agarose (w/v) in Tris / Borate / EDTA (TBE) buffer (89 mM Tris; 89 mM H_3BO_3; 2 mM EDTA, pH 8.0), with 0.5 µg/ml ethidium bromide (Sigma, UK). DNA samples were combined with 5x loading buffer (Fermentas, UK) and the gels electrophoresed at 100 V in TBE buffer. Images were captured using a GelDoc 2000 UV transilluminator with Quantity One software (BioRad, UK).

2.3.5 Restriction endonuclease digests of DNA

PCR amplified DNA products were digested with the relevant restriction enzymes (Table 2.1) to produce compatible ends for ligation reactions. Restriction endonuclease digestion was conducted according to the standard manufacturer's protocol, with incubation at 37°C for approximately 3 hours. The number of units of each restriction enzyme required per µg of DNA was calculated relative to the reference information for the digestion of linear lambda DNA. The volume of restriction enzymes was kept below 10% of the total reaction volume.

2.3.6 Phenol-chloroform DNA extraction and ethanol precipitation

Restriction digested PCR products were purified using phenol extraction and ethanol precipitation. DNA samples were mixed with equal volumes of phenol /

Table 2.1: Primers for the PCR amplification of genes of interest

me	Primer	Sequence (5'-3')	Restriction Site	Template DNA	Prod siz (b
latin	for	TA**CCATGG**AACGGCTGCAGAAGCAACCAC	NcoI	Origene EPB49 (BC017445) Human cDNA Clone	14
	rev	AT**CTCGAG**TCAGAAGAGAGAGGCCTTCTTCTTGAGCTC	XhoI		
l1	for	TA**CCATGG**AACGGCTGCAGAAGCAACCAC	NcoI	pENTR11*FLAG*-dematin	23
	rev	TA**CTCGAG**CTACAGCTCCACGTGTTCCAGGAGGGAAT	XhoI		
l2	for	TA**CCATGG**AACGGCTGCAGAAGCAACCAC	NcoI	pENTR11*FLAG*-dematin	58
	rev	TT**CTCGAG**CTACGGGGGGCATGGCCAGTAGTCG	XhoI		
l3	for	AG**CCATGG**ATTCCCTCCTGGAACACGTGGA	NcoI	pENTR11*FLAG*-dematin	38
	rev	TT**CTCGAG**CTACGGGGGGCATGGCCAGTAGTCG	XhoI		
:1	for	AAG**CCATGG**CGGTTACTTCCAACTTGGGAAAGATGA	NcoI	pENTR11*FLAG*-dematin	48
	rev	AT**CTCGAG**TCAGAAGAGAGAGGCCTTCTTCTTGAGCTC	XhoI		
HP	for	AA**CCATGG**GGGAGAACCTGTACTTCCAGGGCCCAGGCCT	NcoI	pENTR11*FLAG*-dematin	20
	rev	AT**CTCGAG**TCAGAAGAGAGAGGCCTTCTTCTTGAGCTC	XhoI		
)+22	for	TA**CCATGG**ACCAGGCCTGCAGAACGGAGAG	NcoI	pENTR11*FLAG*-dematin	27
	rev	AT**CTCGAG**TCAGAAGAGAGAGGCCTTCTTCTTGAGCTC	XhoI		

Provided are the sequences and details of the PCR primer used in this study. Cloning restriction sites are shown in bold and underlined.

/ chloroform / iso-amyl alcohol (25:24:1 v:v:v ratio), vortexed thoroughly and centrifuged for 15 seconds at 14,000 x g. The top aqueous layer was removed and combined with 1/10 volume of 3 M sodium acetate (pH 5.2), followed by 2.5 volumes of ice cold 100% ethanol and incubated on dry ice for 15 minutes. After a 5-minute centrifugation at 14,000 x g, the supernatant was removed and the pellet washed twice with 1 ml of 70% ethanol. Pellets were dried in an Eppendorf Concentrator Plus (Eppendorf, UK) for 5 minutes and resuspended in the required amount of sterile distilled water.

2.3.7 Preparation of vector DNA

All genes were initially cloned into a pENTR11 entry vector (Figure 2.1) for use with the Gateway® expression system (Invitrogen, UK). The vectors used in this study were modified forms of the commercially available pENTR11, which had been altered to contain either a FLAG or MYC protein tag at the 5' end of the multiple-cloning site. pENTR11*FLAG* or pENTR11*MYC* vectors were digested with the relevant restriction enzymes as in section 2.3.5. The digested vector was then dephosphorylated to minimise self-ligation. This was conducted using 0.5 U/µg vector DNA of CIP alkaline phosphatase (New England Biolabs, UK) with one hour incubation at 37°C. Digested pENTR11 vector DNA was electrophoresed and the desired band (of approximately 2200 bp) was excised from the gel. DNA extraction was conducted using a GenElute Gel Extraction Kit (Sigma, UK) according to the manufacturer's guidelines, and eluted in the appropriate volume of buffer for subsequent procedures.

2.3.8 DNA Ligation and product verification

Following enzyme digests the relevant inserts were ligated into the pENTR11 entry vector in 10 µl reactions with insert : vector DNA ratios of between 1:3 and 3:1, 1 µl T4 DNA ligase buffer and 0.5 units T4 DNA ligase. Samples were incubated at 16°C for 18 hours before transformation in TOP10 *E.coli* cells (section 2.2.3). Overnight cultures inoculated with single colonies were prepared in LB supplemented with 25 µg/ml kanamycin. Test digests with relevant restrictions enzymes were performed to identify successful ligation reactions. Enzymes were chosen to digest both the

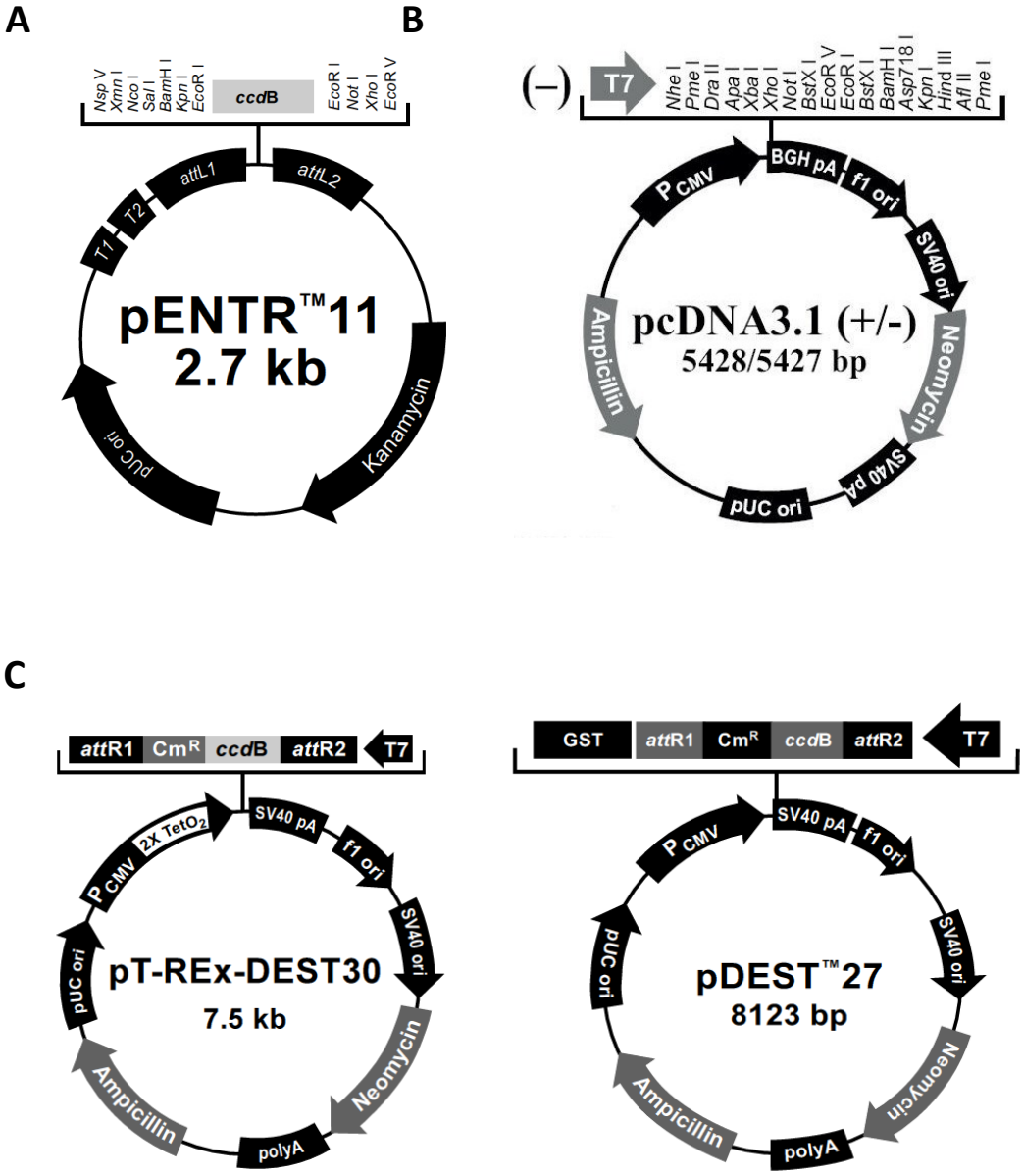

Figure 2.1: Gateway DNA entry and expression vectors used in this study

All DNA constructs were first cloned into the kanamycin resistant pENTR11 entry vector (A) for use with the Invitrogen gateway system. The attL1 and attL2 recombination sites allowed efficient transfer into a variety of mammalian expression vectors - (B) a modified version of the commercial pcDNA3.1 shown here that has with the gateway transfer cassette cloned into the XbaI / HindIII sites (referred to as pcDNA3.1-DEST), and (C) the standard destination vectors pT-Rex-DEST30 and pDEST27. These were selected on the basis of the properties required in each individual experiment. All of the expression vectors express the CMV immediate-early promoter/enhancer for efficient, high-level expression of the recombinant protein, and an ampicillin resistance gene to allow selection.

insert and the vector, and produce DNA fragments that were easily distinguishable from incorrectly ligated products by gel electrophoresis.

2.3.9 Gateway® recombination cloning

Gateway cloning® of successfully ligated constructs from pENTR11 entry vectors into mammalian expression vectors was conducted according to the standard Invitrogen protocol. Reactions of 5 µl containing 75 ng of entry vector DNA in the pENTR11 vector, 75 ng of destination plasmid DNA and 2 µl TE buffer (pH 8.0) were incubated at 25°C for 90 minutes with 1 µl of LR Clonase enzyme II mix (Invitrogen, UK). The reaction was terminated by the addition of 1 µl Proteinase K (Invitrogen, UK), and incubated for 10 minutes at 37°C. The destination vectors used in this study were a version of pcDNA3.1 which was modified to contain the necessary Gateway® recombination sequences, pT-RExDEST30, and pDEST27. These were selected according to the properties required for each specific experiment (see Figure 2.1 for further details). The total 6 µl gateway reaction was transformed into TOP10 competent *E.coli* cells (section 2.2.3). Successfully ligated clones were identified by conducting test digests with the appropriate restriction enzymes.

2.3.10 Plasmids

Details of the pENTR11 entry-vector and pcDNA3.1, pTrexDEST30, and pDEST27 expression-vector plasmids created for use in this study are provided in Table 2.2.

2.3.11 Sequencing of plasmid DNA

Sequencing was performed externally (GATC, UK). Sequencing reactions of 10 µl contained 100-500 ng plasmid DNA and 2.5 µM sequencing primer. The sequences obtained were compared to the expected sequences using Clustal-X alignment software (European Bioinformation Institute, UK). Details of the sequencing primers used are provided in Table 2.3.

Table 2.2: Plasmids created for use in this study

Dematin constructs were first cloned into the pENTR11 entry vector, before gateway transfer into pcDNA3.1, pTrexDEST30, or pDEST27 as required. The protein molecular weight (MW) refers to the mass of the protein product that is expressed upon transfection of mammalian cells with a given construct.

Insert	Vector	Plasmid size (bp)	Protein MW (KDa)	Antibiotic Resistance
Dematin	pENTR11*FLAG*	3957	/	kanamycin
	pTrexDEST30*FLAG*	8335	56.1	ampicillin
	pDEST27*FLAG*	7656	83.4	ampicillin
N1	pENTR11*FLAG*	2773	/	kanamycin
	pcDNA3.1*FLAG*	5501	11.6	ampicillin
	pDEST27*FLAG*	6472	38.9	ampicillin
N2	pENTR11*FLAG*	3127	/	kanamycin
	pcDNA3.1FLAG	5855	24.7	ampicillin
	pDEST27*FLAG*	6826	52.0	ampicillin
N3	pENTR11*FLAG*	2923	/	kanamycin
	pcDNA3.1*FLAG*	5651	18.1	ampicillin
	pDEST27*FLAG*	6622	45.4	ampicillin
C1	pENTR11*FLAG*	2974	/	kanamycin
	pcDNA3.1*FLAG*	5702	22.3	ampicillin
	pDEST27*FLAG*	6673	49.6	ampicillin
DHP	pENTR11*FLAG*	2743	/	kanamycin
	pTrexDEST30*FLAG*	7481	11.5	ampicillin
	pDEST27*FLAG*	6442	38.8	ampicillin
DHP+22	pENTR11*FLAG*	2809	/	kanamycin
	pTrexDEST30*FLAG*	7187	12.7	ampicillin
	pDEST27*FLAG*	6506	40.0	ampicillin

Table 2.3: Sequencing primers used in this study

All cloned and mutagenised plasmids were sequenced to confirm that the correct products had been created. Constructs in the pENTR11 entry vector were sequenced with pENTR11-forward and/or pENTR11-reverse, which recognise the ATTL recombination sites preceding and succeeding the start and stop codons. The T7 primer was used to sequence plasmids in either the pTrexDEST30 or pDEST27 vectors, which both contain a T7 reverse priming site at the C-terminal end of the insert.

Primer	Target	Primer sequence (5' - 3')
pENTR11-forward	attL1	TAAGCAGAAGGCCATCCTCACG
pENTR11-reverse	attL2	GTAACATCAGAGATTTTGAGACAC
T7-forward	T7	TAATACGACTCACTATAGGG
Bgh reverse	Bgh	TAGAAGGCACAGTCGACG

2.3.12 Mutagenesis of plasmid DNA

Single point mutations were introduced in plasmid DNA using the QuikChange Site-Directed Mutagenesis Kit (Stratagene, USA). This was conducted according the standard manufacturer's protocol, except for the use of *Pfu* DNA polymerase instead of *Pfu Turbo*. All mutagenesis reactions were conducted in 25 µl volumes containing 50 ng of template DNA, 60 ng each of sense and antisense primers, 0.2 mM dNTPs, 1x *Pfu* buffer with $MgSO_4$ and 0.5 units *Pfu* DNA polymerase. The following thermal cycling conditions were used:

Initial denaturation	95°C	30 seconds	
Denaturation	95°C	30 seconds	16 cycles
Annealing	55°C	1 minute	
Extension	68°C	2 min / Kb	
Hold	4°C		

The reaction was incubated with 1 µl of *DpnI* for 3 hours at 37°C to digest methylated template DNA. Reactions were transformed into TOP10 *E.coli* as in section 2.2.3, and transformants selected on agar plates containing the appropriate antibiotic. Colonies were used to inoculate 5 ml cultures and the DNA extracted as in section 2.3.1. Where possible the introduced diagnostic restriction site was used to facilitate easy identification of correct mutants (see Table 2.4 and Table 2.5 for specific sites). Multiple amino acid changes in a single plasmid were created by sequentially introducing individual mutations using the above method.

2.3.13 Mutagenesis primers

Primers for the mutagenesis of plasmid DNA were designed according to manufacturer's specifications for use with the QuikChange Site-Directed Mutagenesis Kit. When possible, primers were designed to introduce a diagnostic restriction site into the mutated region, without changing the surrounding amino acid sequence. Mutagenesis was used to introduce serine / threonine to alanine, aspartic acid, or glutamic acid mutations of kinase phosphorylation sites, using the primers provided in Table 2.4 and Table 2.5. Mutagenesis was also for sequence deletions, as detailed in Table 2.6.

Table 2.4: Primers for the mutagenesis of p38 phosphorylation motifs

Serine residues (S) within p38 phosphorylation motifs were mutated to alanine (A), aspartic acid (D), or glutamic acid (E) residues using site directed mutagenesis. Diagnostic restriction sites were introduced to identify positive mutants. Amino acid changes are underlined, with bases in bold type indicating those that are different to the wild-type sequence**.**

Mutation	Primer	Primer sequence 5' - 3'	Restriction site added
S11A	For	CAGAAGCAACCACTTAC**GG**C**G**CCCGGGAGCGTG	NarI GG/CGCC
	Rev	CACGCTCCCGGG**CG**C**C**GTAAGTGGTTGCTTCTG	
S16A	For	CCCGGGAGCGTG**GCG**CCCTCCCGAGATTCCAG	NarI GG/CGCC
	Rev	CTGGAATCTCGGGAGGG**CGC**CACGCTCCCGGG	
S26A	For	CAGTGTGCCTGGC**G**C**C**CCCTCCAGCATCG	NarI GG/CGCC
	Rev	CGATGCTGGAGGG**GG**C**C**GCCAGGCACACTG	
S87A	For	CGCGAGCGCTCGCTG**GCG**CCCAAATCCAC	NarI GG/CGCC
	Rev	GTGGATTTGG**C**G**C**CAGCGAGCGCTCGCG	
S87E	For	CGCGAGCGCTCGCTG**GAG**CCCAAATCCAC	(no site)
	Rev	GTGGATTTGGG**CTC**CAGCGAGCGCTCGCG	
S92A	For	CCCAAATCCACA**GAG**CCCCCACC	NarI GG/CGCC
	Rev	GGTGGGGG**CTC**TGTGGATTTGGG	
S92E	For	CCCAAATCCACA**GAG**CCCCCACC	(no site)
	Rev	GGTGGGGG**CTC**TGTGGATTTGGG	
S96A	For	CCCCCACC**GG**C**G**CCAGAGGTGTGGGCGGACAGCCGG	NarI GG/CGCC
	Rev	CCGGCTGTCCGCCCACACCTCTGG**C**G**CC**GGTGGGGG	
S96E	For	CCCCCACCA**GAG**CCAGAGGTGTGGGCGGACAGCCGG	(no site)
	Rev	CCGGCTGTCCGCCCACACCTCTGG**CTC**TGGTGGGGG	
S105A	For	CGGACAGCCGG**G**C**G**CCTGGAATCATC	NarI GG/CGCC
	Rev	GATGATTCCAGGC**G**C**C**CGGCTGTCCG	
S105E	For	CGGACAGCCGG**GAG**CCTGGAATCATC	(no site)
	Rev	GATGATTCCAGG**CTC**CCGGCTGTCCG	
S383A	For	CTCAAGGGTATTTGCCATG**G**C**G**CCTGAAGAGTTTGGCAAG	NarI GG/CGCC
	Rev	CTTGCCAAACTCTTCAGG**C**G**C**CATGGCAAATACCCTTGAG	
S383D	For	CTCAAGGGTATTTGCCATG**GAT**CCTGAAGAGTTTGGCAAG	BamHI
	Rev	CTTGCCAAACTCTTCAGG**ATC**CATGGCAAATACCCTTGAG	

Table 2.5: Primers for the mutagenesis of 14-3-3 binding motifs

Serine (S) residues within 14-3-3 binding motifs were mutated to alanine (A) residues using site directed mutagenesis. Diagnostic restriction sites were introduced to identify positive mutants. Amino acid changes are underlined, with bases in bold type indicating those that are different to the wild-type sequence.

Mutation	Primer	Primer sequence 5' - 3'	Restriction site added
S22A	For	CCCTCCCGAGATTCC**GCG**GTGCCTGGCTCTCCCTC	SacII CCGC/GG
	Rev	GAGGGAGAGCCAGGCAC**CGC**GGAATCTCGGGAGGG	
S85A	For	CCGCGAGCGCG**CG**CTGTCACCCAAATC	BssHII G/CGCGC
	Rev	GATTTGGGTGACAG**CG**CGCGCTCGCGG	
S269A	For	GGAAAACCCGC**G**C**G**CTGCCTGACCGGAC	BssHII G/CGCGC
	Rev	GTCCGGTCAGGCAG**CG**C**G**CGGGTTTCC	
S289A	For	CGTCTAAATCTTC**AG**C**G**CTCCCCGCCTATGGC	AfeI AGC/GCT
	Rev	GCCATAGGCGGGGAG**C**G**CT**GAAGATTTAGACG	
S333A	For	GGATGGACCGGGGGAA**AGCG**CTGCCCTGTGTGCTGG	AfeI AGC/GCT
	Rev	CCAGCACACAGGGCAG**CGCT**TTCCCCCGGTCCATCC	
S403A	For	CAAGAAGAAGGCC**G**CTCTCTTCTGACTCGAG	(no site)
	Rev	CTCGAGTCAGAAGAG**C**GGCCTTCTTCTTG	

Table 2.6: Mutagenesis primers for the deletion of regions of interest

Site directed mutagenesis was used to delete the headpiece insert of dematin, and the PEST motif. Primer sequences are given, with ___ indicating the region that has been deleted.

Deletion	Construct created	Primer	Primer sequence 5' - 3'
Headpiece Insert (aa 320-341)	Dematin48	For	GGAAGCCCAGGCCTGCAGA___TCTATCCCTATGAAATG
		Rev	CATTTCATAGGGATAGA___TCTGCAGGCCTGGGCTTCC
PEST motif (aa 89-104)	Dematin_ ΔPEST	For	GCGCTCGCTGTCACCC___TCGCCTGGAATCATC
		Rev	GATGATTCCAGGCGA___GGGTGACAGCGAGCGC

2.4 Culture of mammalian cell lines

Cell culture procedures were performed in a class II microbiological safety cabinet (Walker, UK) under sterile conditions. All media and reagents were filter-sterilised through a 0.22 µM filter, and warmed to 37°C prior to use. Cells were maintained in a CO_2 incubator (Sanyo, UK) at 37°C with 5% CO_2 in a humidified atmosphere. Cultured cells were visualised using a Nikon Eclipse TS1500 inverted light-microscope (Nikon, UK).

2.4.1 Culture of HEK293T Cells

Human Embryonic Kidney (HEK) 293T cells (ATCC, USA) were cultured in Dulbecco's Modified Eagles Medium (DMEM; Gibco, UK) supplemented with 10% Foetal Bovine Serum (FBS; Biosera, UK) and 100 units/ml of Penicillin/Streptomycin (PenStrep; Gibco, UK). Cells were removed for passaging by washing with PBS, and pelleted with centrifugation at 130 x g for 4 minutes. Cells were resuspended in the relevant volume of media and seeded in appropriate culture vessels at the required density.

2.4.2 Transient transfection of HEK293T cells using calcium phosphate

24 hours prior to transfection HEK293T cells were seeded at a density of 1.4 x 10^6 cells per 100 mm plate, or 5 x 10^5 cells per 60 mm plate, as required. Media was replaced 2-4 hours before transfection. Per 1 ml of transfection reagent 500 µl DNA/calcium solution (20 µg of plasmid DNA, 50 µl 2.5 M $CaCl_2$ in water) was added dropwise to 500 µl HBS with vortexing, mixed thoroughly and incubated at room temperature for 20 minutes. The solution was added to cells (1 ml / 100 mm plate, 333 µl / 60 mm plate) and incubated at 37°C. Culture media was replaced 24 hours after transfection, and cells lysed for analysis after a further 24 hours.

2.4.3 Culture of C2C12 Cells

C2C12 mouse pre-myocytes (ATCC, USA) were cultured in low-glucose (5.5 mM) DMEM (Gibco, UK) supplemented with 10% FBS and 100 units / ml PenStrep. Cells were removed for passaging with a 5 minute incubation at 37°C with trypsin-EDTA (0.25% v/w trypsin with 0.53 mM EDTA in HBSS; GIBCO, UK), and the enzyme inhibited with 5 ml of culture medium. Cells were centrifuged at 130 x g for 4

minutes and the cells resuspended and seeded as required. Cells were maintained at 10 - 60% confluence to prevent contact mediated differentiation. To differentiate C2C12 cells from myocytes to myotubes, cells were grown to approximately 80% confluence in normal growth medium before being switched to low-serum DMEM containing 2% Horse serum. Cells were incubated at 37°C for 5-10 days as required, and the media replaced every 2-3 days. Differentiation was assessed by monitoring the distinct morphological changes in the cells, from compact individual myocytes to elongated multi-nucleated myotubes.

2.4.4 Transient transfection of C2C12 myocytes by electroporation

C2C12 cells for use in immunofluorescence experiments were transfected using electroporation. Cells at 50-60% confluence were trypsinised, pelleted at 130 x g for 4 minutes, and resuspended in 1 x HBS at a concentration of 2 x 10^6 cells / ml. 10 µg of the relevant DNA was added to each 0.4 cm electroporation cuvette (BioRad, UK), followed by 400 µl of cell solution, and flicked thoroughly to mix. Cells were electroporated using the Gene Pulser MXcell™ Electroporation System, with a ShockPod™ Cuvette Chamber attachment (BioRad, UK), under the following conditions:

Pulse type	Square wave
Number of pulses	1
Pulse duration	25 ms
Capacitance	960 µF
Voltage	350 V
Resistance	∞ Ω

Electroporated cells were transferred to the appropriate culture vesicle containing complete culture media, and incubated at 37°C for 2 days until the desired confluence was reached. Culture media was replaced after 24 hours.

2.4.5 Transient transfection of C2C12 myocytes using PEI

Cells were seeded at a density of 2.8 x 10^6 / 100 mm dish at 24 priors to transfection, to be approximately 60% confluent at the time of transfection. Per 100 mm dish, 800 µl serum-free low-glucose DMEM was combined with 16 µg of DNA. After the addition of 100 µl of 1 mg/ml branched polyethylenimine (PEI; Sigma, UK) samples were immediately pulse-vortexed 15 times. Solutions were incubated at room temperature for 10 minutes before the addition of 5 ml low-glucose DMEM. Culture medium was removed from the cells, and the total volume of transfection mix evenly distributed across the plate. Cells were incubated for 3 hours at 37°C before the addition of a further 5 ml of media. Cells were used for subsequent experiments 48 hours post-transfection.

2.4.6 Activation and inhibition of protein kinases

Cells were treated with a number of different compounds to determine the effects of activation or inhibiting protein kinases of interest. The concentrations and treatment times for each compound are shown in Table 2.7.

2.4.7 Cryopreservation of cell lines

Cells were resuspended in complete culture medium containing 10% DMSO, and aliquotted into 1 ml volumes into cryovials. Vials were placed inside polystyrene inserts to slow the freezing process, and placed at -80°C for 2 days before being transferred to liquid nitrogen for long-term storage. On revival cells were rapidly defrosted in a 37°C waterbath, resuspended in 5 ml of complete culture medium, and centrifuged at 130 x g for 4 minutes to remove all DMSO. Pellets were resuspended in 10 ml complete culture media, seeded in a 10 cm culture dish, and incubated overnight to allow viable cells to adhere.

2.5 Western blotting

Western blots and immunoprecipitation experiments were conducted on C2C12 and HEK293T cell lysates. Where appropriate, cells were first transiently transfected with proteins of interest as in sections 2.4.2 and 2.4.5.

Table 2.7: In vivo activation and inhibition of protein kinases

The kinases AKT, AMPK, p38 and PKA were activated and inhibited in HEK293T and C2C12 cells under the conditions given. p38 was activated through transfection of a pcDNA3.1-MKK6^{DD} construct using the standard method for each cell type. All other compounds were diluted to a 1000 x concentration in DMSO, and then further diluted for use in complete culture media.

Kinase	Product	Name	Company	Concentration	Time
AKT	Activator	Insulin	Gibco	100 nm	1 hour
	Inhibitor	AKT Inhibitor VIII	Calbiochem	10 µM	4 hours
AMPK	Activator	AICAR	Sigma	500 µM	1 hour
	Inhibitor	Compound C	Calbiochem	10 µM	4 hours
p38	Activator	MKK6^{DD}	/	/	/
	Inhibitor	SB203580	Calbiochem	10 µM	4 hours
PKA	Activator	Forskolin	Sigma	10 µM	1 hour
	Inhibitor	H89	Calbiochem	10 µM	4 hours

2.5.1 Cell lysis and protein extraction

For standard western blotting experiments cells were lysed in RIPA buffer (20 mM Tris pH 8.0, 137 mM NaCl, 2 mM EDTA, 10% glycerol, 1% Triton X-100, 0.1% SDS, 0.5% sodium deoxycolate). Cells were washed twice with PBS prior to the addition of lysis buffer (500 µl/100 mm dish; 250 µl/60 mm dish). Cells were scraped from the dishes and incubated on ice for 30 minutes. Lysates were cleared by centrifugation at 13,000 x g for 10 minutes at 4°C. Supernatants were used immediately or stored at -20°C until required.

2.5.2 Protein quantification

Where appropriate the protein content of cell lysates was determined using a Bicinchoninic Acid (BCA) assay (Sigma, UK). Samples were diluted by a factor of 1/5 to 1/20 in lysis buffer between, and 25 µl of each added to a 96-well plate in duplicate. Dilutions of BSA between 0 -1 mg/ml were used as standards. 200 µl of detection reagent was added to each sample well, and the plate incubated at 37°C for 30 minutes. Absorbance was measured on an iMark Microplate Absorbance Reader (BioRad, UK) at 570 nm. A calibration curve of the standard absorbance values versus concentration was produced, and linear regression used to calculate the equation of the trendline. This was used to determine the unknown sample concentrations.

2.5.3 SDS-PAGE separation of proteins

Protein samples were mixed with 5x loading buffer (10% SDS; 10 mM DTT; 20 % glycerol; 0.1 M Tris pH 6.8; 10% blue bromophenol) and heated to 95°C for 5 minutes prior to loading. Proteins were separated on 8 x 8 cm tris-glycine gels prepared at the relevant percentage for optimum separation of the proteins of interest, after passing through a stacking gel (Table 2.8). Pre-stained protein ladder (Fermentas, UK) was used as a size reference. Proteins were separated by electrophoresis at 160 V for 90 minutes in running buffer (2.5 M Tris Base (Foremedium, UK); 192 mM glycine (Fischer, UK); 0.1% SDS (Sigma, UK); pH 8.3).

Table 2.8: Composition of protein stacking and separating gels

Tris-glycine gels of varying acrylamide percentages were selected to provide optimum separation of proteins of interest. The lower portion of the gel was composed of 7.5 ml separating gel (A) with 2.5 ml stacking gel (B) on top. (*APS; ammonium persulphate, SDS; sodium dodecyl sulphate, TEMED; Tetramethylethylenediamine)*

A

Separating Gel (10ml)	**8 %**	**10 %**	**12 %**
Water	4.6 ml	4.0 ml	3.3 ml
1.5 M Tris pH 8.8	2.5 ml	2.5 ml	2.5 ml
10 % SDS	100 µl	100 µl	100 µl
Acrylamide / Bis (30/0.8 %)	2.7 ml	3.3 ml	4.0 ml
10 % APS	90 µl	90 µl	90 µl
TEMED	10 µl	10 µl	10 µl

B

Stacking Gel (5 ml)	
Water	2.94 ml
0.5 M Tris pH 6.8	1.25 ml
10 % SDS	50 µl
Acrylamide / Bis (30/0.8 %)	700 µl
10 % APS	50 µl
TEMED	10 µl

2.5.4 Protein transfer onto nitrocellulose membrane

Following SDS-PAGE separation, proteins were transferred onto nitrocellulose membrane (GE Healthcare, UK) at 40 V for 90 minutes in transfer buffer (12 mM Tris Base; 96 mM glycine; pH 8.3) with 20 % methanol.

2.5.5 Detection of protein by immunoblotting

Non-specific binding sites were blocked with 5% BSA in TBST (137 mM sodium chloride, 20 mM Tris, 0.1% Tween-20; pH 7.6) for 1 hour at room temperature. Membranes were incubated overnight at 4°C with primary antibodies against the relevant proteins. Antibodies were diluted in 5% BSA/TBST at concentrations indicated in Table 2.9. Excess antibody was removed with washes in TBST; 3 x 10 seconds followed by 3 x 10 minutes. Membranes were incubated with secondary antibody in TBST for 1 hour at room temperature, at dilutions shown in Table 2.10. Residual antibody was removed by washing in TBST as before.

2.5.6 Chemiluminescent visualisation of proteins

Proteins were visualised using chemiluminescence. Membranes were incubated with 1 ml of a 1:1 ratio of Supersignal West Pico Stable Peroxidise Solution to Supersignal West Pico Luminol Enhancer Solution (Pierce, UK) for 5 minutes, before the excess solution was removed. Blots were developed on x-ray film (Fujifilm, UK) using a Curix 60 Processor (Agfa, Belgium) with exposure times of 1 second - 60 minutes performed as required.

2.5.7 Relative quantification of protein expression

Western blot exposures were selected to ensure that none of the bands of interest were overexposed. Films were scanned, saved as .tif files and imported into ImageJ (Schneider *et al.*, 2012). Bands were selected and the Gel Analysis feature used to determine the density of each. Values obtained were normalised against control values as appropriate.

Table 2.9: Primary antibodies for western blotting an immunoprecipitation

All primary antibodies were diluted to the concentrations given in 5% BSA/TBST. Antibody dilutions were stored in sealed tubes at 4°C for re-use. Incubation was conducted at the temperatures stated with gentle agitation. *(BSA; bovine serum albumin, IP; immunoprecipitation, O/N; overnight, TBST; tris-buffered saline solution)*

Antibody	Supplier	Host Species	Dilution for western	Amount per IP	Incubation conditions
14-3-3β	Santa Cruz	Rabbit	1/500	1 µg	O/N 4°C
c-MYC	Santa Cruz	Rabbit	1/500	/	RT 1 hour
c-MYC	Serotek	Mouse	/	1 µg	/
Dematin	Santa Cruz	Mouse	1/500	/	O/N 4°C
Dematin	Sigma	Rabbit	/	1 µg	/
FLAG M2	Stratagene	Mouse	1/5000	/	RT 1 hour
FLAG M5	Sigma	Mouse	/	1 µg	/
GAPDH	Abcam	Mouse	1/5000	/	RT 1 hour
MK2	Millipore	Mouse	1/2000	/	O/N 4°C
MK2-phospho	Cell Signalling	Rabbit	1/1000	/	O/N 4°C
MPM2	Millipore	Mouse	1/500	/	O/N 4°C
p38	Cell Signalling	Rabbit	1/1000	/	O/N 4°C
p38-phospho	Cell Signalling	Rabbit	1/1000	/	O/N 4°C

Table 2.10: Secondary antibodies for western blotting

Secondary antibodies of compatible species with the primary used were diluted as stated in TBST, and incubated with gentle agitation. Where lysates had been immunoprecipitated and the protein of interest was of a similar molecular weight to antibody heavy / light-chain, a chain specific antibody was used. All secondary antibodies were HRP-conjugated for compatibility with chemiluminescent detection. *(HC; heavy chain, LC; light chain, TBST; tris-buffered saline solution).*

Antibody	Supplier	Heavy / light chain specificity	Dilution for western	Incubation conditions
anti-Mouse	Pierce	Heavy + Light	1/20,000	O/N 4°C or RT 1 hour
anti-Mouse-LC	Jackson Labs	Light	1/120,000	O/N 4°C or RT 1 hour
anti-Rabbit	Cell Signalling	Heavy + Light	1/20,000	O/N 4°C or RT 1 hour
anti-Rabbit-HC	Jackson Labs	Heavy	1/50,000	O/N 4°C or RT 1 hour

2.6 Immunoprecipitation

Cells for immunoprecipitation (IP) and GST-pulldown assays were lysed in Triton Lysis Buffer (20 mM Tris pH 7.4, 137 mM NaCl, 10% glycerol, 0.5% Triton X-100) in order to maintain protein-protein interactions.

2.6.1 Co-Immunoprecipitation

Cells were lysed immediately prior to IP experiments, and a sample of each lysate retained to confirm protein expression. IP assays were performed using 1 µg of the relevant antibody per sample (Table 2.9), and the antibody-protein complex collected on 15 µl Protein-G-Agarose beads (Millipore, UK) that were equilibrated prior to use by washing 3 x in triton lysis buffer. Following a 3 hours incubation at 4°C, non- specifically bound proteins were removed with a further 3 washes in triton lysis buffer. Lysis buffer was removed, and proteins were eluted with 5x loading buffer and a 5 minute incubation at 95°C.

2.6.2 GST pulldown assay

GST-tagged proteins were purified on GST-bind Resin columns (Millipore, UK). Cells were lysed, and the columns washed and run as in section 2.6.1.

2.6.3 Protein detection and visualisation

Proteins eluted from IP and GST columns were subjected to SDS-PAGE separation and immunoblotting, as detailed in sections 2.5.3 - 2.5.7.

2.7 Mass spectrometry

2.7.1 Protein preparation

Twenty-five 100 mm dishes of HEK293T cells were transfected with pDEST27*FLAG*-dematin using the calcium-chloride method (section 2.4.2). Dematin was purified using a large-scale GST-pulldown assay (section 2.6) with 500 µl of GST-bind resin, and of 5x sample buffer to elute proteins from the beads. Following SDS-PAGE separation (section 2.5.3) the gel was stained for 1 hour with an instant coomassie stain (Expedeon, UK) to detect the eluted proteins. The band corresponding to

dematin was excised from the gel, and lyophilised in a vacuum concentrator (Eppendorf, UK).

2.7.2 Mass spectrometry

Mass spectrometry was conducted externally by Tine Tingholm (Sweden).

2.8 p38 kinase assay

2.8.1 Protein preparation

HEK293T cells were transfected with the required constructs as described in section 2.4.1. Protein was extracted and purified on GST-pulldown columns (section 2.6). After washing 3 x in lysis buffer, columns had an additional final wash with 1 ml of 40 mM Tris, pH 7.5.

2.8.2 Kinase assay

Columns were incubated for 20 minutes at 30°C with 20 µl kinase mix containing 5 µCi γ-ATP ^{32}P and 0.2 µl p38 (Invitrogen, UK) in kinase buffer (40 mM Tris, 10 mM $MgCl_2$, 1 mM DTT). Proteins were eluted with 5x sample buffer, and separated by SDS-PAGE (section 2.5.3).

2.8.3 Protein detection and quantification

Gels were exposed to x-ray film for the required amount of time to detect the bands of interest, from 1 hour to overnight, and films developed as in section 2.5.6.

2.9 Immunofluorescence staining

C2C12 cells were transfected with the relevant constructs in the pTrexDEST30 mammalian expression vector using electroporation (section 2.4.4), and seeded onto 18 mm glass coverslips that were pre-sterilised with 100% ethanol.

2.9.1 Sample processing

Two days after transfection, coverslips were transferred to a 12-well plate and washed twice with PBS. Cells were fixed with 4% paraformaldehyde (PFA) for 10

minutes at room temperature. After two washes in PBS, cells were permeabilised with 1% Triton X-100 in PBS. Cells were then blocked in 3% BSA/TBST for 30 minutes at room temperature.

2.9.2 Fluorescent antibody detection of proteins

Cells were incubated with primary antibody (**Error! Reference source not found.**) in 3% BSA/TBST for 1 hour at room temperature. Unbound primary antibody was removed by washing with PBS for 3 short washes followed by one 15-minute wash with gentle shaking. Cells were incubated in the dark with secondary antibody (**Error! Reference source not found.**) in 3% BSA/TBST for 1 hour at room temperature. Unbound secondary antibody was removed by washing as before. Cells were mounted onto microscope slides using Prolong Gold antifade mountant (Invitrogen, UK). Slides were stored at room temperature overnight to set the mounting medium, and kept at -20°C for long-term storage.

2.9.3 Confocal Microscopy

Images were captured on an inverted TCS SP5 Confocal Laser Scanning Microscope connected to a Leica DM RBE epifluorescence microscope (Leica, Germany). Immunofluorescent staining was examined using a 60x or 100x oil-immersion objective, and images acquired using Leica Microsystem LAS AF AF6000 software, and saved as .tiff files. Sequential scanning was used to prevent bleed-through between channels. For proteins detected with Alexa-Fluor®488 conjugated secondary antibodies a 488nm Argon Laser was used, staining with Alexa Fluor® 568 Phalloidin was imaged with a Ti Sapphire Laser 561nm, and nuclear staining with DAPI was detected using a Blue Diode Laser. The scan speed was set to 550 Hz, and images were taken at a resolution of 512 x 512 pixels. Optical sections were taken at 0.8 µm intervals, and pinhole diameter was set at 1.0 airy unit. Confocal images were processed using the Leica LAS AF Lite software (Leica, UK).

Supplier	Host Species	Dilution	Secondary Antibody / stain	Supplier	Host Species
Santa Cruz	Mouse	1/100	Alexa Fluor® 568 goat anti-mouse IgG (H+L)	Invitrogen	Goat
Stratagene	Mouse	1/200	Alexa Fluor® 488 goat anti-mouse IgG (H+L)	Invitrogen	Goat
			Alexa Fluor® 568 goat anti-mouse IgG (H+L)	Invitrogen	Goat
Santa Cruz	Rabbit	1/200	Alexa Fluor® 488 chicken anti-rabbit IgG (H+L)	Invitrogen	Chicken
/	/	/	Alexa Fluor® 568 Phalloidin	Invitrogen	/
/	/	/	DAPI (4',6-Diamidino-2-Phenylindole, Dihydrochloride)	Invitrogen	/

2.10 Pulse-chase labelling

Cells were maintained in a CO_2 incubator at 37°C with 5% CO_2 in a humidified atmosphere for all incubation steps. A schematic of the experimental protocol is given in Figure 2.2.

2.10.1 Preparation of cells

For experiments using overexpressed protein, C2C12 cells were seeded at a density of 8 x 10^5 cells / p60 dish 48 hours prior to the start of the experiment. Cells were transfected 24 hours later using the PEI method detailed in section 2.4.5.

2.10.2 Activation and inhibition of p38 MAPK

For p38-hyperactivated samples, cells were transfected with 4.6 µg dematin DNA and 1.5µg pcDNA3.1*FLAG*-MKK6 per p60 dish. To assess the effects of p38 inhibition, cells were incubated with the specific inhibitor SB203580 (Table 2.7) for 2 hours prior to the depletion period, and throughout the depletion, labelling, and chase periods.

2.10.3 Labelling of protein with ^{35}S methionine / cysteine

Cells were washed with 3 x 2 ml PBS and incubated for 1 hour in 2 ml of Depletion Medium (cysteine- and methionine-free DMEM (CMF-DMEM; Invitrogen)). Media was aspirated and replaced with 0.5 ml Pulse Medium (CMF-DMEM with 100 µCi / ml ^{35}S labelled methionine and cysteine; Perkin Elmer) for 30 minutes. Cells were washed with 3 x 2 ml PBS, and incubated with 2 ml of Chase Media (DMEM with 1 mM L-cysteine and 3 mM L-methionine).

2.10.4 Cell lysis and immunoprecipitation

Samples were taken at chase intervals of 0-24 hours (measured from the end of the pulse period) as appropriate. At the immediate end of the chase period, cells were washed with 2 x 2ml warm PBS and scraped into 500 µl triton lysis buffer. Lysates were snap frozen in liquid nitrogen and stored at -80°C until all samples had been collected. Cell lysates were immunoprecipitated with an anti-FLAG antibody as described in section 2.6.1, and separated by SDS-PAGE as in section 2.5.3.

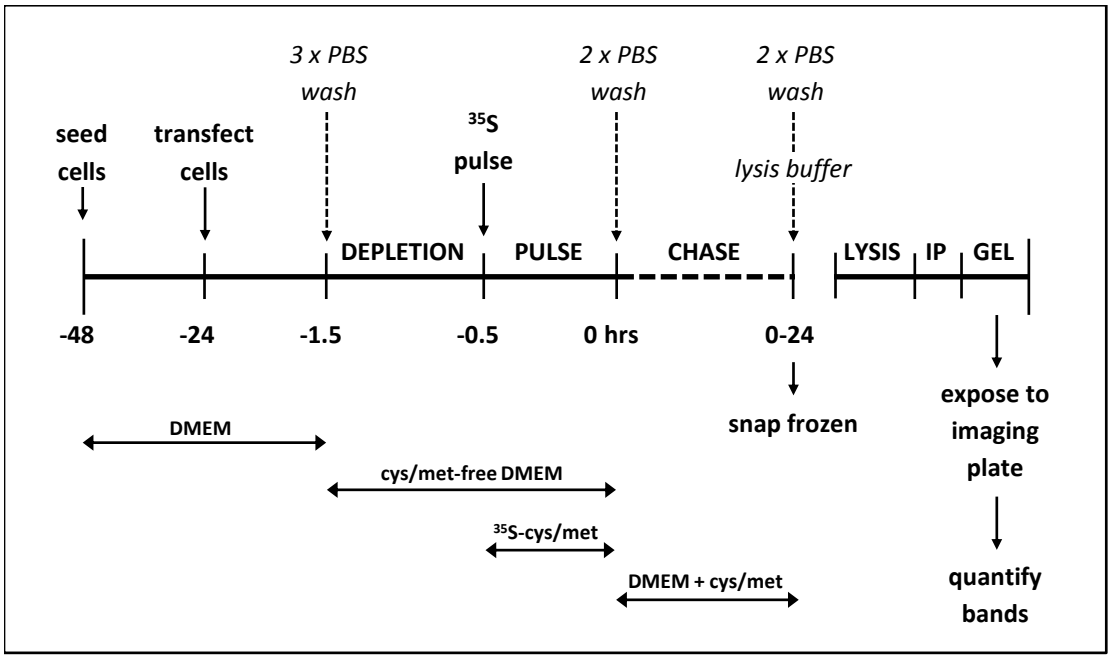

Figure 2.2: Schematic of the experimental protocol for pulse-chase experiments

An outline of the protocol used for pulse-chase experiments, the full details of which are described in the text. (cys; cysteine, IP; immunoprecipitation, met; methionine, PBS; phosphate-buffered saline)

2.10.5 Protein detection and quantification

SDS-PAGE gels were exposed to a white phosphor imaging plate (Fuji, Germany). Plates were imaged on a Typhoon FLA 95000 laser scanner (GE Healthcare). Standard Phosphorimaging settings were used; 635 nm laser with an imaging plate filter. Images were taken at a 10 µm resolution and saved as .tif files.

2.10.6 Statistical analysis

The density of each band was quantified using Image J. Within each treatment, values were normalised to the 0 chase period timepoint. Data presented are means of these normalised values from three independent experiments ± SEM. Statistical analysis was performed using GraphPad Prism 6 (GraphPad, USA). Data was fitted to a one phase decay equation, with the plateau constrained to y=0. Intracellular protein half-life values for each condition were interpolated from the graphs.

2.11 Actin binding and bundling assays

2.11.1 Strep-tag purification

HEK293T cells were co-transfected with the relevant strep-tagged dematin construct, and 14-3-3β, as described in section 2.4.2. Cells were lysed in triton lysis buffer, and the lysates cleared as described in section 2.5.1. Strep-tagged proteins were purified from the lysates on Strep-bind Resin columns (Millipore, UK). Columns were washed and run as in section 2.6.1. Bound proteins were eluted from the columns in 2.5 mM desthiobiotin in triton lysis buffer at room temperature for 10 minutes.

2.11.2 Visualisation of purified proteins

Eluted proteins were separated by SDS-PAGE as in section 2.5.3. Gels were stained with InstantBlue coomassie-based stain (Expedeon, UK) for 1 hour at room temperature to confirm that products of the expected molecular weights had been purified, and the protein-protein interactions were maintained where appropriate.

2.11.3 Preparation of F-actin binding and bundling reactions

Actin binding and bundling reactions were prepared using the same reagents, as detailed in Table 2.11. Reagents were added in the order specified in the table, and mixed after addition of the test protein by gently pipetting up and down three times.

2.11.4 F-actin binding

Samples were incubated at 24°C for 30 minutes, before being centrifuged at 150,000 x g for 1.5 hours at 24°C.

2.11.5 F-actin bundling

Samples were incubated at 24°C for 30 minutes, before being centrifuged at 14,000 x g for 1 hour at 24°C.

2.11.6 Sample processing

Supernatants from the binding and bundling reactions were removed, and combined with 10 µl 5x Laemmli reducing sample buffer. Pellets were resuspended in 30 µl Milli-Q water and pipetted for 2 minutes to fully resuspend. Samples were incubated on ice for 10 minutes before a further 2 minutes of resuspending. Resuspended pellets were combined with 30 µl 2x Laemmli reducing sample buffer.

2.11.7 Visualisation of proteins

SDS-PAGE was used to separate 20 µl of each sample, using the method detailed in section 2.5.3. Proteins were visualised with InstantBlue coomassie-based stain as in 2.11.2.

2.11.8 Protein quantification and analysis

Coomassie stained gels were imaged, and the intensity of the protein bands present in each of the supernatant and pellet samples quantified using ImageJ. The percentage of the protein found in each fraction was then calculated and compared to the control values.

Table 2.11: Composition of the actin binding and bundling reactions

The components of each of the control and test-protein reactions were added in the order listed in the table, and pipetted gently to mix the contents. Samples were then processed for either actin-binding or actin-bundling as described in the text.

ample	F-actin Buffer	F-actin	Test Protein	Protein Buffer	α-actinin	1M Tris pH 6.5
tin only ontrol	/	40 µl	/	10 µl	/	/
tinin only ontrol	40 µl	/	/	/	10 µl	2 µl
ontrol (α- and F-actin)	/	40 µl	/	/	10 µl	2 µl
control (BSA F-actin)	/	40 µl	/	/	/	/
ein only	40 µl	/	10 µl	/	/	/
ein and -actin	/	40 µl	10 µl	/	/	/

3. Regulation of dematin by the p38 MAPK

3.1 Introduction

The p38 MAPK is activated by the specific upstream kinases MKK3 and MKK6 (Raingeaud *et al.*, 1996), and subsequently phosphorylates its substrates at either Ser or Thr residues that are generally followed by a Pro (Cuadrado & Nebreda, 2010). Confirmed substrates of p38 include a number of cytoskeletal components (Trempolec *et al.*, 2013), but the role of p38 in regulating the cytoskeleton is not well defined. Identification of further cytoskeletal-associated p38 substrates will therefore aid in the characterisation of this regulation. Preliminary data obtained in our lab, from both microarray experiments and in vitro kinase assays, identified the actin binding and bundling protein dematin as a novel substrate of the p38 MAPK kinase. Furthermore, sequence analysis identified 13 potential phosphorylation motifs that could be targeted by p38 (Figure 1.2). There is currently a limited understanding of the regulation of dematin, and therefore investigating the potential regulation of dematin by p38 MAPK may offer insights into both the regulation of dematin and the role of p38 in cytoskeletal control.

There are several regions of dematin that could potentially be regulated by p38 phosphorylation. Analysis of the primary sequence of dematin identified the presence of a PEST degradation motif (Rana *et al.*, 1993), which has previously been correlated with protein instability (Rogers *et al.*, 1986). The majority of PEST motifs act as primary destruction signals and must be activated by a second regulatory mechanism, the most common of which is phosphorylation (Rechsteiner & Rogers, 1996). Interestingly the PEST sequence in dematin contains two internal Ser-Pro phosphorylation motifs, and is flanked by a further two sites (Figure 1.2), suggesting that p38 could be a prime candidate for the phospho-regulation of dematin stability.

Most know functions of dematin involve the HP domain, making this region an important target for regulatory phosphorylation. A single p38 phosphorylation motif is located in the HP at Ser^{383} (Figure 1.2). The position of this motif at the extreme end of an α-helix (Figure 1.2 means that phosphorylation of Ser^{383} could potentially induce a localised conformational change in the HP. Recent NMR experiments have demonstrated that PKA phosphorylation of the dematin HP at

Ser^{381} [Ser^{403}] increases its affinity for the normally independent core domain. This change in proximity sterically hinders one of the two actin binding sites, preventing dematin from bundling actin (Chen *et al.*, 2013). Phosphorylation of the HP at Ser^{383} may therefore induce a conformational change that disrupts this function, providing a mechanism through which p38 could regulate actin bundling.

The experiments presented in this chapter aimed to answer the following questions:

1) Is dematin phosphorylated by the p38 MAPK in vivo?
2) Which regions of dematin are phosphorylated by p38?
3) Is degradation of dematin mediated by its PEST motif?
4) Does p38 phosphorylation regulate PEST mediated degradation of dematin?
5) Which region of the core domain does the dematin headpiece bind to?
6) Is this binding regulated by p38 phosphorylation of the headpiece?

3.2 Cloning of dematin constructs

In order to investigate the function and regulation of dematin, a number of constructs were cloned for expression in mammalian cell lines. These included both the 48 and 52 KDa full-length splice variants of dematin that occur in vivo, in addition to a number of truncated dematin constructs for investigations into specific regions of the protein.

3.2.1 Cloning of dematin into the pENTR11 entry vector

PCR was used to amplify the coding region of the Homo sapiens dematin gene (Homo sapiens erythrocyte membrane protein band 4.9 (dematin); BC017445.1), using pCMV6-XL5-dematin as a template. Primers were designed to amplify the dematin gene and add NcoI and XhoI restriction sites onto the 5' and 3' ends of the PCR product respectively in order to facilitate high efficiency, directional, cloning into the pENTR11 gateway entry vector (Figure 3.1). The amplified PCR product and the pENTR11*FLAG* vector were digested with NcoI and XhoI restriction enzymes. The dematin gene was then ligated into the pENTR11*FLAG* vector. This pENTR11*FLAG*-dematin construct was then used as a template for the PCR amplification of a number of truncated dematin constructs. Primers were designed to amplify the following regions of the dematin sequence: dematinN1; aa 0-78, dematinN2; aa 0-196, dematinN3; aa 69-196, dematinC1; aa 261-405 and dematinHP; aa 316-319/342-405. The relative positions of these truncated constructs are shown in the schematic in Figure 3.2. These truncated constructs were cloned into the pENTR11*FLAG* vector using the same method as above.

3.2.2 Cloning of constructs into mammalian expression vectors

The Invitrogen Gateway® recombination system was then used to transfer the constructs into the relevant mammalian expression vectors. Constructs for use in co-immunoprecipitation experiments were transferred to the pTrexDEST30 expression vector, while those for GST-pulldowns were expressed in pDEST27 which creates fusion proteins with an N-terminal GST tag.

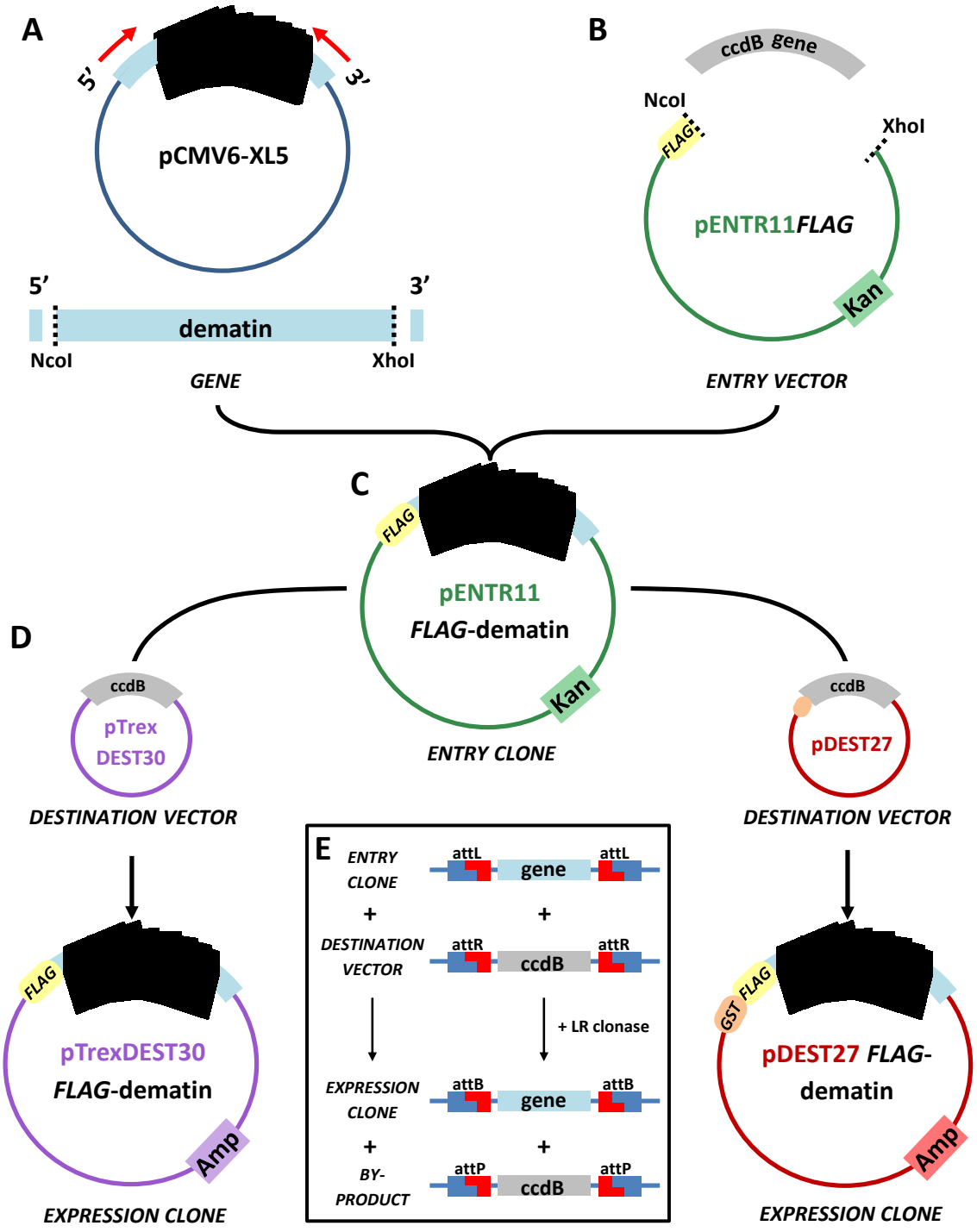

Figure 3.1: Schematic of the cloning approach used in this study

The dematin gene (BC017445.1) was PCR amplified from the pCMV6-XL5 vector (A) using primers which added NcoI and XhoI restriction sites to the N- and C-terminal ends of the product respectively. NcoI / XhoI digests of the PCR product and the entry vector PENTR11*FLAG* (B) were conducted, before ligation of the two using T4 ligase (C). Constructs were then transferred to mammalian expression vectors (D) using the Gateway recombination system.

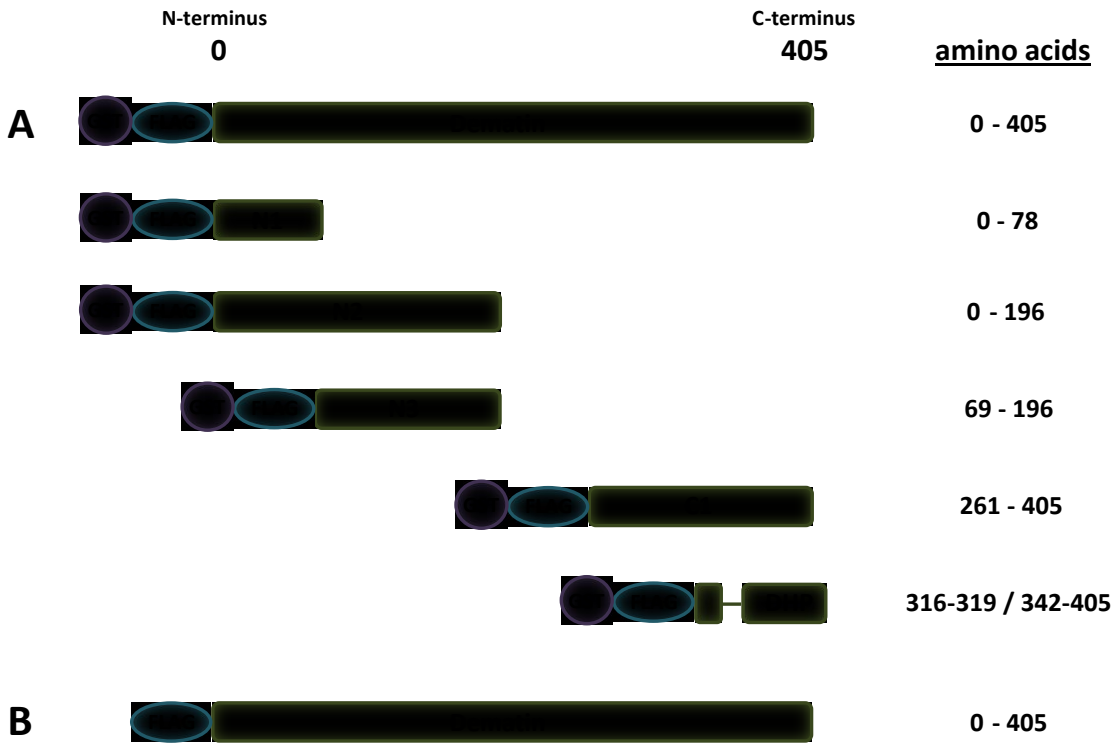

Figure 3.2: Schematic of the basic dematin constructs used in this chapter

Diagram showing the relative positions of full-length dematin and the truncated constructs cloned for use in this chapter. (A) All protein constructs for use in GST-pulldown experiments were expressed in the pDEST27 vector, creating fusion proteins with N-terminal GST tags to facilitate purification and FLAG tags for immuno-detection. (B) Constructs for use in pulse-chase protein degradation experiments were expressed in pTrexDEST30 and had only an N-terminal FLAG tag to minimise the disruption of normal protein function.

3.3 p38 phosphorylation of dematin

Preliminary screening experiments conducted in our lab identified dematin as a novel substrate of the p38 MAPK (Müller; unpublished). Here we aimed to confirm that p38 phosphorylates dematin in vivo as well as in vitro, and to identify the specific regions of dematin that are phosphorylated by p38. Due to its ubiquitous expression patterns, and higher levels of expression than p38β, p38α is the model isoform for research into the p38 MAPK family (Cargnello & Roux, 2011). This study has therefore focused solely on the p38α isoform.

3.3.1 Preliminary screening for novel p38 MAPK substrates

In a protein microarray screen conducted previously in our lab, dematin was identified as a substrate of the p38 MAPK, but not of the other MAPK family kinase ERK5 (Figure 3.3A). An in vitro kinase assay was then conducted which showed that recombinant p38 MAPK was able to phosphorylate dematin, whereas the ERK5 MAPK control was not (Figure 3.3B) (Müller; unpublished). This data provided preliminary evidence that dematin is a novel substrate of the p38 MAPK, and formed the basis of this study.

3.3.2 In vitro phosphorylation of dematin by p38

In vitro kinase assays using recombinant p38 were conducted to determine which regions of dematin are phosphorylated by p38. The pDEST27*FLAG* constructs of full-length dematin and the truncated constructs dematinN1, N2, N3 and C1 (Figure 3.2) were expressed in HEK293T cells. GST-pulldown columns were used to purify the dematin constructs from the cell lysates, and these proteins were then incubated with γ-ATP ^{32}P and recombinant p38α. After separation of the eluted proteins by SDS-PAGE, gels were exposed to radiographic film. Bands were detected for full-length dematin as well as dematinN1, N2, N3, and C1, indicating the presence of incorporated ^{32}P in these proteins (Figure 3.4). This indicates that p38 phosphorylates dematin at multiple sites in vitro, and that phosphorylation occurs within each of the regions covered by the truncated dematinN1, N3 and C1 constructs; aa 0-78, aa 79- 196 and aa 261-405.

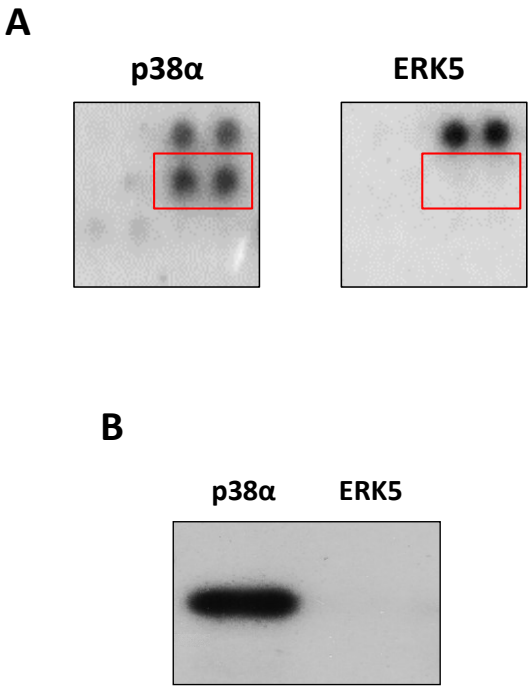

Figure 3.3: Dematin is a novel substrate of the p38 MAPK

Screening experiments were conducted to identify novel substrates of the p38 MAPK. (A) Protein microarray experiments (n=1) were conducted using the Invitrogen ProtoArray® Human Protein Microarray system, consisting of > 9,000 full-length human proteins spotted in duplicate onto a nitrocellulose coated glass slide. The arrays were blocked in 1% BSA, and incubated in kinase buffer with γ-ATP ^{33}P and either recombinant p38α or ERK5 at 30°C for 60 minutes. Following thorough washing, the slides were dried and exposed to a phosphor-imager screen. Images were taken with a phosphor-imager, and processed with the Invitrogen ProtoArray® Prospector software to identify phosphorylated proteins. The regions in red correspond to the dematin spots, indicating that the protein has been phosphorylated by p38α but not ERK5. (B) In vitro kinase experiments (n=3) were conducted to confirm the microarray results. Samples were incubated with γ-ATP ^{32}P and either recombinant p38α or recombinant ERK5. Proteins were separated by SDS-PAGE and exposed to radiographic film. A band corresponding to phosphorylated dematin was detected in the p38α samples but not in the ERK5 sample. This confirmed that recombinant p38α was able to phosphorylate recombinant dematin in vitro, whereas an alternative MAPK family member, ERK5, could not. *(ATP; adenosine tri-phosphate, ERK; extracellular-signal regulated kinase, MAPK; mitogen-activated protein kinase, SDS-PAGE; sodium dodecyl sulphate polyacrylamide gel electrophoresis).*

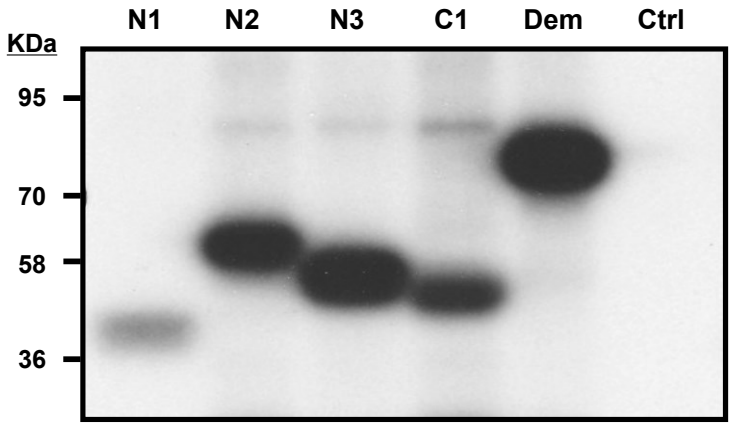

Figure 3.4: Dematin is phosphorylated at multiple sites in vitro by p38α MAPK

In vitro kinase assays were conducted to determine which regions of the dematin are phosphorylated by p38α. pDEST27*FLAG*dematin, dematinN1, dematinN2, dematinN3 and dematinC1 constructs were overexpressed in HEK293T cells, then purified on GST-pulldown columns following cell lysis. Samples were incubated with recombinant p38α and γ-ATP ^{32}P, separated by SDS-PAGE and exposed to radiographic film. Bands were detected in the full-length dematin sample and in all of the truncated constructs. The control sample consisted of p38α / γ-ATP ^{32}P reaction mix in the absence of protein (n=3). *(ATP; adenosine tri-phosphate, SDS-PAGE; sodium dodecyl sulphate polyacrylamide gel electrophoresis).*

3.3.3 Mass spectrometry identification of phosphorylated residues in dematin

Although the kinase assays demonstrated that dematin is phosphorylated by recombinant p38α at multiple sites in vitro, this does not necessarily correlate with the sites that are phosphorylated in vivo. To validate this finding, mass spectrometry was conducted to determine the specific residues in dematin that are phosphorylated by p38 in vivo. HEK293T cells were co-transfected with the pDEST27*FLAG*-dematin construct along with pcDNA3.1*FLAG*-MKK6 to hyper-activate p38. Following cell lysis, proteins were purified on a GST-binding column. The bound proteins were eluted, separated by SDS-PAGE, and stained with coomassie dye. A large band corresponding to GST*FLAG*-dematin was seen in addition to a smaller non-specific band (Figure 3.5A). The GST*FLAG*-dematin band was excised from the gel and lyophilised. Further processing and mass spectrometry detection of phosphorylated peptides was conducted by Dr. Tine Tingholm at Lund University, Sweden.

The mass spectrometry results identified residues within dematin that were phosphorylated under the experimental conditions used. MAPK kinases are known to phosphorylate their targets are either SP or TP motifs, and the primary sequence of dematin contains 13 such sites. A total of 11 phosphorylated SP / TP motifs in dematin were identified, at residues Ser^{11}, Ser^{16}, Ser^{26}, Ser^{87}, Ser^{92}, Ser^{96}, Ser^{105}, Thr^{274}, and Ser^{383}. Four motifs at Ser^{156}, Ser^{307}, Ser^{315} and Thr^{120} were not detected as being phosphorylated (Figure 3.5B).

3.3.4 In vitro validation of the MS identified p38 phosphorylation sites

The mass spectrometry results were then validated in vitro with p38-specific kinase assays. Ser to Ala mutants of the p38 motifs identified as being phosphorylated in the mass spectrometry analysis (Figure 3.5) were created using a site-directed mutagenesis approach. The truncated dematin constructs in the pDEST27*FLAG* vector were used as a template for mutagenesis reactions, and sequential reactions used to mutate all of the p38 sites identified in each fragment. An additional dematinN3 construct was created where only the S92/96 residues which fall within the PEST motif were mutated.

A

B

Phosphorylatable residue	Phosphorylated in mass spectrometry?	Truncated constructs containing this site
Serine 11	YES	N1, N2
Serine 16	YES	N1, N2
Serine 26	YES	N1, N2
Serine 87	YES	N2, N3
Serine 92	YES	N2, N3
Serine 96	YES	N2, N3
serine 105	YES	N2, N3
Threonine 120	/	N2, N3
Serine 156	/	N2, N3
Threonine 274	YES	C1
Serine 307	/	C1
Serine 315	/	C1
Serine 383	YES	C1

Figure 3.5: Phosphorylated MAPK motifs in dematin identified using mass spectrometry

HEK293T cells were co-transfected with pDEST27*FLAG*-dematin and pcDNA3.1*FLAG*-MKK6 to hyper-activate p38. A GST-column was used to purify the lysate, and the eluted proteins were separated by SDS-PAGE and stained with coomassie dye. (A) The band corresponding to GST*FLAG*-dematin was excised from the gel and lypholised. Mass spectrometry detection of phosphorylation sites within the dematin protein sample was conducted externally. (B) This data was then correlated with the potential SP / TP p38 phosphorylation motifs within the dematin sequence (n=1) (*GST; glutathione-S-transferase, MAPK; mitogen-activated protein-kinase, SDS-PAGE, sodium dodecyl sulphate – polyacrylamide gel electrophoresis).*

This produced the following constructs: pDEST27*FLAG*-dematinN1_S11/16/26A (N1-3A), pDEST27*FLAG*-dematinN3_S92/96A (N3-2A), pDEST27*FLAG*dematinN3_S87/92/96/105A (N3-4A), and pDEST27*FLAG*-dematinC1_S274/383A (C1-2A). The in vitro kinase assays were then repeated with both the wild-type constructs and the Ser to Ala mutants. An aliquot of lysate from each sample was subjected to western blot analysis with an anti-FLAG antibody to confirm that the expression levels of the wild-type and mutant constructs were comparable. All blots were scanned and the bands quantified using densitometry software. The intensity of each band was normalised to the expression control, and then the values for mutant constructs were normalised to the comparable wild-type which was given a value of 1.

As seen in the previous experiment (Figure 3.4) each of the dematinN1, N3, and C1 wild-type constructs was phosphorylated by p38 (Figure 3.6). The average band intensity for dematinN1_S11/16/26A had a normalised value of 0.04 compared to wild-type which was set to 1.0 ($p<0.0001$), confirming that p38 phosphorylation of dematin is specific to one or more of these sites. The dematinN3_S92/96A and dematinN3_S87/92/96/105A constructs showed relative expression levels of 0.12 and 0.01 respectively, compared to wild-type dematinN3 ($p<0.0001$). This indicates that dematin is phosphorylated in vitro at one or both of the S92/96 motifs, in addition to one or both of S87/105 motifs. The dematinN3 truncation contains a further two p38 phosphorylation motifs at Thr^{120} and Ser^{156} that were not detected as being phosphorylated in our mass spectrometry analysis. The lack of phosphorylation of the dematinN3_S87/92/96/105A construct confirms this initial finding. Finally phosphorylation of the dematinC1 fragment was abolished in the dematinC1_S274/383A mutant construct ($p<0.0001$), indicating that dematin C1 is phosphorylated at one or more of these sites. Again the dematin C1 regions contained additional p38 phosphorylation motifs, at Ser^{307} and Ser^{315}, which were not detected as being phosphorylated here or in the mass spectrometry analysis.

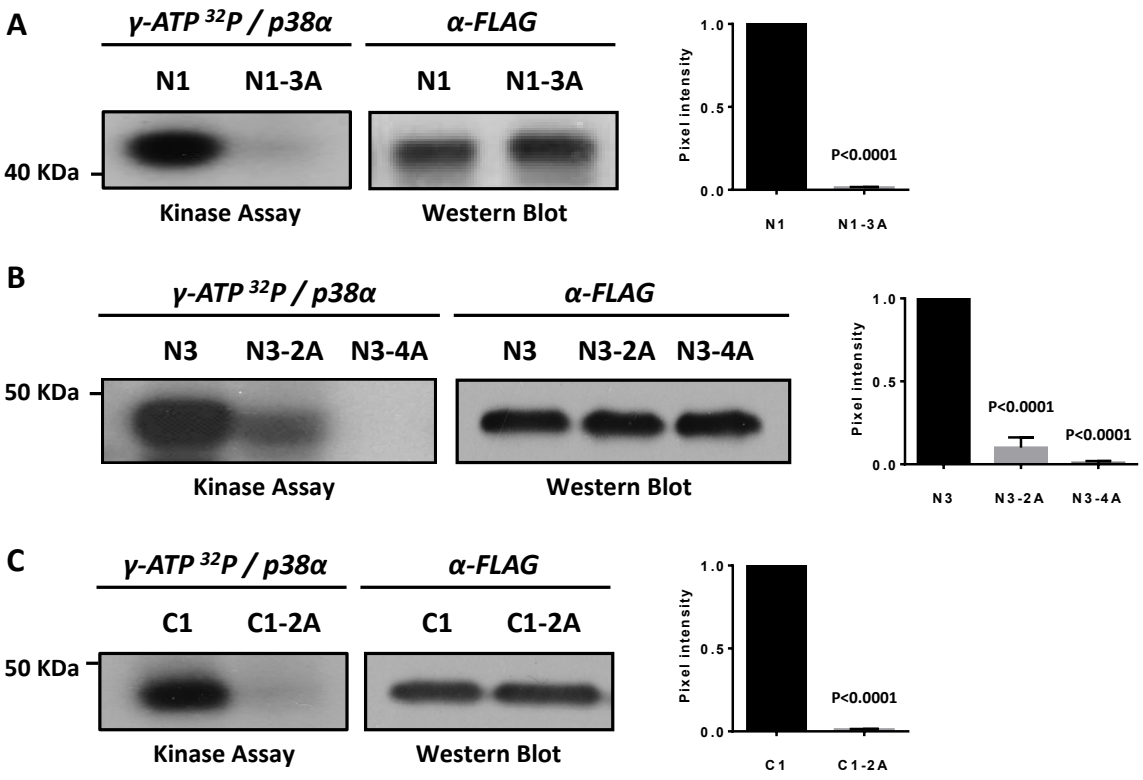

Figure 3.6: In vitro kinase assays of p38 mutant truncated dematin constructs

In vitro kinase assays were conducted to determine whether the phosphorylation of dematin by p38α was specific to the motifs identified. The truncated constructs dematinN1, N3, and C1, along with their corresponding p38 motif mutants in the pDEST27 vector were overexpressed in HEK293T cells, then purified on GST-pulldown columns following cell lysis. Samples were incubated with recombinant p38α and γ-ATP ^{32}P, separated by SDS-PAGE and exposed to radiographic film. Bands were detected in the full-length dematin sample and in all of the truncated constructs. (A) Comparison of dematinN1 (N1) and the dematinN1_S11/16/26A (N3A) construct. (B) Comparison of dematinN3 (N3) and the dematinN3_S92/96A (N3-2A), and dematinN3_S87/92/96/105A (N3-4A) constructs. (C) Comparison of dematinC1 (C1) and the dematinC1_S274/383A (C1-2A) construct. Bands were quantified and normalised against the anti-FLAG expression controls. Normalised values for each mutant were then further normalised to the corresponsing wild-type which was set to 1.0. The statistical significance was determined using an unpaired t-test; (n=3). *(ATP; adenosine tri-phosphate, SDS-PAGE; sodium dodecyl sulphate polyacrylamide gel electrophoresis).*

3.3.5 MPM2-detection of SP / TP phosphorylation sites in vivo

Although the MS analysis provided in vivo phosphorylation data, this technique is not applicable to a high-throughput approach that would be required to characterise specific residues, and therefore a second technique was tested. Western blotting was conducted using an anti-MPM2 antibody that detects context-dependent phosphorylated Ser-Pro and Thr-Pro motifs. The pDEST27*FLAG*dematin and truncated constructs dematinN1, N3, and C1 constructs and their corresponding p38-motif mutants were overexpressed in HEK293T cells and purified from the lysates on GST-pulldown columns. Following SDS-PAGE separation and immunoblotting, membranes were probed with an anti-MPM2 antibody. Blots were then re-probed with an anti-FLAG antibody to confirm that the proteins were expressed. Bands were detected for all constructs (Figure 3.7), indicating that the MPM2 antibody recognises at least one of the phosphorylation motifs in each fragment and is therefore of potential use for analysing the in vivo phosphorylation of dematin. No band was detected with the MPM2 antibody for the dematinN1_S11/16/26A, dematinN3_S87/92/96/105A, and dematinC1_S274/383A constructs (Figure 3.7). This confirms that the antibody is not recognising other non-SP/TP sites within these protein sequences, and that the addition SP/TP phosphorylation motifs in the dematinN3 and dematinC1 are either not phosphorylated in vivo under these experimental conditions, or are not recognised by the antibody.

3.4 PEST mediated degradation of dematin

The presence of a PEST degradation motif in the dematin primary sequence, and the intrinsic instability of the protein, have been reported in the literature but have not been investigated further (Chen *et al.*, 2013; Chen *et al.*, 2009; Rana *et al.*, 1993). Here we aimed to determine whether the PEST motif in dematin does regulate protein stability, to what extent this affects the intracellular half-life of the protein, and whether this degradation is regulated by p38 phosphorylation.

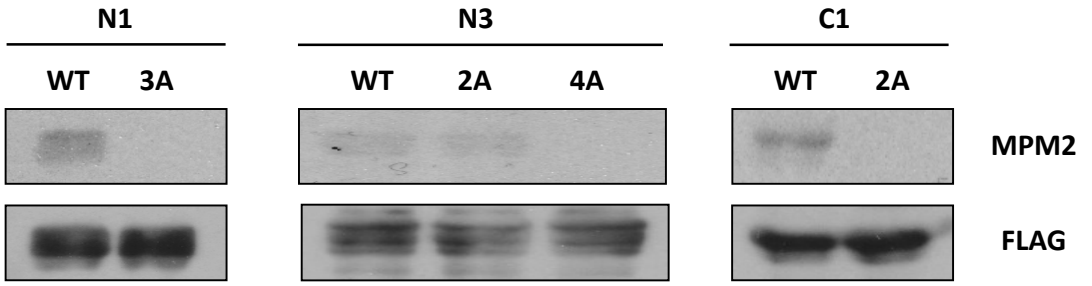

Figure 3.7: In vivo phosphorylation of dematin at SP / TP motifs

The truncated constructs dematinN1, N3, and C1, along with their corresponding p38 motif mutants (dematinN1_S11/16/26A (3A), dematinN3_S92/96A (2A), dematinN3_S87/92/96/105A (4A), dematinC1_S274/383A (2A) in the pDEST27 vector were overexpressed in HEK293T cells, and separated by SDS-PAGE. Following western blotting, membranes were probed with an anti-MPM2 antibody to detect phosphorylated SP/TP motifs (n=3) *(SDS-PAGE; sodium dodecyl sulphate polyacrylamide gel electrophoresis).*

3.4.1 Dematin contains a PEST motif at aa 89-104

The presence of a PEST motif in dematin has been previously reported, but the exact position of this motif is not consistently defined. Rana *et al* (1993) first described the motif at aa 90-103, however Chen *et al* assigned aa 89-102 as the PEST motif (2009). In order to obtain an unbiased definition of the dematin PEST motif for use in this study, the EMBOSS epestfind algorithm was applied (emboss.bioinformatics.nl/cgi-bin/emboss/epestfind). This algorithm conducts a preliminary scan to identify regions of ≥ 12 aa that contain at least one P, D or E and S or T residue which are flanked by positively charged residues. The validity of these initial results in then scored based on two parameters. Firstly the enrichment of D, E, P, S, T residues is expressed as a percentage of the total mass (w/w). The hydrophobicity of the motif is then calculated, using a scale where arginine = 0 to isoleucine = 90. These values are combined to give each motif an overall rating, where the PEST score = 0.55 * DEPST - 0.5 * hydrophobicity index. PEST motifs that meet the required criteria but score below the threshold of 5.0 are considered poor, whilst those above this value are of potential biological interest. The epestfind algorithm was applied to the amino acid sequence of the longer 52 KDa isoform of human dematin (BC017445). Seven potential PEST motifs were identified (Figure 3.8) but six were rated as poor with PEST scores from -27.63 to 4.08. A single viable motif of 14 aa was identified at ^{89}KSTSPPPSPEVWADSR^{104} (Figure 3.8) which was assigned a PEST score of 11.51, with a hydrophobicity index of 34.69 and a DEPST of 52.47 % (w/w). This motif is also present in the sequence of the shorter 48 KDa isoform of dematin.

3.4.2 Intracellular degradation of dematin

The intracellular half-life of the 52 KDa isoform of dematin was determined using pulse-chase degradation experiments. C2C12 cells were transfected with pTrexDEST30*FLAG*-dematin and after 24 hours intracellular stores of sulphur containing amino acids were depleted with a one-hour incubation in cysteine- and methionine-free DMEM. Cells were pulsed with 100 µCi / ml ^{35}S labelled methionine and cysteine for 30 minutes to label all newly synthesised proteins.

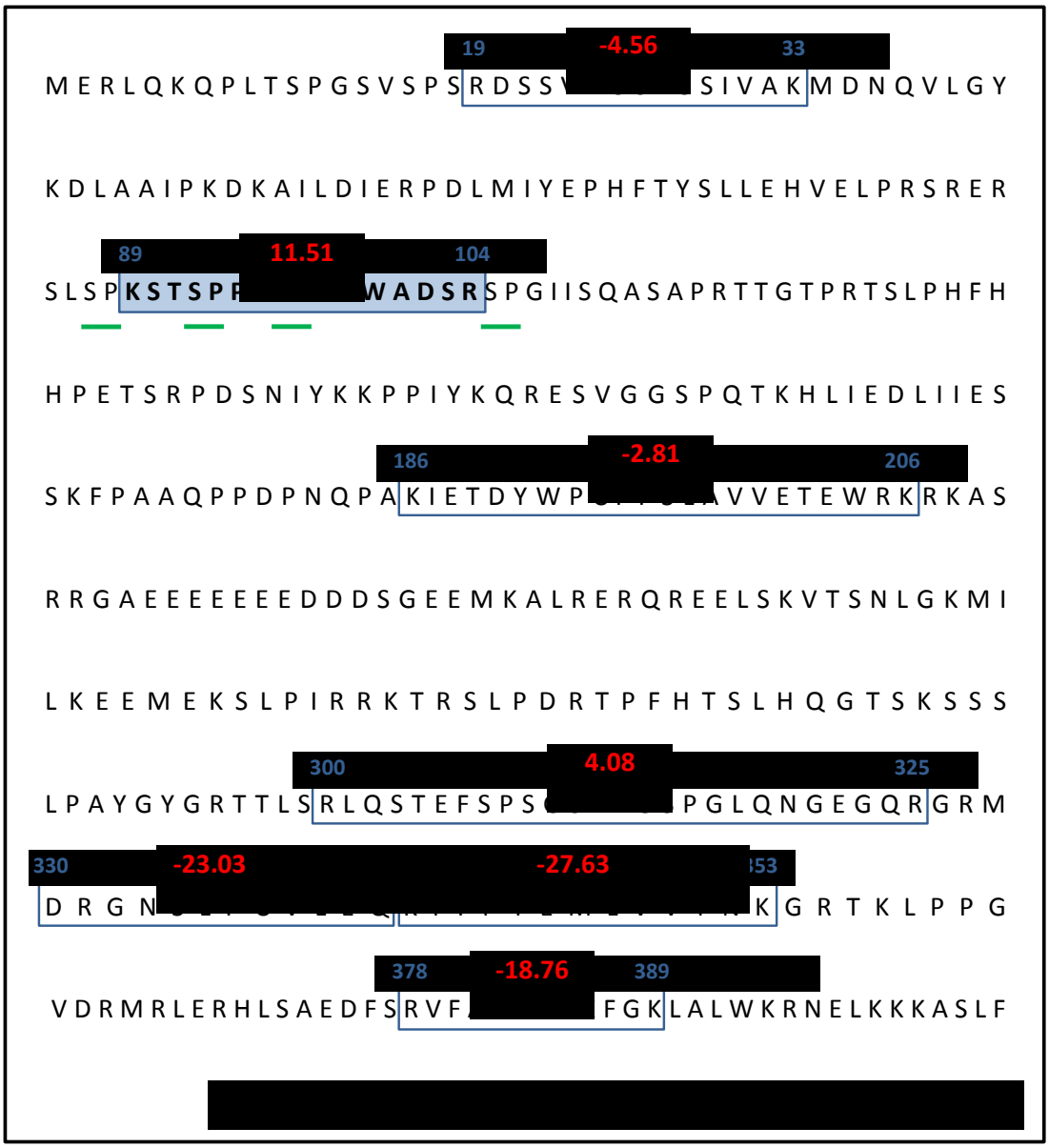

Figure 3.8: PEST motifs in the primary sequence of human dematin

The EMBOSS epestfind algorithm was used to identify potential PEST degradation motifs in the primary sequence of human dematin. The preliminary scan revealed 7 sites in dematin (blue boxes) which were then analysed for enrichment of DEPST residues and hydrophobicity, and given a rating where < 5.0 indicates a poor site while 5.0 and above indicates a site of potential biological interest (red text). The dematin sequence contains a single viable PEST motif at residues 89-104 as indicated by the shaded box. The green lines indicate the p38 phosphorylation motifs both within and flanking the PEST motif.

Cells were thoroughly washed and returned to DMEM media supplemented with excess methionine and cysteine. Samples were taken at chase intervals of 0-20 hours from the immediate end of the pulse period. Cells were lysed, immunoprecipitated with an anti-FLAG antibody, and separated by SDS-PAGE. Gels were exposed to a storage phosphor screen for 48 hours before imaging with a laser scanner. The intensity of each band was quantified using densitometry software, and values were normalised against the 0 timepoint which was taken to be 100%. The intracellular degradation of dematin followed an exponential decay model (Figure 3.9), with a calculated half-life of 5.49 hours (95% confidence interval 5.49 +/- 0.44 hours).

3.4.3 The PEST motif in dematin enhances protein degradation in vivo

In order to determine the effect of the PEST motif on dematin stability, site-directed mutagenesis was employed to create a full-length dematin construct lacking the PEST domain. A primer was designed to delete aa 89-104, creating the pTrexDEST30*FLAG*-dematin_ΔPEST construct. Pulse-chase degradation experiments were repeated as previously using this construct. The data again fitted an exponential decay model (Figure 3.10), with a calculated half-life of 7.64 hours (95% confidence interval 7.64 +/- 0.72 hours). This indicated that the PEST motif in dematin does increase the instability of the protein, and when these values were compared to the wild-type dematin using a t-test this difference was shown to be statistically significant ($p<0.05$).

3.4.4 Potential regulation of dematin stability by p38 MAPK

PEST motifs generally require activation before they mediate degradation of a protein, and this is commonly achieved through phosphorylation at internal serine or threonine residues. The PEST motif in dematin contains two internal p38 phosphorylation sites, and a further two sites flanking either side of the motif. Here we aimed to investigate whether p38 regulates PEST mediated degradation of dematin, and if so which of these four residues are important. Pulse-chase experiments were repeated as previously, but using only four timepoints; 0, 2, 4,

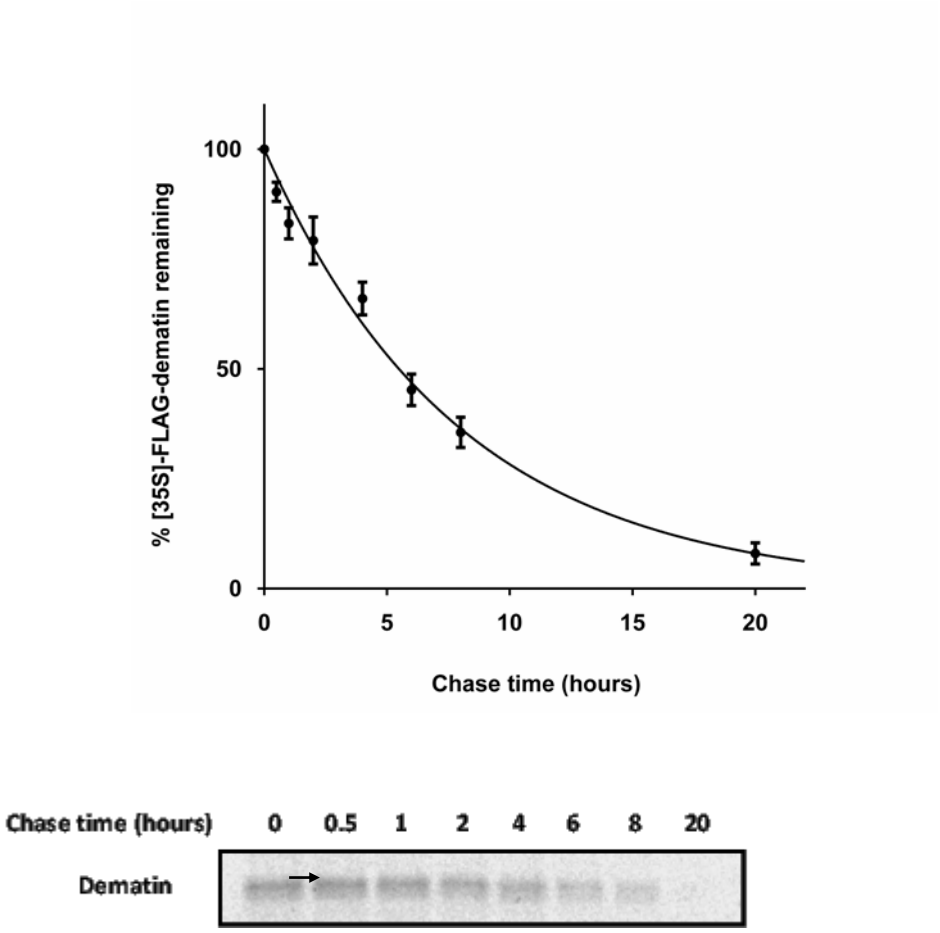

Figure 3.9: Pulse-chase degradation timecourse of overexpressed dematin

C2C12 cells transfected with pTrexDEST30*FLAG*-dematin with depleted of intracellular methionine and cysteine stores before labelling for a 30-minute pulse period with 100 µCi / ml ^{35}S labelled methionine and cysteine. Samples were washed and chased for the time periods indicated in DMEM supplemented with methionine and cysteine. Cells were lysed and the labelled proteins were immunoprecipitated with an anti-FLAG antibody and separated by SDS-PAGE. Following a 48 hour exposure to a phosphor storage plate, imaging was conducted using a laser scanner and bands quantified using densitometry software. Values were normalised to the 0 hour chase timepoint, which was set at 100%. (A) A one-phase decay trendline was fitted to the data, and from this the intracellular half-life of dematin was calculated to be 5.49 hours (+/- 0.44 hours). Data plotted is the mean value ± SEM. (B) A representative image of the gel (n=3).

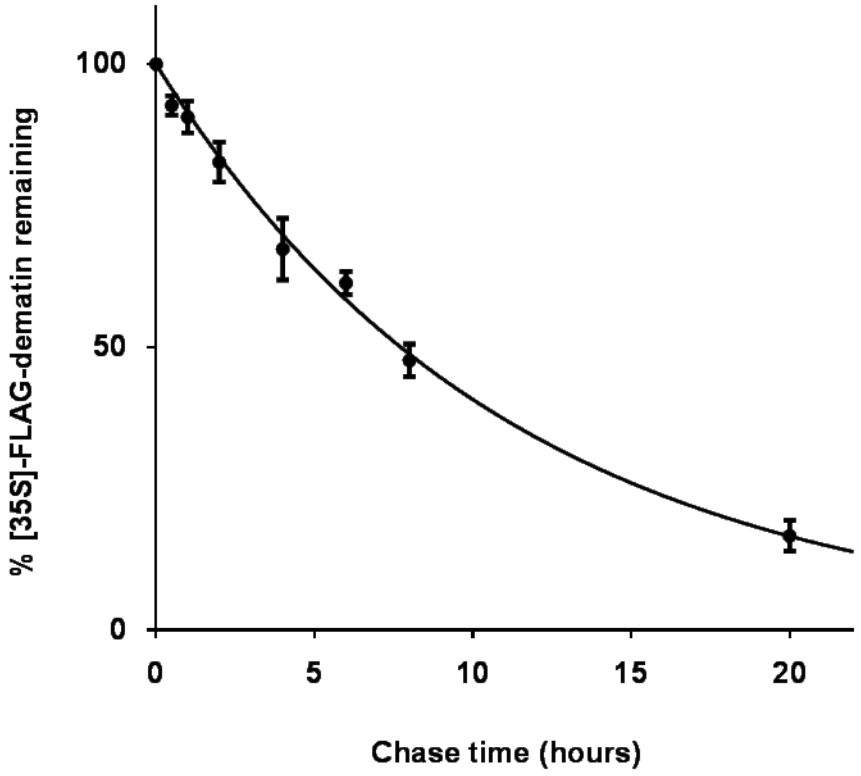

Figure 3.10: The effect deleting the PEST motif on the stability of dematin

C2C12 cells transfected with pTrexDEST30*FLAG*-dematin_ΔPEST were depleted of intracellular methionine and cysteine stores before labelling for a 30-minute pulse period with 100 µCi / ml ^{35}S labelled methionine and cysteine. Samples were chased for the time periods indicated, from 0-20 hours. Cells were lysed and the labelled proteins were immunoprecipitated with an anti-FLAG antibody and separated by SDS-PAGE. Following a 48-hour exposure to a phosphor storage plate, imaging was conducted using a laser scanner and bands quantified using densitometry software. Values were normalised to the 0 hour chase timepoint, which was set at 100%. A one-phase decay trendline was fitted to the data, and from this the intracellular half-life of dematin_ΔPEST was calculated to be 7.64 hours (+/- 0.72 hours). Data plotted is the mean value ± SEM (n=3).

and 8 hours. Data was subsequently plotted on a logarithmic scale to aid the fitting of a trendline to the reduced set of data points. Cells were either pre-incubated with SB203580 to inhibit p38 (and maintained in SB203580 containing solutions throughout the experiment), or co-transfected with $MKK6^{DD}$ to specifically activate p38. The untreated dematin had a calculated mean half-life of 5.98 hours. This increased slightly in the p38 inhibited sample to 6.21 hours, and decreased in the p38 activated dematin to 5.77 hours (Figure 3.11). This indicated that there was a small change towards increased instability upon p38 hyperactivation, however this was not a significant difference.

3.4.5 Potential regulation of dematin stability by PEST phosphorylation

Although p38 phosphorylation had no significant effect on the stability of dematin, there remained a possibility that the PEST motif could be regulated by an alternative kinase. Two sets of mutants were therefore generated to study the effect of PEST phosphorylation on the stability of dematin. The first approach was to create serine to alanine mutants, which were no longer capable of being phosphorylated. A double mutant of the two internal serine residues (Ser^{92} and Ser^{96}), and quadruple mutant of the two internal sites plus two flanking serine residues (Ser^{87} and Ser^{105}) were created: dematin_S92/96A and dematin_S87/92/96/105A. Mutagenesis of the same sites was then used to replace serine residues with negatively charged glutamic acid residues in order to mimic the effects of phosphorylation: dematin_S92/96E and dematin_S87/92/96/105E. The template DNA used for mutagenesis reactions was pTrexDEST30*FLAG*-Dematin.

Wild-type dematin had a calculated mean half-life of 5.98 hours. The mean half-lives of the dematin_S92/96A and dematin_S87/92/96/105A non-phosphorylatable mutants were 6.24 and 6.46 hours respectively. The phospho-mimicking mutants dematin_S92/96E and dematin_S87/92/96/105E had mean half-lives of 6.66 and 6.23 hours (Figure 3.12). None of the mutants had half-lives that were statistically significantly different from the wild-type dematin, indicating that phosphorylation does not appear to affect the stability of dematin via the PEST motif.

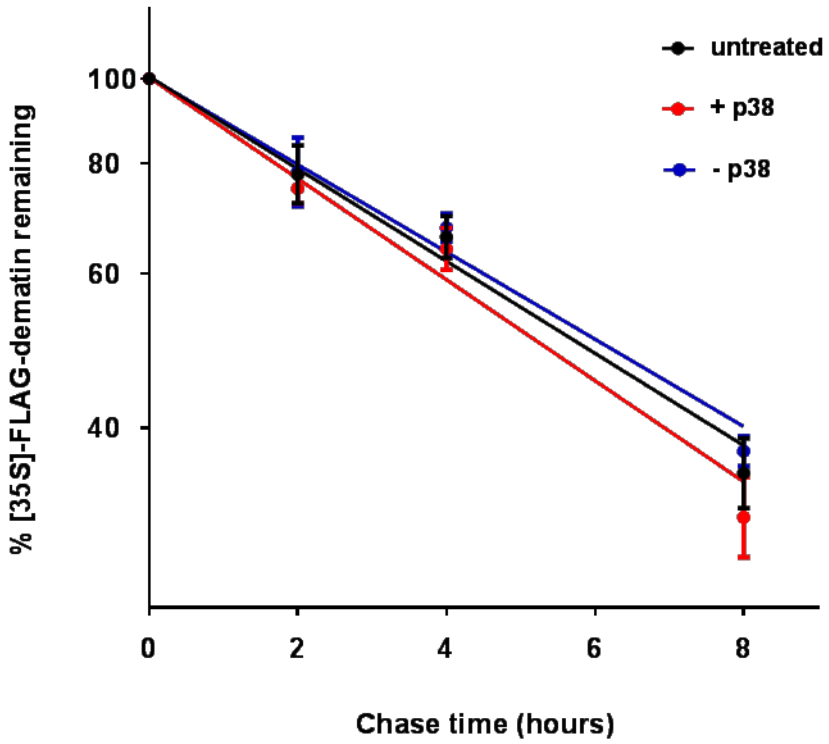

Figure 3.11: The effect of p38 phosphorylation in the stability of dematin

C2C12 cells were transfected with pTrexDEST30*FLAG*-dematin, and either left untreated (untreated), incubated with SB203580 throughout the experiment (-p38), or co-transfected with MKK6 to hyper-activate p38 (+p38). Cells were depleted of intracellular methionine and cysteine stores before labelling for a 30-minute pulse period with 100 µCi / ml ^{35}S labelled methionine and cysteine. Samples were chased for the time periods indicated, from 0-20 hours. Cells were lysed and the labelled proteins were immunoprecipitated with an anti-FLAG antibody and separated by SDS-PAGE. Following a 48-hour exposure to a phosphor storage plate, imaging was conducted using a laser scanner and bands quantified using densitometry software. Values were normalised to the 0 hour chase timepoint, which was set at 100%. Linear trendlines were fitted to the data, and from this the intracellular half-lives were calculated (n=3).

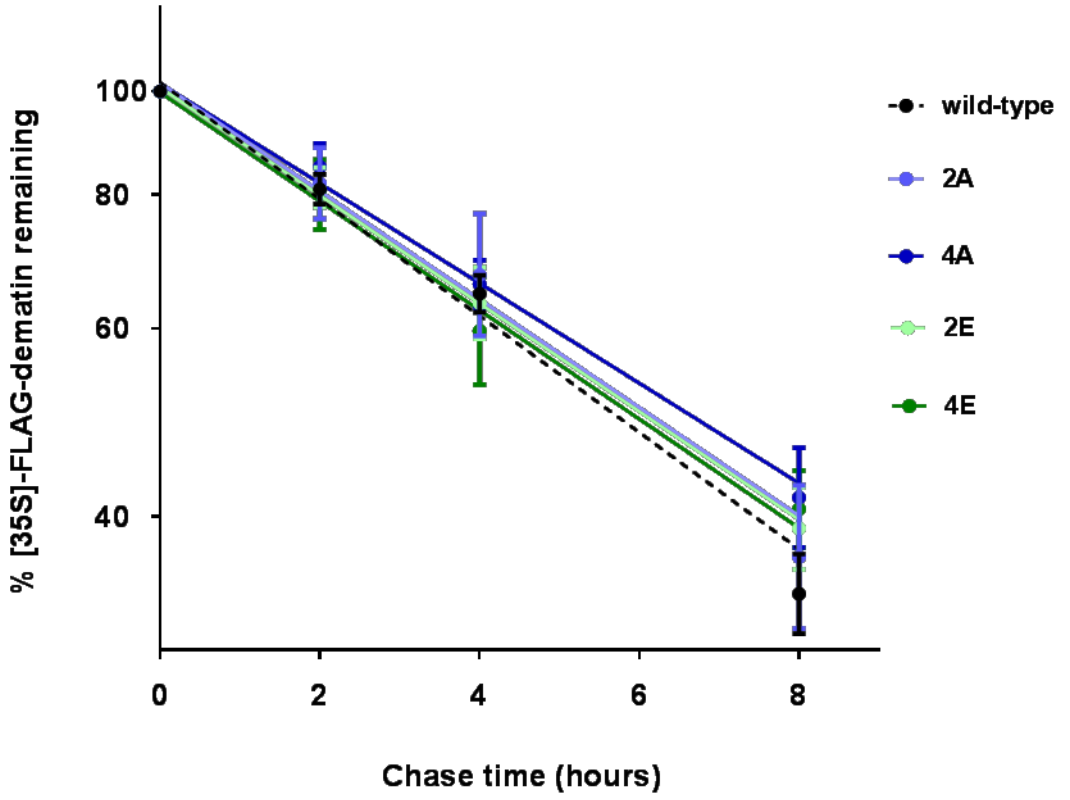

Figure 3.12: The effect of PEST site mutations on the stability of dematin

C2C12 cells were transfected with pTrexDEST30*FLAG*-dematin, -dematinS92/96A (2A), -dematinS87/92/96/105A (4A), -dematinS92/96E (2E), or -dematinS87/92/96/105E (4E). Cells were depleted of intracellular methionine and cysteine stores before labelling for a 30-minute pulse period with 100 µCi / ml ^{35}S labelled methionine and cysteine. Samples were chased for the time periods indicated, from 0-20 hours. Cells were lysed and the labelled proteins were immunoprecipitated with an anti-FLAG antibody and separated by SDS-PAGE. Following a 48-hour exposure to a phosphor storage plate, imaging was conducted using a laser scanner and bands quantified using densitometry software. Values were normalised to the 0 hour chase timepoint, which was set at 100%. Linear trendlines were fitted to the data, and from this the intracellular half-lives were calculated (n=3).

3.5 Regulation of dematin headpiece / core binding by p38

It has recently been shown that phosphorylation of the dematin HP at Ser^{381} [Ser^{403}] induces a conformation change that increases the affinity of the HP for the core domain, which blocks one of the two actin-binding domains and therefore inhibits actin bundling (Chen *et al.*, 2013). Here we aimed to determine which region of the core domain the HP interacts with, in addition to determining whether p38 phosphorylates the dematin HP, and if so whether this phosphorylation has a regulatory effect on the interaction between the HP and core domains.

3.5.1 Binding of the dematin headpiece to the core domain

In order to determine which region of the core domain the dematin HP binds to, cells were co-transfected with pDEST27*FLAG*-dematinHP and either pcDNA3.1DEST*FLAG*-dematin or -dematinN2, -dematinN3 or -dematinC1. Following cell lysis under non-denaturing conditions, GST-pulldown assays were conducted to purify the GST-*FLAG*-dematinHP from solution. The eluted products were subjected to SDS-PAGE separation, transferred onto nitrocellulose membrane, and probed with an anti-FLAG antibody. Full-length dematin co-purified with GST-*FLAG*-dematinHP, but the truncated constructs dematinN2, dematinN3 or dematinC1 did not (Figure 3.13). This demonstrates that the dematin HP does bind to the core region, but suggests that binding occurs in either the region from aa 197-261 that is not covered by these constructs, or binds on the boundary of this region and either the dematinN3 or dematinC1 regions.

3.5.2 The dematin headpiece is phosphorylated in vitro and in vivo at Ser^{383}

In order to investigate whether p38 plays a regulatory role in the interaction between the dematin HP and core domains, it was first necessary to confirm that the dematin HP is phosphorylated by p38. The HP region contains a single p38 motif at Ser^{383}. Observation of the minimised average solution NMR structure of the HP domain confirmed that this motif is located on the external surface of the protein, and therefore would be accessible for p38 phosphorylation (Figure 3.14B). The location of this motif was shown to be at the immediate N-terminal side of the

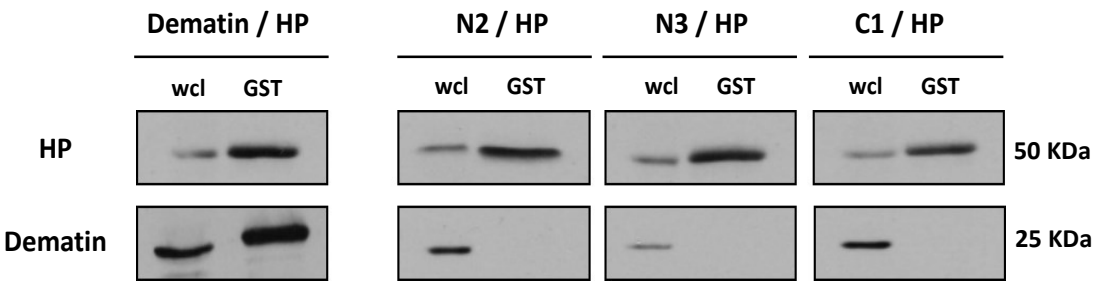

Figure 3.13: The dematin headpiece binds to the core domain at an undefined region.

HEK293T cells were co-transfected with pDEST27*FLAG*-dematinHP and either pcDNA3.1*FLAG*-dematin, -dematinN2, -dematinN3, or -dematinC1. Following cell lysis under non-denaturing conditions, the dematin HP was purified on a GST-pulldown column, and the eluted proteins subjected to SDS-PAGE separation and transfer to nitrocellulose. Membranes were probed with an ant-FLAG antibody (n=3) *(HP; dematin headpiece, GST; glutathione S-transferase, HP; headpiece, wcl; whole-cell lysate)*

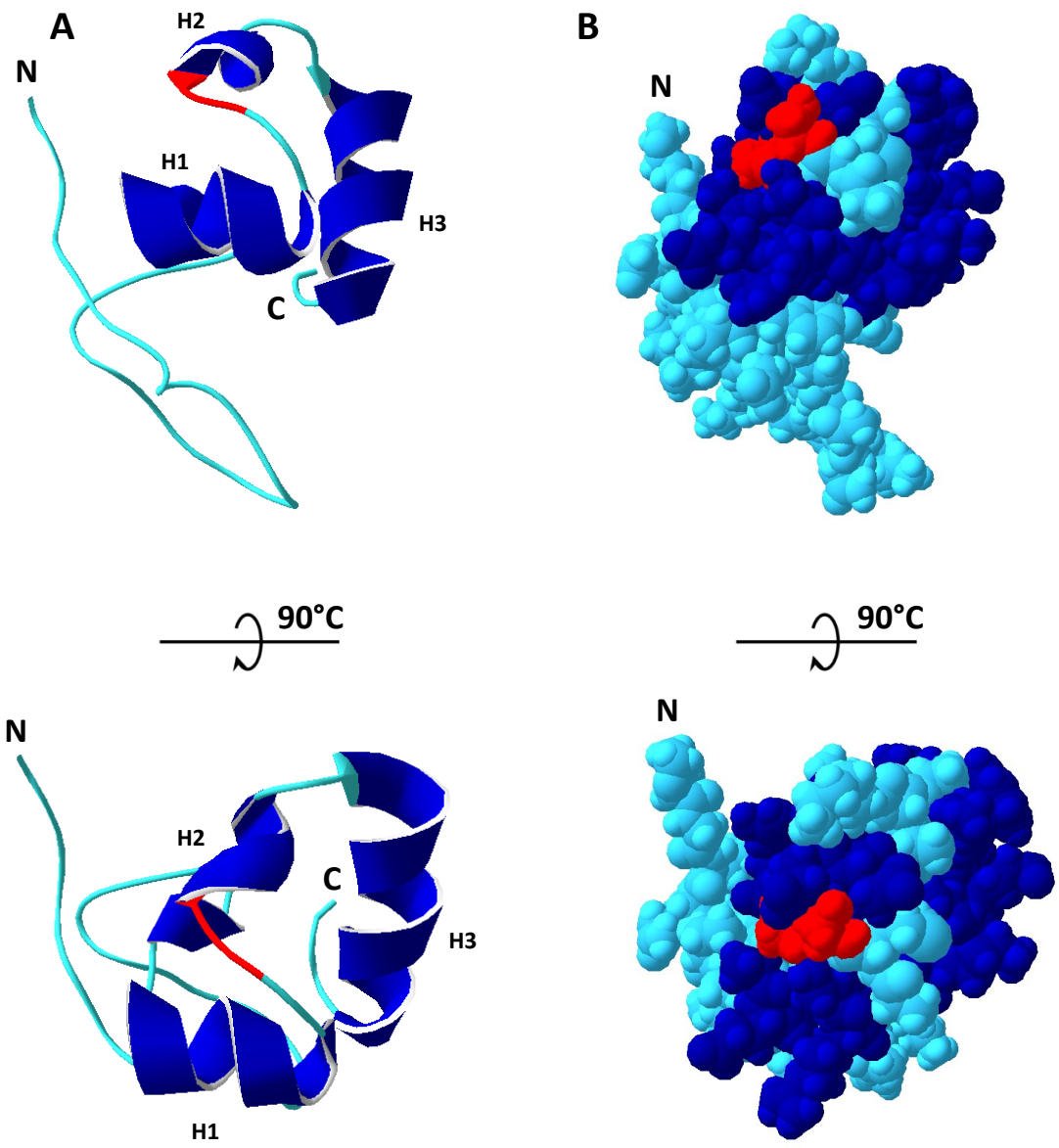

Figure 3.14: Location of Ser^{383} in the folded conformation of the dematin headpiece

A ribbon representation of the minimised average solution NMR structure of the headpiece domain of 48 KDa dematin. The predicted α-helices are shown in dark blue, with the linker regions in light blue. (A) The p38 phosphorylation motif at Ser^{383}-Pro motif is highlighted in red, clearly showing its position at the N-terminal end of helix 2 (H2). (B) The space fill models demonstrate that the Ser^{383}-Pro motif is located on the external surface of the folded protein and therefore accessible for phosphorylation. (The NMR structure was obtained from RCSB Protein Data Bank; structure of the human dematin headpiece domain, 1QZP. The image was created using Swiss-PDB viewer 4.1.0).

second α-helix (Figure 3.14A). This close proximity to the α-helix makes it plausible that phosphorylation of this site could induce a conformational change in the HP, which in turn could affect the HP / core interaction.

In order to determine whether this Ser^{383} motif is phosphorylated by p38 in vitro, kinase assays were repeated using recombinant p38α and the pDEST27*FLAG*-dematinHP (HP) and pDEST27*FLAG*-dematinHP_S383A (HP-A) constructs. The wild-type HP construct was phosphorylated by p38, while the HP-A construct was not ($P<0.0001$; Figure 3.16A). Western blotting experiments using an anti-MPM2 antibody were then used to determine whether this phosphorylation could be detected in vivo. A band was detected for the wild-type dematinHP construct, but not for the dematinHP_S383A mutant (Figure 3.16B). Taken together these results confirm the dematin HP is phosphorylated both in vitro and in vivo at Ser^{383}, and the kinase assay suggests that this phosphorylation is attributable to p38.

3.5.3 Regulation of the dematin headpiece / core interaction by p38

Once it had been demonstrated that the dematin HP and core domains interacted in our system, and that the HP was phosphorylated at Ser^{383} both in vitro and in vivo, the GST-pulldown assays were repeated to determine whether p38 had a regulatory role in this interaction. Site-directed mutagenesis was used to create a second mutant of the dematin HP with the Ser^{383} site mutated to an aspartic acid residue to mimic the negative charge of a phosphate group; pDEST27*FLAG*-dematinHP_S383D (HP-D). Experiments were also repeated in the presence of the p38 inhibitor SB203580, and with $MKK6^{DD}$ co-transfection to hyperactivate p38. Full-length dematin co-purified with the dematin HP under untreated, p38 inhibited, and p38 hyper-activated conditions (Figure 3.16A). This indicated that p38 does no inhibit the core / HP interaction. Equally, full-length dematin co-purified with the HP-S383A and HP-S383D constructs (Figure 3.16B). This suggested that any phospho-mediated change in the dematin HP does not affect the core / HP interaction.

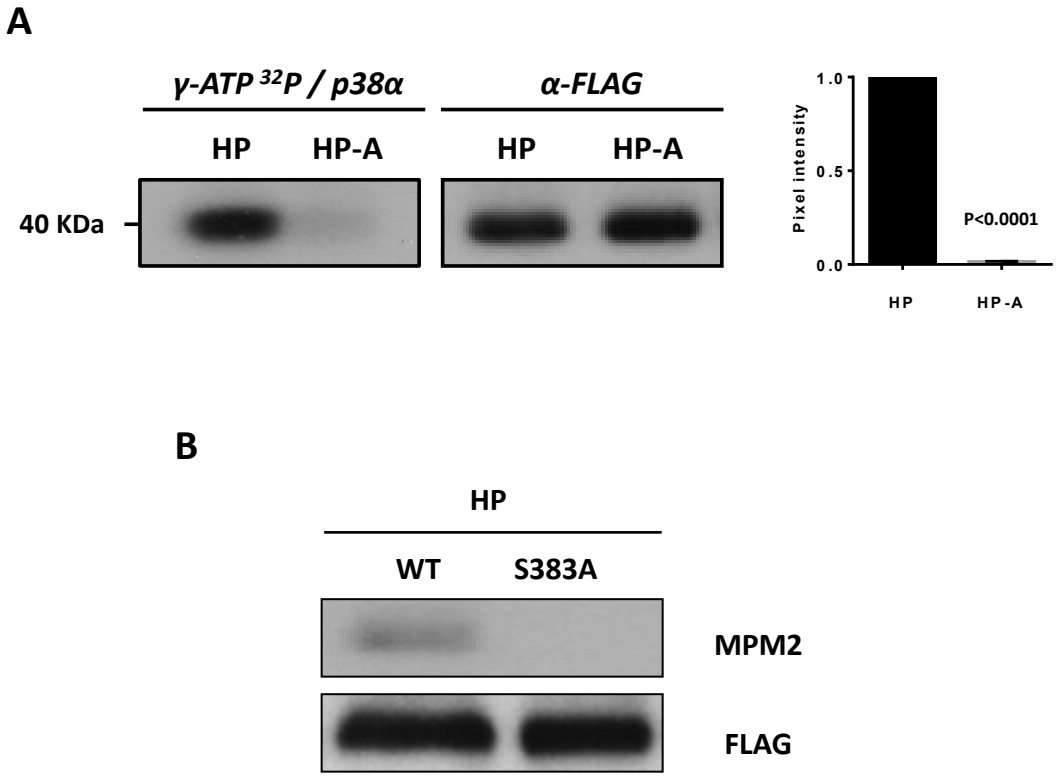

Figure 3.15: The dematin headpiece is phosphorylated at Ser^{383} by p38 MAPK

(A) pDEST27*FLAG*-dematinHP and pDEST27*FLAG*-dematinHP_S383A constructs were overexpressed in HEK293T cells, then purified on GST-pulldown columns following cell lysis. Samples were incubated with recombinant p38α and γ-ATP ^{32}P, separated by SDS-PAGE and exposed to radiographic film. Bands were detected in the full-length dematin sample and in all of the truncated constructs. Bands were quantified and normalised against the anti-FLAG expression controls. Normalised values for the mutant were then further normalised to the wild-type which was set to 1.0. The statistical significance was determined using an unpaired t-test. (B) Cells lysates of the same constructs were immunoblotted with an anti-MPM2 antibody to detect phsophrylated SP/TP motifs with an anti-FLAG control to confirm expression levels were comparable (n=3). *(ATP; adenosine tri-phosphate, SDS-PAGE; sodium dodecyl sulphate polyacrylamide gel electrophoresis).*

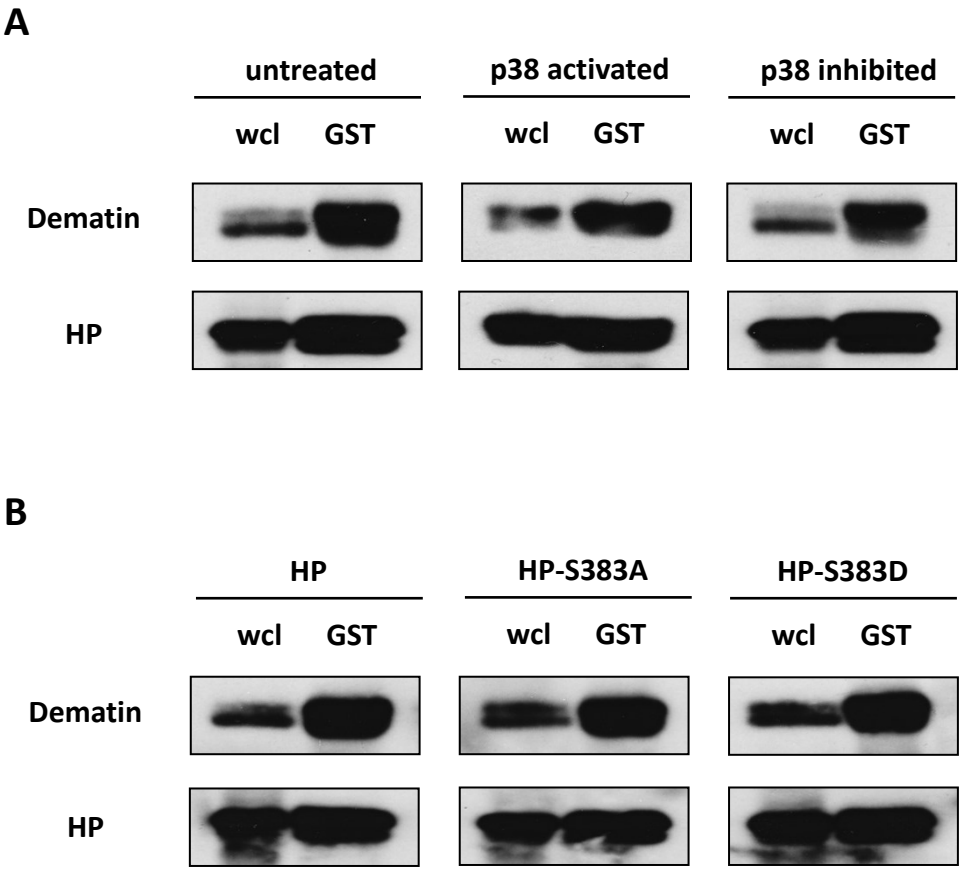

Figure 3.16: Phosphorylation of Ser^{383} does not inhibit the headpiece / core interaction

(A) HEK293T cells were co-transfected with pDEST27*FLAG*-dematinHP and pcDNA3.1*FLAG*-dematin. Cells were either untreated, p38 hyperactivated with MKK6-cotransfection, or p38 inhibited with SB203580. Following cell lysis under non-denaturing conditions, the dematin HP was purified on a GST-pulldown column, and the eluted proteins subjected to SDS-PAGE separation and transfer to nitrocellulose. Membranes were probed with an ant-FLAG antibody. (B) Cells were co-transfected with pDEST27*FLAG*-dematinHP, -dematinHP_S383A, or –dematinHP_S383D, and pcDNA3.1*FLAG*-dematin. Samples were processed as above (n=3) *(HP; dematin headpiece, GST; glutathione S-transferase, HP; headpiece, wcl; whole-cell lysate)*

3.6 Discussion

Here we have confirmed dematin as a novel substrate of the p38α MAPK, and demonstrated that this phosphorylation occurs in vitro and in vivo at multiple sites in both the core and HP regions. The stability of dematin was shown to be regulated by the presence of a PEST degradation motif; however p38 phosphorylation did not regulate this process. Equally, phosphorylation of the HP by p38 did not regulate the association of the HP and core domains.

3.6.1 Dematin is phosphorylated by p38α at multiple sites in vitro and in vivo

It has been estimated that each MAPK family member has around 200-300 substrates (Cuadrado & Nebreda, 2010). To date around 100 substrates of p38α have been identified, which include protein kinases, nuclear proteins including transcription factors, and a wide array of other cytosolic targets (Trempolec *et al.*, 2013). Here we have identified dematin, an actin-binding protein, as a novel substrate of p38α. Other examples of p38 regulating cytoskeletal proteins have been previously documented. Cytoskeletal remodelling in endothelial cells during inflammation has been demonstrated as a result of p38 phosphorylation of HSP27, a protein that enhances F-actin polymerisation and stabilisation (Wang & Doerschuk, 2001). This has also been identified in hepatocytes during ischemia and reperfusion (Keller *et al.*, 2005). Phosphorylation by p38 is also an important regulator of the keratin intermediate filament cytoskeleton (Wöll *et al.*, 2007).

MAPKs including p38 generally phosphorylate their substrates at SP or TP motifs, of which 13 were identified in the primary sequence of 52 KDa dematin. In collaboration with Tine Tingholm (Lund University, Sweden), preliminary mass spectrometry analysis identified 11 phosphorylated motifs in dematin under p38-hyperactivated conditions, at residues Ser^{11}, Ser^{16}, Ser^{26}, Ser^{87}, Ser^{92}, Ser^{96}, Ser^{105}, Thr^{274}, and Ser^{383}. These sites are distributed throughout the dematin sequence, in both the core and HP domains. In support of these results, in vitro kinase assays confirmed that p38α phosphorylates dematin within each of the regions covered by the dematinN1, N3, and C1 constructs; aa 0-78, 79- 196 and 261-405 respectively.

Further mutagenesis to create truncated constructs each containing only a single p38 phosphorylation motif will be required to determine the precise complement of phosphorylation sites.

The preliminary mass spectrometry results presented here identified residues that were phosphorylated under p38 hyper-activated conditions, however this does not confirm that they are directly phosphorylated by p38. It would therefore be useful to repeat the experiment using cells co-transfected with $MKK6^{DD}$ to activate p38, and cells co-transfected with $MKK6^{DD}$ and treated with SB203580 to inhibit p38. By activating and inhibiting p38 simultaneously in the inhibited sample, it will be possible to rule out any non-specific consequences of MKK6 activation. Any differences in phosphorylation profiles at SP / TP motifs between these two samples can be attributed to p38. Those that are the same under both conditions can be attributed to other proline-directed kinases, such as other MAPK family members, which could provide an interesting avenue to investigate further in the future. In addition to the p38 activated and inhibited conditions, a third sample from untreated cells could be used to determine the basal p38 phosphorylation state in these cells. The method used for analysing the preliminary MS sample involved a tryptic digest of dematin and subsequent enrichment of phosphorylated peptides, a process that may results in certain peptides being missed from the screening. In order to increase the likelihood of all peptides being detected future MS will analyse the total protein sample to maximise the chance of detecting each peptide. If certain peptides are not mapped under the experimental conditions, the protocol can then be optimised to increase the detection of these fragments.

In vivo characterisation of dematin phosphorylation by p38 was also conducted using western blotting with anti-MPM2 immuno-detection. This antibody is raised against proteins that are phosphorylated, either directly or indirectly by M-phase-promoting factor, upon entry to mitosis in eukaryotic cells. The limitation of this however is that detection of phosphorylated motifs with this antibody is sequence context dependent, and so although a positive detection is a useful aid, the lack of detection of a peptide is not confirmation that a particular site is not

phosphorylated. The number of sites detected varies with species and cell type, and so sites have to be validated on an individual basis. Detection of the same peptide can also be inconsistent. We have demonstrated that this antibody is capable of detecting full-length dematin, and each of the truncated dematinN1, N3, and C1 regions, as being phosphorylated in vivo. This phosphorylation decreased in the presence of p38 inhibition with SB203580, suggesting that at least some of these motifs are phosphorylated by p38 rather than other proline-directed kinases.

Phosphorylated proteins may also be detected using gel-shift assays, working on the principle that the phosphorylated protein will migrate fractionally slower through an SDS-PAGE gel and therefore be detected as a discreet band of a slightly higher apparent molecular weight than the unphosphorylated form. A band-shift was not detectable for full-length dematin or any of the truncated constructs, even with variation in the percentage acrylamide composition of the gel and total amount of protein loaded (data not shown). An adaptation to this method is now commercially available that consists of a phosphate-retarding component that is added to the SDS-PAGE gel to enhance the migratory difference between the phosphorylated and unphosphorylated protein bands. This method may be useful in future as a tool for validating the MS data. As this is a rapid, high throughput, technique it would be ideal for screening multiple mutant constructs in order to determine the specific motifs that are phosphorylated by p38.

Although p38 is generally considered to phosphorylate substrates at Ser-Pro and Thr-Pro motifs, instances of non-proline-directed phosphorylation have been documented (Cheung et al., 2003; Reynolds et al., 2000). Analysis of known p38α phosphorylation sites indicated that around 85% are either SP or TP motifs, with the others constituting either serine or threonine residues followed by other amino acids (Trempolec *et al.*, 2013). It was therefore important to consider that dematin may be phosphorylated at sites other than the motifs that were initially identified. The p38 mutant constructs dematinN1_S11/16/26A, dematinN3_S87/92/96/105A, and dematinC1_T274A/S383A constructs were not detected as substrates of p38α, in either kinase assays or with MPM2 immuno-detection. This indicates that

dematin is phosphorylated at one or more of the SP / TP motifs within each construct, and not at any non-consensus sites.

3.6.2 Potential phosphorylation of dematin by other p38 isoforms and MAPKs

Four isoforms of p38 have been identified in vivo: p38α, p38β, p38γ, and p38δ. The in vitro kinase assay data presented here looked at the phosphorylation of dematin by p38α, but it remains to be determined whether this is specific or whether other isoforms can fulfil this function. Both the p38α and p38β isoforms display ubiquitous tissue expression, and are sensitive to inhibition by the SB203580 inhibitor, however the p38α isoform is expressed at higher levels in vivo and has therefore become the model isoform for p38 research (Cargnello & Roux, 2011). The p38γ isoform is found mainly in skeletal muscle, and p38δ expressed in the kidney, pancreas, small intestine, and testes (Ono & Han, 2000). HEK293 cells have been shown to express all four p38 subtypes (Junttila *et al.*, 2007; Lawson *et al.*, 2013; Sabio *et al.*, 2010), and therefore the in vivo phosphorylation detected in the mass spectrometry and MPM2 experiments could be attributable to isoforms other than p38α. Activation of p38 was achieved through co-transfection with $MKK6^{DD}$, which is capable of activating all isoforms of p38, however the SB203580 inhibitor used only has an effect on the p38α and p38β isoforms. A band was not detected when lysate from p38 inhibited HEK293T cells was immunoblotted with an anti-phospho p38 antibody. This suggests that the p38δ and p38γ isoforms are not active under these experimental conditions, and therefore we can assume that in the presence of SB203580 there is no signaling through p38. It is possible that these isoforms are inactivate under basal conditions, but are activated upon hyperactivation of p38 through $MKK6^{DD}$ co-transfection, and therefore we cannot completely rule out the involvement of these isoforms. However it seems likely that the p38α and p38β isoforms are the main contributors.

Studies have shown that it is localisation, rather than substrate specificity, which distinguishes between p38α and p38β. Overexpression of the two isoforms in C2C12 cells showed that expression of p38α is ubiquitous, whereas p38β locates only at the cell periphery. Kinase assays confirmed that p38β is catalytically capable

of phosphorylating the same substrates, but is prevented from doing so in vivo due to lack of colocalisation (Knight *et al.*, 2012). Given the lack of substrate specificity between p38α and p38β it is likely that dematin can also be phosphorylated by p38β, however the in vivo localisation pattern of p38β may prevent it from accessing the total pool of dematin.

The consensus recognition motif of p38 is shared by all MAPKs. In our preliminary in vitro kinase and microarray experiments, dematin was identified as a substrate of p38, but not of ERK5. The identified motifs may be targets of the ERK1/2 or JNK pathways however. Both the dematinN3 and dematinC1 constructs contain SP/TP motifs that were not identified as being phosphorylated in the MS analysis. The dematinN3 region has two further p38 motifs at $T^{120}P$ and $S^{156}P$, and dematinC1 has motifs at $S^{307}P$ and $S^{315}P$. These sites were also not detected in either the in vitro kinase or MPM2 assays suggesting that these are not targets for p38 phosphorylation, but they may be regulated by other MAPKs. Due to the broad recognition motif of the MAPK kinases, alternative mechanisms of substrate recognition are required; however this recognition process is not fully understood. The selectivity of MAPKs can be conferred by the presence of docking motifs, which greatly increase the affinity of a kinase for a substrate. These display a far higher affinity for their chosen MAPK over the other MAPK family members, however some crossover in binding does occur (Bardwell *et al.*, 2009) Additionally many substrates do not contain a docking domain, and this therefore does not regulate all interactions. Substrate recognition in these cases is thought to be controlled by availability, concentration, and subcellular localisation (Trempolec *et al.*, 2013).

Dematin may also be phosphorylated at the above sites by non-MAPK kinases. The majority of serine / threonine specific protein kinases and phosphatases favour substrates that don't contain proline residues in the +1 position, as proline cannot act as a hydrogen bond donor. It is therefore unlikely that any of the identified motifs are phosphorylated by such kinases. Proline-directed kinases overcome this by creating an apolar pocket which is unable to bond with the amide nitrogen of other amino acids (Gray *et al.*, 2003). Other proline directed kinases include the

cyclin-dependent kinases (CDKs) and glycogen-synthase kinase-3 (GSK-3). A global analysis of proteins estimated that greater than one quarter of phosphorylation sites were either Ser-Pro or Thr-Pro motifs, suggesting that these proline-directed kinases regulate a larger number of substrates than the non-proline-directed kinases. Of these sites, Ser-Pro motifs greatly outnumbered Thr-Pro sites with by a ratio of 5:1 (Ubersax & Ferrell, 2007), which is reflected in the motifs identified in dematin.

3.6.3 The stability of dematin is regulated by the PEST motif but not p38

The instability of dematin in protein purification experiments has been reported in the literature, but never investigated further or quantified. Here we have used pulse-chase degradation analysis to calculate the intracellular half-life of the 52 KDa isoform of dematin to be 5.49 +/- 0.44 hours. A recent large-scale analysis of over 5000 mammalian proteins calculated the median half-life to be 46 hours (Schwanhäusser *et al.*, 2013). Relative to the total protein complement, this therefore classifies dematin as a short-lived protein. The intracellular half-life of a protein correlates strongly with its in vivo function. Proteins with a high turnover rate have functions that require high temporal regulation, such as roles in signalling pathways that are subjected to considerable variations in requirements. This suggests that cells use the degradation of dematin a mechanism for regulating its function, and that at least some functions of dematin require time-dependent control.

The presence of a PEST motif in dematin has been reported previously, however the exact location of this motif was not consistently defined. The application of the EMBOSS epestfind algorithm enabled an unbiased definition of the PEST sequence, ^{89}KSTSPPPSPEVWADSR^{104}, which was used for subsequent experiments. Deletion of this region confirmed the involvement of the PEST motif in the instability of dematin in vivo, with the calculated half-life of the dematin_ΔPEST deficient construct significantly longer than wild-type dematin at 7.64 +/- 0.72 hours. Activation of PEST motifs has been linked to protein degradation through both the ubiquitin proteasome pathway (Rechsteiner & Rogers, 1996), and the lysosomal

pathway (Zhuang *et al.*, 2012). Determining the mechanism through which this occurs in dematin will provide further insight into the process.

The majority of PEST motifs act as primary degrons, requiring a second activation mechanism to induce protein degradation. Of these mechanisms phosphorylation within the PEST domain is the most prevalent, and the confirmation of active p38 motifs both within and flanking the PEST motif made p38 a likely candidate for this function. Phosphorylation of the dematinN3_S92/96A construct was consistently reduced compared to wild-type, whereas the dematinN3_S87/92/96/105A was unphosphorylated. This suggests that dematin is phosphorylated in vitro by p38α at one or both of the S87 / S105 motifs which flank the PEST domain, in addition to one or both of the S92 / S96 motifs within the PEST domain. However no significant change in degradation was identified in the presence of p38-hyperactivation or inhibition. Equally the stability of dematin could not be significantly increased / decreased through the mutation of the S87/92/96/105 residues to either Ala or Glu residues. This suggests that the PEST-mediated stability of dematin is not regulated by phosphorylation of theses residues. However a trend towards phospho-mediated instability was detected, and therefore there is a possibility that the technique used here was not sensitive enough to detect these changes. Confirming the mechanism that regulates dematin degradation will be beneficial in providing further information on the conditions under which its degradation is enhanced. A small subpopulation of PEST motifs act as primary degrons and don't require activation, so this remains an alternative possibility for dematin.

Although these algorithms act as an indicator of physiologically relevant PEST motifs, not all of these are shown to be important in vivo. Three high-scoring PEST motifs were identified in the sequence of c-Fos; however individual deletion of two of these had no effect on protein stability. In contrast, deletion of the third site had a stabilising effect. It may, however, be that proteins that contain multiple high-scoring PEST motifs rely on each under different circumstances. As dematin only contained a single motif above the threshold this is unlikely to be a mechanism that occurring here. However the threshold is to some extent an arbitrary cut-off value

to determine potential biological significance, and any site with a positive score technically qualifies as a PEST motif. The motif from 300-325 aa was attributed a score of 4.08, and therefore although it is unlikely that this has an impact on stability it remains a possibility.

Previous attempts to overexpress dematin in *E.coli* in order to study the structure of core domain have reportedly been hindered by significant problems with proteolysis (Chen *et al.*, 2009). In an attempt to combat this, the group created a number of mutated constructs. Mutation of Glu^{89} to a lysine residue to switch the charge was not successful; neither was substituting the phosphorylatable sequence $^{90}STS^{92}$ with the non-phosphorylatable $^{90}AAA^{92}$. They were able to prevent proteolysis by deletion the entire PEST motif (which they defined as $^{89}KSTSPPPSPEVWAD^{102}$), however concerns over the effect of removing such a large sequence on the native conformation of the core domain made the construct unsuitable for the desired experiments. The final approach involved mutating all Pro, Glu, Ser, and Thr residues within the motif; Ser / Thr residues were mutated to Ala, Pro to Gly, and Glu to Lys. This new construct containing $^{89}KAAAGGGAGKVWAD^{102}$ was reported to be resistant to proteolysis. These experiments involved the expression of GST- fusion proteins in *E.coli*. Interestingly there has been no documented evidence of the activity of the PEST degradation pathway in prokaryotic organisms. However the deletion results are consistent with the results presented here using the dematin_ΔPEST construct.

Although the PEST motif was identified as a regulator of dematin degradation, it is likely that there are other factors that control dematin stability. The Expasy ProtParam calculator (Gasteiger E., 2005) gives an estimate of the stability of a protein in a test tube, which is referred to as an Instability Index (II) value. This calculation is based upon statistical analysis of 12 unstable and 32 stable proteins, which identified certain dipeptides that had significantly different occurrences between the two groups (Guruprasad *et al.*, 1990). Each of the 400 dipeptides identified were scored according to their instability correlation, and these scores along with the length of the protein sequence to be analysed, are used to

determine the II value of a protein. Values of 40 or below predict that a protein will be stable in a test tube, whereas values above this suggest instability. The II values of the 48 and 52 KDa isoforms of dematin were computed to be 75.74 and 72.04 respectively, which classifies both isoforms as unstable.

3.6.4 The dematin HP / core domain interaction is not regulated by p38

Chen *et al* (2013) recently demonstrated that upon phosphorylation of the dematin HP at Ser^{74} [Ser^{403}] by PKA, a conformational change was induced that increased the affinity of the HP for the core domain, and subsequently inhibited actin bundling. We were able to demonstrate this interaction in our system, with the HP binding to full-length dematin. An interaction was not detected between the HP and truncated constructs dematinN2, N3, or C1. These constructs were initially designed to investigate p38 phosphorylation sites, and 14-3-3 binding motifs, and so do not cover the entire dematin sequence. These results therefore suggest that the HP binds to the core domain either in the region not covered by these constructs (from aa 197-261), or at a site overlapping this untested region and either the dematinN3 or dematinC1 domains. The cloning of further constructs will be required to precisely define the site within the core domain that the HP binds to.

The dematin HP contains a single SP phosphorylation motif at Ser^{383}, and here we have confirmed through MS and MPM2 immunoblotting that this site is phosphorylated in vivo. Furthermore the site was directly phosphorylated by p38α in in vitro kinase assays, and in vivo phosphorylation was detected in the absence but not presence of the p38 inhibitor SB203580. Localisation of this site at the extreme end of an α-alpha helical region, on the external surface of the protein, lead to the hypothesis that phosphorylation of this site might change the conformation of the dematin HP. Using the HP / dematin binding model above, p38-hyperctivation or inhibition were shown to have no effect on the HP / core interaction. Creating constructs where the Ser^{383} phosphorylation site had been mutated either to an non-phosphorylatable Ala residue, or to a phospho-mimicking Glu residue, further validated this finding as no disruption in the HP/core binding was detected. This therefore suggests either that p38 phosphorylation of this site

does not induce a conformational change in the dematin HP, or that the conformational change occurs in a manner that is compatible with the HP / core binding mechanism.

In order to fully characterise the potential change in conformation that occurs in the dematin HP upon phosphorylation of Ser^{383} by p38, it would be useful to determine the structure of the dematinHP_S383A and dematinHP_S383D constructs using solution NMR. Comparison of the resulting structures to the currently available wild-type HP structure would enable an improved understanding of the potential for phosphor-regulation of the HP at Ser^{383}. If a phospho-mediated conformational change can be demonstrated, then p38 may act directly to inhibit actin binding / bundling. The Ser^{383} site is located in the middle of the dematin HP actin-binding motif ^{367}LERHLSAEDFSRVFAM**SP**EEFGKLALWKR^{395} and therefore a p38-mediated conformational change has the potential to directly inhibit actin binding at this motif. This would leave only the core motif able to bind actin, and subsequently would prevent dematin from bundling actin.

4. Dematin interacts with the adaptor protein 14-3-3

4.1 Introduction

14-3-3 proteins are ubiquitously expressed throughout the body, and interact with a vast array of target proteins to regulate important cellular functions (Hermeking & Benzinger, 2006; Kleppe *et al.*, 2011). In humans, seven distinct genes encoding 14-3-3 isoforms β, γ, ε, ζ, η, τ and σ have now been identified (Wang & Shakes, 1996). The interaction between 14-3-3 and a target protein commonly occurs at phosphorylated mode I RSx(pS/pT)xP, or mode II Rxφx(pS/pT)xP motifs, where pS/pT indicates a phosphorylated serine / threonine residue, φ is an aromatic or aliphatic residue, and x is any amino acid (Muslin *et al.*, 1996; Yaffe *et al.*, 1997). In some instances 14-3-3 can also interact with the extreme carboxy-terminus of a protein at a mode III –(pS/pT)x_{1-2}-COOH motif (Coblitz *et al.*, 2005). Although these conserved peptide motifs are the interaction sites in the majority of cases, 14-3-3 displays some flexibility in target binding and there are examples that show motifs that deviate significantly from the above sequences (Johnson *et al.*, 2010).

To date more than 300 14-3-3 binding proteins have been identified, but there are likely to be many others that have yet to be characterised. The primary sequence of dematin contains a number of 14-3-3 consensus motifs (Figure 1.2), and is therefore a likely substrate of 14-3-3. Dematin is both an actin-binding and -bundling protein (Rana *et al.*, 1993), and characterisation of a dematin / 14-3-3 interaction could therefore provide further evidence of an increasing role for the 14-3-3 protein family in regulating the cytoskeleton. In addition, dematin is fairly ubiquitously expressed throughout the body (Kim *et al.*, 1998; Rana *et al.*, 1993) and identifying novel regulatory mechanisms therefore has widespread functional implications.

In the majority of cases, 14-3-3 requires a consensus motif in the target protein to be phosphorylated for binding to occur (Yaffe *et al.*, 1997). As many 14-3-3 binding motifs contain an arginine residue in the -3 position, basophilic serine / threonine kinases commonly phosphorylate these motifs as it correlates with their own consensus motifs. Known regulators of 14-3-3 binding include Akt (Mohammad *et al.*, 2013), PKA (Neukamm *et al.*, 2013), and AMPK (Shen *et al.*, 2013).

In addition to requiring a phosphorylated binding motif, 14-3-3 binding can be negatively regulated by inhibitory phosphorylation of the target protein at residues neighbouring the binding motif. In chapter 3 dematin was identified as a novel substrate of the p38 MAPK. Several of the 14-3-3 binding motifs within dematin either overlap with, or border, p38 phosphorylation sites (Figure 1.2). The potential regulation of the dematin / 14-3-3 interaction by inhibitory p38 phosphorylation will therefore also be investigated.

The experiments presented in this chapter aimed to answer the following questions:

1) Does dematin interact with 14-3-3β in vivo?

2) Which 14-3-3 binding motifs in dematin mediate this interaction?

3) Are these motifs phosphorylated by AKT, AMPK, or PKA?

4) Is the dematin / 14-3-3β interaction regulated by p38 phosphorylation?

4.2 The interaction between dematin and 14-3-3β

The seven human isoforms of 14-3-3 show variation in their subcellular expression patterns, with the β and ζ isoforms preferentially associating with cytosolic and cytoskeletal proteins (Roth et al., 1994). As dematin known to be a cytoskeletal-associated protein, the 14-3-3β isoform was selected as a basis for investigating the potential interaction between dematin and 14-3-3.

4.2.1 The primary sequence of dematin contains seven 14-3-3 binding motifs

14-3-3 family members interact with their target proteins at specific phosphorylated motifs. These can be generally defined as Mode I (Rxx(pS/pT)xP), Mode II (Rxφx(pS/pT)xP), or Mode III (-(pS/pT)x1-2-COOH). This conservation allows potential novel 14-3-3 binding partners to be easily identified by scanning the primary sequences for the presence of these motifs. Two isoforms of dematin exist of 48 and 52 KDa, which differ by a 22-amino acid insert (Figure 4.1). The primary sequences of both isoforms (Homo Sapiens; NP_001107610.1 and NP_001107608.1) were analysed using the Scansite (Obenauer *et al.*, 2003) and Eukaryotic Linear Motif resource (Dinkel *et al.*, 2013) programmes to identify the presence of such motifs. These databases also contain the sequences of non-standard motifs found in other validated 14-3-3 binding proteins, and so are capable of identifying less stringent potential binding sites.

Sequence scans identified six 14-3-3 binding motifs that are found in both dematin isoforms, and an additional motif in the 52 KDa variant (Figure 4.1). Of these seven sites, two were Mode I motifs at $RDSS_{22}VP$ and $RGNS_{333}LP$, the second of which is only found in the longer 52 KDa isoform. There was a single Mode II motif of $RKTRS_{269}LP$, and a Mode III C-terminal $KKKAS_{403}LF$ binding motif. In addition to these sites there were a further three motifs that didn't fit into the strict mode I / II / III groupings - $RERS_{85}LSP$, $RTS_{124}LP$, and $KSSS_{289}LP$.

Figure 4.1: The 14-3-3 consensus motifs in the human dematin sequence

14-3-3 proteins interact with their targets at well-defined sequence motifs. Analysis of the primary sequences of the 48 and 52 KDa splice variants of human dematin identified seven 14-3-3 binding motifs in the longer isoform, and six in the shorter version (yellow boxes). These are numbered according to the amino acid position of the phosphorylatable serine residue in the 52 KDa isoform.

4.2.2 Cloning of dematin constructs for use in this chapter

Dematin constructs were cloned into mammalian expression vectors as described in chapter 3, section 3.2.2. In addition to the constructs used in chapter 3, the shorter 48 KDa isoform of dematin was also cloned using the same method, and was MYC tagged to differentiate it from the 52 KDa isoform. As previously, constructs for GST-pulldown experiments had a GST-tag to facilitate purification, and a FLAG or MYC tag for immuno-detection. Proteins for IP experiments were tagged only with FLAG or MYC. A schematic of the dematin constructs used in this chapter is provided in Figure 4.2.

4.2.3 14-3-3β binds to both the 48 and 52 KDa isoforms of dematin

To determine whether 14-3-3β binds to dematin in vitro, co-immunoprecipitation experiments were conducted in HEK293T cells co-transfected with either pDEST27*FLAG*-dematin and pcDNA3.1*MYC*-14-3-3β or pDEST27*MYC*-dematin48 and pcDNA3.1*FLAG*-14-3-3β. Cells were lysed under conditions which maintained protein-protein interactions, and then immunoprecipitated with either anti-FLAG or anti-MYC antibodies as appropriate. Immunoprecipitates were subjected to SDS-PAGE separation, and immunoblot analysis was conducted using either anti-FLAG or anti-MYC antibodies. Results showed that 14-3-3β co-immunoprecipitated with dematin (Figure 4.3A) and dematin48 (Figure 4.3B). In the reciprocal experiments, both dematin constructs co-immunoprecipitated with 14-3-3β (Figure 4.3). In each experiment the negative control IPs in which dematin or 14-3-3β was expressed alone showed no non-specific protein bands in these regions. This indicates that 14-3-3β interacts with both the 48 KDa and 52 KDa isoforms of dematin.

4.3 Sites of interaction between dematin and 14-3-3β

Following the demonstration of an interaction between dematin and 14-3-3β, the regions of dematin that were involved in this interaction were investigated. Site-directed mutagenesis was used to create constructs with mutated 14-3-3 binding

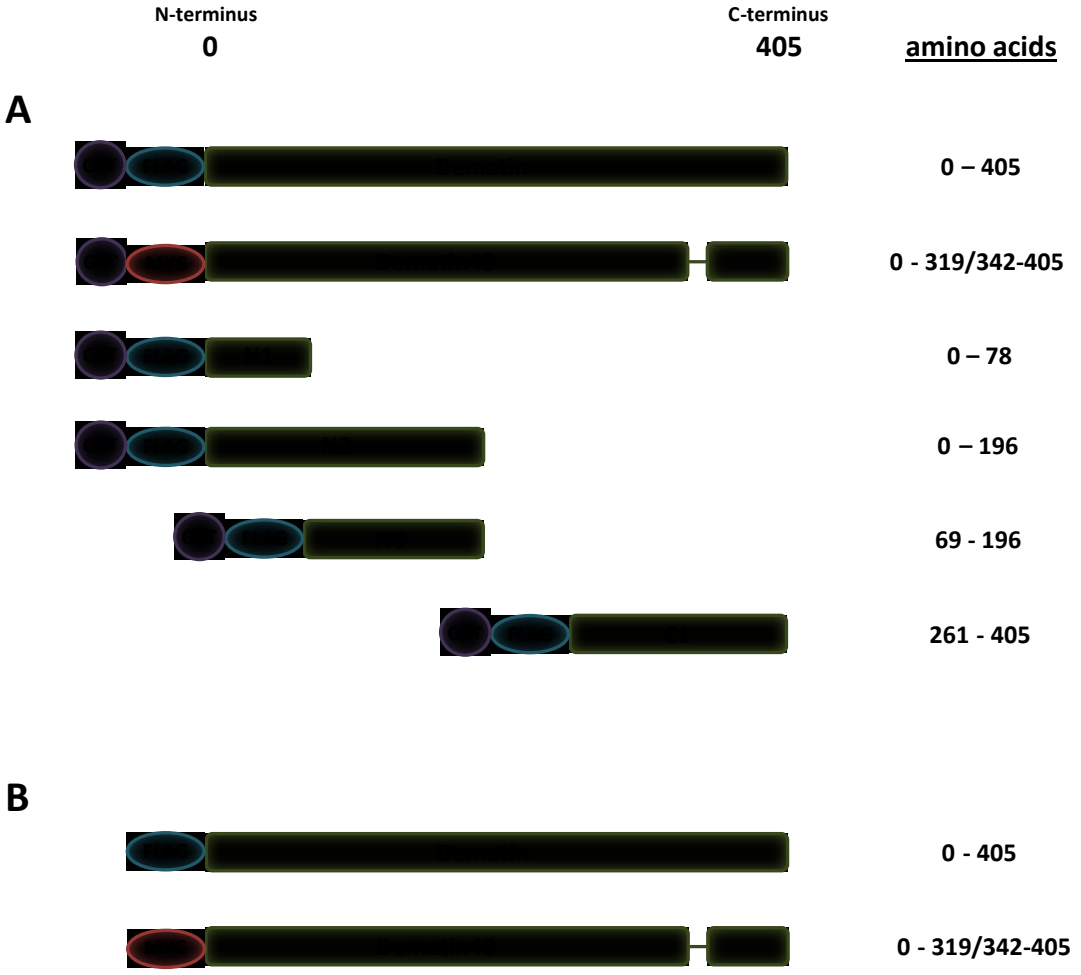

Figure 4.2: Schematic illustrating the dematin constructs used in this chapter

Diagram showing the relative positions of full-length and truncated dematin constructs cloned for use in this chapter, with the tags used for purification and detection. Constructs for use in GST-pulldown experiments (A) all had N-terminal GST-tags followed by either a FLAG or MYC tag. Those for IP experiments (B) had only an N-terminal FLAG or MYC tag. *(GST; glutathione-S-transferase, IP; immunoprecipitation).*

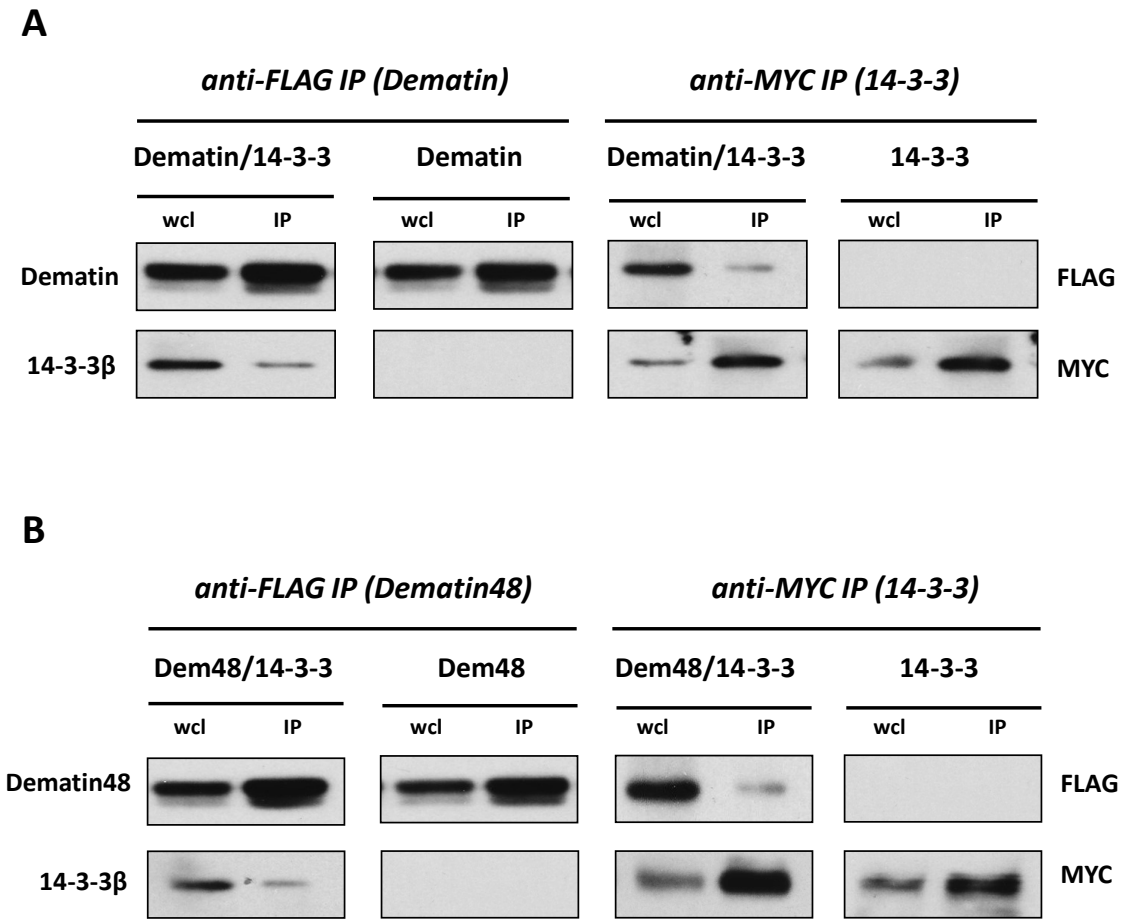

Figure 4.3: Dematin and 14-3-3β co-immunoprecipitate in HEK293T cells

The potential interactions between the 48 and 52 KDa isoforms of dematin and 14-3-3β were investigated using co-immunoprecipitation experiments in HEK293T cells. Cells were co-transfected with pDEST27*FLAG*-Dematin and pcDNA3.1*MYC*-14-3-3β (A) or pDEST27*MYC*-dematin48 and pcDNA3.1*FLAG*-14-3-3β (B) and. Cells lysates were immunoprecipitated with either anti-FLAG, or anti-MYC antibodies, as appropriate to purify dematin, and proteins separated by SDS-PAGE and transferred onto nitrocellulose. Membranes were immunoblotted with anti-FLAG and anti-MYC antibodies of different species from those used for the immunoprecipitation. (n=3) *(SDS-PAGE; sodium dodecyl sulphate polyacrylamide electrophoresis, wcl; whole cell lysate)*

sites, and GST-pulldown experiments repeated with these mutants to determine which sites mediate this interaction.

4.3.1 Full-length dematin contains three phosphorylated 14-3-3 binding motifs

As the majority of interactions between 14-3-3 and its targets require a phosphorylated binding motif, identifying which of the seven motifs within dematin are phosphorylated provided a starting point for determining the active interaction sites. Phosphorylated residues in the 52 KDa isoform of dematin were mapped using mass spectrometry (see chapter 3, section 3.3.3). Analysis of the peptide fragments identified a total of 24 phosphorylated residues under our experimental conditions. Of these phosphorylated residues, 3 corresponded with the previously identified 14-3-3 binding motifs: serine residues 22, 85, and 269 (Table 4.1). This suggested that the motifs RDSS$_{22}$VP, RERS$_{85}$LSP, and RKTRS$_{269}$LP were likely candidates for the dematin / 14-3-3 interaction.

4.3.2 14-3-3β binds to the C-terminal region of dematin

The mass spectrometry analysis identified 3 phosphorylated 14-3-3 binding motifs, which then needed to be tested to determine whether they mediate an interaction with 14-3-3β. To facilitate this, four truncated dematin constructs were cloned, covering the following amino acid ranges: dematinN1 (0-78), dematinN2 (0-96), dematinN3 (69-196) and dematinC1 (261-405). The relative positioning of each construct can be seen in Figure 4.2. These constructs were expressed as fusion proteins in HEK293T cells, and purified on GST-binding columns. Following SDS-PAGE separation and western blotting, membranes were probed for anti-FLAG (dematin) and anti-MYC (14-3-3β) as previously. All four truncated constructs were successfully purified out of the lysate via their GST tags, however 14-3-3β only co-purified with dematinC1 (Figure 4.4). This indicated that under these experimental conditions 14-3-3β binds to the C-terminal region of dematin between aa 261-405, but does not bind to the N-terminal region.

Table 4.1: Dematin contains three phsophorylated 14-3-3 binding motifs

Mass spectrometry was used to identify phosphorylated residues in the 52 KDa isoform of dematin. HEK293T cells were transfected with pDEST27-Flag-Dematin and pcDNA3.1-MKK6^{DD} using calcium phosphate. Cells were lysed and dematin purified on a GST pulldown column, and separated by SDS-PAGE. After coomassie staining, the dematin protein band was excised from the gel and lyophilised. The sample was analysed by mass spectrometry for the presence of phosphorylated residues. These phosphorylation sites were then correlated with known 14-3-3 binding motifs in dematin to determine which of these were phosphorylated.

14-3-3 binding motif	Phosphorylatable residue	Phosphorylated in mass spectrometry?	Truncated constructs containing this site
RDS**S**VP	serine 22	YES	N1, N2
RER**S**LSP	serine 85	YES	N2, N3
RT**S**LP	serine 124	NO	N2, N3
KTR**S**LP	serine 269	YES	C1
KSS**S**LP	serine 289	NO	C1
RGN**S**LP	serine 333	NO	C1
KKKA**S**LF	serine 403	NO	C1

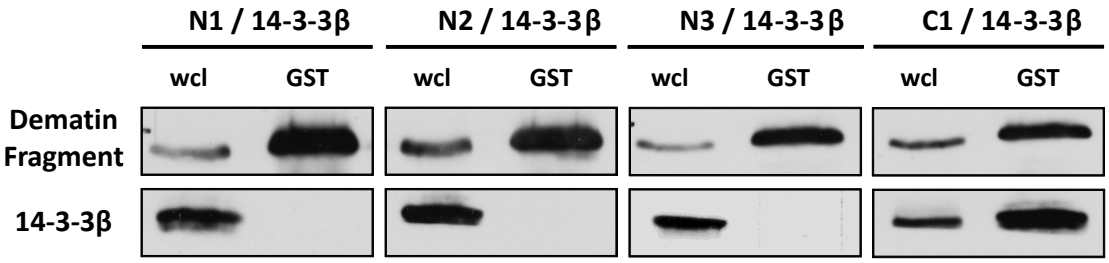

Figure 4.4: Only the C-terminal region of dematin binds to 14-3-3β

Co-immunoprecipitation experiments were conducted to determine which regions of dematin interact with 14-3-3β. HEK293T cells were co-transfected with the truncated dematin constructs N1, N2, N3 and C1 in pDEST27*FLAG* vector, and pcDNA3.1*MYC*-14-3-3β. Cells lysates were purified on GST-pulldown columns, separated by SDS-PAGE and transferred onto nitrocellulose. Membranes were immunoblotted with anti-FLAG and anti-MYC antibodies. The truncated dematin constructs cover the following amino acid ranges relative to the full-length 52 KDa protein: N1 (0-78), N2 (0-96), N3 (69-196) and C1 (261-405). (n=3) *(GST; glutathione S-transferase, wcl; whole cell lysate).*

4.3.3 14-3-3β binds to the C-terminal region of dematin at Ser^{269} and Ser^{333}

Confirming that 14-3-3β co-immunoprecipitated with the dematinC1 provided a starting point for determining the essential 14-3-3 binding motifs within this region. The dematinC1 construct contains four 14-3-3 consensus motifs at residues Ser^{269}, Ser^{289}, Ser^{333,} and Ser^{403}. The mass spectrometry analysis, however, only identified Ser^{269} as being phosphorylated under our experimental conditions. Site-directed mutagenesis was employed to create a C1_S269A mutant with the phosphorylatable serine residue mutated to a non-phosphorylatable alanine residue. The GST-pulldown experiment was then repeated to determine whether the loss of this single binding motif could prevent the interaction between dematinC1 and 14-3-3β. As Figure 4.5 shows, 14-3-3β still co-purified with the dematinC1_S269A mutant. This suggested either that the RKTRS$_{269}$LP motif was not a site of interaction between dematinC1 and 14-3-3β, or that it was not the only site of interaction and that the other site(s) was capable of independent binding in the absence of Ser^{269}.

As none of the Ser^{289}, Ser^{333}, or Ser^{403} residues were detected as being phosphorylated in our mass spectrometry experiments, a systematic approach was taken to determining which of these binding sites were important. Further serine to alanine mutants of the dematinC1 consensus motifs were created that each had three of the four binding sites mutated, leaving only a single binding motif; S289/333/403A, S269/333/403A, S269/289/403A and S269/289/333A. GST-pulldown experiments showed that RKTRS$_{269}$LP (mutant S289/333/403A) and RGNS$_{333}$LP (mutant S269/289/403A) were sufficient to independently bind 14-3-3 in the absence of the other motifs (Figure 4.6). Having a single phosphorylatable motif at Ser^{289} (mutant S269/333/403A) or Ser^{403} (mutant S269/289/333A) was insufficient to maintain the dematinC1 / 14-3-3β interaction (Figure 4.6). A double mutant of dematinC1_S269/333A was then created, to confirm that these two sites were the only motifs in dematinC1 required for 14-3-3β binding. Repetition of the GST-pulldown experiments showed that 14-3-3β no longer co-purified with dematinC1 in the absence of Ser^{269} and Ser^{333} (Figure 4.6).

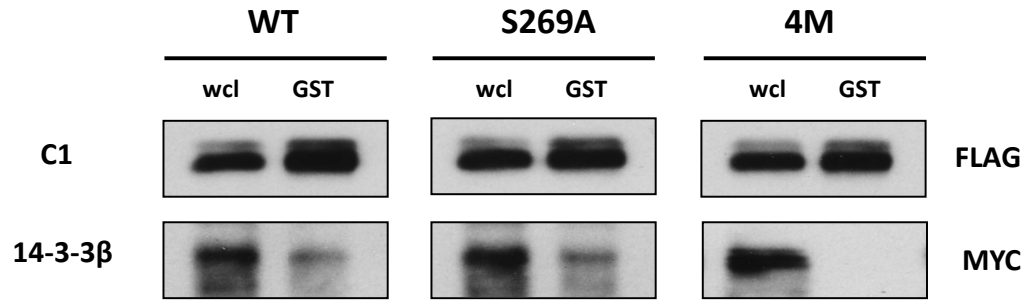

Figure 4.5: Ser^{269} is not the only 14-3-3 binding site in dematinC1

Mass spectrometry identified a single phosphorylated 14-3-3 binding motif in the C-terminal region of dematin at Ser^{269}. Co-immunoprecipitation experiments using a dematin_S269A mutant were conducted to determine whether this was sufficient to abolish the C1 / 14-3-3β interaction. HEK293T cells were co-transfected with the given dematin construct in pDEST27*FLAG* vector, and pcDNA3.1*MYC*-14-3-3β. Cells lysates were purified on GST-pulldown columns, separated by SDS-PAGE, and transferred onto nitrocellulose. Membranes were immunoblotted with anti-FLAG and anti-MYC antibodies. (n=3) *(GST; glutathione S-transferase, wcl; whole cell lysate).*

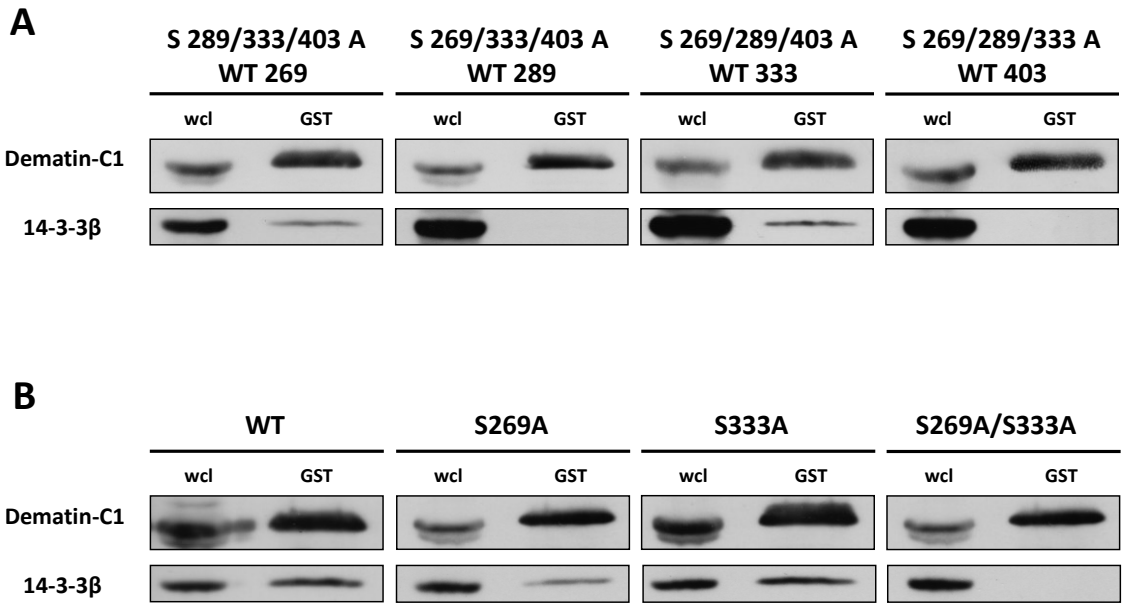

Figure 4.6: C-terminal region of dematin binds 14-3-3β at Ser^{269} and Ser^{333}

HEK293T cells were co-transfected with the stated dematin-C1 construct in the pDEST27*FLAG* vector, and pcDNA3.1*MYC*-14-3-3β. Cells lysates were purified on GST-pulldown columns, separated by SDS-PAGE, and transferred onto nitrocellulose. Membranes were immunoblotted with anti-FLAG and anti-MYC antibodies. Triple mutants with three potential binding sites mutated to alanine residues (A) were first conducted to narrow down the potential sites of interaction. After showing that the S269 and S333 sites were capable of independent binding to 14-3-3β, the double mutant of these sites (B) was tested to confirm that this was sufficient to abolish the interaction. (n=3) *(GST; glutathione S-transferase, wcl; whole cell lysate; WT, wild-type sequence).*

4.3.4 14-3-3β binds to full-length dematin at serine residues 269 and 333

Further mutants were then created in the pDEST27*FLAG*-dematin and pDEST27*FLAG*-dematin48 backbones to determine whether preventing binding at the $RKTRS_{269}LP$ and $RGNS_{333}LP$ motifs was sufficient to prevent the interaction between full-length dematin and 14-3-3β. The GST-pulldown experiments were repeated with these new constructs, and the double S269/333A mutant was again sufficient to abolish the interaction between the 52 KDa isoform of dematin and 14-3-3β (Figure 4.7A). As seen with dematinC1, constructs that contained only one of the two phosphorylated binding motifs were still able to interact with 14-3-3β (Figure 4.7A). The 48 KDa isoform of dematin lacks the $RGNS_{333}LP$ motif, therefore the single S269A mutation was sufficient to abolish the dematin48 / 14-3-3β interaction (Figure 4.7B). From this we can conclude that 14-3-3β binds to the 52 KDa isoform of dematin at the $RKTRS_{269}LP$ and $RGNS_{333}LP$ motifs, and to the 48 KDa isoform at $RKTRS_{269}LP$.

4.4 Candidate kinases for the phosphorylation of 14-3-3 motifs

For an interaction to occur between 14-3-3 and a target protein, phosphorylation of a putative binding motif is generally required. Binding motifs have previously been shown to be phosphorylatable by a range of protein kinases, and here we aimed to determine which kinases were phosphorylating the motifs identified in dematin.

4.4.1 Phosphorylation of dematinC1 at Ser^{269} and Ser^{333}

The amino acid sequences surrounding the Ser^{269} and Ser^{333} phosphorylation sites were scanned for the presence of kinase phosphorylation motifs using the Scansite resource (Obenauer *et al.*, 2003). Protein sequences are compared to the optimal phosphorylation motifs of different Ser/Thr kinases, and given a score depending on how closely the surrounding amino acids correlate with ideal values. High stringency sites are those within the top 0.2% of all sites found in the vertebrate collection of the Swiss-Prot protein database. Medium or low stringency scores indicate that a sequence is within the top 1% or 5% respectively. Ser^{269} was ranked

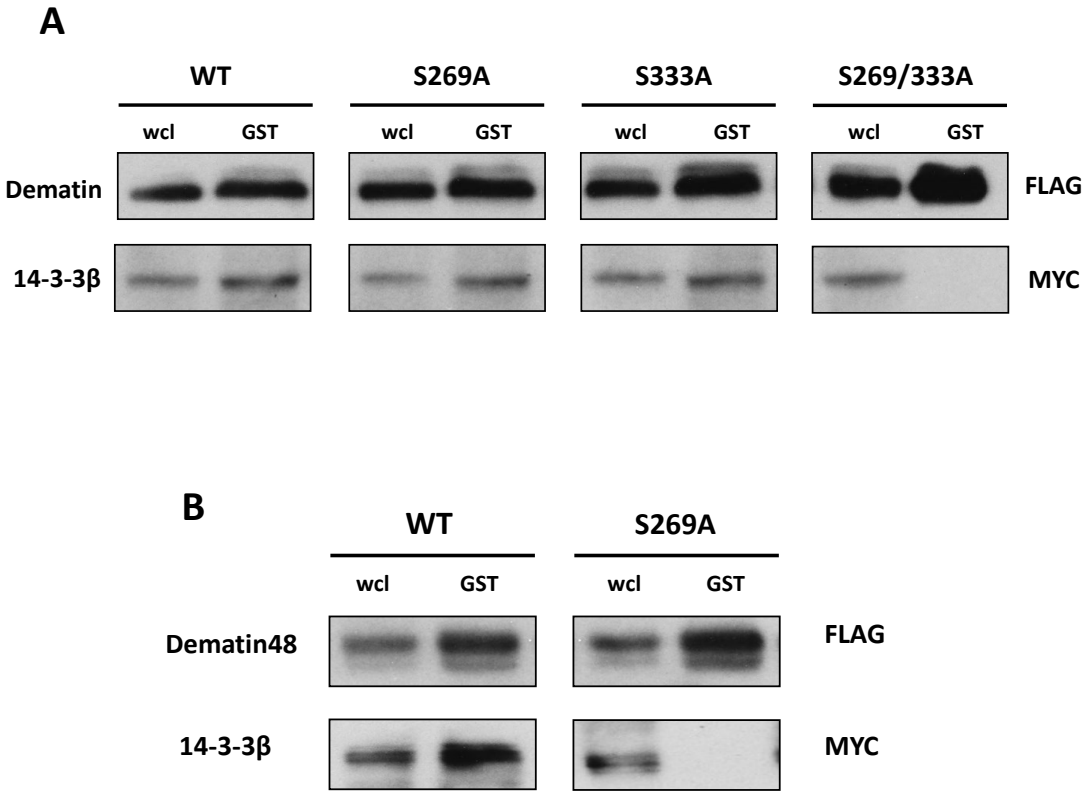

Figure 4.7: Dematin interacts with 14-3-3β at Ser^{269} and Ser^{333}

HEK293T cells were co-transfected with the stated dematin constructs in the pDEST27*FLAG* vector, and pcDNA3.1*MYC*-14-3-3β. (Cells lysates were purified on GST-pulldown columns, separated by SDS-PAGE and transferred onto nitrocellulose. Membranes were immunoblotted with anti-FLAG and anti-MYC antibodies as shown. (A) Interaction between 52 KDa dematin and 14-3-3β. (B) Interaction between 48 KDa dematin and 14-3-3β (n=3) (*GST; glutathione S-transferase, wcl; whole cell lysate)*

as a high stringency Akt site and medium stringency for AMPK and PKA. Ser^{333} was ranked as a medium stringency Akt site and low stringency PKA site. However as these are only predictions, both sites were tested with inhibitors against all three.

GST-pulldown experiments between pDEST27*FLAG*-dematinC1_S269A or pDEST27*FLAG*-dematinC1_S333A and pcDNA3*MYC*-14-3-3β were repeated in the presence of inhibitors of Akt, AMPK, and PKA. Cells were transfected and maintained for 48 hours before 6 hours incubation with inhibitor immediately prior to cell lysis and IP. Inhibition of Akt, AMPK or PKA were insufficient to abolish the interaction between 14-3-3β and dematinC1_333A (Figure 4.8A) or dematinC1_269A (Figure 4.8B). This suggests that under our experimental conditions, Akt, AMPK, or PKA do not phosphorylate the $RKTRS_{269}LP$ and $RGNS_{333}LP$ binding sites in dematin. To confirm the efficacy of the inhibitors used, an inhibitor timecourse could have been conducted using antibodies against phosphorylated downstream targets to quantify the level of inhibition from 0-6 hours.

4.4.2 Phosphorylation of N-terminal 14-3-3 binding motifs

Although the mass spectrometry identified phosphorylated 14-3-3 consensus motifs at serine residues 22 and 85, our standard experimental conditions failed to detect an interaction between the N-terminal of dematin and 14-3-3β. To rule out the possibility that an interaction was not occurring due to these sites not being activated by their physiological kinases under these conditions, we attempted to identify potential regulators of these sites. Sequence analysis identified Ser^{22} as a medium stringency Akt phosphorylation site, and a low stringency PKA site. Ser^{85} was reported to be a high stringency Akt site and low stringency AMPK / PKA.

The GST-pulldown experiments with pDEST27*FLAG*-dematinN2 and pcDNA3.1*MYC*-14-3-3β were repeated immediately after activation of these kinases. Cells were incubated for 1 hour with 100 nm insulin, 500 µM AICAR, or 10 µM forskolin to activate Akt, AMPK, or PKA respectively. Under these conditions, 14-3-3β still did not co-purify with dematinN2 (Figure 4.9A). To determine whether these sites were

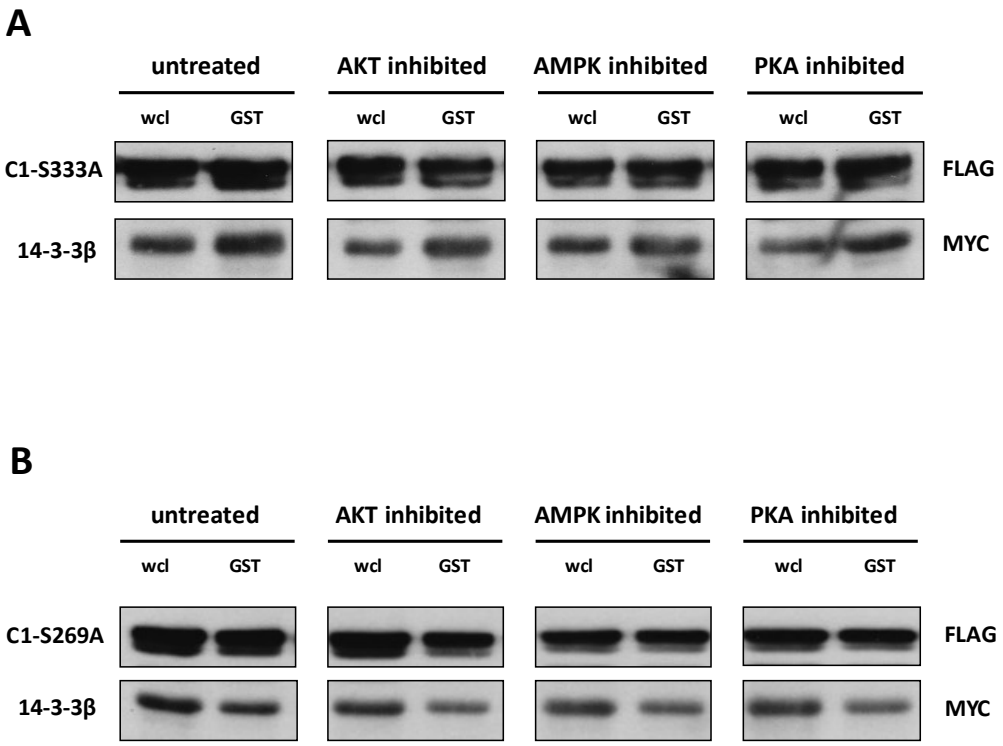

Figure 4.8: Inhibition of Akt, AMPK, or PKA does not inhibit the dematin / 14-3-3β interaction

The interaction between dematin-C1 and 14-3-3β was investigated in the presence on various inhibitors to try and determine whether these kinases phosphorylate either the $RKTRS_{269}LP$ or $RGNS_{333}LP$ motifs. HEK293T cells were co-transfected with pDEST27*FLAG*-dematin_S333A (A) or pDEST27*FLAG*-dematin_S269A (B), and pcDNA3.1*MYC*-14-3-3β. After 48 hours, cells were treated with inhibitors of Akt, AMPK, and PKA for 6 hours. Cells lysates were then purified on GST-pulldown columns, separated by SDS-PAGE and transferred onto nitrocellulose. Membranes were immunoblotted with anti-FLAG and anti-MYC antibodies (n=3) *(GST; glutathione S-transferase, wcl; whole cell lysate)*

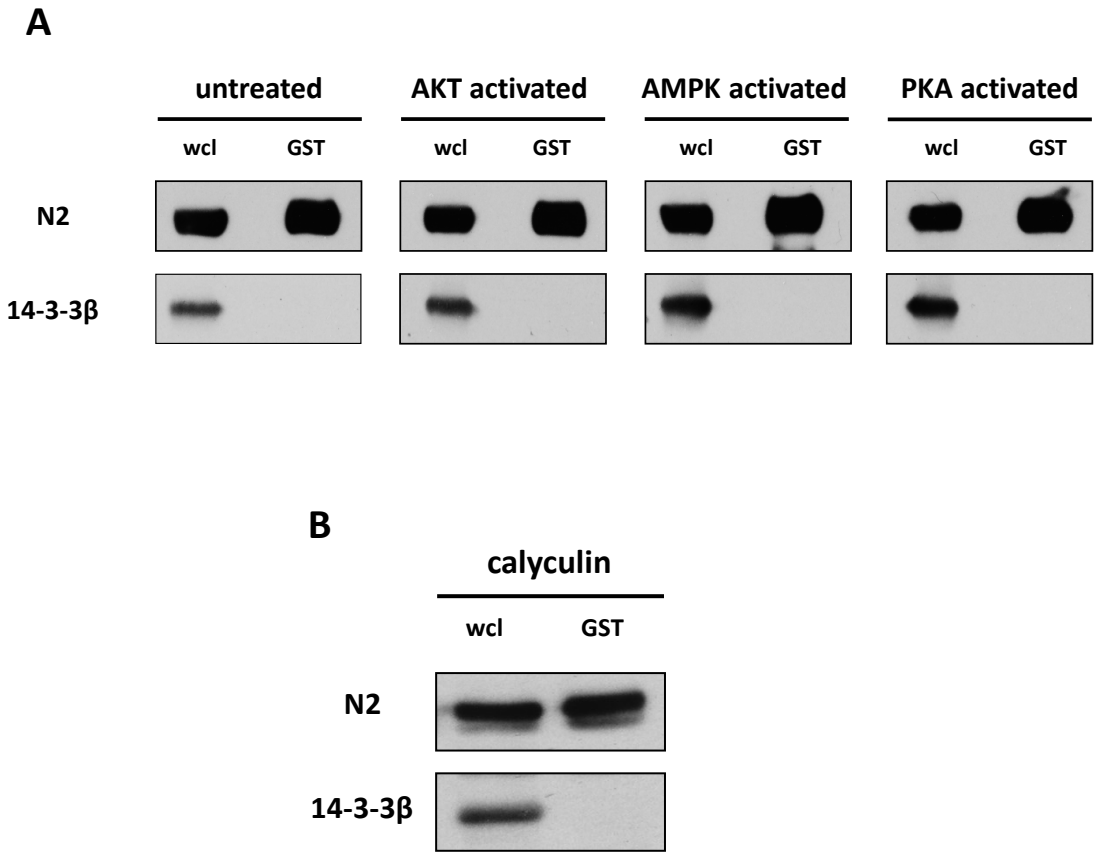

Figure 4.9: Activation of Akt, AMPK, or PKA is not sufficient to induce an interaction between the N-terminal of dematin and 14-3-3β

(A) The N-terminal dematin fragment was treated with compounds to activate Akt, AMPK and PKA to determine whether this could induce an interaction with 14-3-3β. HEK293T cells were co-transfected with pDEST27*FLAG*-dematinN2 and pcDNA3.1*MYC*-14-3-3β. After 48 hours, cells were treated with activators of AKT (100 nM insulin), AMPK (500 µM AICAR), and PKA (10 µM forskolin) for 60 minutes. Cells lysates were then purified on GST-pulldown columns, separated by SDS-PAGE and transferred onto nitrocellulose. Membranes were immunoblotted with anti-FLAG and anti-MYC antibodies. (B) The experiment was repeated following a one-hour incubation with calyculin to inhibit protein phosphatases PP1 and PP2A activity (n=3) *(GST; glutathione S-transferase, wcl; whole cell lysate).*

being phosphorylated by alternative kinases, the experiments were repeated following a 60-minute incubation with 100 nM calyculin. As calyculin inhibits the activity of protein phosphatases PP1 and PP2A, phosphorylation at all sites regulated by these phosphatases will increase under these conditions. As in untreated conditions 14-3-3β still did not co-purify with dematinN2 (Figure 4.9B). This suggests that 14-3-3β does not bind to dematinN2 at phosphorylated residues Ser^{22} and Ser^{85}, or that binding of these sites alone is not sufficient for an interaction. Alternatively, it may be that one or both of these residues are dephosphorylated by phosphatases other than those of the PP1 and PP2A families, and so inhibition with calyculin did not increase phosphorylation at these sites.

4.5 Effect of p38 phosphorylation on 14-3-3β binding

In addition to the kinase required to phosphorylate the binding motif, the ability of 14-3-3 proteins to interact with a target can be regulated by other inhibitory kinases. In chapter 3, dematin was identified as a novel substrate of the p38 MAPK, and we therefore aimed to investigate whether p38 plays a regulatory role in the interaction between dematin and 14-3-3β. This was of particular interest as the 14-3-3 binding motifs at Ser^{22}, Ser^{85}, and Ser^{269} that were identified in the mass spectrometry analysis all contain closely neighbouring or overlapping potential p38 phosphorylation motifs.

4.5.1 The dematinC1/ 14-3-3β interaction is not affected by p38 phosphorylation

The effect of p38 phosphorylation was first tested on the known 14-3-3 binding sites at Ser^{269} and Ser^{333}, with single serine-alanine mutants used to look at the regulation of each site individually. Thr^{274} is a potential p38 phosphorylation motif that neighbours the Ser^{269} 14-3-3 binding motif (Figure 4.10A), and this was identified as being phosphorylated in our mass spectrometry (Chapter 3, Figure 3.5). The GST pulldown experiment between pDEST27*FLAG*-dematinC1_S269A or pDEST27*FLAG*-dematinC1_S333A and pcDNA3.1*MYC*-14-3-3β were repeated under

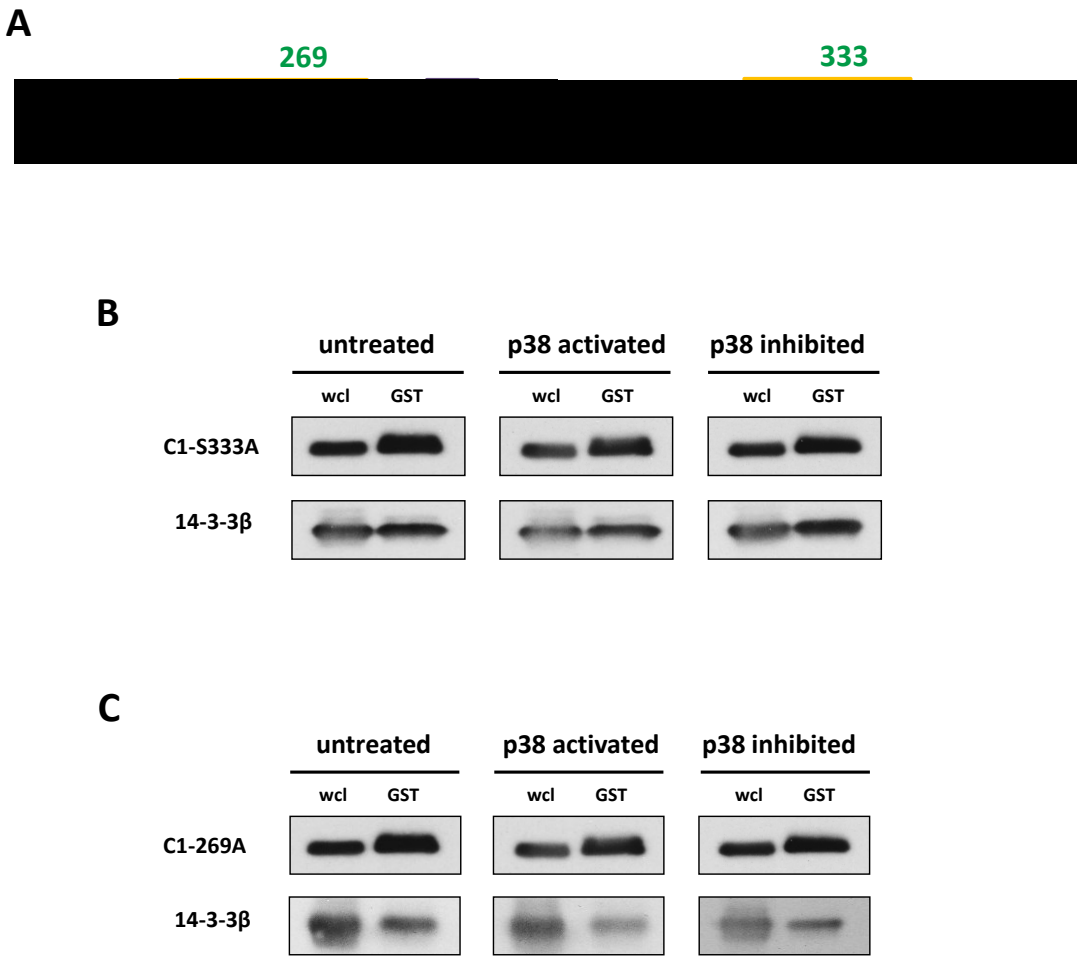

Figure 4.10: Alterations in p38 phosphorylation state do not affect the interaction between 14-3-3β and the C-terminal of dematin

HEK293T cells were co-transfected with pDEST27*FLAG*-dematin_S269A or pDEST27*FLAG*-dematin_S333A, and pcDNA3.1*MYC*-14-3-3β. For p38 activation cells were co-transfected with pcDNA3*FLAG*-MKK6. After 48 hours, p38 inhibited cells were treated with the specific inhibitor SB203580 for 4 hours. Cells lysates were then purified on GST-pulldown columns, separated by SDS-PAGE and transferred onto nitrocellulose. Membranes were immunoblotted with anti-FLAG and anti-MYC antibodies. *(GST; glutathione S-transferase, wcl; whole cell lysate).*

conditions of varying p38 phosphorylation status. p38 was hyper-activated through co-transfected with pcDNA*FLAG*-MKK6^{DD}, a specific upstream activator, or inhibited with a 4 hour incubation with the specific inhibitor SB203580 immediately prior to cell lysis. Alterations in p38 phosphorylation state were insufficient to prevent an interaction between dematinC1 and 14-3-3β at the RKTRS$_{269}$LP (Figure 4.10B) motif or at the RGNS$_{333}$LP motif (Figure 4.10C). This suggests either that these sites are not being phosphorylated by p38, or that p38 phosphorylation of these neighbouring sites does not inhibit dematin / 14-3-3 association.

4.5.2 p38 phosphorylation does not regulate an N-terminal / 14-3-3β interaction

The N-terminal 14-3-3 binding motifs at Ser^{22} and Ser^{85} were unable to mediate an interaction between dematin and 14-3-3. Here we aimed to investigate whether p38 phosphorylation of dematin was inhibiting this interaction by preventing the association of 14-3-3β. Residues Ser^{16}, Ser^{26}, Ser^{87} and Ser^{92} were all phosphorylated in our mass spectrometry analysis of dematin (Chapter 3, Figure 3.5). As can be seen in Figure 4.11A, these phosphorylation sites either closely neighbour or overlap the 14-3-3 binding motif. The co-immunoprecipitation experiments between pDEST27*FLAG*-dematinN1 or dematinN3 and pcDNA3.1*MYC*-14-3-3β were repeated with co-transfection of pcDNA*FLAG*-MKK6^{DD} or incubation with SB203580 inhibitor. No co-immunoprecipitation of 14-3-3β was seen with either dematinN1 (Figure 4.11B) or dematinN3 (Figure 4.11C) under p38 hyper-activated or inhibition conditions. This suggests that the absence of a detectable interaction between 14-3-3β and dematin at the RDSS$_{22}$VP or RERS$_{85}$LSP motifs is not due to p38 phosphorylating neighbouring sites and hindering 14-3-3 binding.

GST-pulldown experiments were conducted using HEK293T cells co-transfected with pDEST27*FLAG*-dematinN1_S16/26A or pDEST27*FLAG*-dematinN3_S87/92A and pcDNA3.1*MYC*-14-3-3β. Co-purification of 14-3-3β was not detected with either the dematinN1_S16/26A (Figure 4.12B), nor dematinN3_S87/92A (Figure 4.12C), constructs. This indicates that the absence of a detectable interaction between dematin and 14-3-3β at the RDSS$_{22}$VP and RERS$_{85}$LSP motifs is not due to the inhibitory phosphorylation of the neighbouring Ser^{16}/ Ser^{26} and Ser^{87} / Ser^{92} residues.

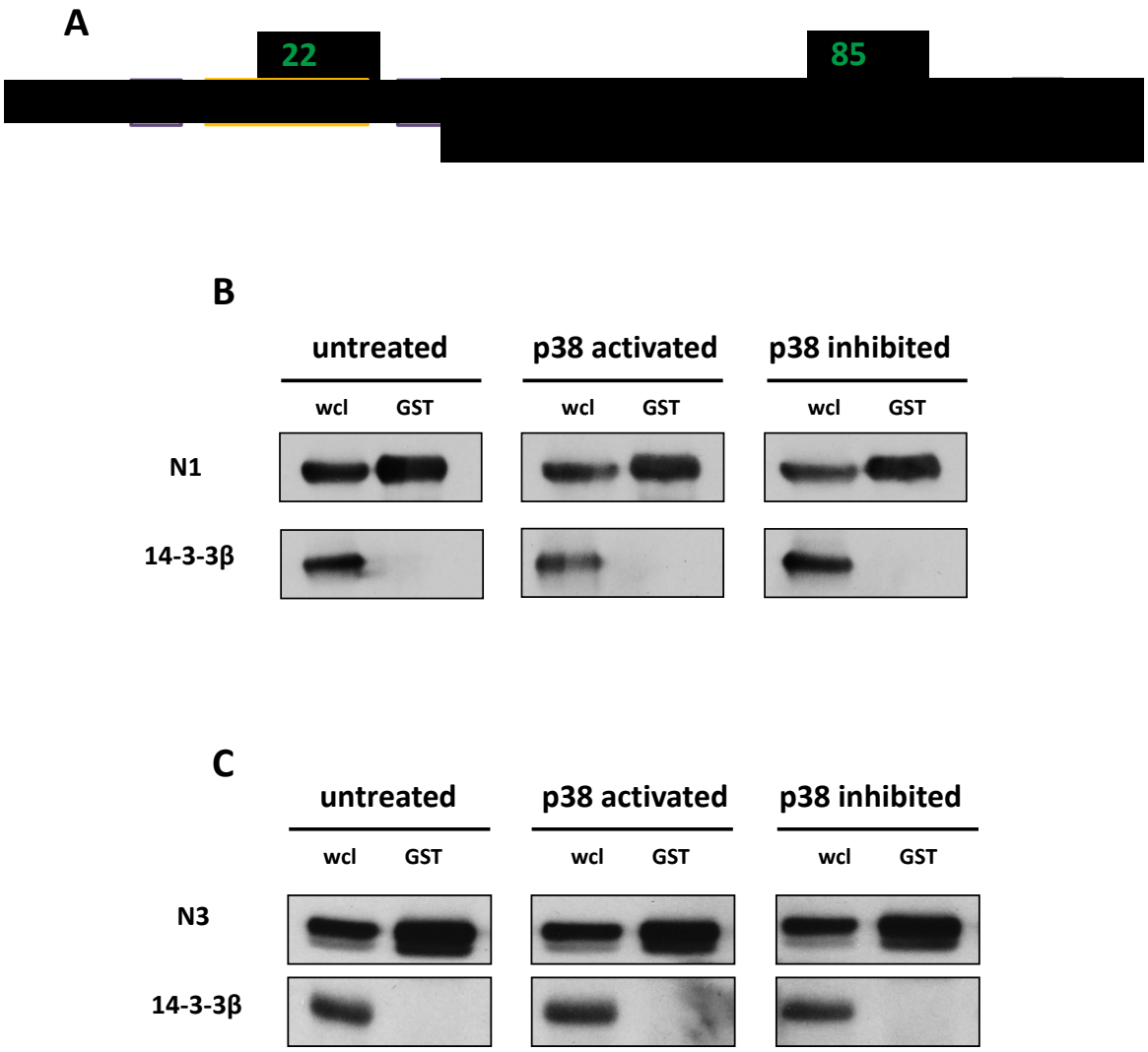

Figure 4.11: Alterations in p38 phosphorylation state are not sufficient to induce and interaction between 14-3-3β and the N-terminal of dematin

HEK293T cells were co-transfected with pDEST27*FLAG*-dematinN1 or dematinN3, and pcDNA3.1*MYC*-14-3-3β. For p38 hyper-activation, cells were co-transfected with pcDNA3*FLAG*-MKK6. After 48 hours, p38 inhibited cells were treated with the specific inhibitor SB203580 for 4 hours. Cells lysates were then purified on GST-pulldown columns, separated by SDS-PAGE and transferred onto nitrocellulose. Membranes were immunoblotted with anti-FLAG and anti-MYC antibodies. *(GST; glutathione S-transferase, wcl; whole cell lysate).*

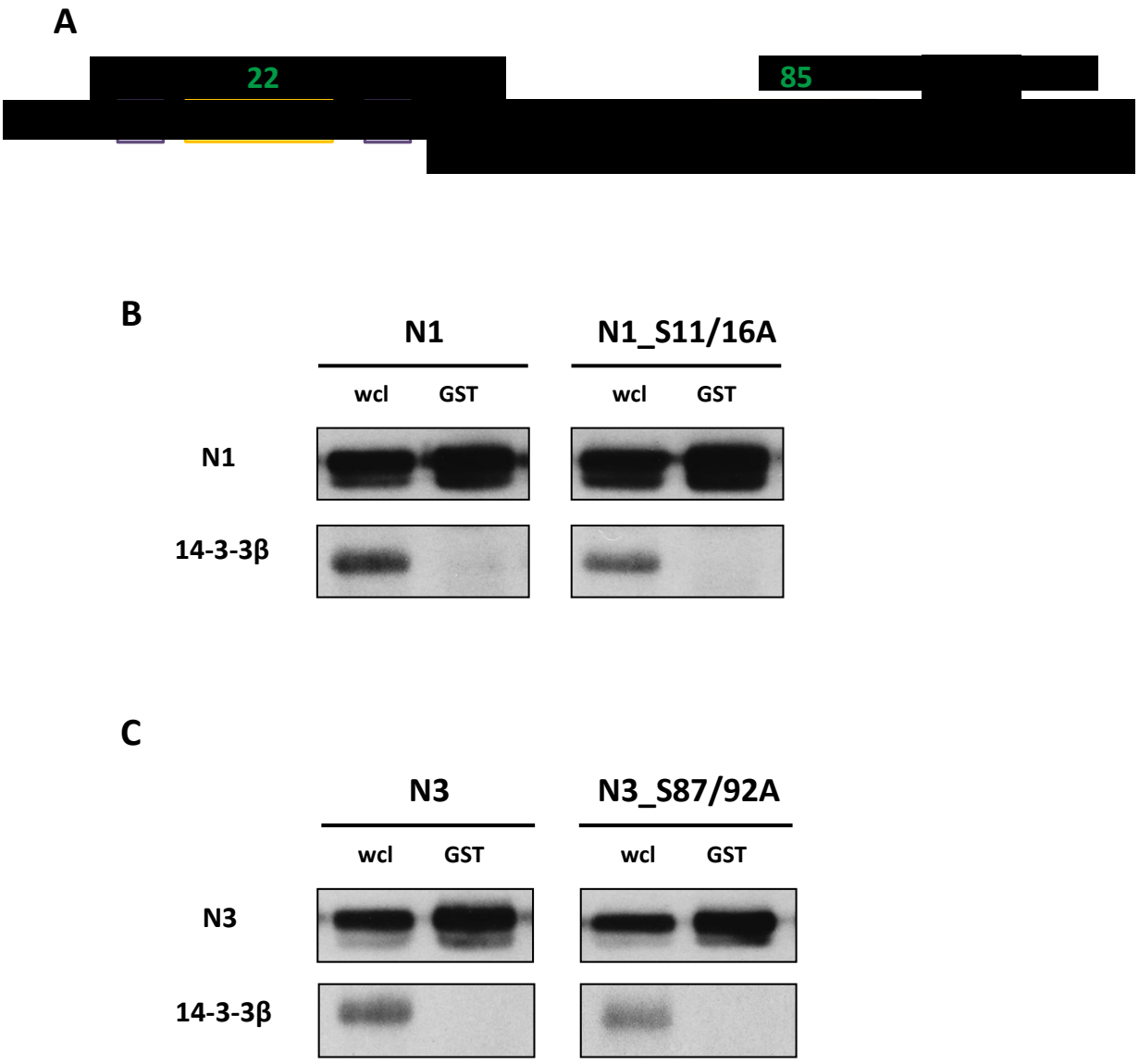

Figure 4.12: Phosphorylation of neighbouring residues does not prevent and N-terminal dematin / 14-3-3β interaction

(A) Site-directed mutagenesis was used to change serine residue neighbouring 14-3-3 motifs to alanine residues. HEK293T cells were co-transfected with (B) pDEST27*FLAG*-dematinN1 / pDEST27*FLAG*-dematinN1_S11/16A or (C) pDEST27FLAG-dematinN3 / pDEST27*FLAG*-dematinN3_S87/92A, and pcDNA3.1*MYC*-14-3-3β. Cells lysates were purified on GST-pulldown columns, separated by SDS-PAGE and transferred onto nitrocellulose. Membranes were immunoblotted with anti-FLAG and anti-MYC antibodies. *(GST; glutathione S-transferase, wcl; whole cell lysate).*

4.6 DISCUSSION

In this chapter we have used co-immunoprecipitation experiments to confirm the interaction between dematin and 14-3-3β, and site-directed mutagenesis to identify $RKTRS_{269}LP$ and $RGNS_{333}LP$ as the specific motifs in dematin to which 14-3-3β binds. Preliminary investigations into the phospho-regulation of the interaction suggest that these sites are not phosphorylated by protein kinases Akt, PKA, or AMPK. Phosphorylation of dematin by the p38 MAPK did not regulate the interaction between dematin and 14-3-3β.

4.6.1 14-3-3β binds to dematin at Ser^{269} and Ser^{333}

Interactions between either the 48 or 52 KDa isoform of human dematin and human 14-3-3β were demonstrated in a series of co-immunoprecipitation experiments. This confirms dematin as one of more than 300 14-3-3 binding partners that have now been identified. The majority of known interactions with 14-3-3 occur via phosphorylated motifs in the target protein, and here we have shown that this is the mechanism exploited by the dematin / 14-3-3β interaction. Serine to alanine mutagenesis of Ser^{269} and Ser^{333} abolished the interaction with 14-3-3β, while neither of the single mutations was sufficient to prevent binding. This indicated that the interaction between 52 KDa dematin and 14-3-3β occurs at the $RKTRS_{269}LP$ and $RGNS_{333}LP$ motifs, while 48 KDa dematin is bound at just $RKTRS_{269}LP$ as it lacks the additional motif at Ser^{333}. Mass spectrometry analysis of 14-3-3 binding motifs identified Ser^{269} as being phosphorylated, however Ser^{333} was not detected. This may be because this site was not phosphorylated under the experimental conditions used, or because the peptide containing this motif was not mapped. The mass spectrometry approach used involved first purifying phosphorylated peptide from the total protein sample, and this technique may not purify all phosphorylated proteins equally.

Lalle *et al* (2011) have subsequently reported an interaction between erythrocyte dematin and plasmodium 14-3-3. This was shown to be dependent upon phosphorylated residues Ser^{124} and Ser^{333}, with Ser to Ala substitutions of each of

these sites showing a reduction in 14-3-3 binding. However the relative reduction in binding cannot be accurately quantified from the data provided, as the western blots show only the band corresponding to the co-immunoprecipitated 14-3-3, and not the amount of dematin itself. Despite the identification of other binding motifs in the dematin sequence, including that at Ser^{269}, mutants of these sites were not created and the group failed to completely abolish the interaction with any of their constructs. It is therefore possible that the $RKTRS_{269}LP$ motif that we have identified is also important for the interaction between dematin and plasmodium 14-3-3. Ser^{124} was not phosphorylated under our mass spectrometry conditions and we were unable to demonstrate an interaction between dematinN3, which contains the $RTS_{124}LP$ motif, and 14-3-3β.

Yaffe (2002) proposed the gatekeeper phosphorylation theory, which states that most proteins with two active binding motifs contain one dominant 'gatekeeper' binding site to which 14-3-3 must always bind first. Binding to this site brings the 14-3-3 dimer into close proximity with the weaker binding site, which is then able to bind to the other 14-3-3 monomer. Although the weaker site is not capable of independent binding, it may need to be bound to confer the full physiological function upon the target protein. Examples of proteins displaying this mechanism include the pro-apoptotic Bcl-2-associated death promoter (BAD) protein; Ser^{136} acts as a gatekeeper site but Ser^{112} is required to stabilise the complex (Chiang *et al.*, 2003). Under serum-starved conditions, the scaffold protein KSR has two phosphorylated 14-3-3 binding motifs at Ser^{297} and Ser^{392} (Cacace *et al.*, 1999). Here Ser^{392} constitutes the gatekeeper site, and mutation of this motif alone is sufficient to constitutively localise KSR1 to the plasma membrane. The gatekeeper theory does not correlate with the binding sites we have identified in dematin, where both the $RKTRS_{269}LP$ and $RGNS_{333}LP$ motifs show comparable, independent binding to 14-3-3β.

4.6.2 Binding of 14-3-3β to the N-terminal domain of dematin was not detected

With the experiments presented here it was not possible to demonstrate an interaction between 14-3-3β and the N-terminal region of dematin. This was

despite the mass spectrometry analysis identifying the $RDSS_{22}VP$ and $RERS_{85}LSP$ binding motifs as being phosphorylated. These motifs were identified as potential Akt, AMPK, and PKA phosphorylation sites, but activation of these kinases was still not sufficient to induce an interaction. Neither was an interaction seen in the presence of the phosphatase inhibitor calyculin; however this is only effective on protein phosphatases 1 and 2A and not on the acid or alkaline phosphatase families. Although the $RDSS_{22}VP$ and $RERS_{85}LSP$ motifs were identified as being phosphorylated, this alone is not sufficient for an interaction with 14-3-3. The sequence surrounding a consensus motif has also been shown to be important for efficient binding (Uchida *et al.*, 2006; Uhart *et al.*, 2011). It may therefore be the incorrect context of these N-terminal motifs that prevents an interaction with 14-3-3β. In addition to the localised context of a motif, its position in the tertiary structure of the target protein is also important. A motif must be fully accessible on the external surface of the target protein when folded in its native conformation. As the N-terminus of dematin is known to be devoid of any significant secondary structure (Chen *et al.*, 2009), a buried binding motif is unlikely to be preventing an interaction with 14-3-3β in this region.

We cannot, however, rule out the possibility that the N-terminal of dematin and 14-3-3β do interact under certain conditions. It is notoriously difficult to detect weak interactions between 14-3-3 and a target protein, and so the absence of a positive interaction at a particular site is not evidence that binding doesn't occur. If a gatekeeper site is mutated, then the interaction with the weak site can also be lost. It is therefore possible that many of the characterised 14-3-3 binding partners have additional motifs to those that have been identified using simple mutagenesis techniques. There remains a possibility that 14-3-3β binds to the N-terminal $RDSS_{22}VP$ and / or $RERS_{85}LSP$ motifs, after first binding to one of the two higher affinity $RKTRS_{269}LP$ and $RGNS_{333}LP$ sites. Although a 14-3-3 dimer can only bind to two phosphorylated residues at once, substrates have been identified that contain more than two active binding sites, and so it would be plausible for dematin to contain active motifs other than the identified sites at Ser^{269} and Ser^{333}. Examples of this include Cdc25B which has three functional binding sites at Ser^{151}, Ser^{230} and

Ser^{323} (Forrest & Gabrielli, 2001; Giles *et al.*, 2003). Regulation of the Raf-1 protein kinase also involves three 14-3-3 sites, at Ser^{259}, Ser^{621}, and a third undetermined site (Tzivion *et al.*, 1998).

4.6.3 Phosphorylation of the 14-3-3 binding motifs in dematin

More than 50 proteins containing two active 14-3-3 binding sites have been identified, and the majority of these have been shown to have a different mode of motif at each interaction site (Johnson *et al.*, 2010). This is the case with dematin, where the identified sites are the Mode I motif $RGNS_{333}LP$, and the Mode II motif $RKTRS_{269}LP$. The differing sequences means that the two sites have the potential to be regulated by different protein kinases, which each have their own sequence recognition motifs. This provides two layers of regulation if both sites are needed for binding (or functional outcome), or alternative methods of activation if only one site is needed.

Despite identifying a number of potential regulatory kinases of the $RKTRS_{269}LP$ and $RGNS_{333}LP$ motifs, inhibition of Akt, AMPK or PKA for 6 hours prior to GST-pulldown experiments was insufficient to abolish the interaction between dematin and 14-3-3β at either of these binding sites. Control western blots for downstream phosphorylated substrates to confirm the inhibition of these kinases were not conducted due to a lack of appropriate antibodies; however the inhibitors were all new and were used at concentrations widely reported in the literature. 14-3-3 binding has previously been shown to directly protect residues from phosphatase-mediated dephosphorylation (Gohla & Bokoch, 2002; Margolis *et al.*, 2003). A 6-hour incubation may therefore be insufficient to dephosphorylate these motifs and reverse the binding. However no decrease in binding was seen with any of the inhibitors tested, suggesting that this is unlikely as some natural turnover would be expected over this time period. Sequence analysis also identified the $RKTRS_{269}LP$ as a low stringency PKC phsohporylation site, but no other potential regulators were identified for the $RGNS_{333}LP$ motif. Contrary to our findings, Lalle *et al.* (2011) demonstrated that PKA phosphorylation of erythrocyte dematin induced an interaction with plasmodium 14-3-3 that was not seen under basal conditions. The

specific PKA phosphorylation sites within erythrocyte dematin were not mapped, however, and therefore this does not confirm that this is a direct effect of PKA itself.

Interestingly, 14-3-3 binding to a substrate can also be regulated by phosphorylation of other residues within the consensus binding motifs. For example phosphorylation of the -2 position in both p52 and Cdc25c inhibits 14-3-3 binding (Bulavin et al., 2003; Waterman et al., 1998). This therefore acts as an additional regulatory mechanism for 14-3-3 binding. Of the 14-3-3 motifs in dematin, two contain phosphorylatable residues at the -2 positions; RK**T**RS$_{269}$LP and K**S**SS$_{289}$LP. A further motif contains a serine residue at the +2 position, RERS$_{85}$L**S**P, which could potentially have the same effect. As Ser^{87} was identified as being phosphorylated in the mass spectrometry results this provided a potential explanation for the lack of binding to the RERS$_{85}$LSP motif, however mutating the Ser^{87} an alanine residue was insufficient to facilitate an interaction.

4.6.4 p38 does not inhibit the interaction between dematin and 14-3-3β

Analysis of the primary sequence of dematin indicated the presence of p38 phosphorylation motifs in close proximity to 14-3-3 binding motifs, in particular at binding motifs RDSS$_{22}$VP, RERS$_{85}$LSP, and RKTRS$_{269}$LP. In chapter 3, dematin was confirmed as a novel substrate of p38 and in vitro kinase assays and MPM2 detection using the truncated dematin constructs indicated that all regions of dematin contain p38 phosphorylation sites. It was therefore hypothesised that p38 may negatively regulate the association of 14-3-3 with dematin by physically hindering binding of the 14-3-3β dimer. However no differences in binding affinity were noted under conditions of p38 activation with the specific upstream activator MKK6^{DD}, or inhibition with SB203580. Equally mutating these sites to non-phosphorylatable alanine residues had no effect on binding, indicating that the site aren't subject to inhibitory phosphorylation by other proline-directed kinases.

4.6.5 Potential for dematin / 14-3-3 interactions in other isoforms and species

Here we have investigated the interaction between human dematin, and human 14-3-3β. Sequence comparison of the seven unique human 14-3-3 isoforms indicated

that there are five distinct blocks of sequence conservation (Wang & Shakes, 1996). These regions are involved in dimer formation, lining of the ligand binding groove, and direct interaction with target proteins. Although there is a high level of sequence and structural conservation between 14-3-3 family members, not all isoforms bind equally to all target proteins. In the majority of cases it seems that binding is not limited to a particular isoform, however several interactions have been identified where a specific isotype is required for binding, or enhances binding. These include KSR1, which is efficiently bound by 14-3-3 isoforms β, γ, η, and ζ, weakly bound by the ϵ and τ isoforms, and unable to bind to 14-3-3 σ (Jagemann *et al.*, 2008). Equally other than 14-3-3σ, which preferentially homodimerises, all isoforms have the potential to hetero-dimerise which increases the potential for regulation (Wilker *et al.*, 2005). This specificity has not been well characterised to date, but may provide an interesting additional level of biological regulation for 14-3-3 interactions. Here were have used 14-3-3β, but the initial screening by Angrand *et al* (2006) identified dematin as a binding partner of 14-3-3ζ. Interestingly, the phosphatase Cdc25 has been shown to bind to 14-3-3β at a different motif to that which 14-3-3σ binds, and the two isoforms have different regulatory effects on Cdc25 (Uchida *et al.*, 2004). It is therefore possible that other motifs in dematin, such as $RDSS_{22}VP$ and $RERS_{85}LSP$, are only recognised by alternative isoforms of 14-3-3. Endogenous co-immunoprecipitation experiments could be conducted to determine which isoforms of 14-3-3 interact with dematin in vivo, facilitated by the commercial availability of isoform-specific 14-3-3 primary antibodies. The motif binding preferences of any interacting isoforms could then be determined using overexpression studies with GST-pulldown assays and site-directed mutagenesis as conducted here.

The expression patterns of particular 14-3-3 isoforms in mammals has been shown to be dependent upon the tissue or cell type in question, but all types investigated express more than one isoform (Aitken, 2006). Subcellular variations in expression patterns are also seen, and isoform-specific variations have also been proposed to determine the subcellular localisation of 14-3-3 proteins. The β and ζ isoforms preferentially associate with the cytosol and cytoskeletal proteins, while the γ

isoform associates with phospholipids (Roth *et al.*, 1994). As dematin is a cytoskeletal-associated protein the β and ζ isoforms are most likely to be expressed in the same subcellular locations in vivo. This suggests that if dematin has any isoform-specific preferences then it is more likely to be with one of these forms.

The N-terminal region of 14-3-3 isoforms display the highest degree of variability, and it is these regions which are important for dimer formation. This variation is thought to limit the number of homo- or hetero-dimeric complexes which form, and preferences in dimerisation partners could potentially affect the functional outcome of these interactions. In our experiments only 14-3-3β was overexpressed and therefore monomers were forced to create homo-dimeric complexes, as remaining monomeric is thermodynamically unfavourable (Chaudhri *et al.*, 2003). Overexpressed 14-3-3β is also be capable of dimerising with other isoforms found endogenously within the cell, however endogenous expression levels are expressed at comparatively low levels and are therefore not likely to affect the overall patterns seen.

5. Regulation of dematin localisation and actin binding / bundling by 14-3-3

5.1 Introduction

Actin binding proteins such as dematin are responsible for coordinating the dynamic actin structures found within the cell (dos Remedios *et al.*, 2003). Two main types of structure exist in vivo; actin networks, and actin bundles. The formation of both structures is coordinated by actin crosslinking proteins, such as dematin, which hold filaments in place (Blanchoin *et al.*, 2014). Dematin contains two actin binding motifs, one in the HP and a second in the core region (Vardar *et al.*, 2002). As each site operates independently, a single dematin monomer can bind to two AFs and bundle them together (Chen *et al.*, 2013).

In chapter 4 dematin was confirmed as a substrate of the adaptor protein 14-3-3β, and the specific motifs mediating this interaction in the 52 KDa isoform were identified as $RKTRS_{269}LP$ and $RGNS_{333}LP$. The 14-3-3 family are important regulatory molecules that can modulate a range of effects on their binding targets. These effects can be due to 14-3-3 changing the structure of the target protein, changing the subcellular localisation of the target protein, or acting as a scaffold to enhance the binding properties of the target protein. Altering the localisation of a protein can result from 14-3-3 masking specific sequences or structural features in the target. This can impinge on the normal function of the protein by physically separating it from the other proteins and co-factors it either requires or regulates (Bridges & Moorhead, 2005). The ability to bind actin is an essential property of all known functions of dematin, and relies on the presence of specific actin-binding sequence motifs. Masking of these motifs could therefore provide a mechanism through which 14-3-3 binding could regulate the actin binding function dematin.

The experiments presented in this chapter aimed to answer the following questions:

1. Where does dematin localise in C2C12 skeletal muscle cells?
2. Does 14-3-3 binding affect the subcellular localisation of dematin?
3. Which 14-3-3 binding sites have an effect on the localisation of dematin?
4. Does 14-3-3 association affect the actin binding ability of dematin?
5. Does 14-3-3 association affect the actin bundling ability of dematin?

5.2 Subcellular localisation of dematin in C2C12 cells

Dematin expression has been demonstrated in skeletal muscle tissue; however the subcellular localisation of the protein has not been investigated. Here we used the C2C12 murine skeletal muscle cell line to characterise the subcellular expression pattern of dematin.

5.2.1 Constructs used in this chapter

The constructs used in this chapter were cloned into the pTrexDEST30 mammalian expression vector using the Invitrogen Gateway® recombination system, as described in chapter 3, section 3.2. DNA constructs for use in confocal imaging experiments were tagged with epitope tags to facilitate immuno-detection (Figure 5.1): a FLAG tag on the 52 KDa isoform, and a MYC tag on the 48 KDa variant. The dematin construct created for use in actin binding and bundling experiments was PCR amplified with an N-terminal Strep-tag to facilitate efficient protein purification.

5.2.2 Subcellular localisation of dematin in C2C12 cells

C2C12 cells were seeded onto glass coverslips and transfected with pTrexDEST30*FLAG*-dematin. After 48 hours cells were fixed with 4 % PFA, permeabilised in 0.2% triton X-100, blocked with 3% BSA, and incubated with either an anti-dematin or anti-FLAG primary antibody. This was followed by an Alexa Fluor® 568 goat anti-mouse IgG antibody with DAPI to stain the nuclei. Cells were imaged on a confocal microscope with sequential scanning between wavelengths. Expression of dematin was detected throughout the cytosol in a fairly uniform distribution, and in the membrane protrusions. The staining observed using the anti-dematin and anti-FLAG primary antibodies was comparable, and no staining was observed in the primary only or secondary only controls (Figure 5.2).

5.3 The effect of 14-3-3β association on dematin localisation

One well characterised function of the 14-3-3 family of proteins is the ability to change the subcellular localisation of a target protein upon binding. In order to

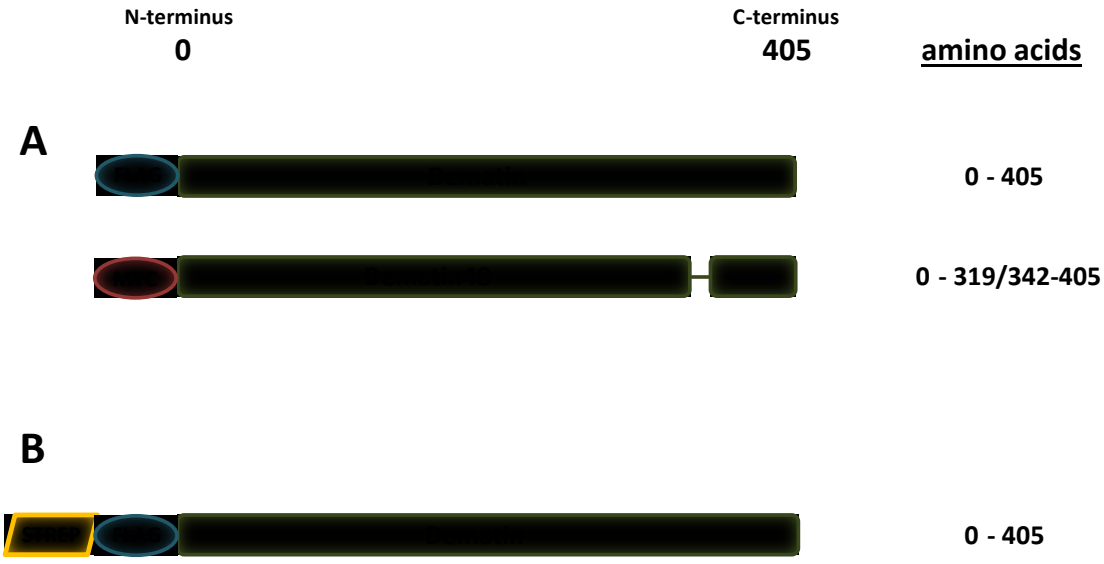

Figure 5.1: Schematic of the dematin constructs used in this chapter

Diagram showing the relative positions, and epitope tags, of the dematin constructs cloned for use in this chapter. (A) The constructs used for imaging experiments had either FLAG or MYC tags to facilitate immunodetection. (B) The dematin construct for use in actin-binding and bundling assays had a Strep-tag to enable efficient purification of the protein, and a FLAG tag to facilitate immunodetection.

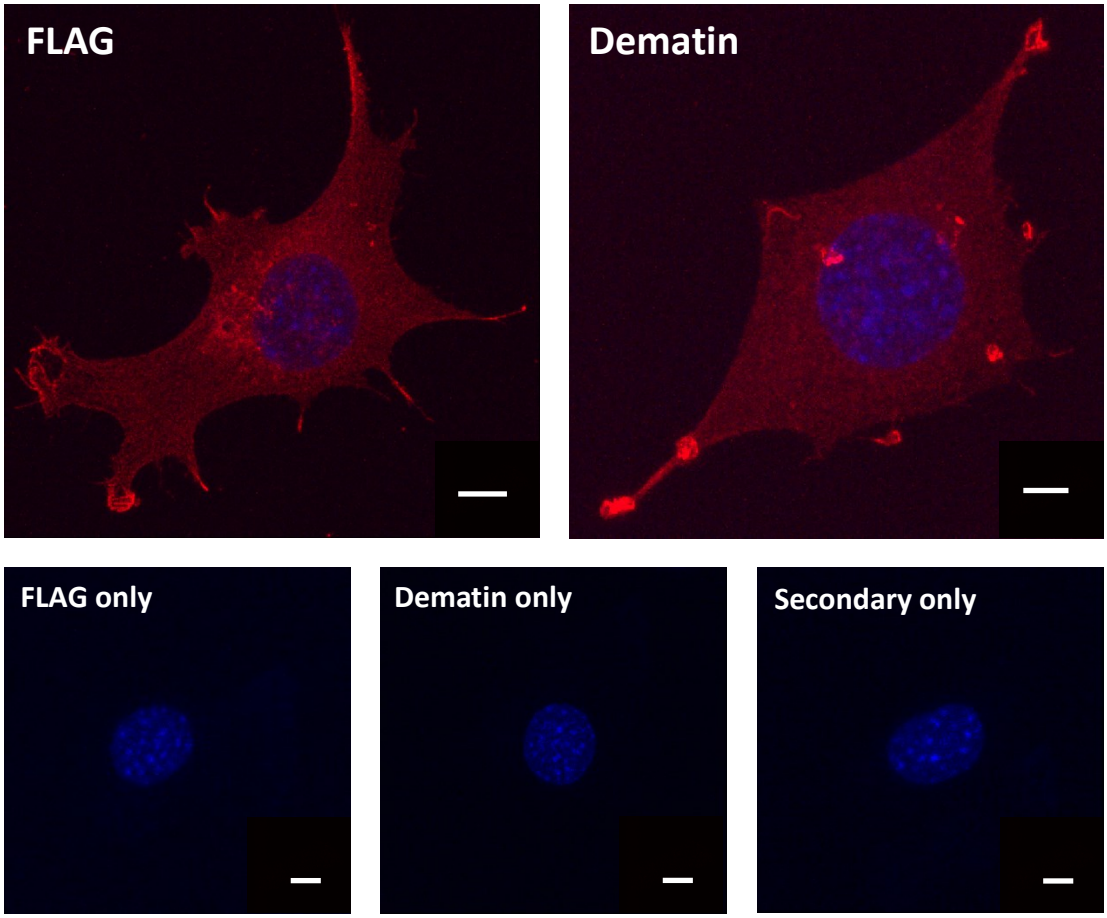

Figure 5.2: Localisation of overexpressed dematin in C2C12 cells

C2C12 cells were seeded onto glass coverslips and transfected with pTrexDEST30*FLAG*-dematin. After 24 hours cells were fixed with 4 % PFA, permeabilised in 0.2 % triton X-100, and blocked in 3 % BSA/PBS. Cells were incubated at room temperature for one hour with either an anti-FLAG or anti-dematin primary antibody, before washing in PBS. Dematin was detected with an Alexa Fluor® 568 goat anti-mouse IgG antibody (red), and cell nuclei visualised with DAPI (blue). Following further washes in PBS, followed by water, cells were mounted onto coverslips using Mowiol. Cells were visualised on an SP5 Confocal Laser Scanning Microscope with a 100 x oil objective. Controls show cells incubated with FLAG or dematin primary antibody and no secondary, or with only secondary antibody. Scale bars indicate 10 µm. Representative images from three independent experiments. (BSA; bovine serum albumin, PBS; phosphate buffered saline, PFA; paraformaldehyde).

determine whether this effect is seen in dematin, the subcellular localisation of the wild-type dematin isoforms with 14-3-3β bound were compared to the 14-3-3 binding mutant forms of dematin.

5.3.1 Localisation of dematin and dematin_S269/333A in C2C12 cells

Localisation of 52 KDa wild-type dematin was first compared to the dematin_S239/333A mutant that is unable to bind to 14-3-3β. C2C12 cells were seeded, transfected, and stained using the same method as in section 5.2.2. Dematin was visualised with Alexa Fluor® 488 goat anti-mouse IgG fluorescent secondary antibody. The F-actin cytoskeleton was stained with Alexa Fluor® 568 conjugated Phalloidin, a toxin originating from the death cap mushroom *Amanita phalloides*. This prevents depolymerisation of AFs by binding at the interface between individual actin monomers, and therefore acts as a convenient stain when conjugated to a fluorescent probe. Images were captured of z-sections through the central region of the cells at the point where the F-actin staining was most defined. Images of the dematin and F-actin staining were merged to visually determine the extent of apparent co-localisation between the two proteins.

As previously the wild-type 52 KDa had a disperse distribution throughout the cytosol. The dematin staining showed minimal co-localisation with the F-actin cytoskeleton when the two images were merged (Figure 5.3). The staining pattern of the dematin_S269/333A construct was markedly different, having an obviously striated patterning, which correlated with the image of the Phalloidin staining. On merging the two images, extensive co-localisation between dematin_S269/333A and actin is indicated by the yellow pixels. These results suggest that binding of 14-3-3β to dematin is preventing it from co-localising with the F-actin cytoskeleton.

5.3.2 Localisation of dematin_S269A and dematin_S333A in C2C12 cells

In order to determine whether binding of 14-3-3β to the 52 KDa isoform of dematin at both of the identified RKTRS$_{269}$LP and RGNS$_{333}$LP motifs is required to change the subcellular localisation of dematin, the imaging experiments were repeated with

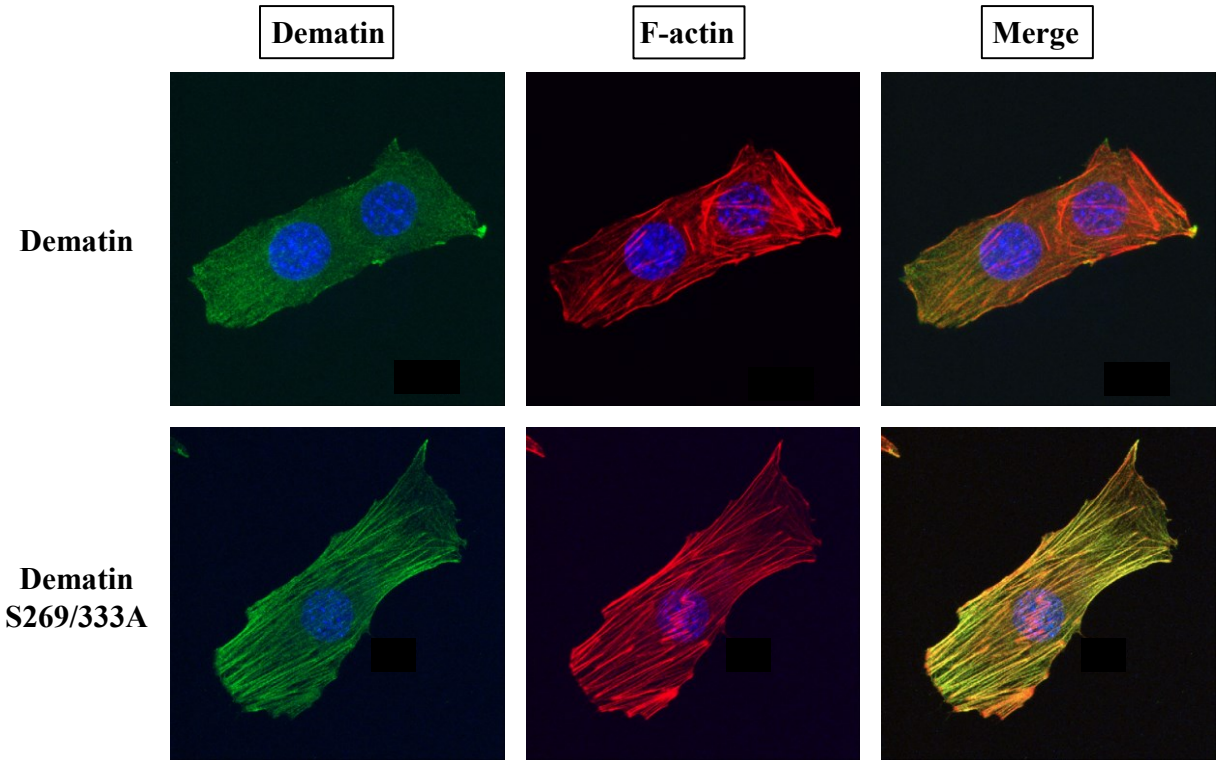

Figure 5.3: The effect of 14-3-3β binding on dematin localisation in C2C12 cells

C2C12 cells were seeded onto glass coverslips and transfected with either pTrexDEST30*FLAG*-dematin or pTrexDEST30*FLAG*-dematin_S269/333A. After 24 hours cells were fixed with 4 % PFA, permeabilised in 0.2 % triton X-100, and blocked in 3 % BSA/PBS. Cells were incubated at room temperature for one hour with an anti-FLAG antibody, before washing in PBS. Dematin was detected with an Alexa Fluor® 488 goat anti-mouse IgG antibody (green), F-actin stained with Alexa Fluor® 568 Phalloidin (red), and cell nuclei visualised with DAPI (blue). Following further washes in PBS, followed by water, cells were mounted onto coverslips using Mowiol. Cells were visualised on an SP5 Confocal Laser Scanning Microscope with a 60 x oil objective. Images were captured of z-sections through the central region of the cells at the point where the F-actin staining was most defined. Representative images from three independent experiments. (BSA; bovine serum albumin, PBS; phosphate buffered saline, PFA; paraformaldehyde).

the pTrexDEST30*FLAG*dematin_S269A and pTrexDEST30*FLAG*dematin_S333A constructs. The staining pattern observed for each of these single mutants is comparable to wild-type dematin, with a fairly disperse pattern throughout the cytosol. Again little co-localisation with F-actin was detected (Figure 5.4). These observations suggest that binding of 14-3-3β to either the $RKTRS_{269}LP$ or$RGNS_{333}LP$ motif is sufficient for preventing dematin from co-localising with F-actin.

5.3.3 Localisation of dematin48 and dematin48_S269A in C2C12 cells

In chapter 3, the 48 KDa isoform of dematin was shown to bind to 14-3-3 via a single motif at $RKTRS_{269}LP$. Localisation of the dematin48 and dematin48_S269A constructs was visualised to determine whether 14-3-3 binding had the same regulatory effect as in the 52 KDa isoform of dematin. As in the longer isoform, dematin48 was expressed throughout the cytosol and showed little co-localisation with F-actin (Figure 5.5). The dematin48_S269A construct had a comparable staining pattern to the dematin_S269/333A mutant, with a definite striated staining that co-localised with the F-actin staining. This suggests that 14-3-3β has the same regulatory effect on the 48 KDa isoform as demonstrated in the 52 KDa isoform, and prevents localisation of dematin with the F-actin cytoskeleton.

5.4 The effect of 14-3-3β association on the actin binding and bundling properties of dematin

Changes in subcellular localisation of a substrate upon 14-3-3 binding can result from the substrate being blocked from interacting with a protein it would normally associate with. The confocal imaging results suggested that 14-3-3 prevents dematin from associating with F-actin, and this was therefore investigated using quantitative assays. As dematin has been identified as both an actin-binding and actin-bundling protein, the effect of 14-3-3β binding on each of these properties was determined.

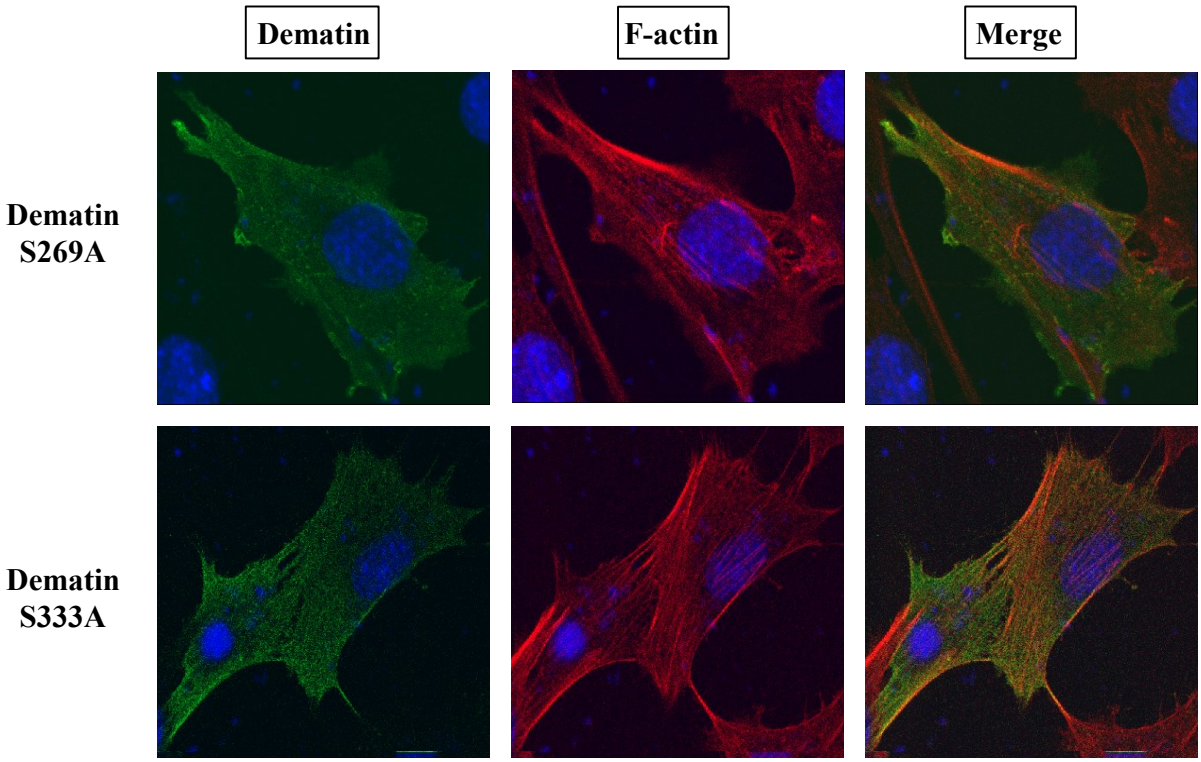

Figure 5.4: Localisation of dematin_S269A and dematin_S333A in C2C12 cells

C2C12 cells were seeded onto glass coverslips and transfected with either pTrexDEST30*FLAG*-dematin_S269A or pTrexDEST30*FLAG*-dematin_S333A. After 24 hours cells were fixed with 4 % PFA, permeabilised in 0.2 % triton X-100, and blocked in 3 % BSA/PBS. Cells were incubated at room temperature for one hour with an anti-FLAG antibody, before washing in PBS. Dematin was detected with an Alexa Fluor® 488 goat anti-mouse IgG antibody (green), F-actin stained with Alexa Fluor® 568 Phalloidin (red), and cell nuclei visualised with DAPI (blue). Following further washes in PBS, followed by water, cells were mounted onto coverslips using Mowiol. Cells were visualised on an SP5 Confocal Laser Scanning Microscope with a 100 x oil objective. Images were captured of z-sections through the central region of the cells at the point where the F-actin staining was most defined. Representative images from three independent experiments. (BSA; bovine serum albumin, PBS; phosphate buffered saline, PFA; paraformaldehyde).

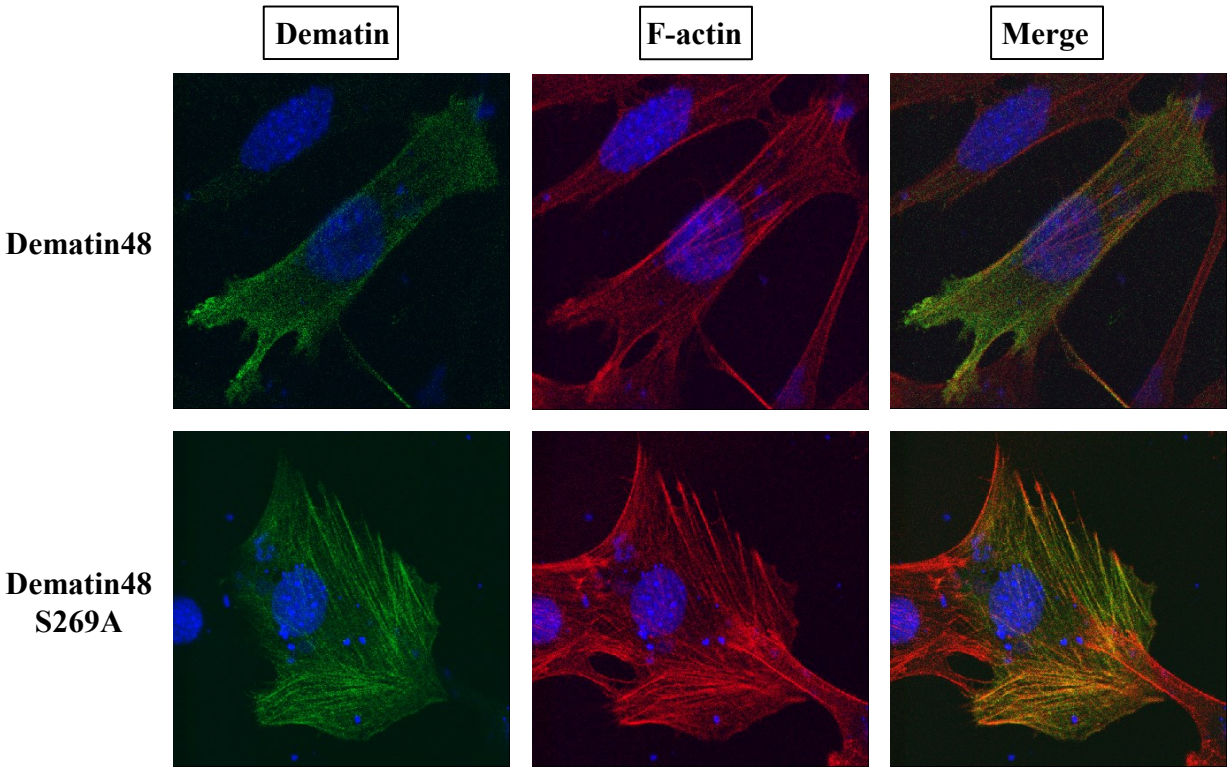

Figure 5.5: Localisation of dematin48 and dematin48_S269A in C2C12 cells

C2C12 cells were seeded onto glass coverslips and transfected with either pTrexDEST30*MYC*-dematin48 or pTrexDEST30*MYC*-dematin48_S269A. After 24 hours cells were fixed with 4 % PFA, permeabilised in 0.2 % triton X-100, and blocked in 3 % BSA/PBS. Cells were incubated at room temperature for one hour with an anti-FLAG antibody, before washing in PBS. Dematin was detected with an Alexa Fluor® 488 goat anti-mouse IgG antibody (green), F-actin stained with Alexa Fluor® 568 Phalloidin (red), and cell nuclei visualised with DAPI (blue). Following further washes in PBS, followed by water, cells were mounted onto coverslips using Mowiol. Cells were visualised on an SP5 Confocal Laser Scanning Microscope with a 100 x oil objective. Images were captured of z-sections through the central region of the cells at the point where the F-actin staining was most defined. Representative images from three independent experiments. (BSA; bovine serum albumin, PBS; phosphate buffered saline, PFA; paraformaldehyde).

5.4.1 Constructs used for actin-binding and bundling experiments

Purified dematin was required for both the actin-binding and -bundling assays. To facilitate this, the wild-type dematin and dematin_S269/333A sequences were PCR amplified with an N-terminal Strep-tag. A strep-tag was chosen as it enables efficient purification of the protein, but the short tag sequence should not interfere with normal protein function.

5.4.2 The dematin - 14-3-3β interaction is maintained upon Strep-purification

The Strep-tag purification procedure was optimised to ensure that the protein could be efficiently eluted from the Strep-resin, and importantly that upon elution of the wild-type dematin construct 14-3-3β remained bound to dematin. HEK293T cells were co-transfected with pTrexDEST30*FLAG*-dematin and pcDNA3.1*MYC*-14-3-3β. After 48 hours cells were lysed under non-denaturing conditions and incubated with Strep-Tactin resin. After thorough washing of the beads, the remaining bound protein was eluted with 2.5 mM desthiobiotin. This eluted protein fraction, along with a sample of the original cell lysate, was subjected to SDS-PAGE separation and western blotting. The membrane was probed with an anti-FLAG antibody to detect dematin, and anti-MYC to detect 14-3-3β. As Figure 5.6 shows, elution of Strep*FLAG*-dematin from the strep column resulted in the successful co-elution of 14-3-3β.

5.4.3 14-3-3β regulation of the actin-binding ability of dematin

Each of the Strep*FLAG*-dematin and Strep*FLAG*-dematin_S269/333A proteins were assayed for their actin binding ability. In the control reaction the relevant protein was combined with freshly polymerised rabbit skeletal muscle F-actin, with the negative control reaction containing only protein and polymerisation buffer. Further control reactions were conducted containing proteins with known actin-binding activities. An F-actin only control was conducted to ensure that the actin was correctly polymerised, and that these polymers pelleted upon centrifugation. BSA, a protein known to have no actin-binding ability, was incubated with F-actin as

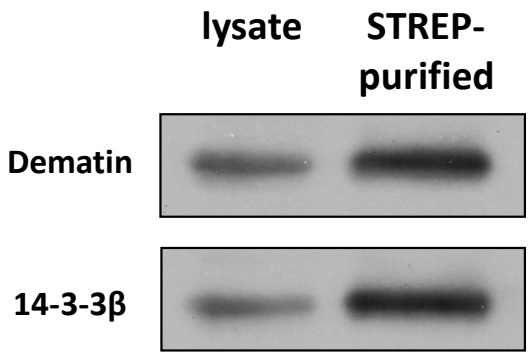

Figure 5.6: Co-purification of STREP-dematin and 14-3-3β

HEK293T cells were co-transfected with pTrexDEST30-STREP*FLAG*-dematin and pcDNA3.1*MYC*14-3-3β. Cells were lysed under non-denaturing conditions, and the cleared proteins incubated for 3 hours with Strep-Tactin resin. After thorough washing of the beads, the remaining bound protein was eluted with 2.5 mM desthiobiotin. This eluted protein fraction, along with a sample of the original cell lysate, was subjected to SDS-PAGE separation before immunoblotting with anti-FLAG (dematin) and anti-MYC (14-3-3β) antibodies (n=3).

a measure of non-specific sedimentation. Finally the well-characterised actin-binding protein α-actinin was used as a positive control. Two reactions were conducted, one with and one without F-actin, to ensure that the reaction worked and that it was specific interaction that was causing sedimentation. Samples were incubated at 24°C for 30 minutes, before centrifugation at 150,000 x g for 1.5 hours at 24°C to sediment the F-actin. The supernatant and pellet samples from each reaction were resuspended in 2 x Laemmlli reducing sample buffer and separated by SDS-PAGE. Control gels were stained with coomassie dye, whereas test protein gels were subjected to western blotting and immunodetection with an anti-FLAG antibody.

The control reactions confirmed that upon centrifugation at 150,000 x g for 1.5 hours F-actin alone is found almost exclusively in the pellet fraction (Figure 5.7A). α-actinin, a known actin binding protein, did not sediment when assayed alone but co-sedimented when incubated with F-actin. Finally the negative control confirmed that proteins which do not bind to actin remain in the supernatant fraction. When assayed in the absence of F-actin, only a very small proportion of the Strep*FLAG*-dematin and Strep*FLAG*-dematin_S269/333A test proteins were found in the pellet fraction (Figure 5.7B), with proportional values of 3.16% and 3.96% respectively. Statistical analysis confirmed that there was no significant difference between the sedimentational properties of these proteins. In the presence of polymerised actin, both constructs were found in higher proportions in the pellet fractions, confirming that they both bound to actin; Strep*FLAG*-dematin at 27.11% and Strep*FLAG*-dematin_S269/333A at 41.34%. This indicates that binding of 14-3-3β to dematin reduces dematin's actin-binding ability. This equated to a statistically significant 42.8% reduction in actin binding between the dematin_S269/333A and wild-type dematin constructs (Figure 5.7C).

5.4.4 14-3-3β regulation of the actin-bundling ability of dematin

Actin-bundling reactions and control were set up in the same way as in the actin-binding experiment, but bundles were separated with a lower speed centrifugation

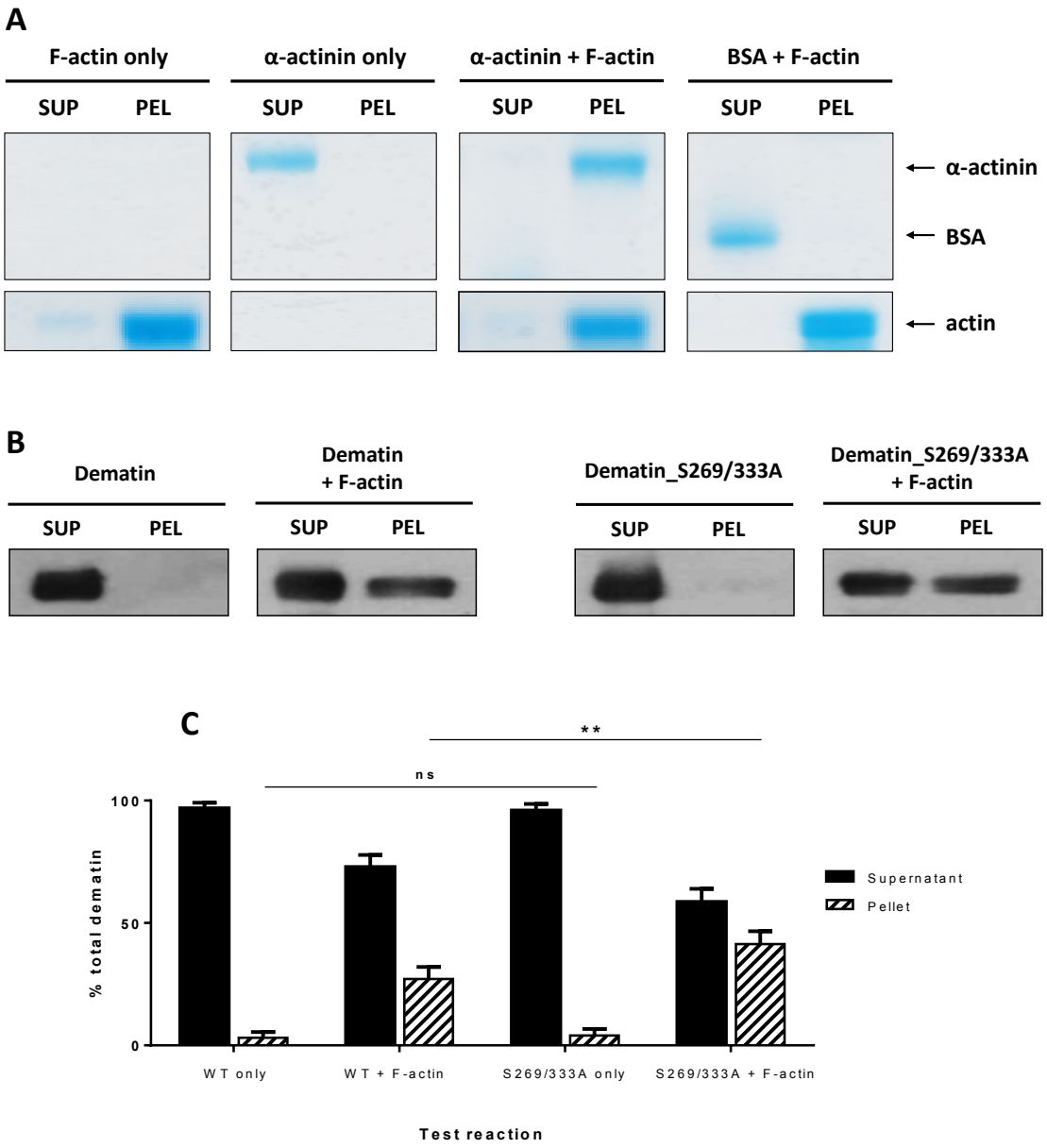

Figure 5.7: The effect of 14-3-3β binding on the actin-binding ability of dematin

Strep*FLAG*-dematin/14-3-3β and Strep*FLAG*-dematin_S269/333A dematin were purified from HEK293T cells lysates on Strep-Tactin columns. Test reactions were set up containing the eluted protein and skeletal muscle F-actin, with controls containing protein in polymerisation buffer. Samples were incubated at 24°C for 30 minutes before centrifugation at 150,000 x g for 1.5 h at 24°C. Aliquots of the supernatant and pellet fractions were analysed. (A) Control reactions of F-actin only, α-actinin (a known actin binding protein) alone and as a positive control with F-actin, and a negative control of BSA (which has no actin-binding ability) with F-actin. (B) Test reaction of wild-type dematin and the dematin_S269/333A mutants alone and with F-actin, visualized with anti-FLAG immunoblotting. (C) Quantification of the amount of protein in the pellet and supernatant fractions, with data presented as mean values + SEM (n=3). (SUP; supernatant, PEL; pellet).

at 14,000 x g for 1 hour at 24°C. In the absence of test protein, the majority of F-actin was retained in the supernatant fraction indicating that there was little non-specific bundling occurring. α-actinin remained in the supernatant when assayed alone, but co-sedimented with F-actin in the positive control reaction. The BSA negative control was comparable to the F-actin only sample, with both proteins found predominantly in the supernatant (Figure 5.8A). In the absence of F-actin, Strep*FLAG*-dematin and Strep*FLAG*-dematin_S269/333A were found predominantly in the supernatant, with mean values of 3.96% and 5.40% respectively (Figure 5.8B). There was no significant difference between the sedimentation properties of these proteins at 14,000 x g (Figure 5.8C). In the F-actin test reactions, both proteins displayed actin-bundling ability (Figure 5.8B). The proportion of dematin protein in the pellets increased to 51.96% and 74.31% for the Strep*FLAG*-dematin and Strep*FLAG*-dematin_S269/333A constructs respectively (Figure 5.8C). This indicated that binding of 14-3-3β to dematin reduces its actin-bundling ability by a statistically significant 30.08%.

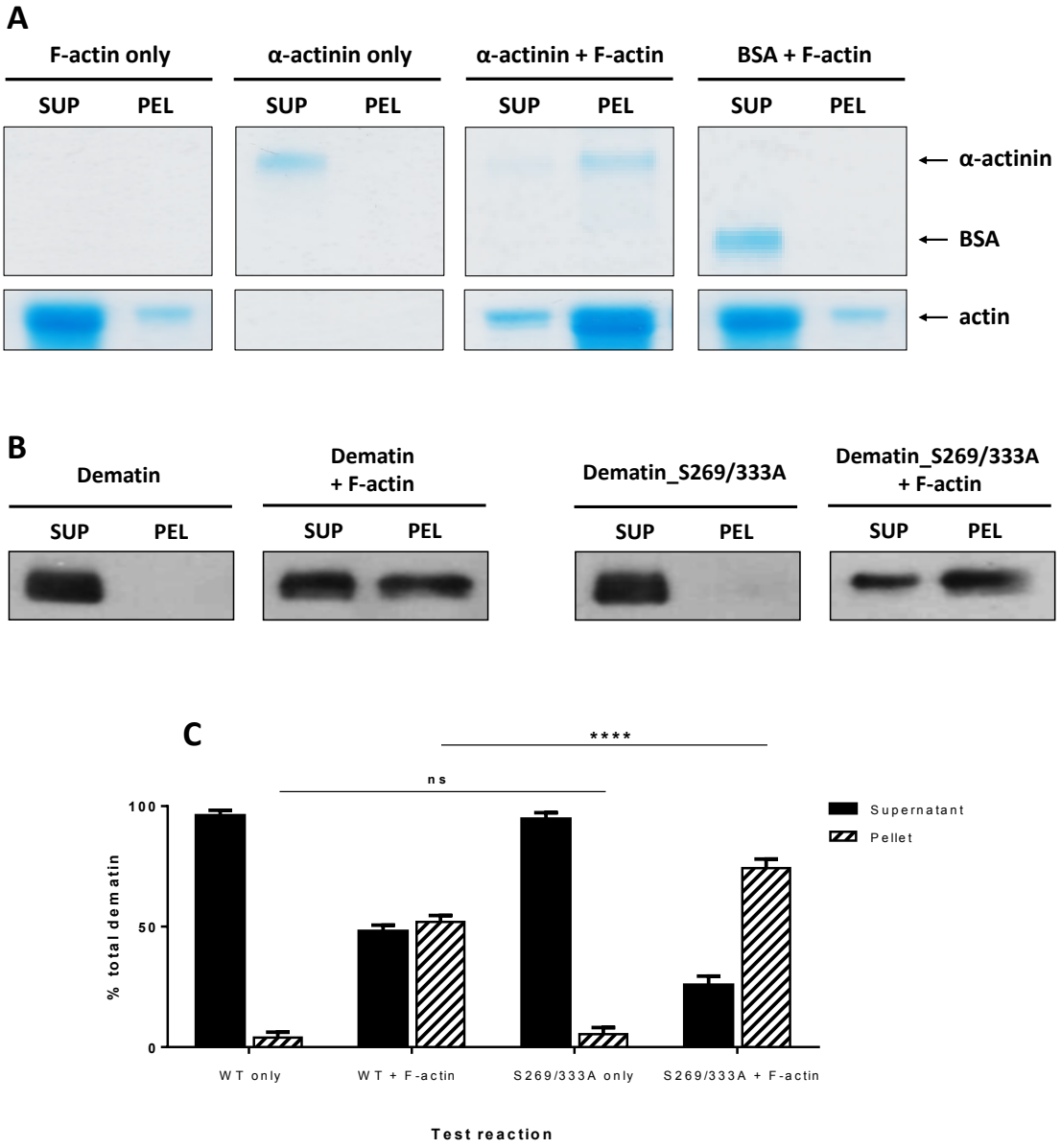

Figure 5.8: The effect of 14-3-3β binding on the actin-bundling ability of dematin

Strep*FLAG*-dematin/14-3-3β and Strep*FLAG*-dematin_S269/333A dematin were purified from HEK293T cells lysates on Strep-Tactin columns. Test reactions were set up containing the eluted protein and skeletal muscle F-actin, with controls containing protein in polymerisation buffer. Samples were incubated at 24°C for 30 minutes before centrifugation at 14,000 x g for 1 h at 24°C. Aliquots of the supernatant and pellet fractions were analysed. (A) Control reactions of F-actin only, α-actinin (a known actin bundling protein) alone and as a positive control with F-actin, and a negative control of BSA (which has no actin-bundling ability) with F-actin. (B) Test reaction of wild-type dematin and the dematin_S269/333A mutants alone and with F-actin, visualized with anti-FLAG immunoblotting. (C) Quantification of the amount of protein in the pellet and supernatant fractions, with data presented as mean values + SEM (n=3). (SUP; supernatant, PEL; pellet).

5.5 Discussion

In this chapter 14-3-3 has been shown to regulate the subcellular localisation of dematin, preventing its association with the F-actin cytoskeleton. This was shown to require only one of the $RKTRS_{269}LP$ or $RGNS_{333}LP$ consensus motifs in dematin to be bound by 14-3-3. The localisation of dematin with F-actin was further confirmed in sedimentation based actin-binding and -bundling assays, which revealed that both the actin-binding and bundling abilities of dematin are decreased upon association with 14-3-3.

5.5.1 14-3-3β binding regulates the subcellular localisation of dematin

The subcellular localisation of overexpressed dematin in the C2C12 skeletal muscle cell line was visualised using immunodetection and confocal microscopy. Dematin expression was observed throughout the cytosol, but not in the nucleus. The pattern of dematin staining was fairly uniform in distribution and did not correlate with the expected patterns for a protein contained within a specific subcellular organelle. Despite the widespread expression profile of dematin, there is currently little published data on its subcellular localisation in different tissues and cell lines. Expression of dematin in mouse embryonic fibroblasts (MEFs) was detected in the cytosol, and in membrane protrusions (Mohseni & Chishti, 2008a), mimicking the results observed here in C2C12 cells. Conversely, dematin staining in platelets produced a well-defined punctate staining pattern that did not correlate with the pattern seen here in C2C12 cells. Approximately two thirds of protein expression was located at the periphery of the cell, with a second cluster at the centre of the platelet. This central pool was shown to co-localise with protein disulphide isomerase (PDI), located in the dense tubular system (DTS) of the platelet, which is involved in thrombus formation (Wieschhaus *et al.*, 2012).

Attempts were also made to visualise the subcellular localisation of endogenous dematin in C2C12 cells, however this was unsuccessful due to the low protein expression levels. It was not possible to detect dematin expression in the lysate of undifferentiated C2C12 cells using western blotting, and immunocytochemical

detection was also not possible in these cells. Differentiation of C2C12 cells from myocytes to myoblasts was associated with a gradual increase in dematin expression levels that can be detected using immunoblotting (data not shown). This increase was visible from day one of differentiation, and increased at each timepoint taken up to day 10. However it was not possible to successfully differentiate these cells on glass coverslips as would be required for immunocytochemical staining. If this technique can be optimised in future then it will be useful to confirm that the distribution of endogenous dematin correlates with the expressed constructs used here.

The 14-3-3 family are known to have a broad range of effects on their targets, which can be generally classified as physically changing the structure of a substrate, altering its subcellular localisation, or acting as a scaffold to increase the likelihood of the substrate interacting with another protein. Here 14-3-3β has been shown to regulate the subcellular localisation of dematin, preventing its colocalisation with the F-actin cytoskeleton. Whereas overexpressed wild-type dematin had a uniform distribution throughout the cytosol, dematin_S269/333A localised to Phalloidin stained F-actin.

In chapter 4, both the $RKTRS_{269}LP$ and $RGNS_{333}LP$ binding sites in dematin were shown to be high affinity motifs that are capable of independently mediating a stable interaction with 14-3-3β. Here co-localisation experiments using the dematin_S269A and dematin_S333A constructs revealed that association of 14-3-3β with either of the motifs was sufficient to reduce the localisation of dematin to the F-actin cytoskeleton. The staining patterns observed were comparable to the wild-type protein localisation, however further experiments will be required as this technique is non-quantitative. It is therefore not possible to conclude whether the full functional effect of 14-3-3 binding is achieved through single-site binding, or whether the phenotype observed is actually an intermediate state on the spectrum between unbound and double-bound 14-3-3. If the dematin_S333A construct is shown to have full actin binding / bundling abilities $RKTRS_{269}LP$

The locations of 14-3-3 binding sites within a target can provide preliminary information on the likely functional role of 14-3-3 binding. Paired binding sites are often found on either side of important functional domains, meaning that binding of the 14-3-3 dimer masks these sequences, and therefore alters the function of the target protein (Silhan *et al.*, 2009). Analysis of the amino acid sequence between the $RKTRS_{269}LP$ and $RGNS_{333}LP$ binding sites does not identify any known protein motifs that may be masked by 14-3-3 binding. Dematin is known to contain two actin-binding motifs, one in the HP domain and a second in the core region. The HP motif is located within the ^{367}LERHLSAEDFSRVFAMSPEEFGKLALWKR^{395} region, whereas the core motif has not been defined. It is therefore plausible that the core motif is located between the $RKTRS_{269}LP$ and $RGNS_{333}LP$ motifs, and is directly masked upon binding of 14-3-3. Alternatively 14-3-3 binding may inhibit the HP actin-binding site. The available NMR structure of the dematin HP is from the 48 KDa isoform, which is lacking the HP insert and therefore the region containing the $RGNS_{333}LP$ motif is not mapped. It is possible that although 14-3-3 does not directly mask the HP actin-binding region, the 3D conformation of the protein may be such that binding of 14-3-3 physically obscures the actin-binding motif. Interestingly, the two 14-3-3 interaction sites are situated on either side of dematin core / HP boundary (at aa 315). The core domain of dematin is intrinsically disordered, and therefore binding of the rigid 14-3-3 dimer may also affect the structure of the surrounding protein.

One difficulty in interpreting the images presented here arises from the non-uniform nature of the actin cytoskeleton. The natural variation in F-actin staining patterns between cells hinders the determination of subtle mutation-specific changes in dematin localisation. In future it may be beneficial to co-transfect cells with both a wild-type and a 14-3-3 mutant construct, one with an N-terminal FLAG tag the other with a MYC tag. As the primary FLAG and MYC antibodies used for detection are raised in different species, the constructs could be detected with compatible Alexa Fluor® 488 and Alexa Fluor® 633 conjugated secondary antibodies (which would also allow co-detection of F-actin with Alexa Fluor® 568 conjugated Phalloidin). This would permit images to be taken of the distribution of both wild-

type and 14-3-3 mutant forms of dematin in the same cell, and facilitate the direct comparison of subcellular expression patterns. This would be particularly useful for comparing wild-type dematin with the single-site mutations dematin_S269A, and dematin_S333A, as it was not possible to determine any differences in the data presented here due to the intrinsic variability of the actin staining patterns.

Although imaging experiments act as a useful tool for visualising the subcellular distribution of a protein they are prone to inaccuracies in interpretation, and colocalisation data alone is therefore not sufficient evidence of a biological effect. Imaging data can be quantified using co-localisation software, which attempts to determine whether there is a spatial overlap between the pixels in the two different fluorophore images. Ultimately however it is essential that potential findings are validated using biochemical assays, particularly when looking at potential interactions between two proteins. Attempts were made to quantify the degree of co-localisation in the images presented here; however the method could not be suitably optimised to provide consistent results.

5.5.2 14-3-3β regulates the actin-binding and -bundling properties of dematin

The observations from the imaging localisation data were validated using quantitative F-actin binding and bundling assays. Experiments were conducted on the Strep*FLAG*-dematin and Strep*FLAG*-dematin_S269/333A constructs. Both proteins were shown to have both actin-binding and -bundling function, but these properties decreased by 42.8% and 30.08% respectively upon 14-3-3 β association. This adds to an increasing body of evidence of 14-3-3 as a regulator of the actin cytoskeleton. It was originally believed that 14-3-3 interacted directly with actin (Chen & Yu, 2002), but in line with the data presented here it is now evident that this interaction is actually an indirect mechanism involving the regulation of actin-binding proteins (Birkenfeld *et al.*, 2003). A significant amount of wild-type dematin bound to and bundled F-actin, despite the localisation experiments showing little spatial correlation between the two. This may be a true result, indicating that 14-3-3 is only a partial regulator of the actin-binding activity of dematin. Although there wasn't an obvious correlation between wild-type dematin and actin distribution in

the cells, dematin was found throughout the cytosol and therefore it would be plausible to imagine that a significant proportion could still be bound to actin. Alternatively this may be an artefact of the experiment. Although western blotting was used to confirm that 14-3-3 co-eluted with the wild-type dematin, it was not possible to confirm what proportion of the purified dematin was bound by 14-3-3. Equally it was not possible to determine whether any of the bound 14-3-3 dissociated during the course of the assay. It is therefore possible that a proportion of the actin-bound dematin was actually no longer associated with 14-3-3, which may partially or fully explain the binding and bundling activity seen here.

The results presented here act as a basis for understanding the general regulatory function of the dematin / 14-3-3β interaction, through characterisation of the wild-type and binding-inhibited dematin_S269/333A constructs. Now that the efficacy of the technique has been demonstrated, it will be possible to characterise the actin regulatory properties of the single dematin_S269A and dematin_S333A mutants. This will confirm whether binding at a single motif is sufficient to induce the full physiological function. In addition the shorter 48 KDa isoform of dematin will be assayed, along with the corresponding dematin48_S269A mutant. The results presented in chapter 4 suggest that the 52 KDa isoform of dematin interacts with 14-3-3β at residues RKTRS$_{269}$LP and RGNS$_{333}$LP, whereas the 48 KDa isoform only interacts at RKTRS$_{269}$LP. The two isoforms may therefore not bind to 14-3-3 with equal affinity. When a synthetic peptide with two 14-3-3 binding motifs was compared to a similar peptide with only one site, the strength of interaction with 14-3-3 was over 30 times greater (Yaffe *et al.*, 1997). It will be interesting to see what difference this makes to the physiological regulation of the two isoforms when 14-3-3 is bound.

The constructs used in the actin-binding and -bundling experiments were re-cloned with an N-terminal Strep-tag for purification rather than the previously used GST-tag. Under standard purification conditions GST-fusion proteins have been demonstrated to dimerise via the GST-tag. There is no evidence of dimerisation of Strep-fusion proteins, which was essential for the actin-bundling experiments in

particular as the increased molecular weight of the dimerised complex may have produced a false positive pelleting of dematin. Strep-tags are small and chemically inert and so should not interfere with the folding or activity of a recombinant protein, and therefore it was not necessary to cleave the tag prior to the experimentation. Equally the desthiobiotin was not removed through dialysis or gel filtration, as this is compatible with the experimental design used here.

5.5.3 Physiological regulation of the dematin / 14-3-3β interaction

To date it has not been possible to identify the kinases that are responsible for phosphorylating the $RKTRS_{269}LP$ and $RGNS_{333}LP$ binding sites, and so further characterisation of these motifs will be required. Equally identifying the phosphatases that negatively regulate these sites via dephosphorylation will also be important. Identification of the regulatory kinases will be important for confirming the physiological regulation of the interaction between endogenous dematin and 14-3-3. Inhibition of these kinases will provide a mechanism for abolishing the dematin / 14-3-3 interaction which should mimic the effect of the dematin_S269/333A mutant used here. Identification of these kinases will also provide information on the signalling pathways that are involved in regulating the dematin / actin interaction, allowing for the study of the upstream regulators of dematin. Interestingly a number of other actin-binding proteins that have now been identified as 14-3-3 substrates, including SSH1L and cortactin, are phosphorylated by PKD.

Analysis of 14-3-3 substrates that contain two active sites demonstrated that in the majority of cases these proteins contained two different modes of binding motif (Johnson et al., 2010). This is the case with dematin, where the identified sites are the mode I motif $RGNS_{333}LP$, and the mode II motif $RKTRS_{269}LP$. These differing sequences are targets for both shared, and unique, subsets of protein kinases. If the two sites are phosphorylated by different kinases then this provides two layers of regulation if both sites are needed for binding (or functional outcome), or alternative methods of activation if only one site is needed. Localisation experiments suggest that both the single dematin_S269A and dematin_S333A

mutants are capable of altering the subcellular localisation of dematin, although it remains to be determined exactly what level of functional effect they confer. Based upon this preliminary data, the dematin / 14-3-3β interaction has the potential to be regulated by two different kinase pathways.

5.5.4 Potential function of the dematin N-terminal 14-3-3 binding motifs

The experiments conducted in chapter 4 were unable to verify an interaction between the N-terminal region of dematin and 14-3-3β, despite the mass spectrometry analysis identifying the $RDSS_{22}VP$ and $RERS_{85}LSP$ motifs as being phosphorylated. This may be a true negative result or it may be that these are lower affinity sites which require cooperative binding or specific conditions, making them difficult to characterise. Paired binding sites are frequently located within highly disordered protein regions, explaining how 14-3-3 association can have such a dramatic effect on the tertiary structure of a target protein (Obsilova *et al.*, 2008). The N-terminal region of dematin is known to be intrinsically disordered (Chen *et al.*, 2009), and so binding at the $RDSS_{22}VP$ and $RERS_{85}LSP$ motifs could be predicted to significantly alter the conformation of dematin. If an interaction at these sites can be demonstrated in the future, then this could be an important mechanism for regulating the structure and therefore function of dematin.

Based upon the experiments performed to date, the 48 KDa isoform of dematin binds to 14-3-3β at the $RKTRS_{269}LP$ motif. As 14-3-3 dimers are known to simultaneously bind to two motifs, this suggests that either there is a second low-affinity binding site that we have not been able to characterise, or that the second site is occupied by a different protein. It is possible that either the $RDSS_{22}VP$ or $RERS_{85}LSP$ motif are required for binding in the 48 KDa isoform of dematin, but not in the 52 KDa isoform where having two high-affinity sites would take binding preference. If only a single site in dematin is bound, then this would enable 14-3-3 to act as a scaffold protein and bring a second interacting protein into close proximity with 48 KDa dematin. Alternatively 14-3-3 may act to bring together two monomers of 48 KDa dematin.

6. General Discussion

6.1 Introduction

Dematin is an actin-binding and -bundling protein that was first identified in erythrocytes, where it is important for creating a stabilising linkage between the actin cytoskeleton and the cell membrane (Khan *et al.*, 2008; Siegel & Branton, 1985). Despite the ubiquitous expression pattern of dematin throughout the body, little research has been conducted into understanding its functions in non-erythroid tissues. Several roles have been described for dematin, including as a potential tumour suppressor, regulator of calcium mobilisation in platelets, and enhancer of wound healing (Lutchman *et al.*, 1999; Mohseni & Chishti, 2008a; Wieschhaus *et al.*, 2012). Interestingly the function of dematin in metabolically active tissues has not been investigated, despite confirmation of its expression in both skeletal muscle and adipose tissue, and validation of its direct interaction with the basal glucose transporter GLUT1 (Azim *et al.*, 1995; Khan *et al.*, 2008; Mohseni & Chishti, 2008b). Equally little is known about how dematin is regulated in vivo, in particular with respect to its well-characterised and fundamental ability to both bind and bundle F-actin. The work presented in this thesis aimed to gain an understanding of the function and regulation of dematin, using skeletal muscle as a model system. In particular the project had two broad aims:

1) *To confirm dematin as a substrate of the p38 MAPK, and determine the effects of p38 phosphorylation on the stability of dematin, and on the dematin core / HP interaction.*

2) *To determine whether dematin is a substrate of the 14-3-3 family of adaptor proteins, characterise the nature of the interaction, and identify the physiological function of 14-3-3 binding.*

This chapter brings together the findings of this thesis in relation to the above aims, summarising both the results themselves and their significance in furthering our understanding of the function and regulation of dematin. The wider implications of these findings, and future research areas of interest, are also discussed.

6.2 Regulation of dematin by the p38 MAPK

The experiments presented here confirm dematin as a substrate of the p38 MAPK, both in vitro and in vivo. Multiple phosphorylation sites were identified in both the core and HP domains using mass spectrometry, in vitro kinase assays, and in vivo detection approaches. The regions of dematin that were identified as being phosphorylated by p38 are summarised in Figure 6.1A.

The unstable nature of dematin was confirmed in pulse-chase experiments where dematin was shown to have a short in-vivo half-life, which was linked at least in part to the presence of a PEST degradation motif. As phosphorylation of intrinsic Ser and Thr residues is known to be the most common mechanism through which PEST motifs are activated, this lead to the hypothesis that p38 may regulate the stability of dematin. Although a trend towards instability was seen under p38-hyperactivated conditions, there was no significant effect (Figure 6.1B). Equally no significant change in stability was seen when Ser / Thr residues were mutated to Ala or Glu, suggesting that phosphorylation may not be the activation method in place here. It therefore remains to be determined how exactly the PEST motif is regulated, or whether it even requires a secondary activation mechanism. Elucidating this will provide further information on the function and regulation of dematin by identifying the conditions under which its degradation is enhanced.

The HP domain is an important region that mediates most of the known functions of dematin. Here p38 was shown to phosphorylate the HP at Ser^{383} (Figure 6.1C). PKA phosphorylation of the HP was recently shown to inhibit actin-bundling by inducing binding of the HP to the core domain. As Ser^{383} is located at the end of an α-helix, we speculated that phosphorylation of this site may cause a conformational change that could inhibit the HP / core interaction. Based on the experiments to date, the HP appears to bind to the core domain at a site either within or overlapping the aa 197-261 region. No regulatory effect of p38 phosphorylation on this interaction was identified (Figure 6.1C). It remains to be determined whether p38 phosphorylation of Ser^{383} does indeed induce a conformational change in the HP, and whether this could directly regulate the actin-binding ability of dematin.

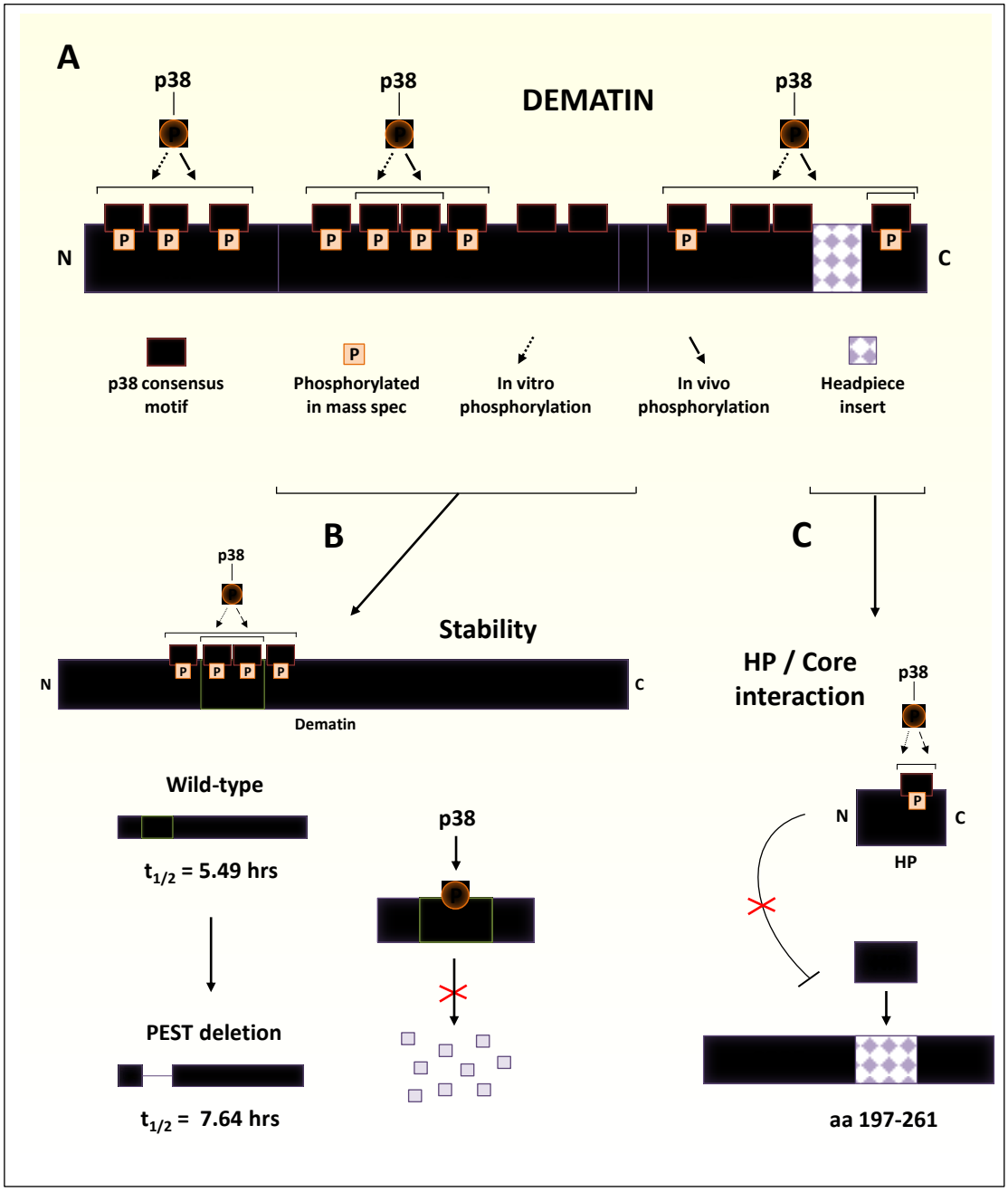

Figure 6.1: Summary of the effects of p38 phosphorylation of dematin

A schematic representation of the p38 phosphorylation sites in dematin that were identified in this thesis (A), and the effects of p38 phosphorylation on the PEST-mediated stability of dematin (B), and on the interaction between the dematin core and headpiece domains (C).

6.3 Regulation of dematin by 14-3-3

The data presented in chapter 4 confirmed dematin as a novel substrate of the 14-3-3 family, with the experiments in chapter 5 beginning to elucidate the function of this interaction. Seven 14-3-3 consensus motifs were identified in the primary sequence of the 52 KDa dematin isoform, and through Co-IP and mutagenesis approaches, two active binding sites were identified at $RKTRS_{269}LP$ and $RGNS_{333}LP$ (Figure 6.2A). These were both shown to be high affinity binding sites, each capable of independently binding to 14-3-3β. The shorter 42 KDa isoform lacks the $RGNS_{333}LP$ sequence, and appeared to bind only the $RKTRS_{269}LP$ motif. Interestingly the original mass spectrometry analysis also identified he N-terminal $RDSS_{22}VP$ and $RERS_{85}LSP$ motifs as being phosphorylated. We therefore cannot rule out the possibility that these are lower affinity sites that may have important functional roles that have yet to be determined.

To date it has not been possible to determine the kinases responsible for phosphorylating these motifs, but Akt, AMPK, and PKA were ruled out as regulators of these sites. Identification of these regulatory kinases, in addition to their opposing phosphatases, will aid in confirming the physiological regulation of the interaction in addition to providing further information on the pathways that are involved in regulating this process. Despite identifying p38 phosphorylation motifs in close proximity to the 14-3-3 binding sites, phosphorylation by p38 did not negatively regulate the dematin / 14-3-3 interaction (Figure 6.2A).

Association of 14-3-3 was shown to alter the subcellular distribution of dematin. Inhibiting binding at either one of the $RKTRS_{269}LP$ or $RGNS_{333}LP$ motifs reduced the apparent localisation of dematin with the F-actin cytoskeleton (Figure 6.2B). Dematin is well characterised as an actin-binding and -bundling protein, but the regulation of these functions are not well understood. The experiments presented here provide evidence that binding of 14-3-3 to dematin regulates dematin's ability to both bind and bundle F-actin. Actin sedimentation assays confirmed that localisation images and revealed that binding of 14-3-3 to dematin resulted in a significant decrease in both actin binding and actin bundling (Figure 6.2B).

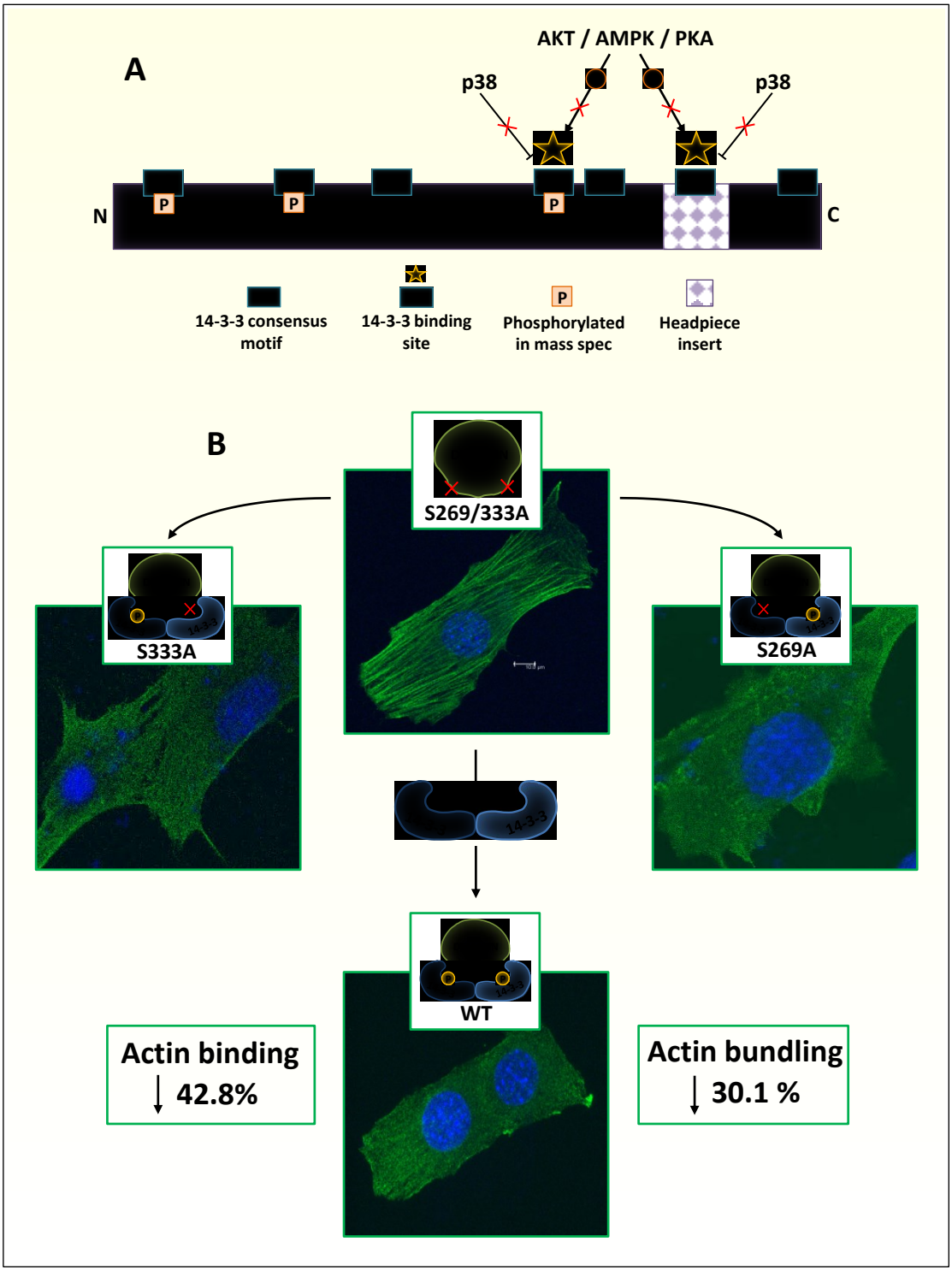

Figure 6.2: Summary of the effect of 14-3-3 regulation on dematin

A schematic representation of the interaction between dematin and 14-3-3, confirming the identified sites of interaction (A), and the effect of 14-3-3 binding on the subcellular localisation and actin binding/bundling properties of dematin (B).

6.4 Relevance of these findings in cytoskeletal remodelling

The confirmation of dematin as a substrate of 14-3-3β adds to increasing evidence of essential roles for 14-3-3 proteins in the regulation of the actin cytoskeleton. What was initially considered to be a coordination of actin by 14-3-3 is now known to be an indirect regulatory mechanism via control of actin-binding and -bundling proteins. The regulation of actin binding and bundling by 14-3-3 identified here in skeletal muscle cells has implications for the regulation of dematin in many other cells types. Dematin is ubiquitously expressed, and both 14-3-3 and actin are found in all tissues, suggesting the potential for a conserved regulatory mechanism.

The ability of dematin to regulate the actin cytoskeleton has been linked to its control of RhoA. In the GTP-bound state, RhoA acts upon two known effector proteins, Rho-associated coiled-coil containing protein kinase 1a (ROCK1) and (diaphanous homolog 1 (Drosophila) (DIAPH1), to regulate actin dynamics and control cell migration. Fibroblasts from dematin HPKO mice showed defects in migration as a result of enhanced adhesive properties and elevated FAK activation, leading to the confirmation that dematin operates upstream of RhoA and FAK, and acts as a suppressor of RhoA activation (Mohseni & Chishti, 2008a). Activation of RhoA is mediated by RhoGEFs, while RhoGAPs return RhoA to the inactive GDP-bound state. A third set of proteins, the RhoGDIs, can tether RhoA in an inactive complex. Cytoskeletal-associated proteins can coordinate RhoA activity through direct interaction with these factors. The regulation of this process in dematin has not been defined, however a direct interaction between dematin and the GEFs RasGRF2, and GEF domain of Trio, has been demonstrated. There is no direct evidence for the binding of dematin to RhoGAPs but other ABPs, such as actopaxin and VRP1, spatially and temporally regulate RhoGAPs thereby inhibiting Rho activity. Equally no direct binding has been confirmed between dematin and any RhoGDIs.

As a direct interaction between dematin and GEFs but not GAPs or GDIs has been demonstrated, current evidence suggests that the negative regulation of RhoA by dematin is most likely to be as a result of dematin binding to RhoGEFs and preventing nucleotide exchange. Identification of 14-3-3 as a novel regulator of the

actin-binding and -bundling functions of dematin raises the possibility that this interaction may also regulate RhoA. The interaction between dematin and the GEF RasGRF2 was localised to residues 224-383 in the 48 KDa dematin isoform. This overlaps with the RKTRS$_{269}$LP 14-3-3 binding motif identified here, which suggests that binding of 14-3-3 to dematin could potentially displace RasGRF2. Although RasGRF2 bound to dematin, it was only capable of catalysing the nucleotide exchange of Rac1 and not RhoA. However the DH-domain of other GEFs is likely to bind to dematin in the same region. 14-3-3 could therefore act as a positive regulator of RhoA activation by binding to dematin, thereby preventing dematin from tethering GEFs to the actin cytoskeleton where they are unable to activate RhoA (Figure 6.3). The above model would also be relevant to a dematin / GDI interaction if an interaction between dematin and any GDI proteins is identified in future. Equally this could be applied to the regulation of a dematin / GAP interaction if the mechanism was reversed, and 14-3-3 instead acted as a negative regulator of RhoA. In this instance dematin would tether GAP to the actin cytoskeleton in the RhoA active state, and 14-3-3 binding to dematin would release GAP allowing for nucleotide hydrolysis.

The involvement of 14-3-3 in mediating the RhoA suppressive activity of an actin-regulating protein has previously been demonstrated in kidney ankyrin repeat protein (Kank). Although the precise mechanism of this regulation is not understood, the AKT mediated association of Kank with 14-3-3 resulted in a reduction in actin stress fibre formation and decreased insulin-induced migration.

14-3-3 has also been shown to bind directly to GEFs, including the RhoA activators p190GEF and AKAP-Lbc. Based on the data collected here binding of 14-3-3 to the 48 KDa isoform of dematin occurs at only the RKTRS$_{269}$LP motif, thereby leaving one free binding site in the 14-3-3 dimer. The ability of 14-3-3 to bind to two independent proteins to act as a scaffold protein has been well documented. It is therefore possible that 14-3-3 could enhance the interaction between dematin and a GEF via this alternative mechanism, and subsequently prevent RhoA activation.

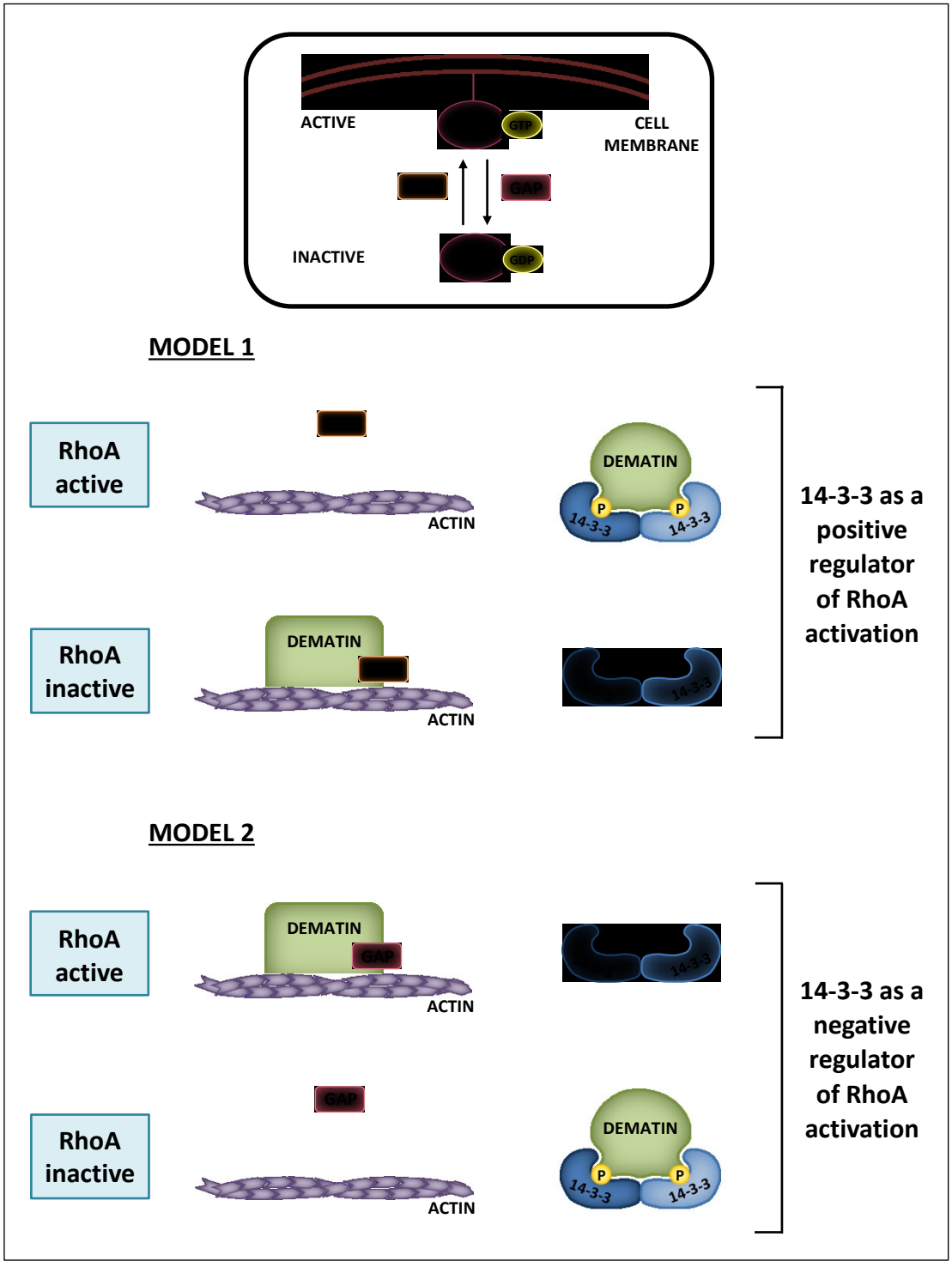

Figure 6.3: Potential mechanisms of dematin/14-3-3 regulating RhoA activation

The cytoskeletal regulator RhoA is activated by guanine nucleotide exchange factors (GEFs) and returned to an inactive state by GTPase activating proteins (GAPs). Dematin is known to suppress RhoA activation, and here has been shown to be a substrate of 14-3-3. Model 1 proposes a potential role for 14-3-3 in preventing dematin from retaining GEFs at the actin cytoskeleton, thereby activating RhoA. Model 2 proposes a potential role for 14-3-3 in preventing dematin from retaining GAPs at actin cytoskeleton, thereby inactivating RhoA.

Although the 52 KDa isoform of dematin was shown to mediate an interaction with 14-3-3 via both the $RKTRS_{269}LP$ and $RGNS_{333}LP$, each of these were high affinity sites and capable of independent binding. If future investigation determines that these motifs are activated by different kinases, then it is plausible that under certain conditions 52 KDa dematin only associated with 14-3-3 via one motif thereby facilitating the co-binding of a GEF.

6.4.1 Implications of these findings for wound healing

Relatively few functions of dematin have been characterised, but expression has been confirmed in fibroblasts and platelets, both of which are essential for normal wound healing. Platelets are essential for preventing blood loss via their aggregation and fibrin formation, and also secrete factors that promote tissue repair. Fibroblast involvement includes aiding in the breakdown of the fibrin clot and forming extracellular matrix structures to support other recruited cells. The expression pattern of dematin in fibroblasts was shown to be comparable to that observed here in C2C12 cells (Mohseni & Chishti, 2008a). Dematin HPKO fibroblasts displayed impaired cell migration in culture, and this corresponded to markedly decreased wound healing vivo (Mohseni & Chishti, 2008a). Dematin therefore has an essential role in fibroblast migration, and 14-3-3 regulation could represent a mechanism through which the actin cytoskeleton is regulated in this process. The subcellular localisation of a protein is not always consistent between cells types however, and this has been demonstrated in platelets where dematin expression was visualised as discrete puncta that localised with the cell periphery (Wieschhaus *et al.*, 2012). This regulatory mechanism identified here may therefore not be relevant to the regulation of platelets, as dematin in these cells may be confined to specific intracellular vesicles, and therefore not in direct contact with the actin cytoskeleton. This does not rule out a possible function of the dematin / 14-3-3 interaction in these cells however as 14-3-3 binding to a protein can mediate multiple functions depending on the context of the interaction. Equally it is possible that this mechanism is not important in circulating conditions, but that upon activation regulation of actin becomes more important.

6.4.2 Implications for these findings in cancer

Tumour cells are known to subvert the actin cytoskeleton in order to fulfil their growth, motile, and invasive requirements, and alterations in the expression pattern and activity of actin-bundling proteins correlate with tumour formation and cancer progression. In order to metastasise from the primary tumour location, cancerous cells coordinate actin bundles to form membrane protrusions with sufficient mechanical force to invade the surrounding tissues. However the mechanisms by which tumour cells manipulate the normal physiological actin-bundling processes are not well understood. The dematin gene has been localised to chromosome 8p21.1 in humans, at a region between two markers (D8S258 and D8S137) that are frequently deleted in prostate cancer (Azim *et al.*, 1995; Lutchman *et al.*, 1999). Deletions in this region have also been confirmed in breast, colon, and bladder cancers. This lead to the suggestion that dematin may function as a tumour suppressor, which was validated by the finding that the majority of 8p21.1-linked prostate tumours displayed a loss of dematin heterozygosity (Lutchman *et al.*, 1999).

As important regulators of cell migration, the RhoA family has naturally been linked to invasion and metastasis in cancer cells. Importantly, activation of the RhoA pathway correlates closely with the invasive and metastatic potential of a tumour, thus explaining why loss of dematin (a RhoA suppressor) results in a highly metastatic prostate cancer phenotype. Activation of RhoA is thought to induce a metastatic phenotype via two mechanisms: involvement in membrane protrusions, and promotion of invadopodia. A strong correlation is also emerging between 14-3-3 and a wide variety of cancers with numerous suggested pro-oncogenic roles for these proteins, in particular with regards to invasion and metastasis. Whilst dematin has been shown to be downregulated in human prostate tumours, isoforms of 14-3-3 including 14-3-3τ and 14-3-3ε were shown to be overexpressed.

6.4.3 Implications for these findings in diabetes and obesity

Expression of dematin has been confirmed in skeletal muscle (Azim *et al.*, 1995; Rana *et al.*, 1993) and adipose tissue (Mohseni & Chishti, 2008b), the two main metabolic tissues of the body, and it is therefore plausible that dematin may have

specific metabolic functions that have yet to be determined. Dematin HPKO mice are reported to display an obese phenotype (data referenced in the text but not shown (Khan *et al.*, 2008)), suggesting defects in glucose control. A small-scale animal study also showed a complete loss of erythroid dematin in diabetic animals (Kaymaz *et al.*, 2005), however expression levels in skeletal muscle and adipocytes has never been measured. The potential involvement of dematin in glucose uptake is supported by the finding that dematin binds directly to the basal glucose transporter GLUT1 in erythrocytes, where it provides shape and mechanical stability to the cell (Khan *et al.*, 2008). This interaction has been replicated in our lab in C2C12 skeletal muscle cells between overexpressed dematin (due to the low endogenous levels in undifferentiated cells) and endogenous GLUT1 (data not shown). The region of GLUT1 that was shown to bind dematin is highly homologous between GLUT1 and the insulin-stimulated GLUT4 transporter, leading to speculation that dematin may also bind to other GLUT family members. This would provide a mechanism through which glucose transport and the actin cytoskeleton are connected via dematin. GLUT4 is responsible for insulin-stimulated glucose uptake in skeletal muscle and adipose tissue, and is mis-regulated in both diabetes and obesity. Under basal conditions GLUT4 is almost exclusively found in intracellular storage vesicles. Upon stimulation with insulin, increased recruitment of GLUT4 to the cell surface enables dramatic increases in glucose uptake, a process which is dependent upon coordination of the actin cytoskeleton.

To date it has not been possible to confirm an interaction between dematin and GLUT4 in Co-IP experiments in our lab. One explanation for this is that the interaction is not stable, and therefore sufficient amounts are not bound at any one time to be detectable using this technique. Whereas the interaction between dematin and GLUT1 provides mechanical support to erythrocytes and therefore needs to be a sustained interaction, the proposed function of dematin in GLUT4 translocation would be more transient. In this thesis dematin has been identified as a substrate of the 14-3-3 protein family. As 14-3-3 proteins have previously been implicated in the regulation of glucose uptake, this raises the interesting possibility that they may mediate a dematin / GLUT4 interaction. Consistent with this

hypothesis, the dematin / 14-3-3 interaction identified here was maintained under both basal and insulin-stimulated conditions (data not shown). In addition to this, an essential role for 14-3-3 in glucose uptake through the regulation of GLUT4 membrane translocation has previously been documented. GLUT4 translocation is coordinated by Rab-mediated vesicular transport, which requires inhibitive binding of 14-3-3 to Rab-GAPs such as AS160 to function. Mice overexpressing a mutant form of AS160 that cannot bind to 14-3-3 display reduced GLUT4 translocation.

The confirmation of dematin as a substrate of the p38 MAPK also has implications for the regulation of glucose homeostasis. There is increasing evidence that the MAPK family are important regulators of metabolism, with a potential involvement of p38 signalling in insulin resistance and type II diabetes mellitus (T2DM) now emerging (Gehart *et al.*, 2010). Insulin resistance, T2DM, and obesity are associated with high glucose concentrations, increased plasma free fatty acid levels and inflammatory cytokines, all stress factors which have been implicated in the activation of p38 signalling (Cuadrado & Nebreda, 2010). This correlates with elevated basal p38 phosphorylation levels in skeletal muscle and adipocytes in patients with these conditions (Carlson *et al.*, 2003; Koistinen *et al.*, 2003). The nature of p38 involvement in these processes, however, has yet to be clearly defined. The identification of dematin as a p38 substrate raises the possibility that dematin phosphorylation is elevated in metabolic disorders, and the effect of this on actin-regulation by dematin will require further investigation.

6.5 Conclusion

The data presented in this thesis provides the first evidence for the regulation of human dematin by the p38 MAPK and the adaptor protein 14-3-3. In particular, a novel mechanism for regulating the actin-binding and -bundling function of dematin via an interaction with 14-3-3 has been demonstrated. Given the ubiquitous nature of dematin, 14-3-3, and p38, the results presented here are likely to be of significance far beyond the regulation of skeletal muscle. Regulation of the actin-cytoskeleton underlies many essential cellular processes, and these findings

therefore have consequences for all of the currently known functions of dematin, from its structural role in erythrocytes to its potential function as a tumour suppressor and regulator of wound healing. In addition, this provides a basis for more in depth characterisation of the metabolic functions of dematin, including the potential for regulating trafficking of GLUT4 and glucose uptake, which have implications for obesity and diabetes.

7. References

Adams, R. H., Porras, A., Alonso, G., Jones, M., Vintersten, K., Panelli, S., Valladares, A., Perez, L., Klein, R. & Nebreda, A. R. (2000) Essential role of p38alpha MAP kinase in placental but not embryonic cardiovascular development. *Mol Cell*, 6 (1): 109-116.

Agarwal-Mawal, A., Qureshi, H. Y., Cafferty, P. W., Yuan, Z., Han, D., Lin, R. & Paudel, H. K. (2003) 14-3-3 connects glycogen synthase kinase-3 beta to tau within a brain microtubule-associated tau phosphorylation complex. *J Biol Chem*, 278 (15): 12722-12728.

Aitken, A. (2006) 14-3-3 proteins: a historic overview. *Semin Cancer Biol*, 16 (3): 162-172.

Aitken, A., Baxter, H., Dubois, T., Clokie, S., Mackie, S., Mitchell, K., Peden, A. & Zemlickova, E. (2002) Specificity of 14-3-3 isoform dimer interactions and phosphorylation. *Biochem Soc Trans*, 30 (4): 351-360.

Aitken, A., Howell, S., Jones, D., Madrazo, J. & Patel, Y. (1995) 14-3-3 alpha and delta are the phosphorylated forms of raf-activating 14-3-3 beta and zeta. In vivo stoichiometric phosphorylation in brain at a Ser-Pro-Glu-Lys MOTIF. *J Biol Chem*, 270 (11): 5706-5709.

Anderson, R. B., Newgreen, D. F. & Young, H. M. (2006) Neural crest and the development of the enteric nervous system. *Adv Exp Med Biol*, 589 181-196.

Andrianantoandro, E. & Pollard, T. D. (2006) Mechanism of actin filament turnover by severing and nucleation at different concentrations of ADF/cofilin. *Mol Cell*, 24 (1): 13-23.

Angrand, P. O., Segura, I., Völkel, P., Ghidelli, S., Terry, R., Brajenovic, M., Vintersten, K., Klein, R., Superti-Furga, G., Drewes, G., Kuster, B., Bouwmeester, T. & Acker-Palmer, A. (2006) Transgenic mouse proteomics identifies new 14-3-3-associated proteins involved in cytoskeletal rearrangements and cell signaling. *Mol Cell Proteomics*, 5 (12): 2211-2227.

Anong, W. A., Franco, T., Chu, H., Weis, T. L., Devlin, E. E., Bodine, D. M., An, X., Mohandas, N. & Low, P. S. (2009) Adducin forms a bridge between the erythrocyte membrane and its cytoskeleton and regulates membrane cohesion. *Blood*, 114 (9): 1904-1912.

Aouadi, M., Laurent, K., Prot, M., Le Marchand-Brustel, Y., Binétruy, B. & Bost, F. (2006) Inhibition of p38MAPK increases adipogenesis from embryonic to adult stages. *Diabetes*, 55 (2): 281-289.

Ashwell, J. D. (2006) The many paths to p38 mitogen-activated protein kinase activation in the immune system. *Nat Rev Immunol*, 6 (7): 532-540.

Athwal, G. S., Huber, J. L. & Huber, S. C. (1998) Phosphorylated nitrate reductase and 14-3-3 proteins. Site of interaction, effects of ions, and evidence for an amp-binding site on 14-3-3 proteins. *Plant Physiol*, 118 (3): 1041-1048.

Azim, A. C., Kim, A. C., Lutchman, M., Andrabi, S., Peters, L. L. & Chishti, A. H. (1999) cDNA sequence, genomic structure, and expression of the mouse dematin gene (Epb4.9). *Mamm Genome*, 10 (10): 1026-1029.

Azim, A. C., Knoll, J. H., Beggs, A. H. & Chishti, A. H. (1995) Isoform cloning, actin binding, and chromosomal localization of human erythroid dematin, a member of the villin superfamily. *Journal of Biological Chemistry*, 270 (29): 17407-17413.

Baboshina, O. V. & Haas, A. L. (1996) Novel multiubiquitin chain linkages catalyzed by the conjugating enzymes E2EPF and RAD6 are recognized by 26 S proteasome subunit 5. *J Biol Chem*, 271 (5): 2823-2831.

Bachmair, A., Finley, D. & Varshavsky, A. (1986) In vivo half-life of a protein is a function of its amino-terminal residue. *Science*, 234 (4773): 179-186.

Bardwell, A. J., Frankson, E. & Bardwell, L. (2009) Selectivity of docking sites in MAPK kinases. *J Biol Chem*, 284 (19): 13165-13173.

Beardmore, V. A., Hinton, H. J., Eftychi, C., Apostolaki, M., Armaka, M., Darragh, J., McIlrath, J., Carr, J. M., Armit, L. J., Clacher, C., Malone, L., Kollias, G. & Arthur, J. S. (2005) Generation and characterization of p38beta (MAPK11) gene-targeted mice. *Mol Cell Biol*, 25 (23): 10454-10464.

Bellon, S., Fitzgibbon, M. J., Fox, T., Hsiao, H. M. & Wilson, K. P. (1999) The structure of phosphorylated p38gamma is monomeric and reveals a conserved activation-loop conformation. *Structure*, 7 (9): 1057-1065.

Bennett, V. (1989) The spectrin-actin junction of erythrocyte membrane skeletons. *Biochimica et Biophysica Acta*, 988 (1): 107-121.

Benzinger, A., Muster, N., Koch, H. B., Yates, J. R. & Hermeking, H. (2005) Targeted proteomic analysis of 14-3-3 sigma, a p53 effector commonly silenced in cancer. *Mol Cell Proteomics*, 4 (6): 785-795.

Birkenfeld, J., Betz, H. & Roth, D. (2003) Identification of cofilin and LIM-domain-containing protein kinase 1 as novel interaction partners of 14-3-3 zeta. *Biochem J*, 369 (Pt 1): 45-54.

Blanchoin, L., Boujemaa-Paterski, R., Sykes, C. & Plastino, J. (2014) Actin dynamics, architecture, and mechanics in cell motility. *Physiol Rev*, 94 (1): 235-263.

Boston, P. F., Jackson, P., Kynoch, P. A. & Thompson, R. J. (1982) Purification, properties, and immunohistochemical localisation of human brain 14-3-3 protein. *J Neurochem*, 38 (5): 1466-1474.

Brancho, D., Tanaka, N., Jaeschke, A., Ventura, J. J., Kelkar, N., Tanaka, Y., Kyuuma, M., Takeshita, T., Flavell, R. A. & Davis, R. J. (2003) Mechanism of p38 MAP kinase activation in vivo. *Genes Dev*, 17 (16): 1969-1978.

Briata, P., Forcales, S. V., Ponassi, M., Corte, G., Chen, C. Y., Karin, M., Puri, P. L. & Gherzi, R. (2005) p38-dependent phosphorylation of the mRNA decay-promoting factor KSRP controls the stability of select myogenic transcripts. *Mol Cell*, 20 (6): 891-903.

Bridges, D. & Moorhead, G. B. (2005) 14-3-3 proteins: a number of functions for a numbered protein. *Sci STKE*, 2005 (296): re10.

Brummer, T., Larance, M., Herrera Abreu, M. T., Lyons, R. J., Timpson, P., Emmerich, C. H., Fleuren, E. D., Lehrbach, G. M., Schramek, D., Guilhaus, M., James, D. E. & Daly, R. J. (2008) Phosphorylation-dependent binding of 14-3-3 terminates signalling by the Gab2 docking protein. *EMBO J*, 27 (17): 2305-2316.

Bukau, B., Weissman, J. & Horwich, A. (2006) Molecular chaperones and protein quality control. *Cell*, 125 (3): 443-451.

Bunney, T. D., van Walraven, H. S. & de Boer, A. H. (2001) 14-3-3 protein is a regulator of the mitochondrial and chloroplast ATP synthase. *Proc Natl Acad Sci U S A*, 98 (7): 4249-4254.

Butler, M. P., O'Connor, J. J. & Moynagh, P. N. (2004) Dissection of tumor-necrosis factor-alpha inhibition of long-term potentiation (LTP) reveals a p38 mitogen-activated protein kinase-dependent mechanism which maps to early-but not late-phase LTP. *Neuroscience*, 124 (2): 319-326.

Cacace, A. M., Michaud, N. R., Therrien, M., Mathes, K., Copeland, T., Rubin, G. M. & Morrison, D. K. (1999) Identification of constitutive and ras-inducible phosphorylation sites of KSR: implications for 14-3-3 binding, mitogen-activated protein kinase binding, and KSR overexpression. *Mol Cell Biol*, 19 (1): 229-240.

Canagarajah, B. J., Khokhlatchev, A., Cobb, M. H. & Goldsmith, E. J. (1997) Activation mechanism of the MAP kinase ERK2 by dual phosphorylation. *Cell*, 90 (5): 859-869.

Cargnello, M. & Roux, P. P. (2011) Activation and function of the MAPKs and their substrates, the MAPK-activated protein kinases. *Microbiol Mol Biol Rev*, 75 (1): 50-83.

Carlier, M. F., Laurent, V., Santolini, J., Melki, R., Didry, D., Xia, G. X., Hong, Y., Chua, N. H. & Pantaloni, D. (1997) Actin depolymerizing factor (ADF/cofilin) enhances the

rate of filament turnover: implication in actin-based motility. *J Cell Biol*, 136 (6): 1307-1322.

Carlson, C. J., Koterski, S., Sciotti, R. J., Poccard, G. B. & Rondinone, C. M. (2003) Enhanced basal activation of mitogen-activated protein kinases in adipocytes from type 2 diabetes: potential role of p38 in the downregulation of GLUT4 expression. *Diabetes*, 52 (3): 634-641.

Chan, T. A., Hermeking, H., Lengauer, C., Kinzler, K. W. & Vogelstein, B. (1999) 14-3-3Sigma is required to prevent mitotic catastrophe after DNA damage. *Nature*, 401 (6753): 616-620.

Chaudhri, M., Scarabel, M. & Aitken, A. (2003) Mammalian and yeast 14-3-3 isoforms form distinct patterns of dimers in vivo. *Biochem Biophys Res Commun*, 300 (3): 679-685.

Chen, H., Khan, A. A., Liu, F., Gilligan, D. M., Peters, L. L., Messick, J., Haschek-Hock, W. M., Li, X., Ostafin, A. E. & Chishti, A. H. (2007) Combined deletion of mouse dematin-headpiece and beta-adducin exerts a novel effect on the spectrin-actin junctions leading to erythrocyte fragility and hemolytic anemia. *Journal of Biological Chemistry*, 282 (6): 4124-4135.

Chen, L., Brown, J. W., Mok, Y. F., Hatters, D. M. & McKnight, C. J. (2013) The allosteric mechanism induced by protein kinase A (PKA) phosphorylation of dematin (band 4.9). *J Biol Chem*, 288 (12): 8313-8320.

Chen, L., Jiang, Z. G., Khan, A. A., Chishti, A. H. & McKnight, C. J. (2009) Dematin exhibits a natively unfolded core domain and an independently folded headpiece domain. *Protein Science*, 18 (3): 629-636.

Chen, X. Q. & Yu, A. C. (2002) The association of 14-3-3gamma and actin plays a role in cell division and apoptosis in astrocytes. *Biochem Biophys Res Commun*, 296 (3): 657-663.

Cheung, P. C., Campbell, D. G., Nebreda, A. R. & Cohen, P. (2003) Feedback control of the protein kinase TAK1 by SAPK2a/p38alpha. *EMBO J*, 22 (21): 5793-5805.

Chiang, C. W., Kanies, C., Kim, K. W., Fang, W. B., Parkhurst, C., Xie, M., Henry, T. & Yang, E. (2003) Protein phosphatase 2A dephosphorylation of phosphoserine 112 plays the gatekeeper role for BAD-mediated apoptosis. *Mol Cell Biol*, 23 (18): 6350-6362.

Clark, A. R. & Dean, J. L. (2012) The p38 MAPK Pathway in Rheumatoid Arthritis: A Sideways Look. *Open Rheumatol J*, 6 209-219.

Coblitz, B., Shikano, S., Wu, M., Gabelli, S. B., Cockrell, L. M., Spieker, M., Hanyu, Y., Fu, H., Amzel, L. M. & Li, M. (2005) C-terminal recognition by 14-3-3 proteins for surface expression of membrane receptors. *J Biol Chem*, 280 (43): 36263-36272.

Collins, A., Warrington, A., Taylor, K. A. & Svitkina, T. (2011) Structural organization of the actin cytoskeleton at sites of clathrin-mediated endocytosis. *Curr Biol*, 21 (14): 1167-1175.

Courson, D. S. & Rock, R. S. (2010) Actin cross-link assembly and disassembly mechanics for alpha-Actinin and fascin. *J Biol Chem*, 285 (34): 26350-26357.

Cuadrado, A. & Nebreda, A. R. (2010) Mechanisms and functions of p38 MAPK signalling. *Biochem J*, 429 (3): 403-417.

Cuenda, A. & Rousseau, S. (2007) p38 MAP-kinases pathway regulation, function and role in human diseases. *Biochim Biophys Acta*, 1773 (8): 1358-1375.

Derick, L. H., Liu, S. C., Chishti, A. H. & Palek, J. (1992) Protein immunolocalization in the spread erythrocyte membrane skeleton. *European Journal of Cell Biology*, 57 (2): 317-320.

Dinkel, H., Van Roey, K., Michael, S., Davey, N. E., Weatheritt, R. J., Born, D., Speck, T., Krüger, D., Grebnev, G., Kuban, M., Strumillo, M., Uyar, B., Budd, A., Altenberg, B., Seiler, M., Chemes, L. B., Glavina, J., Sánchez, I. E., Diella, F. & Gibson, T. J. (2013) The eukaryotic linear motif resource ELM: 10 years and counting. *Nucleic Acids Res*,

dos Remedios, C. G., Chhabra, D., Kekic, M., Dedova, I. V., Tsubakihara, M., Berry, D. A. & Nosworthy, N. J. (2003) Actin binding proteins: regulation of cytoskeletal microfilaments. *Physiol Rev*, 83 (2): 433-473.
Doolittle RF. Redundancies in protein sequences. In: Fasman GD, editor. Prediction of protein structure and the principles of protein conformation. New York: Plenum Press; 1989. pp. 599–623.

Dérijard, B., Raingeaud, J., Barrett, T., Wu, I. H., Han, J., Ulevitch, R. J. & Davis, R. J. (1995) Independent human MAP-kinase signal transduction pathways defined by MEK and MKK isoforms. *Science*, 267 (5198): 682-685.
Doolittle RF. Redundancies in protein sequences. In: Fasman GD, editor. Prediction of protein structure and the principles of protein conformation. New York: Plenum Press; 1989. pp. 599–623.
Eiseler, T., Döppler, H., Yan, I. K., Kitatani, K., Mizuno, K. & Storz, P. (2009) Protein kinase D1 regulates cofilin-mediated F-actin reorganization and cell motility through slingshot. *Nat Cell Biol*, 11 (5): 545-556.

Eiseler, T., Hausser, A., De Kimpe, L., Van Lint, J. & Pfizenmaier, K. (2010) Protein kinase D controls actin polymerization and cell motility through phosphorylation of cortactin. *J Biol Chem*, 285 (24): 18672-18683.

Feng, Y. & Walsh, C. A. (2004) The many faces of filamin: a versatile molecular scaffold for cell motility and signalling. *Nat Cell Biol*, 6 (11): 1034-1038.

Fischer, A., Baljuls, A., Reinders, J., Nekhoroshkova, E., Sibilski, C., Metz, R., Albert, S., Rajalingam, K., Hekman, M. & Rapp, U. R. (2009) Regulation of RAF activity by 14-3-3 proteins: RAF kinases associate functionally with both homo- and heterodimeric forms of 14-3-3 proteins. *J Biol Chem*, 284 (5): 3183-3194.

Ford, J. C., al-Khodairy, F., Fotou, E., Sheldrick, K. S., Griffiths, D. J. & Carr, A. M. (1994) 14-3-3 protein homologs required for the DNA damage checkpoint in fission yeast. *Science*, 265 (5171): 533-535.

Forrest, A. & Gabrielli, B. (2001) Cdc25B activity is regulated by 14-3-3. *Oncogene*, 20 (32): 4393-4401.

Frank, B. S., Vardar, D., Chishti, A. H. & McKnight, C. J. (2004) The NMR structure of dematin headpiece reveals a dynamic loop that is conformationally altered upon phosphorylation at a distal site. *Journal of Biological Chemistry*, 279 (9): 7909-7916.

Freshney, N. W., Rawlinson, L., Guesdon, F., Jones, E., Cowley, S., Hsuan, J. & Saklatvala, J. (1994) Interleukin-1 activates a novel protein kinase cascade that results in the phosphorylation of Hsp27. *Cell*, 78 (6): 1039-1049.

Gasteiger E., H. C., Gattiker A., Duvaud S., Wilkins M.R., Appel R.D., Bairoch A. (2005) *Protein Identification and Analysis Tools on the ExPASy Server*. Humana Press.

Gehart, H., Kumpf, S., Ittner, A. & Ricci, R. (2010) MAPK signalling in cellular metabolism: stress or wellness? *EMBO Rep*, 11 (11): 834-840.

Ghoda, L., Phillips, M. A., Bass, K. E., Wang, C. C. & Coffino, P. (1990) Trypanosome ornithine decarboxylase is stable because it lacks sequences found in the carboxyl terminus of the mouse enzyme which target the latter for intracellular degradation. *J Biol Chem*, 265 (20): 11823-11826.

Ghoda, L., van Daalen Wetters, T., Macrae, M., Ascherman, D. & Coffino, P. (1989) Prevention of rapid intracellular degradation of ODC by a carboxyl-terminal truncation. *Science*, 243 (4897): 1493-1495.

Giles, N., Forrest, A. & Gabrielli, B. (2003) 14-3-3 acts as an intramolecular bridge to regulate cdc25B localization and activity. *J Biol Chem*, 278 (31): 28580-28587.

Glotzer, M. (2005) The molecular requirements for cytokinesis. *Science*, 307 (5716): 1735-1739.

Gohla, A. & Bokoch, G. M. (2002) 14-3-3 regulates actin dynamics by stabilizing phosphorylated cofilin. *Curr Biol*, 12 (19): 1704-1710.

Goley, E. D. & Welch, M. D. (2006) The ARP2/3 complex: an actin nucleator comes of age. *Nat Rev Mol Cell Biol*, 7 (10): 713-726.

Gonda, D. K., Bachmair, A., Wünning, I., Tobias, J. W., Lane, W. S. & Varshavsky, A. (1989) Universality and structure of the N-end rule. *J Biol Chem*, 264 (28): 16700-16712.

Gray, C. H., Good, V. M., Tonks, N. K. & Barford, D. (2003) The structure of the cell cycle protein Cdc14 reveals a proline-directed protein phosphatase. *EMBO J*, 22 (14): 3524-3535.

Guruprasad, K., Reddy, B. V. & Pandit, M. W. (1990) Correlation between stability of a protein and its dipeptide composition: a novel approach for predicting in vivo stability of a protein from its primary sequence. *Protein Eng*, 4 (2): 155-161.

Hall, A. (2009) The cytoskeleton and cancer. *Cancer Metastasis Rev*, 28 (1-2): 5-14.

Han, J., Jiang, Y., Li, Z., Kravchenko, V. V. & Ulevitch, R. J. (1997) Activation of the transcription factor MEF2C by the MAP kinase p38 in inflammation. *Nature*, 386 (6622): 296-299.

Han, J., Lee, J. D., Jiang, Y., Li, Z., Feng, L. & Ulevitch, R. J. (1996) Characterization of the structure and function of a novel MAP kinase kinase (MKK6). *J Biol Chem*, 271 (6): 2886-2891.

Herman, I. M. (1993) Actin isoforms. *Curr Opin Cell Biol*, 5 (1): 48-55.

Hermeking, H. & Benzinger, A. (2006) 14-3-3 proteins in cell cycle regulation. *Semin Cancer Biol*, 16 (3): 183-192.

Hirsch, S., Aitken, A., Bertsch, U. & Soll, J. (1992) A plant homologue to mammalian brain 14-3-3 protein and protein kinase C inhibitor. *FEBS Lett*, 296 (2): 222-224.

Hofmann, K. & Falquet, L. (2001) A ubiquitin-interacting motif conserved in components of the proteasomal and lysosomal protein degradation systems. *Trends Biochem Sci*, 26 (6): 347-350.

Hollenbach, E., Neumann, M., Vieth, M., Roessner, A., Malfertheiner, P. & Naumann, M. (2004) Inhibition of p38 MAP kinase- and RICK/NF-kappaB-signaling suppresses inflammatory bowel disease. *FASEB J*, 18 (13): 1550-1552.

Holmes, K. C., Popp, D., Gebhard, W. & Kabsch, W. (1990) Atomic model of the actin filament. *Nature*, 347 (6288): 44-49.

Houde, M., Laprise, P., Jean, D., Blais, M., Asselin, C. & Rivard, N. (2001) Intestinal epithelial cell differentiation involves activation of p38 mitogen-activated protein

kinase that regulates the homeobox transcription factor CDX2. *J Biol Chem*, 276 (24): 21885-21894.

Huang, H., Ryu, J., Ha, J., Chang, E. J., Kim, H. J., Kim, H. M., Kitamura, T., Lee, Z. H. & Kim, H. H. (2006) Osteoclast differentiation requires TAK1 and MKK6 for NFATc1 induction and NF-kappaB transactivation by RANKL. *Cell Death Differ*, 13 (11): 1879-1891.

Huang, S. F., Xiao, S., Renshaw, A. A., Loughlin, K. R., Hudson, T. J. & Fletcher, J. A. (1996) Fluorescence in situ hybridization evaluation of chromosome deletion patterns in prostate cancer. *Am J Pathol*, 149 (5): 1565-1573.

Hunter, R. W., Mackintosh, C. & Hers, I. (2009) Protein kinase C-mediated phosphorylation and activation of PDE3A regulate cAMP levels in human platelets. *J Biol Chem*, 284 (18): 12339-12348.

Husain-Chishti, A., Faquin, W., Wu, C. C. & Branton, D. (1989) Purification of erythrocyte dematin (protein 4.9) reveals an endogenous protein kinase that modulates actin-bundling activity. *Journal of Biological Chemistry*, 264 (15): 8985-8991.

Husain-Chishti, A., Levin, A. & Branton, D. (1988) Abolition of actin-bundling by phosphorylation of human erythrocyte protein 4.9. *Nature*, 334 (6184): 718-721.

Ichijo, H., Nishida, E., Irie, K., ten Dijke, P., Saitoh, M., Moriguchi, T., Takagi, M., Matsumoto, K., Miyazono, K. & Gotoh, Y. (1997) Induction of apoptosis by ASK1, a mammalian MAPKKK that activates SAPK/JNK and p38 signaling pathways. *Science*, 275 (5296): 90-94.

Ichimura, T., Isobe, T., Okuyama, T., Takahashi, N., Araki, K., Kuwano, R. & Takahashi, Y. (1988) Molecular cloning of cDNA coding for brain-specific 14-3-3 protein, a protein kinase-dependent activator of tyrosine and tryptophan hydroxylases. *Proc Natl Acad Sci U S A*, 85 (19): 7084-7088.

Ichimura, T., Isobe, T., Okuyama, T., Yamauchi, T. & Fujisawa, H. (1987) Brain 14-3-3 protein is an activator protein that activates tryptophan 5-monooxygenase and tyrosine 3-monooxygenase in the presence of Ca2+,calmodulin-dependent protein kinase II. *FEBS Lett*, 219 (1): 79-82.

Isomaa, V. V., Pajunen, A. E., Bardin, C. W. & Jänne, O. A. (1983) Ornithine decarboxylase in mouse kidney. Purification, characterization, and radioimmunological determination of the enzyme protein. *J Biol Chem*, 258 (11): 6735-6740.

Jagemann, L. R., Pérez-Rivas, L. G., Ruiz, E. J., Ranea, J. A., Sánchez-Jiménez, F., Nebreda, A. R., Alba, E. & Lozano, J. (2008) The functional interaction of 14-3-3

proteins with the ERK1/2 scaffold KSR1 occurs in an isoform-specific manner. *J Biol Chem*, 283 (25): 17450-17462.

Jiang, Y., Chen, C., Li, Z., Guo, W., Gegner, J. A., Lin, S. & Han, J. (1996) Characterization of the structure and function of a new mitogen-activated protein kinase (p38beta). *J Biol Chem*, 271 (30): 17920-17926.

Jiang, Z. G. & McKnight, C. J. (2006) A phosphorylation-induced conformation change in dematin headpiece. *Structure*, 14 (2): 379-387.

Jin, J., Smith, F. D., Stark, C., Wells, C. D., Fawcett, J. P., Kulkarni, S., Metalnikov, P., O'Donnell, P., Taylor, P., Taylor, L., Zougman, A., Woodgett, J. R., Langeberg, L. K., Scott, J. D. & Pawson, T. (2004) Proteomic, functional, and domain-based analysis of in vivo 14-3-3 binding proteins involved in cytoskeletal regulation and cellular organization. *Curr Biol*, 14 (16): 1436-1450.

Johnson, C., Crowther, S., Stafford, M. J., Campbell, D. G., Toth, R. & MacKintosh, C. (2010) Bioinformatic and experimental survey of 14-3-3-binding sites. *Biochem J*, 427 (1): 69-78.

Johnson, G. V. & Bailey, C. D. (2003) The p38 MAP kinase signaling pathway in Alzheimer's disease. *Exp Neurol*, 183 (2): 263-268.

Jones, D. H., Martin, H., Madrazo, J., Robinson, K. A., Nielsen, P., Roseboom, P. H., Patel, Y., Howell, S. A. & Aitken, A. (1995) Expression and structural analysis of 14-3-3 proteins. *J Mol Biol*, 245 (4): 375-384.

Junttila, M. R., Ala-Aho, R., Jokilehto, T., Peltonen, J., Kallajoki, M., Grenman, R., Jaakkola, P., Westermarck, J. & Kähäri, V. M. (2007) p38alpha and p38delta mitogen-activated protein kinase isoforms regulate invasion and growth of head and neck squamous carcinoma cells. *Oncogene*, 26 (36): 5267-5279.

Kaksonen, M., Toret, C. P. & Drubin, D. G. (2005) A modular design for the clathrin- and actin-mediated endocytosis machinery. *Cell*, 123 (2): 305-320.

Kaksonen, M., Toret, C. P. & Drubin, D. G. (2006) Harnessing actin dynamics for clathrin-mediated endocytosis. *Nat Rev Mol Cell Biol*, 7 (6): 404-414.

Kaymaz, A. A., Tamer, S., Albeniz, I., Cefle, K., Palanduz, S., Ozturk, S. & Salmayenli, N. (2005) Alterations in rheological properties and erythrocyte membrane proteins in cats with diabetes mellitus. *Clin Hemorheol Microcirc*, 33 (2): 81-88.

Keller, M., Gerbes, A. L., Kulhanek-Heinze, S., Gerwig, T., Grutzner, U., van Rooijen, N., Vollmar, A. M. & Kiemer, A. K. (2005) Hepatocyte cytoskeleton during ischemia and reperfusion--influence of ANP-mediated p38 MAPK activation. *World J Gastroenterol*, 11 (47): 7418-7429.

Khaitlina, S., Fitz, H. & Hinssen, H. (2013) The interaction of gelsolin with tropomyosin modulates actin dynamics. *FEBS J*, 280 (18): 4600-4611.

Khan, A. A., Hanada, T., Mohseni, M., Jeong, J.-J., Zeng, L., Gaetani, M., Li, D., Reed, B. C., Speicher, D. W. & Chishti, A. H. (2008) Dematin and adducin provide a novel link between the spectrin cytoskeleton and human erythrocyte membrane by directly interacting with glucose transporter-1. *Journal of Biological Chemistry*, 283 (21): 14600-14609.

Khanna, R., Chang, S. H., Andrabi, S., Azam, M., Kim, A., Rivera, A., Brugnara, C., Low, P. S., Liu, S.-C. & Chishti, A. H. (2002) Headpiece domain of dematin is required for the stability of the erythrocyte membrane. *Proceedings of the National Academy of Sciences of the United States of America*, 99 (10): 6637-6642.

Kim, A. C., Azim, A. C. & Chishti, A. H. (1998) Alternative splicing and structure of the human erythroid dematin gene. *Biochimica et Biophysica Acta*, 1398 (3): 382-386.

Kim, A. C., Peters, L. L., Knoll, J. H., Van Huffel, C., Ciciotte, S. L., Kleyn, P. W. & Chishti, A. H. (1997) Limatin (LIMAB1), an actin-binding LIM protein, maps to mouse chromosome 19 and human chromosome 10q25, a region frequently deleted in human cancers. *Genomics*, 46 (2): 291-293.

Kisselev, A. F., Akopian, T. N., Woo, K. M. & Goldberg, A. L. (1999) The sizes of peptides generated from protein by mammalian 26 and 20 S proteasomes. Implications for understanding the degradative mechanism and antigen presentation. *J Biol Chem*, 274 (6): 3363-3371.

Kleppe, R., Martinez, A., Døskeland, S. O. & Haavik, J. (2011) The 14-3-3 proteins in regulation of cellular metabolism. *Semin Cell Dev Biol*, 22 (7): 713-719.

Knight, J. D., Tian, R., Lee, R. E., Wang, F., Beauvais, A., Zou, H., Megeney, L. A., Gingras, A. C., Pawson, T., Figeys, D. & Kothary, R. (2012) A novel whole-cell lysate kinase assay identifies substrates of the p38 MAPK in differentiating myoblasts. *Skelet Muscle*, 2 5.

Kobayashi, M., Nishita, M., Mishima, T., Ohashi, K. & Mizuno, K. (2006) MAPKAPK-2-mediated LIM-kinase activation is critical for VEGF-induced actin remodeling and cell migration. *EMBO J*, 25 (4): 713-726.

Koistinen, H. A., Chibalin, A. V. & Zierath, J. R. (2003) Aberrant p38 mitogen-activated protein kinase signalling in skeletal muscle from Type 2 diabetic patients. *Diabetologia*, 46 (10): 1324-1328.

Kuma, Y., Sabio, G., Bain, J., Shpiro, N., Márquez, R. & Cuenda, A. (2005) BIRB796 inhibits all p38 MAPK isoforms in vitro and in vivo. *J Biol Chem*, 280 (20): 19472-19479.

Kumagai, A. & Dunphy, W. G. (1999) Binding of 14-3-3 proteins and nuclear export control the intracellular localization of the mitotic inducer Cdc25. *Genes Dev*, 13 (9): 1067-1072.

Lavoie, J. N., Lambert, H., Hickey, E., Weber, L. A. & Landry, J. (1995) Modulation of cellular thermoresistance and actin filament stability accompanies phosphorylation-induced changes in the oligomeric structure of heat shock protein 27. *Mol Cell Biol*, 15 (1): 505-516.

Lawson, S. K., Dobrikova, E. Y., Shveygert, M. & Gromeier, M. (2013) p38α mitogen-activated protein kinase depletion and repression of signal transduction to translation machinery by miR-124 and -128 in neurons. *Mol Cell Biol*, 33 (1): 127-135.

Lieleg, O., Schmoller, K. M., Claessens, M. M. & Bausch, A. R. (2009) Cytoskeletal polymer networks: viscoelastic properties are determined by the microscopic interaction potential of cross-links. *Biophys J*, 96 (11): 4725-4732.

Liu, C. Y., Zha, Z. Y., Zhou, X., Zhang, H., Huang, W., Zhao, D., Li, T., Chan, S. W., Lim, C. J., Hong, W., Zhao, S., Xiong, Y., Lei, Q. Y. & Guan, K. L. (2010) The hippo tumor pathway promotes TAZ degradation by phosphorylating a phosphodegron and recruiting the SCF{beta}-TrCP E3 ligase. *J Biol Chem*, 285 (48): 37159-37169.

Liu, D., Bienkowska, J., Petosa, C., Collier, R. J., Fu, H. & Liddington, R. (1995) Crystal structure of the zeta isoform of the 14-3-3 protein. *Nature*, 376 (6536): 191-194.

Loetscher, P., Pratt, G. & Rechsteiner, M. (1991) The C terminus of mouse ornithine decarboxylase confers rapid degradation on dihydrofolate reductase. Support for the pest hypothesis. *J Biol Chem*, 266 (17): 11213-11220.

Lutchman, M., Pack, S., Kim, A. C., Azim, A., Emmert-Buck, M., van Huffel, C., Zhuang, Z. & Chishti, A. H. (1999) Loss of heterozygosity on 8p in prostate cancer implicates a role for dematin in tumor progression. *Cancer Genetics & Cytogenetics*, 115 (1): 65-69.

Mackintosh, C. (2004) Dynamic interactions between 14-3-3 proteins and phosphoproteins regulate diverse cellular processes. *Biochem J*, 381 (Pt 2): 329-342.

Manning, G., Whyte, D. B., Martinez, R., Hunter, T. & Sudarsanam, S. (2002) The protein kinase complement of the human genome. *Science*, 298 (5600): 1912-1934.

Margolis, S. S., Walsh, S., Weiser, D. C., Yoshida, M., Shenolikar, S. & Kornbluth, S. (2003) PP1 control of M phase entry exerted through 14-3-3-regulated Cdc25 dephosphorylation. *EMBO J*, 22 (21): 5734-5745.

Marinissen, M. J., Chiariello, M. & Gutkind, J. S. (2001) Regulation of gene expression by the small GTPase Rho through the ERK6 (p38 gamma) MAP kinase pathway. *Genes Dev*, 15 (5): 535-553.

Martens, G. J., Piosik, P. A. & Danen, E. H. (1992) Evolutionary conservation of the 14-3-3 protein. *Biochem Biophys Res Commun*, 184 (3): 1456-1459.

Masters, S. C., Pederson, K. J., Zhang, L., Barbieri, J. T. & Fu, H. (1999) Interaction of 14-3-3 with a nonphosphorylated protein ligand, exoenzyme S of Pseudomonas aeruginosa. *Biochemistry*, 38 (16): 5216-5221.

Mohammad, D. K., Nore, B. F., Hussain, A., Gustafsson, M. O., Mohamed, A. J. & Smith, C. I. (2013) Dual phosphorylation of Btk by Akt/protein kinase b provides docking for 14-3-3ζ, regulates shuttling, and attenuates both tonic and induced signaling in B cells. *Mol Cell Biol*, 33 (16): 3214-3226.

Mohandas, N. & An, X. (2006) New insights into function of red cell membrane proteins and their interaction with spectrin-based membrane skeleton. *Transfusion Clinique et Biologique*, 13 (1-2): 29-30.

Mohseni, M. & Chishti, A. H. (2008a) The headpiece domain of dematin regulates cell shape, motility, and wound healing by modulating RhoA activation. *Molecular & Cellular Biology*, 28 (15): 4712-4718.

Mohseni, M. & Chishti, A. H. (2008b) Erythrocyte dematin is a candidate gene for Marie Unna hereditary hypotrichosis and related hairloss disorders. *Am J Hematol*, 83 (5): 430-432.

Mohseni, M. & Chishti, A. H. (2009) Regulatory models of RhoA suppression by dematin, a cytoskeletal adaptor protein. *Cell Adhesion & Migration*, 3 (2): 191-194.

Montagnac, G., Echard, A. & Chavrier, P. (2008) Endocytic traffic in animal cell cytokinesis. *Curr Opin Cell Biol*, 20 (4): 454-461.

Moore, B. E. a. P., V. J. (1967) Specific acid proteins of the nervous system

Muslin, A. J., Tanner, J. W., Allen, P. M. & Shaw, A. S. (1996) Interaction of 14-3-3 with signaling proteins is mediated by the recognition of phosphoserine. *Cell*, 84 (6): 889-897.

Müller, J., Ory, S., Copeland, T., Piwnica-Worms, H. & Morrison, D. K. (2001) C-TAK1 regulates Ras signaling by phosphorylating the MAPK scaffold, KSR1. *Mol Cell*, 8 (5): 983-993.

Nagata-Ohashi, K., Ohta, Y., Goto, K., Chiba, S., Mori, R., Nishita, M., Ohashi, K., Kousaka, K., Iwamatsu, A., Niwa, R., Uemura, T. & Mizuno, K. (2004) A pathway of

neuregulin-induced activation of cofilin-phosphatase Slingshot and cofilin in lamellipodia. *J Cell Biol*, 165 (4): 465-471.

Neukamm, S. S., Ott, J., Dammeier, S., Lehmann, R., Häring, H. U., Schleicher, E. & Weigert, C. (2013) Phosphorylation of serine 1137/1138 of mouse insulin receptor substrate (IRS) 2 regulates cAMP-dependent binding to 14-3-3 proteins and IRS2 protein degradation. *J Biol Chem*, 288 (23): 16403-16415.

Obenauer, J. C., Cantley, L. C. & Yaffe, M. B. (2003) Scansite 2.0: Proteome-wide prediction of cell signaling interactions using short sequence motifs. *Nucleic Acids Res*, 31 (13): 3635-3641.

Obsil, T., Ghirlando, R., Anderson, D. E., Hickman, A. B. & Dyda, F. (2003) Two 14-3-3 binding motifs are required for stable association of Forkhead transcription factor FOXO4 with 14-3-3 proteins and inhibition of DNA binding. *Biochemistry*, 42 (51): 15264-15272.

Obsil, T., Ghirlando, R., Klein, D. C., Ganguly, S. & Dyda, F. (2001) Crystal structure of the 14-3-3zeta:serotonin N-acetyltransferase complex. a role for scaffolding in enzyme regulation. *Cell*, 105 (2): 257-267.

Obsilova, V., Herman, P., Vecer, J., Sulc, M., Teisinger, J. & Obsil, T. (2004) 14-3-3zeta C-terminal stretch changes its conformation upon ligand binding and phosphorylation at Thr232. *J Biol Chem*, 279 (6): 4531-4540.

Obsilova, V., Nedbalkova, E., Silhan, J., Boura, E., Herman, P., Vecer, J., Sulc, M., Teisinger, J., Dyda, F. & Obsil, T. (2008) The 14-3-3 protein affects the conformation of the regulatory domain of human tyrosine hydroxylase. *Biochemistry*, 47 (6): 1768-1777.

Obsilova, V., Vecer, J., Herman, P., Pabianova, A., Sulc, M., Teisinger, J., Boura, E. & Obsil, T. (2005) 14-3-3 Protein interacts with nuclear localization sequence of forkhead transcription factor FoxO4. *Biochemistry*, 44 (34): 11608-11617.

Oda, T., Iwasa, M., Aihara, T., Maéda, Y. & Narita, A. (2009) The nature of the globular- to fibrous-actin transition. *Nature*, 457 (7228): 441-445.

Ono, K. & Han, J. (2000) The p38 signal transduction pathway: activation and function. *Cell Signal*, 12 (1): 1-13.

Otterbein, L. R., Graceffa, P. & Dominguez, R. (2001) The crystal structure of uncomplexed actin in the ADP state. *Science*, 293 (5530): 708-711.

Pavlov, D., Muhlrad, A., Cooper, J., Wear, M. & Reisler, E. (2007) Actin filament severing by cofilin. *J Mol Biol*, 365 (5): 1350-1358.

Perrin, B. J. & Ervasti, J. M. (2010) The actin gene family: function follows isoform. *Cytoskeleton (Hoboken)*, 67 (10): 630-634.

Peterburs, P., Heering, J., Link, G., Pfizenmaier, K., Olayioye, M. A. & Hausser, A. (2009) Protein kinase D regulates cell migration by direct phosphorylation of the cofilin phosphatase slingshot 1 like. *Cancer Res*, 69 (14): 5634-5638.

Pollard, T. D. (1986) Rate constants for the reactions of ATP- and ADP-actin with the ends of actin filaments. *J Cell Biol*, 103 (6 Pt 2): 2747-2754.

Pollard, T. D. (2010) Mechanics of cytokinesis in eukaryotes. *Curr Opin Cell Biol*, 22 (1): 50-56.

Pollard, T. D., Blanchoin, L. & Mullins, R. D. (2000) Molecular mechanisms controlling actin filament dynamics in nonmuscle cells. *Annu Rev Biophys Biomol Struct*, 29 545-576.

Pollard, T. D. & Cooper, J. A. (2009) Actin, a central player in cell shape and movement. *Science*, 326 (5957): 1208-1212.

Pozuelo Rubio, M., Geraghty, K. M., Wong, B. H., Wood, N. T., Campbell, D. G., Morrice, N. & Mackintosh, C. (2004) 14-3-3-affinity purification of over 200 human phosphoproteins reveals new links to regulation of cellular metabolism, proliferation and trafficking. *Biochem J*, 379 (Pt 2): 395-408.

Pring, M., Weber, A. & Bubb, M. R. (1992) Profilin-actin complexes directly elongate actin filaments at the barbed end. *Biochemistry*, 31 (6): 1827-1836.

Raingeaud, J., Gupta, S., Rogers, J. S., Dickens, M., Han, J., Ulevitch, R. J. & Davis, R. J. (1995) Pro-inflammatory cytokines and environmental stress cause p38 mitogen-activated protein kinase activation by dual phosphorylation on tyrosine and threonine. *J Biol Chem*, 270 (13): 7420-7426.

Raingeaud, J., Whitmarsh, A. J., Barrett, T., Dérijard, B. & Davis, R. J. (1996) MKK3- and MKK6-regulated gene expression is mediated by the p38 mitogen-activated protein kinase signal transduction pathway. *Mol Cell Biol*, 16 (3): 1247-1255.

Rana, A. P., Ruff, P., Maalouf, G. J., Speicher, D. W. & Chishti, A. H. (1993) Cloning of human erythroid dematin reveals another member of the villin family. *Proceedings of the National Academy of Sciences of the United States of America*, 90 (14): 6651-6655.

Rechsteiner, M. (1990) PEST sequences are signals for rapid intracellular proteolysis. *Semin Cell Biol*, 1 (6): 433-440.

Rechsteiner, M. & Rogers, S. W. (1996) PEST sequences and regulation by proteolysis. *Trends Biochem Sci*, 21 (7): 267-271.

Reid, M., Takakuwa, Y., Conboy, J., Tchernia, G. & Mohandas, N. (1990) Glycophorin C content of human erythrocyte membrane is regulated by protein 4.1. *Blood*, 75 (11): 2229-2234.

Reményi, A., Good, M. C., Bhattacharyya, R. P. & Lim, W. A. (2005) The role of docking interactions in mediating signaling input, output, and discrimination in the yeast MAPK network. *Mol Cell*, 20 (6): 951-962.

Rittinger, K., Budman, J., Xu, J., Volinia, S., Cantley, L. C., Smerdon, S. J., Gamblin, S. J. & Yaffe, M. B. (1999) Structural analysis of 14-3-3 phosphopeptide complexes identifies a dual role for the nuclear export signal of 14-3-3 in ligand binding. *Mol Cell*, 4 (2): 153-166.

Rock, K. L., Gramm, C., Rothstein, L., Clark, K., Stein, R., Dick, L., Hwang, D. & Goldberg, A. L. (1994) Inhibitors of the proteasome block the degradation of most cell proteins and the generation of peptides presented on MHC class I molecules. *Cell*, 78 (5): 761-771.

Rogers, S., Wells, R. & Rechsteiner, M. (1986) Amino acid sequences common to rapidly degraded proteins: the PEST hypothesis. *Science*, 234 (4774): 364-368.

Roth, D., Morgan, A., Martin, H., Jones, D., Martens, G. J., Aitken, A. & Burgoyne, R. D. (1994) Characterization of 14-3-3 proteins in adrenal chromaffin cells and demonstration of isoform-specific phospholipid binding. *Biochem J*, 301 (Pt 1) 305-310.

Rousseau, S., Dolado, I., Beardmore, V., Shpiro, N., Marquez, R., Nebreda, A. R., Arthur, J. S., Case, L. M., Tessier-Lavigne, M., Gaestel, M., Cuenda, A. & Cohen, P. (2006) CXCL12 and C5a trigger cell migration via a PAK1/2-p38alpha MAPK-MAPKAP-K2-HSP27 pathway. *Cell Signal*, 18 (11): 1897-1905.

Sabio, G., Cerezo-Guisado, M. I., Del Reino, P., Iñesta-Vaquera, F. A., Rousseau, S., Arthur, J. S., Campbell, D. G., Centeno, F. & Cuenda, A. (2010) p38gamma regulates interaction of nuclear PSF and RNA with the tumour-suppressor hDlg in response to osmotic shock. *J Cell Sci*, 123 (Pt 15): 2596-2604.

Sakabe, K., Teramoto, H., Zohar, M., Behbahani, B., Miyazaki, H., Chikumi, H. & Gutkind, J. S. (2002) Potent transforming activity of the small GTP-binding protein Rit in NIH 3T3 cells: evidence for a role of a p38gamma-dependent signaling pathway. *FEBS Lett*, 511 (1-3): 15-20.

Satoh, J., Nanri, Y. & Yamamura, T. (2006) Rapid identification of 14-3-3-binding proteins by protein microarray analysis. *J Neurosci Methods*, 152 (1-2): 278-288.

Schneider, C. A., Rasband, W. S. & Eliceiri, K. W. (2012) NIH Image to ImageJ: 25 years of image analysis. *Nat Methods*, 9 (7): 671-675.

Schwanhäusser, B., Busse, D., Li, N., Dittmar, G., Schuchhardt, J., Wolf, J., Chen, W. & Selbach, M. (2013) Corrigendum: Global quantification of mammalian gene expression control. *Nature*, 495 (7439): 126-127.

Seimiya, H., Sawada, H., Muramatsu, Y., Shimizu, M., Ohko, K., Yamane, K. & Tsuruo, T. (2000) Involvement of 14-3-3 proteins in nuclear localization of telomerase. *EMBO J*, 19 (11): 2652-2661.

Shen, C. H., Yuan, P., Perez-Lorenzo, R., Zhang, Y., Lee, S. X., Ou, Y., Asara, J. M., Cantley, L. C. & Zheng, B. (2013) Phosphorylation of BRAF by AMPK Impairs BRAF-KSR1 Association and Cell Proliferation. *Mol Cell*,

Siegel, D. L. & Branton, D. (1985) Partial purification and characterization of an actin-bundling protein, band 4.9, from human erythrocytes. *The Journal of Cell Biology*, 100 (3): 775-785.

Silhan, J., Vacha, P., Strnadova, P., Vecer, J., Herman, P., Sulc, M., Teisinger, J., Obsilova, V. & Obsil, T. (2009) 14-3-3 protein masks the DNA binding interface of forkhead transcription factor FOXO4. *J Biol Chem*, 284 (29): 19349-19360.

Simon, C., Simon, M., Vucelic, G., Hicks, M. J., Plinkert, P. K., Koitschev, A. & Zenner, H. P. (2001) The p38 SAPK pathway regulates the expression of the MMP-9 collagenase via AP-1-dependent promoter activation. *Exp Cell Res*, 271 (2): 344-355.

Simone, C., Forcales, S. V., Hill, D. A., Imbalzano, A. N., Latella, L. & Puri, P. L. (2004) p38 pathway targets SWI-SNF chromatin-remodeling complex to muscle-specific loci. *Nat Genet*, 36 (7): 738-743.

Smirnov, S. L., Isern, N. G., Jiang, Z. G., Hoyt, D. W. & McKnight, C. J. (2007) The isolated sixth gelsolin repeat and headpiece domain of villin bundle F-actin in the presence of calcium and are linked by a 40-residue unstructured sequence. *Biochemistry*, 46 (25): 7488-7496.

Stevenson, R. P., Veltman, D. & Machesky, L. M. (2012) Actin-bundling proteins in cancer progression at a glance. *J Cell Sci*, 125 (Pt 5): 1073-1079.

Swanson, K. D. & Ganguly, R. (1992) Characterization of a Drosophila melanogaster gene similar to the mammalian genes encoding the tyrosine/tryptophan hydroxylase activator and protein kinase C inhibitor proteins. *Gene*, 113 (2): 183-190.

Takekawa, M., Adachi, M., Nakahata, A., Nakayama, I., Itoh, F., Tsukuda, H., Taya, Y. & Imai, K. (2000) p53-inducible wip1 phosphatase mediates a negative feedback regulation of p38 MAPK-p53 signaling in response to UV radiation. *EMBO J*, 19 (23): 6517-6526.

Takekawa, M., Maeda, T. & Saito, H. (1998) Protein phosphatase 2Calpha inhibits the human stress-responsive p38 and JNK MAPK pathways. *EMBO J*, 17 (16): 4744-4752.

Tobias, J. W., Shrader, T. E., Rocap, G. & Varshavsky, A. (1991) The N-end rule in bacteria. *Science*, 254 (5036): 1374-1377.

Toker, A., Sellers, L. A., Amess, B., Patel, Y., Harris, A. & Aitken, A. (1992) Multiple isoforms of a protein kinase C inhibitor (KCIP-1/14-3-3) from sheep brain. Amino acid sequence of phosphorylated forms. *Eur J Biochem*, 206 (2): 453-461.

Trempolec, N., Dave-Coll, N. & Nebreda, A. R. (2013) SnapShot: p38 MAPK substrates. *Cell*, 152 (4): 924-924.e921.

Tzivion, G., Luo, Z. & Avruch, J. (1998) A dimeric 14-3-3 protein is an essential cofactor for Raf kinase activity. *Nature*, 394 (6688): 88-92.

Tzivion, G., Luo, Z. J. & Avruch, J. (2000) Calyculin A-induced vimentin phosphorylation sequesters 14-3-3 and displaces other 14-3-3 partners in vivo. *J Biol Chem*, 275 (38): 29772-29778.

Ubersax, J. A. & Ferrell, J. E. (2007) Mechanisms of specificity in protein phosphorylation. *Nat Rev Mol Cell Biol*, 8 (7): 530-541.

Uchida, S., Kubo, A., Kizu, R., Nakagama, H., Matsunaga, T., Ishizaka, Y. & Yamashita, K. (2006) Amino acids C-terminal to the 14-3-3 binding motif in CDC25B affect the efficiency of 14-3-3 binding. *J Biochem*, 139 (4): 761-769.

Uchida, S., Kuma, A., Ohtsubo, M., Shimura, M., Hirata, M., Nakagama, H., Matsunaga, T., Ishizaka, Y. & Yamashita, K. (2004) Binding of 14-3-3beta but not 14-3-3sigma controls the cytoplasmic localization of CDC25B: binding site preferences of 14-3-3 subtypes and the subcellular localization of CDC25B. *J Cell Sci*, 117 (Pt 14): 3011-3020.

Uhart, M., Iglesias, A. A. & Bustos, D. M. (2011) Structurally constrained residues outside the binding motif are essential in the interaction of 14-3-3 and phosphorylated partner. *J Mol Biol*, 406 (4): 552-557.

Van Der Hoeven, P. C., Van Der Wal, J. C., Ruurs, P., Van Dijk, M. C. & Van Blitterswijk, J. (2000) 14-3-3 isotypes facilitate coupling of protein kinase C-zeta to Raf-1: negative regulation by 14-3-3 phosphorylation. *Biochem J*, 345 Pt 2 297-306.

Vardar, D., Chishti, A., Frank, B., Luna, E., Noegel, A., Oh, S., Schleicher, M. & McKnight, C. (2002) Villin-type headpiece domains show a wide range of F-actin-binding affinities. *Cell Motil Cytoskeleton*, 52 (1): 9-21.

Varshavsky, A. (1991) Naming a targeting signal. *Cell*, 64 (1): 13-15.

Verzijl, N., DeGroot, J., Thorpe, S. R., Bank, R. A., Shaw, J. N., Lyons, T. J., Bijlsma, J. W., Lafeber, F. P., Baynes, J. W. & TeKoppele, J. M. (2000) Effect of collagen turnover on the accumulation of advanced glycation end products. *J Biol Chem*, 275 (50): 39027-39031.

Vocke, C. D., Pozzatti, R. O., Bostwick, D. G., Florence, C. D., Jennings, S. B., Strup, S. E., Duray, P. H., Liotta, L. A., Emmert-Buck, M. R. & Linehan, W. M. (1996) Analysis of 99 microdissected prostate carcinomas reveals a high frequency of allelic loss on chromosome 8p12-21. *Cancer Res*, 56 (10): 2411-2416.

Vugmeyster, L. & McKnight, C. J. (2009) Phosphorylation-induced changes in backbone dynamics of the dematin headpiece C-terminal domain. *Journal of Biomolecular NMR*, 43 (1): 39-50.

Wang, B., Yang, H., Liu, Y. C., Jelinek, T., Zhang, L., Ruoslahti, E. & Fu, H. (1999) Isolation of high-affinity peptide antagonists of 14-3-3 proteins by phage display. *Biochemistry*, 38 (38): 12499-12504.

Wang, Q. & Doerschuk, C. M. (2001) The p38 mitogen-activated protein kinase mediates cytoskeletal remodeling in pulmonary microvascular endothelial cells upon intracellular adhesion molecule-1 ligation. *J Immunol*, 166 (11): 6877-6884.

Wang, W. & Shakes, D. C. (1996) Molecular evolution of the 14-3-3 protein family. *J Mol Evol*, 43 (4): 384-398.

Waterman, M. J., Stavridi, E. S., Waterman, J. L. & Halazonetis, T. D. (1998) ATM-dependent activation of p53 involves dephosphorylation and association with 14-3-3 proteins. *Nat Genet*, 19 (2): 175-178.

Wegner, A. & Engel, J. (1975) Kinetics of the cooperative association of actin to actin filaments. *Biophys Chem*, 3 (3): 215-225.

Wieschhaus, A. J., Le Breton, G. C. & Chishti, A. H. (2012) Headpiece domain of dematin regulates calcium mobilization and signaling in platelets. *J Biol Chem*, 287 (49): 41218-41231.

Wilker, E. W., Grant, R. A., Artim, S. C. & Yaffe, M. B. (2005) A structural basis for 14-3-3sigma functional specificity. *J Biol Chem*, 280 (19): 18891-18898.

Woodcock, J. M., Murphy, J., Stomski, F. C., Berndt, M. C. & Lopez, A. F. (2003) The dimeric versus monomeric status of 14-3-3zeta is controlled by phosphorylation of Ser58 at the dimer interface. *J Biol Chem*, 278 (38): 36323-36327.

Wu, Z., Woodring, P. J., Bhakta, K. S., Tamura, K., Wen, F., Feramisco, J. R., Karin, M., Wang, J. Y. & Puri, P. L. (2000) p38 and extracellular signal-regulated kinases regulate the myogenic program at multiple steps. *Mol Cell Biol*, 20 (11): 3951-3964.

Wöll, S., Windoffer, R. & Leube, R. E. (2007) p38 MAPK-dependent shaping of the keratin cytoskeleton in cultured cells. *J Cell Biol*, 177 (5): 795-807.

Würtele, M., Jelich-Ottmann, C., Wittinghofer, A. & Oecking, C. (2003) Structural view of a fungal toxin acting on a 14-3-3 regulatory complex. *EMBO J*, 22 (5): 987-994.

Xiao, B., Smerdon, S. J., Jones, D. H., Dodson, G. G., Soneji, Y., Aitken, A. & Gamblin, S. J. (1995) Structure of a 14-3-3 protein and implications for coordination of multiple signalling pathways. *Nature*, 376 (6536): 188-191.

Yaffe, M. B. (2002) How do 14-3-3 proteins work?-- Gatekeeper phosphorylation and the molecular anvil hypothesis. *FEBS Lett*, 513 (1): 53-57.

Yaffe, M. B., Rittinger, K., Volinia, S., Caron, P. R., Aitken, A., Leffers, H., Gamblin, S. J., Smerdon, S. J. & Cantley, L. C. (1997) The structural basis for 14-3-3:phosphopeptide binding specificity. *Cell*, 91 (7): 961-971.

Zhai, J., Lin, H., Shamim, M., Schlaepfer, W. W. & Cañete-Soler, R. (2001) Identification of a novel interaction of 14-3-3 with p190RhoGEF. *J Biol Chem*, 276 (44): 41318-41324.

Zhao, B., Li, L., Tumaneng, K., Wang, C. Y. & Guan, K. L. (2010) A coordinated phosphorylation by Lats and CK1 regulates YAP stability through SCF(beta-TRCP). *Genes Dev*, 24 (1): 72-85.

Zhuang, X., Northup, J. K. & Ray, K. (2012) Large putative PEST-like sequence motif at the carboxyl tail of human calcium receptor directs lysosomal degradation and regulates cell surface receptor level. *J Biol Chem*, 287 (6): 4165-4176.